The Variation in Results of Standardized Tests to Determine the Yield Strength of Structural Steel

by

Kevin Barry Clinch, B.S.

Thesis

Presented to the Faculty of the Graduate School of

The University of Texas at Austin

in Partial Fulfillment

of the Requirements

for the Degree of

Masters of Science in Engineering

The University of Texas at Austin

December 1997

The Variation in Results of Standardized Tests to Determine the Yield Strength of Structural Steel

Approved by
Supervising Committee:

_____

_____

Acknowledgments

I am grateful to have had the opportunity to work with Dr. Michael Engelhardt, my advisor, who kept me focused and whose sense of humor made graduate research entertaining.

The staff of Ferguson Structural Engineering Laboratory provided valuable advice and assistance throughout the project.

Mostly, I would like to thank Gini Barton whose absence inspired me to work harder.

December 1997

Abstract

The Variation in Results of Standardized Tests to Determine the Yield Strength of Structural Steel

Kevin Barry Clinch, M.S.E.

The University of Texas at Austin, 1997

Supervisor: Dr. Michael Engelhardt

Independent tests of mill-certified structural steel have obtained yield strengths which differ significantly from those reported by the mill. A study to identify the causes of this discrepancy focuses on the standardized test procedures employed to determine yield strength and includes a review of published material related to yield point phenomena and mechanical testing, a comparison of ASTM Standards with foreign and international standards, and an experimental program to evaluate the significance of the various test parameters on yield strength determination. Test results indicate that the variation in yield strength due to the use of different machines and testing speeds may account for only a small portion of the reporteddiscrepancy between mill certificates and independent tests.

Table of Contents

List of Tables

List of Figures

List of Illustrations

Chapter 1: Introduction

1.1 BACKGROUND

Yield strength is a key material property used in the design of steel structures. Significant discrepancies between the value of yield stress assumed by a designer and the actual yield stress of the material provided in the structure can pose safety concerns. For example, under gravity and wind loads, if the actual yield stress of the steel is substantially less than assumed in design, the safety of the structure may be compromised. On the other hand, if the actual yield stress is larger than assumed in design, the safety of the structure under earthquake loading may be adversely affected. The Code (*Uniform* 1994; "NEHRP" 1994) philosophy for the design of earthquake resistant steel structures anticipates that yielding will occur in selected ductile elements of the framing system. The yielding of these ductile elements is intended to serve as a fuse to the forces transferred to the more brittle elements of the frame. For example, in a moment frame, yielding of the beam limits the forces transmitted to the beam-to-column connection, thereby protecting against connection failure. Yielding of the beams also limits the forces transmitted to the columns, thereby preventing potential instability of the column or the development of a soft story. If the actual yield strength of the beam is substantially greater than that assumed by the designer, then the connection may fail or a column may buckle before sufficient ductility is developed by the frame to prevent collapse. One of the factors thought to contribute to the moment connection failures in the 1994 Northridge Earthquake

was the observation that the actual yield stress of A36 beams was in fact likely much higher than 36 ksi (“Interim” 1995).

Considering the full range of loading conditions for a structure, it is important that the actual yield stress of steel neither significantly exceed nor significantly fall short of the yield stress used in design. For most grades of steel used in the United States, ASTM *Standards* (referred to herein as the *Standards*) typically specify only a minimum yield strength. For each heat of steel produced by a steel mill, conformance with the minimum specified yield strength is evaluated by standardized tensile tests specified by the *Standards* and reported on mill certificates.

As noted above, in earthquake resistant design of steel structures, the use of minimum specified yield stress values can be problematic. Recent codes and design guidelines for earthquake resistant steel structures (“Interim” 1995; *Seismic* 1997) explicitly recognized this problem, and employ the use *expected yield strength* values for the design of critical frame elements. The expected yield strength values are based on statistical data from mill test reports (“Statistical” 1994).

Mill tests are a critical element in the design of steel structures. These tests establish conformance with minimum specified yield stress values and form the basis for the expected yield strength values introduced in recent seismic codes. Recently, however, the validity of yield strengths reported on mill test reports have been called into question. Independent tensile tests conducted as part of experimental programs on steel moment connections have obtained yield strengths which, in some cases, have been significantly less than that reported on

the mill certificate. (Shuey 1996; Uang 1995; Schriber 1996). For example, the mill certificate for a W36x150 beam tested by Uang (1995) reported a yield stress of 58.6 ksi (based on web coupons). Independent tests by Uang showed a yield stress of 46.2 ksi in the web and 41.5 ksi in the flange. Shuey (1996) also tested a W36x150 beam with a mill certificate yield stress of 58.0 ksi. Independent tensile tests showed a yield stress of 48 ksi in the web and 42 ksi in the flange. The actual plastic moment of this W36x150 beam was 35 percent less than the value calculated using the mill certificate yield stress. Such large discrepancies are an issue of concern. Interestingly, the Northridge Earthquake has heightened awareness that the actual yield stress of steel may considerably exceed minimum specified values and the need to account for this "overstrength" in design. However, the observations noted above that the actual yield stress may, in fat, be significantly lower than mill certificate values is also of great concern in non-seismic design.

Large discrepancies between yield stress values reported on mill certificates and values reported in independent tensile tests is the motivation for this study. Possible reasons for these discrepancies include:

- variations in the definition of yield stress (upper vs. lower yield stress, offset yield stress, etc.);
- variations caused by the sampling location of the tensile coupon; and
- variations caused by the use of different testing equipment and procedures including the rate at which the specimen is tested and the type of tensile testing machine used.

The study focuses on the final factor noted above, i.e., the influence of test equipment and the loading rate on the measured yield stress.

A number of researchers (e.g., Fry 1940; Lessells and Barr 1965; Gray and Sharp 1989) have suggested that some variation in the yield strength of the same material is due to the response of the machine in which the specimen is tested. Hydraulic machines can sometimes report a higher yield strength than mechanical machines. The increase in strain rate following yield, i.e., the plastic strain rate, will vary with machine type. The ASTM *Standards* do not seem to address either of these issues.

It has long been known that the yield strength of steel increases with strain rate. In specifying maximum and minimum testing rates, the *Standards* provide different criteria to account for different machine types used in production testing. Neither is a direct measure of strain rate. The actual strain rate resulting from the two different criteria may be significantly different.

By specifying a minimum rate, the *Standards* implicitly prohibit the use of a static yield test. Research conducted in the late 1950's at Lehigh University (Tall and Ketter 1958) found close correlation between static yield tests and stub column tests. This suggests that the static yield is a structurally significant measure of yield strength. One of the goals of the present study is to evaluate the reliability of the static yield test when different machines and different testing speeds are employed.

1.2 STUDY OBJECTIVES

The objectives of the study are::

- to investigate the variability of measured yield strength values inherent in the ASTM *Standards* by conducting tests which satisfy the *Standard* but which employ different procedures and measures;
- to validate the reported influence of machine type and strain rate on the upper and lower yield strengths;
- to determine if the static yield is independent of machine type and strain rate; and
- to recommend improvements to the *Standards* based on test findings.

1.3 SCOPE OF INVESTIGATION

The study focuses on the standardized test procedures employed to determine yield strength and includes a review of published material related to yield point phenomena and mechanical testing; a comparison of ASTM *Standards* with foreign and international standards; and an experimental program to evaluate the significance of various testing procedures on yield strength determination.

All experimental work was conducted at the Phil M. Ferguson Structural Engineering Laboratory and the Construction Materials Laboratory of the University of Texas at Austin. Thirty-three plate specimens were tested using four different machines at a number of different rates. An additional twelve specimens were tested as part of a parallel study sponsored by the American Institute of Steel Construction.

The test data and results are presented and the implications of the data with respect to standardized tensile testing of steel are discussed.

1.4 CODES AND SPECIFICATIONS

The ASTM *Standards* which are relevant to the study are listed below in Table 1-1. Included are the publication dates of the editions which were reviewed. Further discussion of the ASTM specifications regarding the determination of the yield strength of steel is presented in Section 2.5.

Table 1-1: ASTM *Standards* relevant to the study

Standard		Edition
A36	Carbon Structural Steel	Jun-94
A6	General Requirements for Rolled Structural Steel	
	Bars, Plates, Shapes and Sheet Piling	Jun-94
A370	Mechanical Testing of Steel Products	Sep-95
E6	Standard Terminology Relating to Methods of Mechanical Testing	Feb-89
E8	Tension Testing of Metallic Materials	Mar-96
E83	Practice for Verification and Classification of Extensometers	Mar-96

Chapter 2: Literature Review

2.1 YIELD POINT PHENOMENA IN STEEL

The tensile stress - strain curve of mild steel exhibits a well defined elastic - plastic transition in what is termed a yield point phenomenon. The transition may be accompanied by a yield drop, i.e. a sudden drop in stress once yielding begins, or the stress-strain curve may simply flatten out. See Figure 2-1.

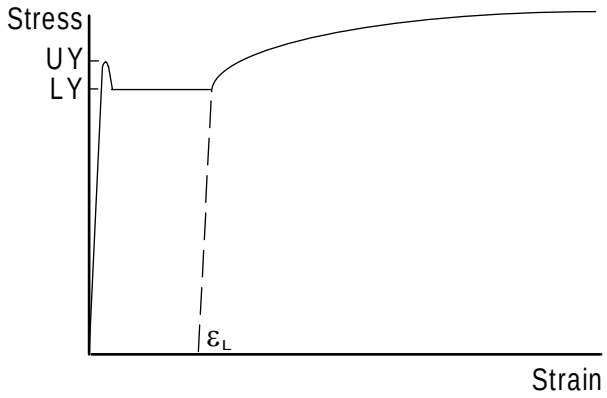

Figure 2-1: Typical stress-strain curve showing upper yield, lower yield and Luders strain, ε_L.

General references on the yield point phenomenon include Hall (1970), Meyers and Chawla (1984), Dieter (1986) and Haasen (1996). Ingwall (1970) summarized the research on yield point phenomenology. Li and Chou (1970) reviewed the various models of yielding.

2.1.1 Yield Point Theories

There are two theories which explain the yield point phenomenon: the theory of impurity locking and the theory of dislocation dynamics.

The theory of impurity locking is most often attributed to the work of Cottrell and Bilby (1949). Dislocations, which are imperfections in the crystallographic structure of the metal and which facilitate slip among blocks of the crystal, are locked by solute atoms such as carbon and nitrogen. At a load just prior to the upper yield, some dislocations become mobile at regions of stress concentrations such as at the shoulders of the test specimen. These dislocations spread across randomly distributed grains and pile-up at the grain boundaries. The upper yield occurs when the stress concentration due to the pile-up combines with the applied stress in the next grain to unlock more dislocations and that grain yields. In this way a plastic zone spreads and develops into a Luders band which propagates along the specimen.

The fundamental flow process at the start of yielding and at further propagation is the same. The often-observed yield drop represents the difference between the applied stress required to unlock the dislocations and the applied stress to move them. Loosening of dislocations in the unyielded grains is facilitated by plastic flow in the adjacent yielded grains. This allows grain boundary breakthrough to occur at a lower stress.

The theory of dislocation dynamics is based on the experiments done by Johnson and Gilman (1959). A number of researchers have advanced the theory including Hahn (1962), Butler (1962) and Hahner (1993). In cases where the

dislocations are strongly pinned, the Cottrell theory does not hold and new dislocations must be generated for yielding to occur.

As the stress, τ, on the material approaches the upper yield, the velocity, υ, of the few mobile dislocations increases according to

$$\upsilon = A\tau^m \tag{2-1}$$

where *A* and *m* are constants. As the dislocations reach very high speeds, rapid multiplication occurs. The relation between the strain rate, $\dot{\varepsilon}$, the mobile dislocation density, ρ, and the dislocation velocity, υ, is given by

$$\dot{\varepsilon} = \rho\upsilon b \tag{2-2}$$

where *b* is the Burgers vector. Assuming the strain rate is constant throughout the test, the increase in mobile dislocation density requires a lower velocity and the stress falls to the lower yield according to equation 2-1.

The premise of a constant strain rate is fundamental to this theory, though it is has been observed in these tests (Chapter 4) and many others (e.g., Gray and Sharp 1989; Johnson and Murray 1967) that the strain rate increases at the onset of yield. Also, there appears to be a contradiction in the relationship between the dislocation density and the velocity of the dislocations. If the strain rate is constant, dislocation multiplication cannot occur as the velocity increases.

The application of one of these theories to steel is not consistent in the literature. Some recent papers suggest that a combination of the two may be appropriate. Petch (1988) provides a brief synopsis of the current understanding of yield point. His explanation follows the Cottrell theory but explains the yield drop in terms of dislocation multiplication. Hahner (1993) attributes yielding to

the softening effect of rapid dislocation multiplication and has developed a model which includes this and dislocation pile-ups.

2.1.2 Strain Rate Sensitivity

A comprehensive explanation of strain rate sensitivity of yield strength could not be found in the literature. Most general references on metallurgy (Hall 1970; Dieter 1986; Meyers and Chawla 1984) provide only a mathematical expression to describe the effect of strain rate on the yield strength. A physical explanation in terms of yield point phenomena is often absent.

A number of analytical models are presented in the literature (Hahn 1962; Christian 1964; Moon and Vreeland 1967). Most of these are based on the Johnson and Gilman theory presented above and attempt to show that strain rate sensitivity and the Luders band front velocity are related to dislocation velocity characteristics. Stress is related to the velocity of the dislocations, Eq. (2-1), which is, in turn, proportional to the applied strain rate according to Eq. (2-2).

An important point to be made is that the strain rate, $\dot{\varepsilon}$, of Eq. (2-2) and, in fact, the strain rate referred to in most metallurgical discussions, is the local strain rate occurring at the front of the Luders band, not the overall strain rate measured by the extensometer. It is the latter which is reported in mechanical testing.

During yielding, nearly all plastic deformation occurs at the front of the Luders band. See Figure 2-2. Assuming all bands to be propagating within the gage length of the extensometer, the rate of deformation at the band front will be less than the rate of deformation reported by the extensometer by a factor

equaling the total number of bands. However, since the plastic deformation increases from zero to ε_L over only a few grain diameters, the local strain rate will always be many times greater than the strain rate reported by the extensometer even for a large number of bands. Figure 2-3 illustrates this for the case of a constant strain rate test. The strain gage in the diagram represents a differential length of the specimen similar to a Luders band front.

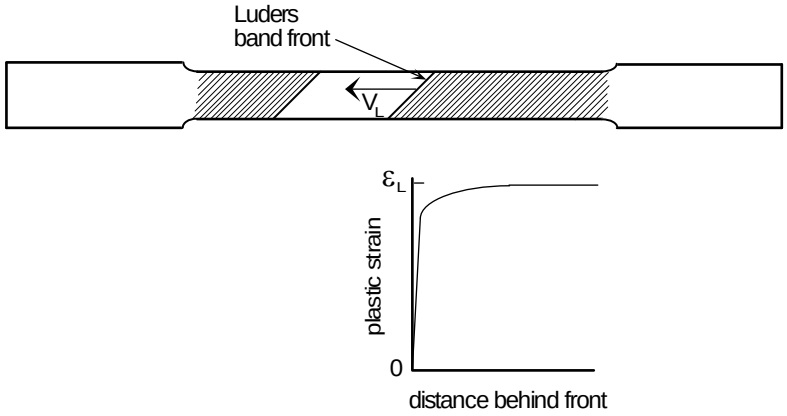

Figure 2-2: Schematic drawing of the Luders band showing the Luders band strain profile and the Luders strain, ε_L

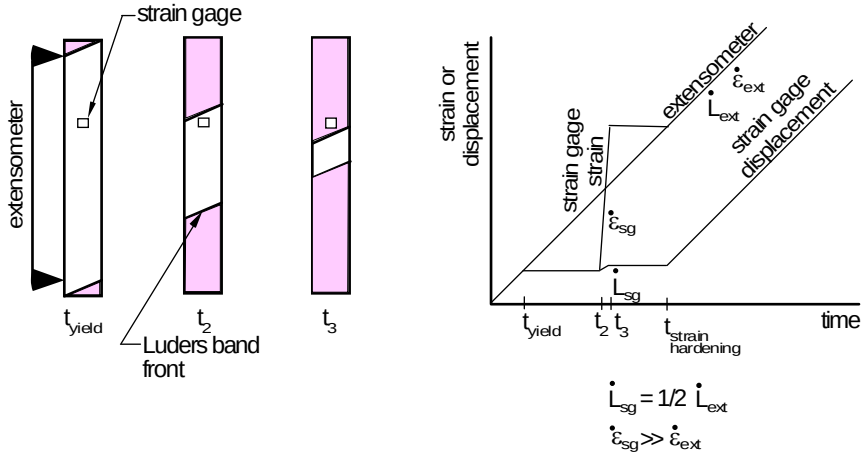

Figure 2-3: Local strain rate and local rate of deformation for a constant strain rate test.

The equation for strain rate at the Luders band front, $\dot{\varepsilon}_L$, is

$$\dot{\varepsilon}_L = \frac{V_L}{Nt} \tag{2-3}$$

where V_L is the velocity of the Luders band front, N is the number of fronts, t is the thickness of the front, in effect, the gage length.

Hutchison (1973) argues that the velocity of the Luders front, not the overall applied strain rate, is the important parameter during yield propagation. Therefor, the number of Luders bands is important. Butler (1962) reached a similar conclusion. Kraft (1962) conducted high speed tests and showed that the lower yield stress increased with the Luders front velocity.

2.2 VARIATION OF YIELD STRENGTH IN ROLLED STEEL PLATES AND SHAPES

2.2.1 Studies of Variation

A number of studies have shown that the yield strength of steel can vary between producers, within a heat and within a rolled section.

Withey (1928) reported the variation in yield point between different locations in a rolled shape to be less than the variation between different shapes. He found the weighted yield point in tension for a given shape was a good measure of the strength of that shape in compression.

Figure 2-4 shows the variation of strength in a wide flange beam included in a text by Massonet and Save (1965), though no reference is provided.

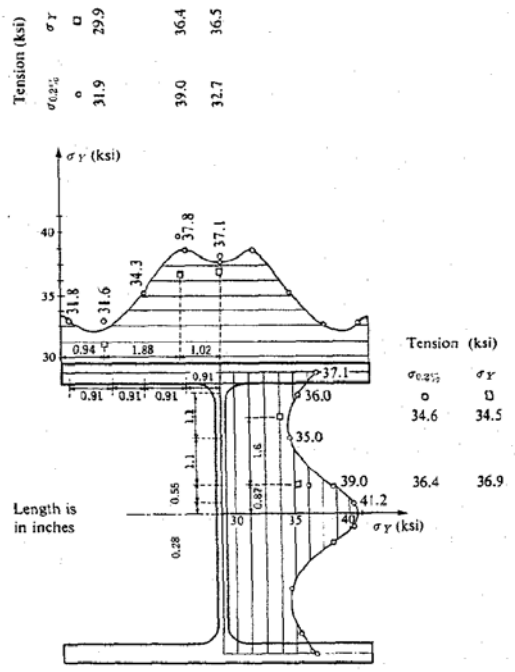

Figure 2-4: Distribution of yield strength over a wide flange shape (Massonet and Save 1965)

Tall and Alpsten (1969) report the variation of yield strength across the flange of a HE 200 B section. See Figure 2-5. The yield strength varies between 32.8 and 41.9 ksi which is equivalent to almost 30 percent. They also report that the variation for a 2" and a 3 1/2" thick steel plate was less than the H-shape. The width of the test specimen was taken in the direction of plate thickness. The

higher strengths were recorded for the outer specimens and the lower strengths were near the middle.

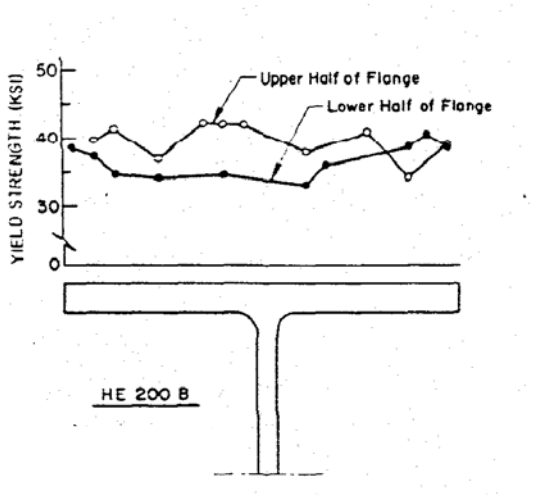

Figure 2-5: Distribution of yield strength over a wide flange shape (Tall and Alpsten 1969)

In the 1970's, the American Iron and Steel Institute sponsored a study of the variation of tensile properties in carbon steel plates and shapes ("Variation" 1974). Variation within a heat, within an ingot, within a plate and within a rolled shape were reported. The former two were determined from tests on plate material. A number of mills submitted test data from predetermined sampling

locations including one corresponding to the ASTM specifications. This was considered the reference test. The results compare the properties from all sampling locations to the reference specimen.

Selected results are shown in Table 2-1. The "difference" noted in the table is the average of all tests minus the reference test.

Table 2-1: Yield point variations in rolled plates and shapes ("Variation" 1974)

Product	Type of Variation	No. of Tests	Differences (ksi)	
			Average	Std Deviation
Plates	within heat	1828	-0.76	2.617
	within ingot	1145	-0.385	2.400
	within plate	1064	-0.016	1.938
Shapes	within flanges	715	-2.649	3.908
	within webs	718	0.152	3.588
	whole section	1433	-1.246	4.003

In addition to these results, the study reported an 86% probability that a test taken from a plate will give a value greater than 36 ksi and, in shapes, there is a 78% probability that a test at other than the official location will exhibit a yield point above 36 ksi.

A study sponsored by the Structural Shape Producers Council ("Statistical" 1994) analyzed the results from 57,930 mill certificates from six producers over a period of one year. The results showed that the average yield strength reported on the mill certificate for A36 steel was just below 50 ksi.

2.2.2 Sources of Variation

The following section is based largely on the texts by Cottrell (1967), Dieter (1986) and Callister (1994).

The yield strength and the ductility of steel are affected by the carbon content. See Figure 2-6.

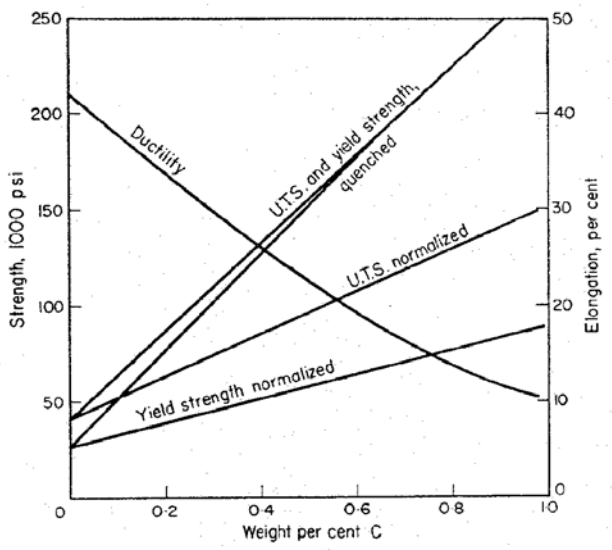

Figure 2-6: Effect of carbon on strength and ductility of plain carbon steel (Cottrell 1967)

A considerable amount of variation over the cross-section and along the length of a shape is introduced in the production process. The webs, being thinner than the flanges, require more hot working during the rolling process. The grains are broken down into finer sizes and, as a result, the strength increases according to the Hall-Petch relationship

$$\sigma_y = \sigma_o + k_y d^{-1/2} \tag{2-4}$$

In this relationship, d is the average grain diameter and σ_0 and k_y are constants for a given material. Further, the interior of the thicker flanges cool slower than that of the web resulting in greater grain growth and a subsequent reduction in strength.

Straightening of the section by plastic deformation occurs after it has cooled. This process is described alternatively as cold working or work hardening and results in an increase in strength and a decrease in ductility. Indications of this plastic deformation on the surface of the rolled shape include the yield lines seen on the flanges and the flaking of mill scale in the K-line region of the web. See Illustration 2-1.

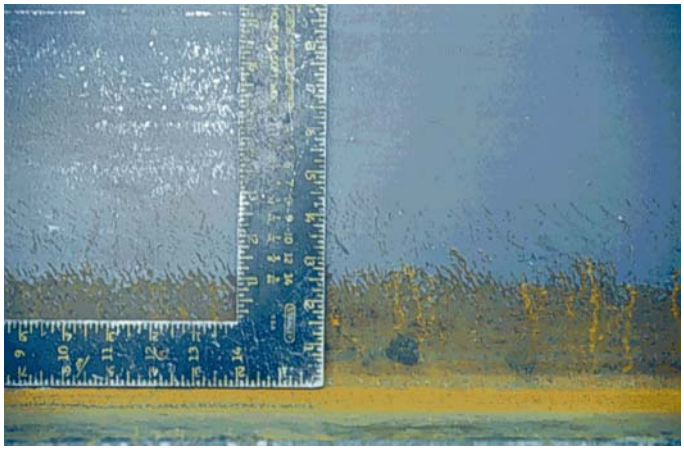

Illustration 2-1: Indication of yielding on surface of web at the K-line

If the steel is heated, the cold-worked dislocation structure becomes more unstable until the metal softens and reverts to a strain-free condition. This

process is called annealing and restores the ductility lost in the cold working process. The increase in strength from cold working is also removed. Normalizing is an annealing process in which the steel is heated up and then allowed to cool at air temperature.

The effects of cold working and annealing are shown in Figure 2-7.

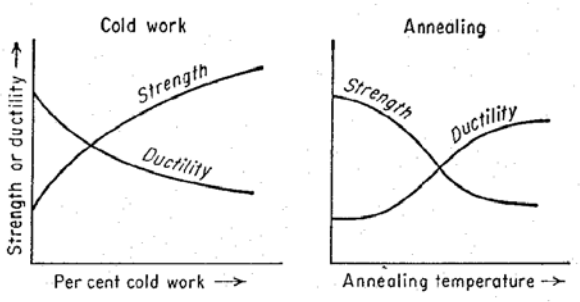

Figure 2-7: Effect of cold working and annealing (Dieter 1986)

The re-appearance of the yield point in cold worked metals is termed strain aging. This is caused by the diffusion of carbon and nitrogen atoms to the dislocations during the aging period to form new atmospheres of interstitials anchoring the dislocations. Strain aging occurs quickly if the material is heated at a relatively low temperature after unloading or is left to age at room temperature for several days.

Strain-aged steels have a lower strain rate sensitivity (Dieter 1986).

2.3 INFLUENCE OF TESTING PROCEDURES ON THE YIELD STRENGTH

2.3.1 Strain Rate

A number of investigators have demonstrated the increase in yield strength with strain rate. As a point of reference in reviewing the following figures, the strain rates measured in tests which satisfy the ASTM A370 specifications typically range from about 10^{-4} to 10^{-1} in/in/min.

Fry (1940) compared the yield point values from a number of tests conducted at different rates and using a number of different testing machines. See Figure 2-8. The strain rate was found by recording the time required for the load to increase from 1000 lbs to 7500 lbs (5 ksi to 38 ksi). He found the increase in yield point value which corresponded to a three fold increase in strain rate was of about the same order as the scatter due to material variation.

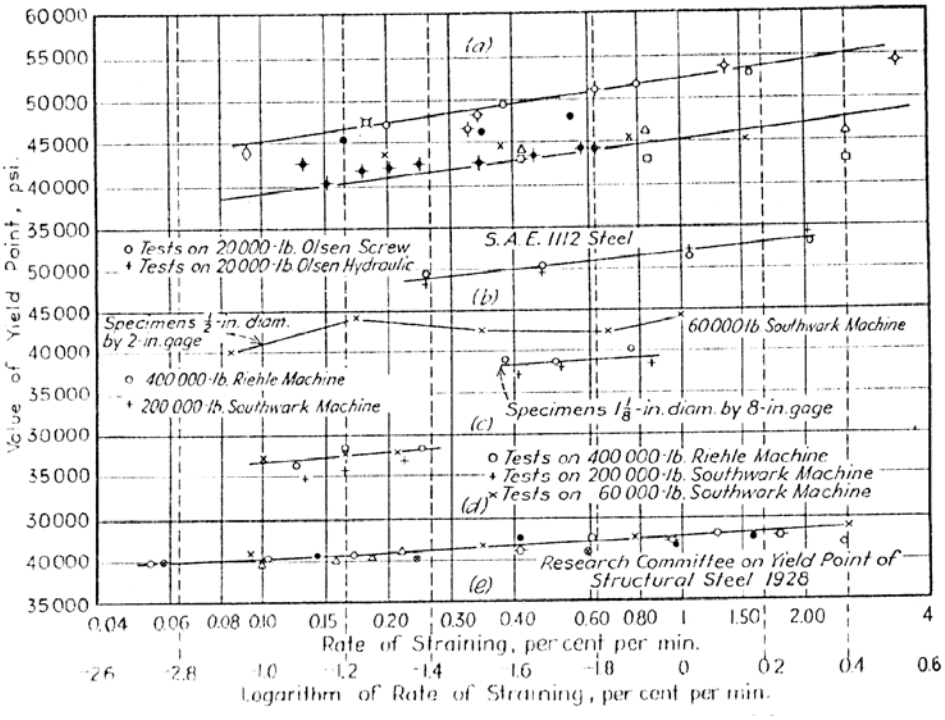

Figure 2-8: Strain rate sensitivity of yield point values (Fry 1940).

Manjoine (1944) reported the yield point and the stress at a number of different points along the stress-strain curve and plotted these against strain rate. See Figure 2-9. He does not describe how he determined the strain rate.

However, he used a mechanical machine with a constant crosshead speed and described it as a constant strain-rate machine. Since the crosshead speed will roughly equal the strain rate only during yielding (see Section 2.3.2.1), it is assumed that the reported strain rates are plastic strain rates.

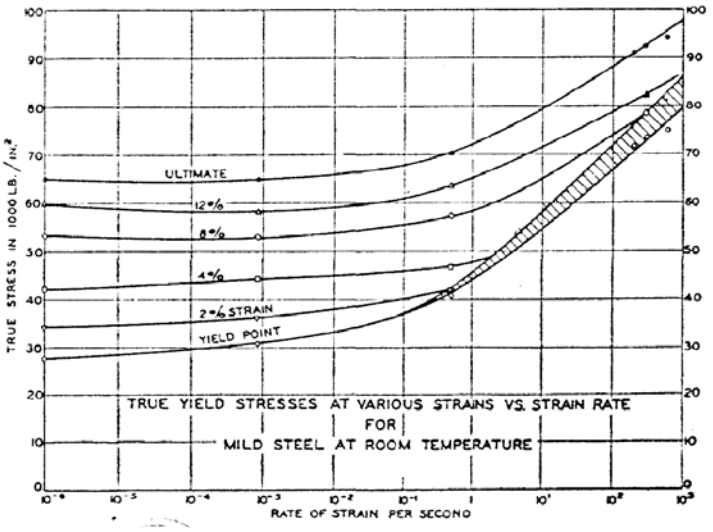

Figure 2-9: Yield stresses at various strains versus strain rate (Manjoine 1944)

Johnson and Murray (1967) found the yield strength to increase linearly with the log of strain rate. See Figure 2-10. For an increase in the strain rate of 10 times, the yield strength increased about 1.4 ksi. The strain rates were found by plotting strain with a time stamp during the test. Though it is not stated explicitly, it is assumed the reported strain rates are plastic.

Chang and Lee (1987) used a closed loop machine in extensometer control mode and found a 14% increase in the lower yield when the strain rate was increased from 10^{-5} to 10^{-3} in/in/sec. See Figure2-11. By unloading the specimen

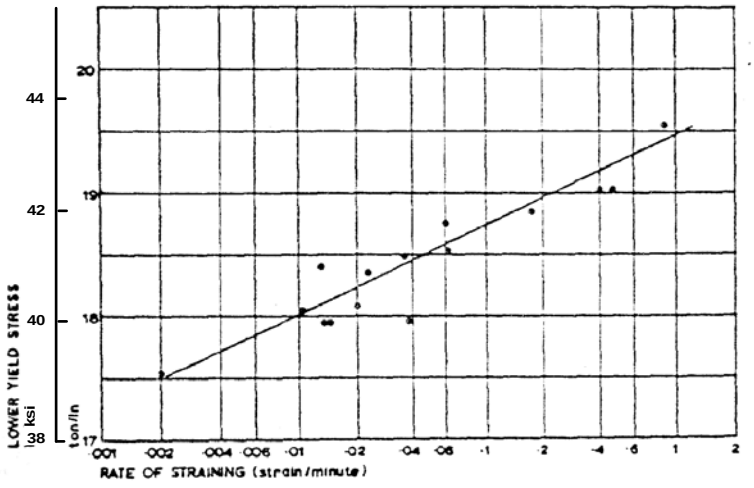

Figure 2-10: Effect of strain rate on lower yield of carbon steel (Johnson and Murray 1967).

during yielding and then reloading at a rate of 10^{-2} in/in/sec the yield strength was increased 27%.

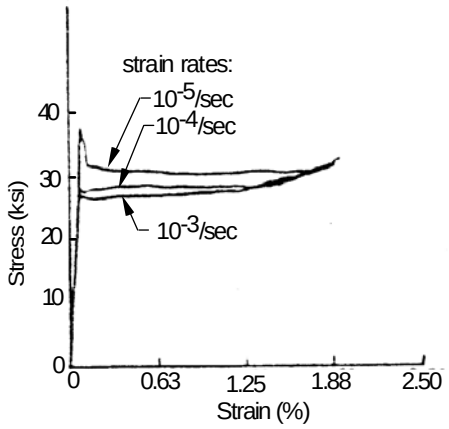

Figure 2-11: Effect of strain rate on lower yield (Chang and Lee 1987)

Gray and Sharp (1989) confirmed Johnson and Murray's conclusions regarding strain rate sensitivity. However, they found that it varied with the machine type and suggested this was a function of the number of Luders bands present during yielding. See Section 2.3.2.

2.3.2 Testing Machines

It is assumed that most production testing is conducted using open loop mechanical and/or hydraulic machines. Open loop machines feature an adjustable control mechanism which regulates the speed of the test but is not able to maintain a constant strain rate or constant loading rate throughout the test. In order to accomplish this, hydraulic machines must be equipped with a servo-control system which reads the strain or ram deformation output and feeds it back to the ram to maintain a constant strain rate or rate of deformation. These machines are called closed loop.

The machine type and mode of control can influence the determination of yield strength. In tests using open loop machines, the strain rate will vary considerably during a test. Variations in yield strength corresponding to these strain rates have been observed. The deformation characteristics of the machine and the response of the machine to changes in the specimen stiffness at yield will affect the path of the load deformation curve from the upper yield to the lower yield. Recent tests suggest that closed loop machines provide the most accurate determination of yield strength (Gray and Sharp 1989).

Control of Strain Rate The settings on most mechanical and hydraulic machines which control the speed of the test do not control the strain rate.

Mechanical machines can be run at a constant crosshead speed only when there is no specimen under load, termed the free-running crosshead speed. During a test, the restraint against crosshead movement provided by the specimen causes deformations in the machine which effectively reduce the rate of displacement in the gauge length to be less than the free-running crosshead speed. Figure 2-12, which is typical of tests conducted as part of this study, illustrates this. At the onset of yielding, the rate of deformation will increase suddenly to roughly equal the free-running crosshead speed as the specimen stiffness approaches zero. The loading train is free to move, albeit in the deformed position, as if no specimen were under load. At the onset of strain hardening, the specimen regains some stiffness and the deformation of the machine is resumed.

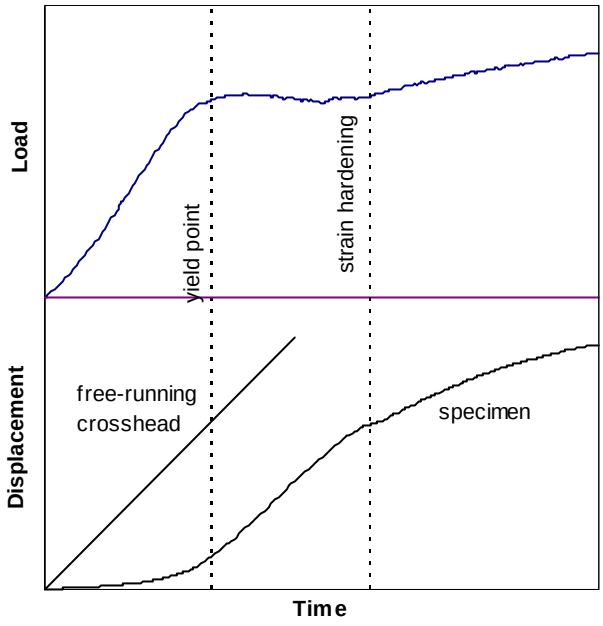

Figure 2-12: Load-time curve and corresponding displacement-time curve for specimen and free-running crosshead displacement

A note regarding Figure 2-12: the rate of separation of the crossheads during a test is not the same as the rate of specimen displacement measured by the extensometer since slip is occurring in the grips (Guiu and Pratt 1964; Hockett and Gillis 1971).

Fry (1940) observed that only a small fraction of the crosshead travel appears as strain in the specimen and suggested the need to characterize machines by a mechanical modulus. Rao et al. (1964) recognized the effect of machine stiffness on strain rate and proposed the use of a static yield test to eliminate its influence (See Section 2.4.1). Hamstad and Gillis (1966) and Lessells and Barr (1965) provided a physical and an analytical description of effective strain rates in constant crosshead speed tests. Johnson and Murray (1967) estimated the variation in tests conducted in accordance with British and ISO testing specifications due to machine hardness. They considered hardness ratios ranging from 20 to 400 and elastic strain rates ranging from roughly 10^{-4} /min to 10^{-3} /min and predicted the maximum variation for all cases to be 2.69 ksi.

The ratio of plastic strain rate, $\dot{\varepsilon}_{pl}$, to elastic strain rate, $\dot{\varepsilon}_{el}$, for a given test is termed the hardness ratio, *H*.

$$H = \frac{\dot{\varepsilon}_{pl}}{\dot{\varepsilon}_{el}} \tag{2-5}$$

The hardness ratio is a function of the machine stiffness and the size of the specimen being tested

$$H = 1 + \left(\frac{EA}{KL_o} \right) \tag{2-6}$$

where E, A and L_o are the Young's modulus, the cross sectional area and the original gauge length of the specimen and K is the testing machine stiffness. The hardness ratio will always be greater than 1.0. Only for a perfectly rigid machine or a specimen with zero stiffness ($E = 0$) would the ratio equal 1.0. The relationship above has been used to quantify the stiffness of testing machines. Some values cited in the literature are listed in Table 2-2. The stiffness of three typical test specimens are also shown for comparison. The specimen stiffness can be many times that of the machine.

Table 2-2: Machine and specimen stiffnesses

Machine	K (kip/in)	Specimen	K (kip/in)
Hamstad and Gillis (1966)			
nr	41.5	0.505" diameter round	2600
nr	26	0.25" x 1.5" plate	1200
nr	100	0.625" x 1.5" plate	3000
nr	77.9 to 166.5		
Hockett and Gillis (1971)			
10 kip Instron	414		
nr: not reported			

This relationship seems counter-intuitive when one considers the size of most test machine components relative to the specimen. A more plausible explanation for the observed effect of machine deformations comes from Hockett and Gillis (1971). Their test results showed machine stiffness to be highly nonlinear, varying not only from test to test but also throughout a given test. They concluded that elastic deformations of the elements in the loading train (crossheads, lead screws, etc.) contribute only a small amount to the machine

deflection. Instead, they attributed the major portion of machine deformations to non-elastic elements such as slip in the grips or platens, deformation of the load cell and insulation, the taking up of bearing clearances and the extrusion of lubricant. An example of the significance of these elements is provided by Gray and McCombe (1992) who found that a machine's hardness increased from 10 to 25 when the grips were changed from screw type to wedge. Apparently, the stiffness of the machine is only partly related to its loading capacity.

Meyers and Chawla (1984) disagree with Hockett and Gillis and cite a number of studies which maintain that machine stiffness is linear.

Gray and Sharp (1989) have reported hardness ratios ranging from 12 to 84 for hydraulic machines and from 4 to 15 for mechanical machines. Lessells and Barr (1965) report a hardness ratio of 20 for the mechanical machine used in their tests and quote Krisch and Schweitzer as having found hardness ratios as high as 300 for hydraulic machines. In general, mechanical machines are stiffer than hydraulic machines which leads to higher hardness ratios for the latter.

ASTM regulates the speed of the test in the elastic range only. Plastic strain rates much greater than the specified elastic strain are likely to occur. The European Standard ("Tensile" 1990) specifies a maximum plastic strain rate. See Section 2.7. Recognizing that most test machines cannot be set to control the plastic strain rate, the European standards have required that a machine's hardness, termed compliance, be determined experimentally. This value is used to determine the required elastic strain rate to achieve the desired plastic strain rate. However, Gray and Sharp suggest that the compliance calibration procedure

"is more honored in the breach than in observance" and report that the procedure may be removed from the standards.

Influence of Machine Stiffness on Yield Drop The path of the load deformation curve from the upper yield to the lower yield will depend on the type of machine. See Figure 2-13. In the case of the mechanical machine, the upper yield is typically followed by an immediate drop in load to the lower yield (curve AB). The hydraulic machine will report a more gradual drop and, according to some authors (Lessells and Barr 1965; Hall 1970; Meyers and Chawla 1984), may in some extreme cases not reach the lower yield (curve AE). This may lead to erroneous results when reporting the 0.5% total elongation or the 0.2% offset yield strengths.

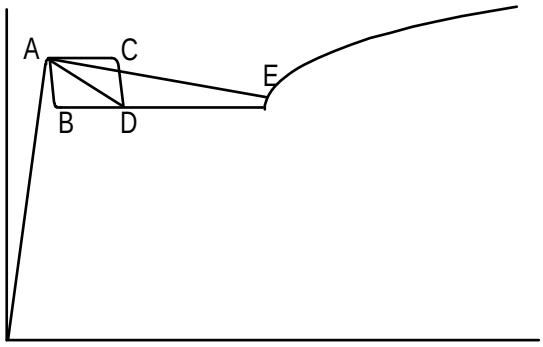

Figure 2-13: Effect of machine stiffness on stress-strain curve adapted from Lessells and Barr (1965)

Recalling that the test machine components deform under the load of a test, the machine can therefore be modeled as a spring with a characteristic stiffness. At yield, the load required to propagate yielding is less than the load to initiate yielding and so the load will drop. The spring, i.e., the machine, will

contract to reach equilibrium with the load in the specimen. For a stiff spring, this contraction will be a small amount equal to the deformation occurring between A and B in Figure 2-13. For a very soft machine, this contraction will be larger and could be greater than the yield point elongation of the specimen. In this case, the machine will reach equilibrium with the specimen at some point in the strain hardening range (curve AE).

Davis (1938) references the work of Siebel and Schwaigerer who demonstrated this hypothesis. By fitting springs around specimens to modify the machines compliance, they were able to convert a hard machine to a very soft machine and no yield drop was observed. Tanaka and Ishikawa (1976) conducted similar experiments and reported stress-strain curves, shown in Figure 2-14, which confirm the influence of machine stiffness, K_m, on the yield drop.

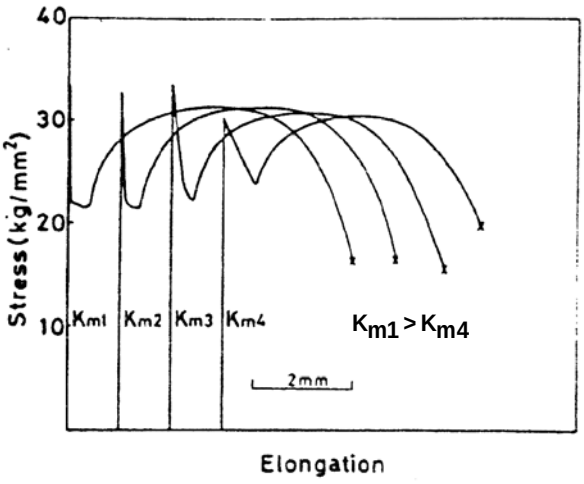

Figure 2-14: Stress-elongation curves obtained by four testing systems of different stiffnesses (Tanaka and Ishikawa 1976)

Aside from carefully controlled experiments such as these, there does not appear to be much evidence in the literature to support the notion that the common testing machine is soft enough to report a yield drop similar to curve AE in Figure 2-13. Instead, the more common curve, and the one cited by Lessells and Barr as being typical of their results, is that of ACD. Due to the softness of the machine, the load will not reach equilibrium with the specimen until the machine has contracted an amount equal to that occurring between A and D. The upper plateau, curve AC, is caused by the load measuring device which has a longer response time and thus will hold the load (Lessells and Barr 1965).

Open Loop vs. Closed Loop Machines Programming an initial strain rate and maintaining it throughout the test is possible only with a closed-loop system. Closed-loop systems with extensometer control read the strain and adjust the hydraulic pressure acting on the ram to maintain the specified strain rate. These machines can also be operated in displacement control. Since the ram displacement transducer measures the sum of the specimen strain and the deformation occurring in the grips and the load train, the strain rate will vary during deformation controlled tests.

Gray and Sharp (1989) conducted a number of tests to compare open loop and closed loop machines. They found the scatter band in the lower yield strength to be narrowest for the extensometer controlled tests, +/- 1.7 ksi, versus +/-3.0 ksi for the open loop machines. They also found that the extensometer controlled tests (i.e., closed loop) reported lower yield strengths than the open loop machines and that the strain rate sensitivity was less. See Figure 2-15.

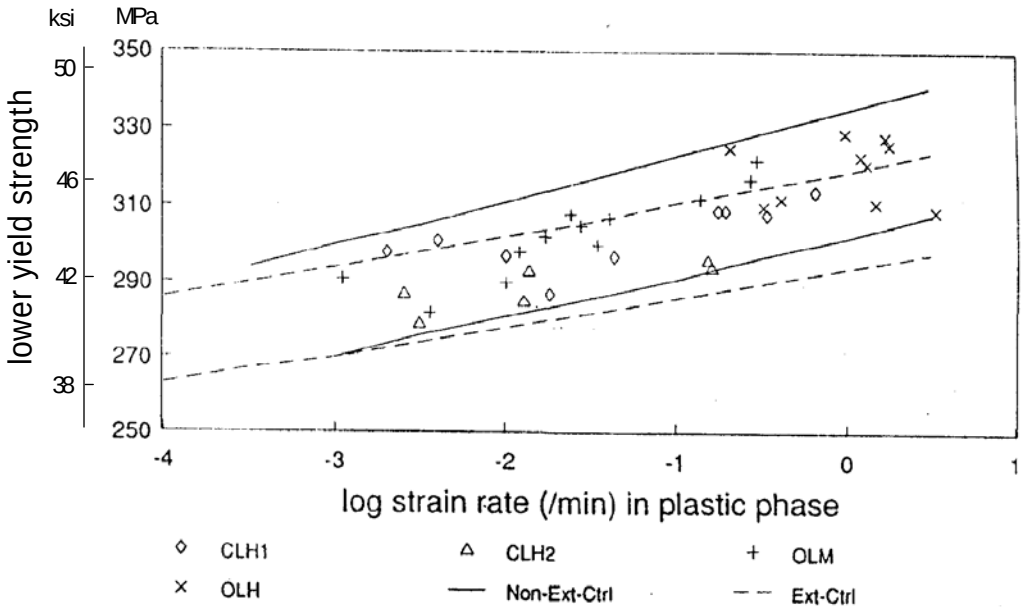

Figure 2-15: Lower yield strengths reported by open loop (OLH and OLM) vs. closed loop (CLH1 and CLH2) machines (Gray and Sharp 1989)

By plotting lower yield strength versus the measured plastic strain rate for all tests, they eliminated the variable of hardness ratio and still found greater scatter and higher yield strengths for the open loop machines. They concluded that when the specimen begins to yield, the strain rate control of the closed loop machine allows a greater portion of the specimen to start yielding. With more Luders bands forming, the strain rate at the front of each band will be less and the lower yield strength will be less as a result.

The scatter band shown in Figure 2-15 represents variations in the material tested. Gray and Sharp conclude that it would be unreasonable to expect much less scatter than that given by the extensometer controlled tests.

2.4 STATIC YIELD TEST

2.4.1 Background

Research conducted in the late 1950's at Lehigh University suggested the use of a static yield test as a reliable indicator of the yield strength of steel. The test involves stopping the machine during yielding of the specimen and recording the load after three minutes. Tall and Ketter (1958) reference the unpublished work of Marshman[1] whose tests showed that the load always fell to the same value. They cite a number of observations in support of the validity of the static yield test: that the strain increases as the load drops, jogging of the machine while in the static yield position does not change the value, and no strain reversal is detected. They conducted a number of stub column and coupon tests, determining the static yield for both, and found very close correlation in the results. In testing 24 tension coupons from the flange and web each and 24 stub columns, they found the average ratio of stub column yield strength to weighted coupon strength to be 99.5%. Though it is not explicitly stated, it is assumed that the coupons came from the same rolled section as the stub column specimens.

Rao et al (1964) proposed using static yield to eliminate the effect of increasing strain rate at yield and proposed a method to predict the static yield stress from a standard coupon test.

Chang and Lee (1987) used a closed loop machine and found the static yield to be influenced by the strain rate history.

---

[1] "The Influence of Plastic Strain Rate on the Yield Strength of Mild Steel," Lehigh University, June 1956.

2.4.2 Related Research

No research related to the static yield test was found in the metallurgical and mechanical engineering literature. The term and the test seem to be restricted to structural engineering literature. A description of the static yield in metallurgical terms is difficult to attempt since the models for the yielding of mild steel are not entirely agreed upon nor is there a well-accepted physical explanation for the change in yield strength with strain rate.

The area of research most closely related to the static yield test is stress relaxation. These tests involve stopping the machine and recording the load after a length of time which can vary considerably. Some important findings in this research are applicable to an examination of the validity of the static yield test.

It has long been recognized that relaxation of the machine affects the results of stress relaxation tests. Guiu and Pratt (1964) found that machine relaxation increases with the applied load and with the speed of the crossheads. In their tests, almost all relaxation occurred in the first 3 to 6 seconds after the machine had been stopped. Meyers et al. (1979) found that a considerable amount of relaxation was concentrated at the grips. Another source is the oil layers between the screws. As the oil is driven out of the region by the load, the machine relaxes. Gillis (1997) described a “dry test” in which all of the lubricant is flushed out on an Instron screw driven machine and the stiffness is increased enormously. Unfortunately, none of the literature which was reviewed provides any data regarding the magnitude of the load drop.

The length of the static yield test, three minutes, exceeds the time for stress relaxation tests reported by Meguid and Malvern (1982). They used a

closed-loop hydraulic machine with extensometer control and measured the relaxation of mild steel after 60 seconds. This suggests that stress relaxation may influence the results of the static yield test.

2.5 ASTM SPECIFICATIONS REGARDING THE YIELD STRENGTH OF STEEL

2.5.1 Specimen Sampling and Geometry

Table 2-3 summarizes the requirements for specimen sampling and specimen geometry in the ASTM *Standards*. The sampling location is reportedly in the process of being changed from the web to the flange (Frank 1997).

Table 2-3: ASTM requirements for specimen sampling and geometry

Parameter	Requirement	Standard & Section
Location in Section	from web	A6 11.3.2
Longitudinal Axis	parallel to rolling direction	A6 11.2
Shape & Dimensions	t < 3/4" 1 1/2" or 1/2" wide flat plate w/ 8" gage length	A6 11.5.2.1
	t < 4" 1 1/2" wide flat plate w/ 8" gage length	A370 Fig 3
	t > 3/4" 0.50" diameter round w/ 2" gage length	A6 11.5.2.3 A370 Fig 4

2.5.2 Speed of Test

Table 2-4 summarizes the specifications governing the speed of the test. The *Standards* specify two different measures of rate to account for different types of machines and modes of control. The first applies to the case of mechanical machines with crosshead speed control. The second, the rate of stressing, applies to machines equipped with a device to indicate the rate of

loading. When no device exists, the rate of loading must be determined experimentally. Presumably this measure of rate applies only to the case of hydraulic machines.

Table 2-4: ASTM specifications governing the speed of the test

Measure	Stage of Loading	Maximum Rate	Minimum Rate	Standard & Section
Mechanical Machines				
free-running crosshead speed	zero to 0.5 Fy 0.5 Fy thru yield determination strain hardening to fracture	any rate 1/16 in/min[a] 1/2 in/min[a]	any rate 1/160 in/min[a] 1/20 in/min[a]	A370 11.4.1
rate of separation of the crossheads	zero to 0.5 Fy 0.5 Fy thru yield determination strain hardening to fracture	any rate 1/16 in/min[a] 1/2 in/min[a]	any rate 1/160 in/min[a] 1/20 in/min[a]	A370 11.4.2
Hydraulic Machines				
rate of stress	zero to 0.5 Fy 0.5 Fy thru yield determination strain hardening to fracture	any rate 100 ksi/min not specified	any rate 10 ksi/min not specified	A370 11.4.3
General				
rate of strain	elastic elastic	0.0625 in/in/min 0.0033 in/in/min	0.00625 in/in/min 0.00033 in/in/min	from 11.4.2 from 11.4.3

[a] per inch of reduced section

Maximum and minimum rates are specified for the stage of the test between 0.5 Fy and the determination of yield point or yield strength. After this the *Standards* permit an increase in the crosshead speed for the remainder of the test but do not provide criteria for machines without crosshead speed control. Presumably, the rate of hydraulic machines are increased to some rate roughly equivalent to the crosshead speed specifications.

In the case of mechanical machines, the *Standards* provide two options for crosshead speed control. The free-running crosshead speed, i.e., the dial, can be set within the limits shown in Table 2-4 or it can be adjusted so that the actual

rate of separation of the crossheads falls with these limits. As an example, a specimen with an 8” gage length and a 9” reduced section can be tested with a maximum free-running crosshead speed set at 0.563 in/min for the stage of the test between 0.5Fy and the determination of yield point or yield strength. For a machine with a hardness ratio of 4, the actual rate of separation of the crossheads will be around 0.14 in/min. Alternatively, the free-running crosshead speed, i.e., the dial, can be adjusted so that the actual rate of separation of the crossheads equals 0.563 in/min. For the same machine, the free-running crosshead speed would equal about 2.25 in/min. The plastic strain rate will correspond to this higher crosshead speed.

The *Standards* do not specify strain rates explicitly but the rate of stressing and the rate of separation of the crossheads imply maximum elastic strain rates of 0.0033 in/in/min and 0.0625 in/in/min, respectively. There is no provision which states that either should control. Strain rates during plastic yielding are not addressed.

2.5.3 Yield Strength Determination

There are a number of methods for determining the yield point and the yield strength which the *Standards* recognize for the purpose of characterizing the strength of the steel. These are listed in Table 2-5. In the case of A36 steel, the *Standards* specify that the minimum yield *point* for the material shall be 36 ksi (ASTM A36 8.3) and that the yield *strength* may be substituted for the yield point (ASTM A6 11.7.2). Since the “top of the knee on the stress-strain curve” is defined as one measure of the yield point, the use of the upper yield peak to

represent the strength of the material is permitted. Selection of one of the other methods such as the 0.5% total elongation could report a different value of yield strength.

Table 2-5: ASTM methods for determining the yield strength of steel

Yield Definition	Methods of Determination	Standard & Section
Yield Point	Drop of the beam or Halt the Pointer Method	A370 13.1.1
	Autographic Diagram Method	A370 13.1.2
	(top of the knee on the stress-strain diagram)	
	Total Extension Under Load Method	A370 13.1.3
	Extension=0.005 in/in of gage length	
Yield Strength	Offset Method	A370 13.2.1
	Offset = 0.002 in/in of gage length	A6 11.7.3
	Extension Under Load Method	A370 13.2.2
	Extension=0.005 in/in of gage length	A6 11.7.3

The “drop of the beam” method refers to older machines which employed a balance arm and poise to indicate load. It is unlikely that this type of machine is still used in production testing. Davis et al. (1941) describe some of the older testing machines and procedures.

2.5.4 Acceptable Variation

The *Standards* recognize some variation in the tensile properties of material within a heat and within a section. In Appendix A2 of ASTM A6, the *Standards* reference the study sponsored by AISI (see Section 2.2.1) and its conclusions of one standard deviation equals approximately 8% of the required yield strength. The *Standards* advise engineers to “use sound engineering judgment when using tension test results shown on the mill test reports.”

2.6 THE YIELD STRENGTH IN STRUCTURAL DESIGN

2.6.1 Tension Test vs. Structural Behavior

The relationship between the results of the tension test and the behavior of a structural member has been treated by a number of authors. Leblois and Massonet (1972) reviewed the various models dating back to 1913 which relate the upper and lower yield of the tension test to the flexural behavior of a cross section. They conducted a number of careful tests on small specimens in pure bending to demonstrate that the maximum elastic moment could exceed that predicted by the classical theory by about 50 per cent. They recognize, however, that in actual structures, residual stresses, surface defects, small eccentricities in loading and other factors obviate the results of their tests.

Tall and Ketter (1958), mentioned in Section 2.4.1, found very close correlation between stub column tests and tension tests when the static yield is employed for both.

Alpsten (1970) studied the theoretical interaction between yielding properties and residual stresses in a section to compare the significance of the upper and lower yield. By assuming a residual stress distribution, zero strain hardening and plane sections remain plane, he developed force-deformation curves for sections in pure tension and compression and moment-curvature curves for sections in weak axis bending. Despite an upper yield which was assumed to be 20% greater than the lower yield, the capacity of the section was only slightly increased by the considering the upper yield in the analysis.

2.6.2 Allowance for Yield Strength Variation in the *LRFD Specification*

Strength reduction factors in the *LRFD Specification* (*Load* 1993) account for the variation in yield strength. Galambos and Ravindra (1978) summarize the development of these factors and other material properties to be used as a basis for the Specifications. The strength reduction factors are determined by

$$\Phi = \frac{R_m}{R_n} \exp(-\alpha\beta V_R) \tag{2-7}$$

in which R_m = mean resistance, computed with mean material and cross sectional properties; R_n = the nominal resistance, determined for specified material properties and handbook sectional properties; α and β are respectively, linearizing and reliability factors; and V_R = the coefficient of variation of the resistance

$$V_R = \sqrt{V_M^2 + V_F^2 + V_P^2} \tag{2-8}$$

In this equation, *M* refers to the variability of the material properties, while *F* and *P* are due to uncertainties of the "fabrication' process and of "professional" assumptions.

The coefficient of variation for yield stress in the flanges and the web were chosen to be 0.10 and 0.11, respectively, and the mean values of strength are 1.05Fy and 1.10Fy for 36 ksi steel. Each of these values was arrived at after an analysis of selected, published data and, eventually, by a certain amount of judgment.

The test data for the yield strength came from three sources. (It appears that there may be an error in the paper. Tests on plate steel in the United Kingdom are listed as one of the three sources of data while the text indicates otherwise. A review of subsequent issues of the *Journal* did not find an errata.)

The great majority of the roughly 7300 samples were from the web. Thus only a few samples were used to arrive at the properties of the flanges. The mean yield stress from each set of data was then scaled down to the static yield value using the equations proposed by Rao et al (1964).

The coefficients of variation appear to be based wholly on interpretation of the data from the three sources.

2.7 FOREIGN CODES AND STANDARDS

The foreign standards reviewed in this section are listed in Table 2-6. Most of the countries of Western Europe are members of the European Committee for Standardization. These standards have replaced those of the individual countries. The status of adoption of ISO 6892 is not clear, though the provisions of ISO 6892 - 1984 are nearly identical both in format and in content to EN 10 002-1.

Table 2-6: Foreign standards.

Organization and Standard	Edition
National Standards of Canada	
CAN/CSA-G40.20-M92	
General Requirements for Rolled or Welded Structural Quality Steel	Jan-92
European Standard	
EN 10 002-1 : 1990	
Tensile Testing of Metallic Materials, Part 1. Method of test at ambient temperature	Mar-90
International Standards Organization	
ISO 6892-1984	
Metallic Materials - Tensile Testing	1984

The rates of testing specified by these standards are summarized in Table 2-7. The rates specified in ISO 6892 are the same as EN 10 002-1. The Canadian specification for the rate of separation of the crossheads during elastic loading, assumed to be the actual rate of separation, is less than the equivalent ASTM specification by a factor of 26 times. The elastic rate of stressing in the European Standard is more than twice as high as that prescribed by ASTM. While ASTM does not specify plastic strain rates, the limit in the European Standard is about the same as the highest plastic strain rates measured in tests which satisfy the ASTM specifications (see Chapter 4).

Table 2-7: Testing speeds in foreign standards

Measure	Stage of Loading	Maximum Rate	Minimum Rate	Section
National Standards of Canada CAN/CSA-G40.20-M92				
rate of	zero to 0.5 Fy	any rate	any rate	8.2.1
separation of the	0.5 Fy thru yield determination	0.0024 in/min[a]	0.0006 in/min[a]	8.2.2
crossheads	strain hardening to fracture	0.0197 in/min[a]	0.0197 in/min[a]	8.2.3
European Standard EN 10 002-1 : 1990				
rate of stress	zero thru yield determination	261 ksi/min	52 ksi/min	10.1.2.1[b]
rate of strain	zero thru yield determination	0.009 in/in/min	0.0018 in/in/min	from 10.1.2.1
rate of strain	during yield	0.15 in/in/min	0.015 in/in/min	10.1.2.2[c]

[a] per inch of L_o

[b] for determining the upper yield

[c] for determining the lower yield

The standards which were reviewed did not state that the material must satisfy a minimum upper yield or lower yield. This requirement is probably located in the material specifications. However, both upper and lower yield are defined in the European Standard. The lower yield is defined as the lowest value during

yielding. The 0.5% total elongation and the 0.2% offset seem reserved for materials without a yield point, i.e., without an elastic-plastic transition.

Chapter 3: Description of Test Program

A test program was developed to investigate the influence of testing variables on the determination of yield strength. The primary objective of the program was to quantify the variation in results from tests which satisfy the ASTM *Standards* and compare this to the observed discrepancy between mill certificates and independent tests (see Chapter 1).

The program included two parallel studies. In the first, specimens were obtained from a plate and tested in four machines at a number of different speeds. In the second, a length of web material from a wide flange beam was cut into specimens and tested as part of a "Round Robin" sponsored by the American Institute of Steel Construction[2] . These tests compared two machines and a wider range of testing speeds than the plate tests.

A secondary objective was to investigate the validity of the static yield test. The results of the static yield tests were compared and a number of machine relaxation tests were conducted.

3.1 TEST SPECIMENS

Forty five test coupons and sixteen practice coupons were cut from a single 4'-0" x 8'-0" x 1/4" thick plate of A36 steel. See Figure 3-1. A 3'-0" x 6'-6" plate was ordered for the test specimens. The steel supplier included the

[2] To be published in 1997.

“drops” from the remainder of the 4’-0” x 8’-0” plate. The larger of these was used to make the practice specimens.

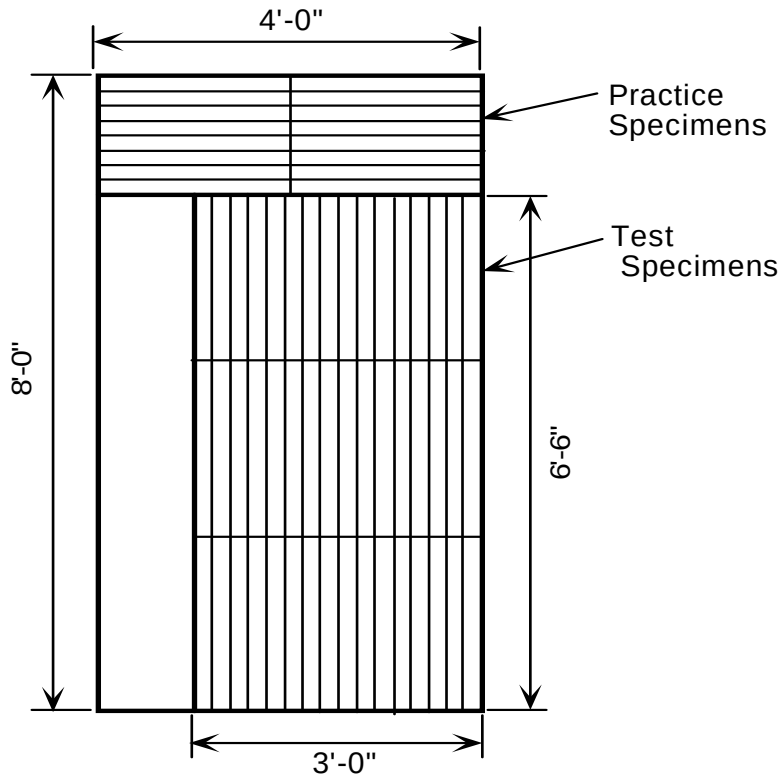

Figure 3-1: Plate and specimen layout

The plates were sheared to 2 1/4” wide by approximately 24” long pieces by a local fabricator.

A second set of test specimens were torch-cut from the web of a W36x150, A36 steel. See Figure 3-2.

No mill certificates was obtained for either the plate or the web material.

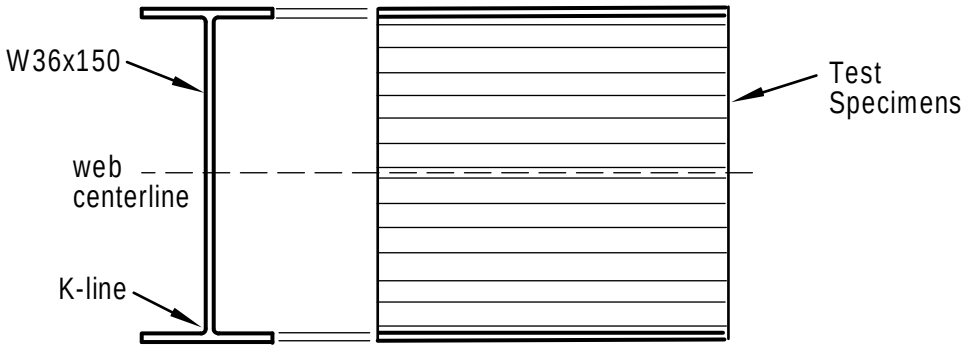

Figure 3-2: W36x150 specimen layout

All specimens were machined to the dimensions and tolerances specified in ASTM ("Standard" 1994). Burs along the machined edge were filed off to improve the accuracy of cross section measurements. Areas of each specimen are listed in Tables 4-3 and 4-7.

3.2 TEST MACHINES

Four different test machines with different modes of control were used in the study.

1) Tinius Olsen 120,000 pound capacity screw-driven machine. See Illustration 3-1. The specimen is held in the crossheads by manually-tightened wedge grips. The rate of deformation is controlled by dialing-in a crosshead speed. This speed is the rate of separation of the crossheads when no specimen is under load. The load is measured by a system of levers supported on knife edges. As the load is applied, the displacement

of the levers is measured by a displacement transducer. This signal is sent to a dial with a leading pointer to indicate peak loads.

2) Satek 600,000 pound capacity hydraulic machine. See Illustration 3-2. The specimen is held in the crossheads by hydraulically-controlled wedge grips. The speed of the test is controlled by two dials which regulate the flow of oil to and from the hydraulic ram for loading and unloading the specimen, respectively. The load is measured by two electronic load cells which are located in the fixed crosshead. The dial indicator is broken. The load is reported by a digital read-out.

3) Southwark-Emery 60,000 pound hydraulic machine. See Illustration 3-3. The specimen is held by manually-tightened wedge grips. The speed of the test is controlled in the same way as the Satek. The load is measured by an arrangement of springs, an air supply and an air bellows called a modified Bourdon tube. Davis et al. (1941) describe the operation of this system. The load is reported by a dial with a leading pointer to indicate peak loads.

4) Riehle 600,000 pound capacity screw-driven machine. See Illustration 3-4. The wedge grips were broken so the specimen was held by a clevis and pin arrangement. The clevis was manufactured by MTS. The pin was a 1/2" diameter high strength bolt with the threads excluded from the bearing surface. The ends of the specimen were reinforced with 1/4"

plates welded to both sides. See Illustration 3-5. The rate of deformation is controlled in

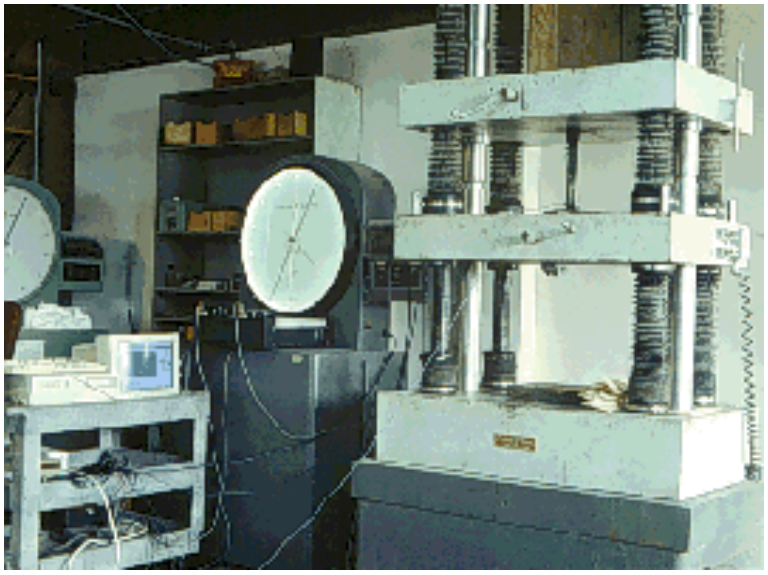

Illustration 3-1: Tinius-Olsen testing machine with data acquisition system

Illustration 3-2: Satek testing machine

Illustration 3-3: Southwark-Emery testing machine with data acquisition system

Illustration 3-4: Riehle testing machine.

the same way as the Tinius-Olsen. The load is measured by four electronic load cells which are located in the moving crosshead. The dial indicator is broken. The load is reported by a digital read-out.

Illustration 3-5: Gripping arrangement for Riehle testing machine

3.3 INSTRUMENTATION AND DATA ACQUISITION

The data acquisition system for each test consisted of an extensometer, an uniterruptible power supply (UPS), a data plotter, a signal conditioner and a computer. See Figure 3-3. In two cases, the machines were modified to report load in terms of voltage.

3.3.1 Power Supply and Grounding

In order to reduce the amount of noise in the output, all components except the load cell were powered through a UPS (American Power Conversion Back-UPS 280) which was itself plugged into the outlet located on the side of the test machine in use. This created a common floating ground.

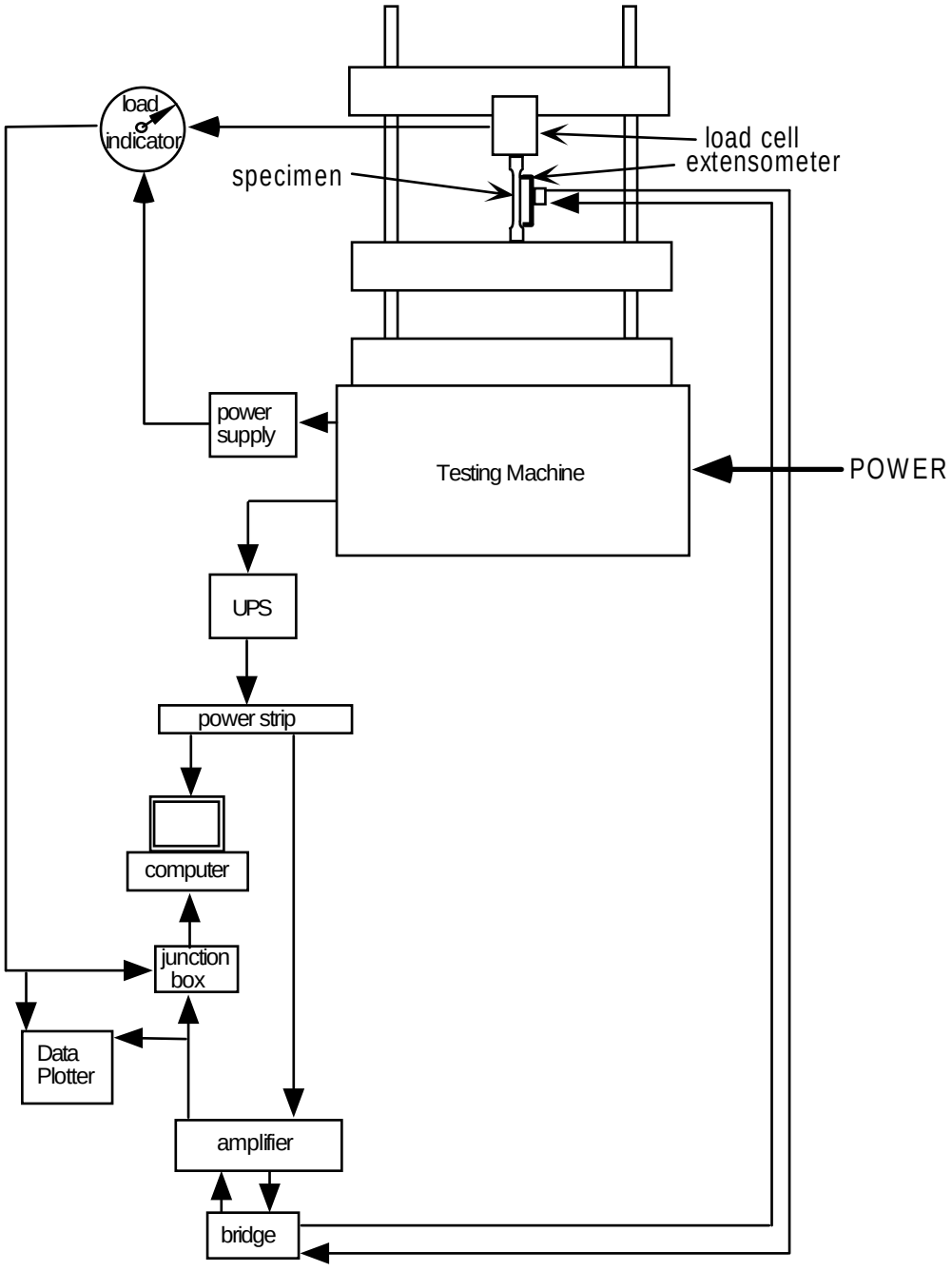

Figure 3-3: Data acquisition block diagram

3.3.2 Extensometer

Strain was measured using an Epsilon 3542 SP extensometer with an 8” gage length and a 2” extension. This type of extensometer uses a strain gauged sensor element and is powered by DC voltage. The fixed error of strain is less than 0.0001 and thus the extensometer is classified as B-1 in ASTM (“Standard” 1996).

A strain gage signal conditioner (Measurements Group, Inc. Strain Gage Conditioning Amplifier 2310) served as the power supply and the output amplifier for the extensometer. Excitation was set at 10 volts. The output signal was amplified 500 times so that the output would be in volts rather than millivolts.

3.3.3 Electronic Modifications to Load Indicating Systems

In the case of the Satek and the Riehle test machines, the computer recorded the amplified voltage reported by the electronic load cells. The Tinius-Olsen and Southwark-Emery machines had been modified so that the load measuring system would report an electronic output. Both machines were fitted with a power supply. In the case of the Southwark-Emery, an LVDT was placed in series with the springs to convert spring displacement to voltage. In the case of the Tinius-Olsen, a potentiometer was placed in series with the dial gears to convert the rotation of the dial to a voltage output.

3.3.4 Lab View

The amplified signal from the extensometer and the signal from each load cell were recorded using a PC equipped with a National Instruments Lab View-

based program. Two programs were used during the test program. Most tests were recorded using MDE2 which is designed to read voltage (scans) at time intervals specified by the user. The total number of scans is also specified by the user. These settings varied with the speed of the test and were chosen to achieve the best resolution while avoiding data files which were too large to analyze. Later tests used KHF2 which records voltage only as it changes. The change in voltage to trigger a reading is specified by the user. This program is able to plot the stress-strain curve in real-time and resulted in much smaller data files.

3.3.5 Data Plotter

Prior to the development of KHF2, the data plotter was necessary to observe the stress-strain curve during the test. The data plotter also shows better resolution than the Lab View at small strains. See Section 4.4.2.

3.4 TEST VARIABLES

The primary test variables in this study were machine type and the speed of the test. See Table 3-1 for plate specimens and Table 3-2 for W36x150 specimens. The four different machines and control modes are described in Section 3.2.

For the plate specimens, three rates were chosen for each machine: the rate corresponding to the maximum allowed by ASTM; the rate corresponding to the minimum allowed by ASTM; and a rate in between these two limits. Two specimens were tested at each rate. Three specimens were tested using the Tinius Olsen machine at rates matching those from previous tests using the three other

machines. The tests at the maximum rate were chosen for this comparison. In the same way, two pairs of specimens were tested using the Satek and the Southwark-

Table 3-1: Plate specimen test variables

Specimen	Tinius-Olsen Crosshead Speed	Satek Loading Rate	Southwark Loading Rate	Riehle Crosshead Speed	Notes
N1	0.05 in/min				ASTM min rate
D1	0.05 in/min				ASTM min rate
I1	0.2 in/min				
I3	0.2 in/min				
D3	0.5 in/min				ASTM max rate
N3	0.5 in/min				ASTM max rate
H2	match P2				
I2	match C2				
J2	match C1				
E1	0.5 in/min				
M1	0.5 in/min				
G1		10 ksi/min			ASTM min rate
K1		10 ksi/min			ASTM min rate
H3		50 ksi/min			
J3		50 ksi/min			
B2		100 ksi/min			ASTM max rate
P2		100 ksi/min			ASTM max rate
E3		match D3			
M3		match N3			
H1			10 ksi/min		ASTM min rate
J1			10 ksi/min		ASTM min rate
G3			50 ksi/min		
K3			50 ksi/min		
O2			100 ksi/min		ASTM max rate
C2			100 ksi/min		ASTM max rate
E2			match D3		
M2			match N3		
O1				0.05 in/min	ASTM min rate
C1				0.05 in/min	ASTM min rate
F2				0.2 in/min	
L2				0.2 in/min	
O3				0.5 in/min	ASTM max rate
C3				0.5 in/min	ASTM max rate

Table 3-2: W36x150 specimen test variables

Specimen	Tinius-Olsen Crosshead Speed	Satek Loading Rate	Notes
3A	0.4 in/min		ASTM Max rate
2A		100 ksi/min	ASTM max rate
1A		10 ksi/min	ASTM min rate
4A	0.05 in/min		ASTM min rate
5A	1.5 in/min		
6A	0.4 in/min		ASTM max rate
4B	0.4 in/min		ASTM max rate
5B	0.05 in/min		ASTM min rate
6B	1.5 in/min		
1B		100 ksi/min	ASTM max rate
2B		10 ksi/min	ASTM min rate
3B	0.4 in/min		ASTM max rate

Emery machines at elastic stressing rates to match the highest elastic strain rate of the Tinius-Olsen tests.

For the W36 web material, the testing procedures for the innermost six specimens were dictated by the Round Robin specifications. The specimens nearest the K-line were tested using the same procedures as the two specimens at the centerline in order to bracket the results. The remaining four specimens were tested using the Satek machine at maximum and minimum rates.

In general, test variables were assigned to the specimens based on their original location in the plate and in the web in order to facilitate comparison of results. See Figure 3-4 for plate layout and Figure 3-5 for W36 web layout.

3.5 BASE LINE YIELD STRENGTH

In order to compare the influence of different machines and rates of testing, a base line yield strength was established for the plate specimens. Twelve specimens taken from the corners and at regular intervals within the plate were tested using the Tinius-Olsen screw-driven machine at a crosshead speed of 0.2 in/min. These specimens are shown shaded in Figure 3-4. The yield strength of each of the remaining specimens was predicted by interpolation. This value of yield strength is defined as the base line yield strength. The results of subsequent tests which employed different testing procedures could then be compared to this value.

The yield strength corresponding to the ASTM definitions of yield point, i.e., the top of the knee on the stress-strain curve and the 0.5% total extension under load ("Standard" 1994), and the static yield were recorded for comparison.

3.6 TEST PROCEDURES

Prior to conducting a series of tests on a given machine, the crosshead speed or valve settings necessary to obtain the desired rate were determined experimentally. A number of practice specimens were tested at various settings and the results were analyzed to determine the strain rate or stressing rate during the second half of the elastic range. This is the range specified by ASTM. The practice specimens were the same size as the actual test specimens and were cut from the same material. See Figure 3-1.

T-O 0.20 in/min **B3**	Rhiele 0.5 in/min **C3**	T-O 0.5 in/min **D3**	Satek match D3 **E3**	T-O 0.20 in/min **F3**	S-E 50 ksi/min **G3**	Satek 50 ksi/min **H3**	T-O 0.2 in/min **I3**	Satek 50 ksi/min **J3**	S-E 50 ksi/min **K3**	T-O 0.20 in/min **L3**	Satek match N3 **M3**	T-O 0.5 in/min **N3**	Rhiele 0.5 in/min **O3**	T-O 0.20 in/min **P3**
Satek 100 ksi/min **B2**	S-E 100 ksi/min **C2**	T-O 0.20 in/min **D2**	S-E match D3 **E2**	Rhiele 0.2 in/min **F2**	T-O 0.20 in/min **G2**	T-O match P2 **H2**	T-O match C2 **I2**	T-O match C1 **J2**	T-O 0.20 in/min **K2**	Rhiele 0.2 in/min **L2**	S-E match N3 **M2**	T-O 0.20 in/min **N2**	S-E 100 ksi/min **O2**	Satek 100 ksi/min **P2**
T-O 0.20 in/min **B1**	Rhiele 0.05 in/min **C1**	T-O 0.05 in/min **D1**	T-O 0.5 in/min **E1**	T-O 0.20 in/min **F1**	Satek 10 ksi/min **G1**	S-E 10 ksi/min **H1**	T-O 0.2 in/min **I1**	S-E 10 ksi/min **J1**	Satek 10 ksi/min **K1**	T-O 0.20 in/min **L1**	T-O 0.5 in/min **M1**	T-O 0.05 in/min **N1**	Rhiele 0.05 in/min **O1**	T-O 0.20 in/min **P1**

Figure 3-4: Plate specimen layout and test variables

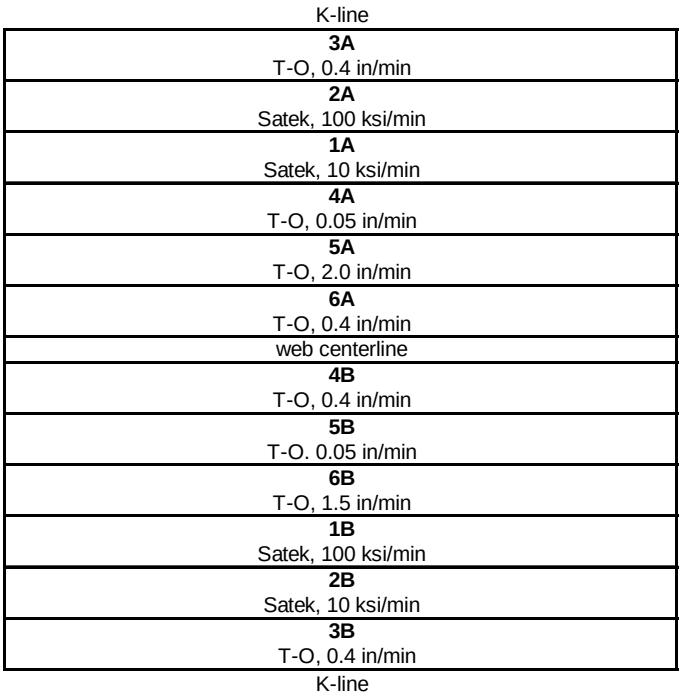

Figure 3-5: W36x150 web specimen layout and test variables

At the start of each test, the specimen was placed in the grips, aligned vertically using a spirit level, then locked in place. The frequency and total number of scans to be recorded by Lab View were specified. The test was then commenced. The initial setting of crosshead speed or oil flow was maintained (i.e., hands-off) through yield of the specimen. Immediately after yielding, a static load test was conducted. In the case of the mechanical machines, the crosshead was stopped and the machine disengaged for three minutes. For the hydraulic machines, the valves were turned off and, in the case of the Satek, the pump turned off for three minutes. After the static yield test was completed, the machine was re-engaged to the initial settings and the specimen loaded through

fracture. Strain data was typically recorded up to near-ultimate load. The specimen deformation at this load corresponded to the maximum range of the extensometer.

3.7 Machine Relaxation Tests

A number of tests were run to determine the amount of load drop which occurs if the machine is stopped during elastic loading. This should demonstrate that a portion of the static yield drop can be attributed to the relaxation of the machine.

A test specimen was stressed to near ultimate then unloaded and allowed to strain age. This created a test piece with a stiffness very similar to the typical specimen but with a higher yield strength. In each machine, the strain-aged specimen was loaded to the lower yield of the typical test specimen and the machine stopped for three minutes. The amount of load drop was recorded at the end of that time.

This test is not a direct comparison of the machine behavior during the static yield test because it does not account for the change occurring in the machine due to the yielding of the specimen. Specifically, the sudden change in stiffness of the specimen at yield causes relaxation in the machine. See section 2.3.2. It should also be noted that there is a more formal procedure for determining machine relaxation (Meyers et al. 1979).

Chapter 4: Results

4.1 MACHINE BEHAVIOR

4.1.1 Measured vs. Intended Testing Rates

The measured testing rates, shown in Tables 4-1 and 4-2, did not always match the intended rates listed in Tables 3-1 and 3-2. In the case of the mechanical machines, the free-running crosshead speed was measured using the extensometer attached to the two ends of a broken specimen. The measured speed typically differed from the dial setting. In the case of the hydraulic machines, practice tests were run and the rate of stressing was determined by fitting a straight line to the stress-time curve between 0.5Fy and 0.9Fy. The flow of oil was adjusted on subsequent tests until the intended stressing rate was achieved. Unfortunately, a given setting of the dial did not always reproduce the same rate of stressing.

Two tests were run on the Southwark-Emery machine at stressing rates to match the elastic strain rate of the 0.5 in/min tests on the Tinius-Olsen machine. The resulting stressing rate was 600 ksi/min. The loading rate of the Satek machine seemed to have an upper bound. The higher stressing rate could not be achieved despite opening the valve almost completely.

4.1.2 Strain Rate Control vs. Machine

Measured Strain Rates The measured elastic and plastic strain rates are listed in Table 4-1 and 4-2 and are plotted against rate category for each machine in Figures 4-1 and 4-2. Similar to the stressing rate calculation, the elastic rate

Table 4-1: Testing speeds and measured strain rates for plate specimens; (a) base line specimens; (b) test specimens

(a)

Specimen	Intended Rate		Measured Rate		Elastic Strain Rate (in/in/min)	Plastic Strain Rate (in/in/min)	Hardness Ratios	Machine Stiffness (kip/in)
Tinius-Olsen								
B1	0.2	in/min	0.34	in/min	0.01141	0.03667	3.21	597
F1	0.2	in/min	0.34	in/min	0.01098	0.03537	3.22	588
L1	0.2	in/min	0.34	in/min	0.01069	0.03016	2.82	730
P1	0.2	in/min	0.34	in/min	0.01015	0.02915	2.87	702
D2	0.2	in/min	0.34	in/min	0.01681	0.05168	3.08	643
G2	0.2	in/min	0.34	in/min	0.01499	0.05157	3.44	529
K2	0.2	in/min	0.34	in/min	0.01498	0.05246	3.50	525
N2	0.2	in/min	0.34	in/min	0.01343	0.04503	3.35	559
B3	0.2	in/min	0.34	in/min	0.01176	0.03668	3.12	619
F3	0.2	in/min	0.34	in/min	0.00862	0.02617	3.04	642
L3	0.2	in/min	0.34	in/min	0.00910	0.02612	2.87	698
P3	0.2	in/min	0.34	in/min	0.01272	0.02956	2.32	987

was found by performing a regression analysis of the strain-time curve between 0.5Fy and 0.9Fy. For plastic strain rate, the line was fitted to the data between $1.1\varepsilon_y$ and the start of the static yield test. Stress-time and strain-time curves with regression lines for all tests are shown in Appendix A3.

Each data point in Figure 4-1(a) and 4-2(a) represents one test which is closest to the intended testing rate. In the case of the Satek machine, the data

point is the average of two tests, one greater and one less than 100 ksi/min. The lines labeled maximum and minimum strain rates correspond to the stressing rate limits. The strain rates from tests conducted using the Tinius-Olsen are higher than the other machines and are often greater than the maximum strain rate.

(b)

Specimen	Intended Rate		Measured Rate		Elastic Strain Rate (in/in/min)	Plastic Strain Rate (in/in/min)	Hardness Ratios	Machine Stiffness (kip/in)
Tinius-Olsen								
N1	0.05	in/min	0.10	in/min	0.00245	0.00719	2.94	681
D1	0.05	in/min	0.10	in/min	0.00336	0.01017	3.02	650
I1	0.2	in/min	0.34	in/min	0.00872	0.02676	3.07	633
I3	0.2	in/min	0.34	in/min	0.01388	0.03864	2.78	730
D3	0.5	in/min	0.67	in/min	0.02221	0.07856	3.54	523
N3	0.5	in/min	0.67	in/min	0.02125	0.06274	2.95	683
H2	0.05	in/min	0.10	in/min	0.00437	0.01686	3.86	453
I2	0.05	in/min	0.10	in/min	0.00234	0.01106	4.74	347
J2	0.05	in/min	0.10	in/min	0.00347	0.00915	2.64	789
E1	0.5	in/min	0.67	in/min	0.02149	0.06576	3.06	625
M1	0.5	in/min	0.67	in/min	ext stick	0.07319	NR	NR
Satek								
G1	10	ksi/min	36	ksi/min	0.00200	0.01369	6.84	224
K1	10	ksi/min	35	ksi/min	0.00180	0.01534	8.50	175
H3	50	ksi/min	53	ksi/min	0.00150	0.02201	14.63	97
J3	50	ksi/min	45	ksi/min	0.00189	0.02505	13.28	106
B2	100	ksi/min	61	ksi/min	0.00258	0.02679	10.37	138
P2	100	ksi/min	63	ksi/min	0.00335	0.02589	7.74	192
E3	600	ksi/min	147	ksi/min	0.00767	0.09326	12.16	117
M3	600	ksi/min	174	ksi/min	0.00959	0.08327	8.68	170
Southwark-Emery								
H1	10	ksi/min	33	ksi/min	0.00103	0.01045	10.17	141
J1	10	ksi/min	9	ksi/min	0.00042	0.00291	6.93	218
G3	50	ksi/min	47	ksi/min	0.00184	0.01233	6.70	228
K3	50	ksi/min	62	ksi/min	0.00290	0.01935	6.68	232
O2	100	ksi/min	150	ksi/min	0.00753	0.04432	5.89	268
C2	100	ksi/min	125	ksi/min	0.00523	0.03962	7.58	197
E2	600	ksi/min	507	ksi/min	0.03186	0.17633	5.53	287
M2	600	ksi/min	508	ksi/min	0.03056	0.17133	5.61	281
Riehle								
O1	0.05	in/min	0.07	in/min	0.00024	0.00166	6.88	222
C1	0.08	in/min	0.07	in/min	0.00033	0.00224	6.85	224
F2	0.2	in/min	0.14	in/min	0.00265	0.01670	6.30	246
L2	0.2	in/min	0.14	in/min	0.00218	0.01686	7.73	194
O3	0.5	in/min	0.41	in/min	0.00659	0.05300	8.05	187
C3	0.5	in/min	0.41	in/min	0.00577	0.04964	8.61	172

Table 4-2: Testing speeds and measured strain rates for W36x150 web specimens

Specimen	Machine	Intended Rate		Measured Rate		Elastic Strain Rate (in/in/min)	Plastic Strain Rate (in/in/min)	Hardness Ratios	Machine Stiffness (kip/in)
3A	Tinius-Olsen	0.4	in/min	0.50	in/min	0.00937	0.07800	8.33	486
2A	Satek	100	ksi/min	115	ksi/min	0.00348	0.03109	8.92	459
1A	Satek	10	ksi/min	11	ksi/min	0.00037	0.00504	13.50	288
4A	Tinius-Olsen	0.05	in/min	0.07	in/min	0.00148	0.00738	4.99	895
5A	Tinius-Olsen	2	in/min	2.00	in/min	0.04702	0.20035	4.26	1095
6A	Tinius-Olsen	0.4	in/min	0.50	in/min	0.00784	0.05134	6.55	979
4B	Tinius-Olsen	0.4	in/min	0.50	in/min	0.00937	0.07396	7.89	533
5B	Tinius-Olsen	0.05	in/min	0.07	in/min	0.00152	0.00757	4.99	923
6B	Tinius-Olsen	1.5	in/min	1.60	in/min	0.02956	0.16574	5.61	792
1B	Satek	100	ksi/min	58	ksi/min	0.00180	0.03090	17.20	224
2B	Satek	10	ksi/min	8	ksi/min	0.00026	0.00346	13.16	297
3B	Tinius-Olsen	0.4	in/min	0.50	in/min	NR	NR	NR	NR

The data points in Figure 4-1(b) and 4-2(b) are the plastic strain rates for the tests plotted in Figure 4-1(a) and 4-2(a). The scatter is more narrow since the hydraulic machines have a higher hardness ratio. No limit lines are shown since ASTM does not limit strain rates in the plastic range.

Hardness Ratio and Machine Stiffness Calculations The hardness ratios calculated from the test results are listed in Tables 4-1 and 4-2. Recall that stiffer machines correspond to lower hardness ratios. The hydraulic machines have higher hardness ratios than the mechanical machines, i.e., the hydraulic machines are softer than the mechanical machines. The Tinius-Olsen machine reports the lowest hardness ratio (highest stiffness). All values are less than those reported in the literature. See Table 2-2.

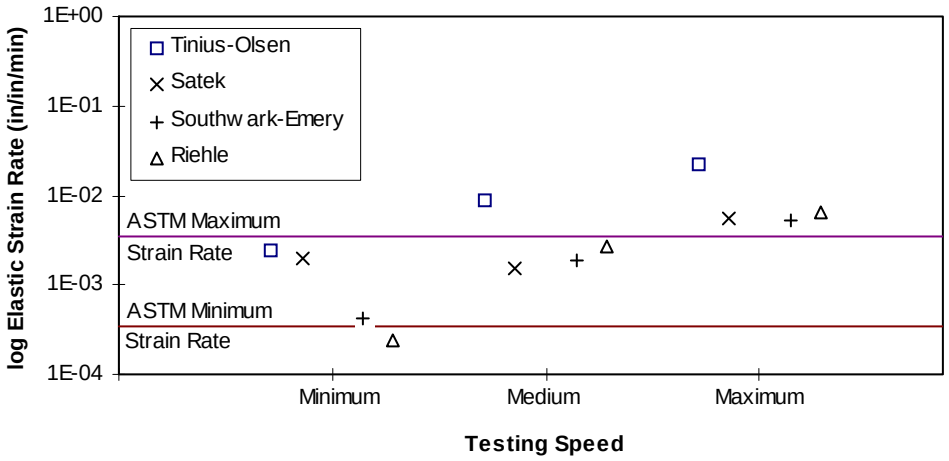

(a)

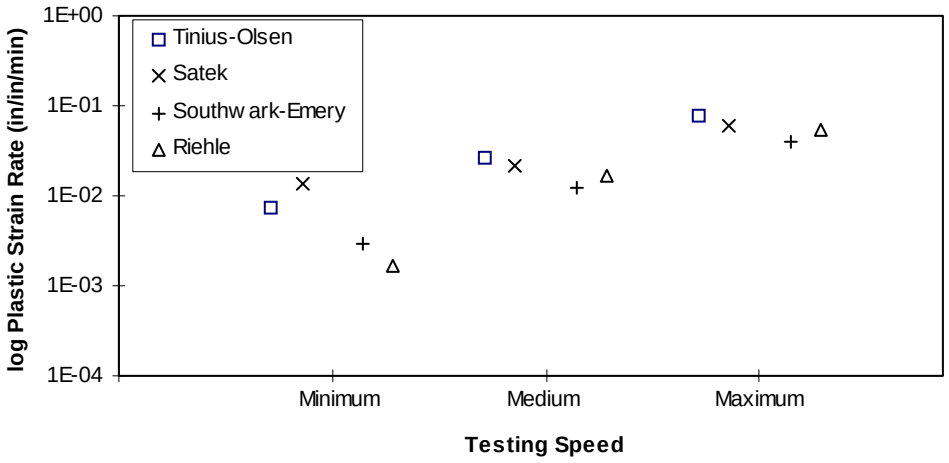

(b)

Figure 4-1: Strain rates at minimum, medium, and maximum test speeds for plate specimens: (a) elastic strain rate, and; (b) plastic strain rate

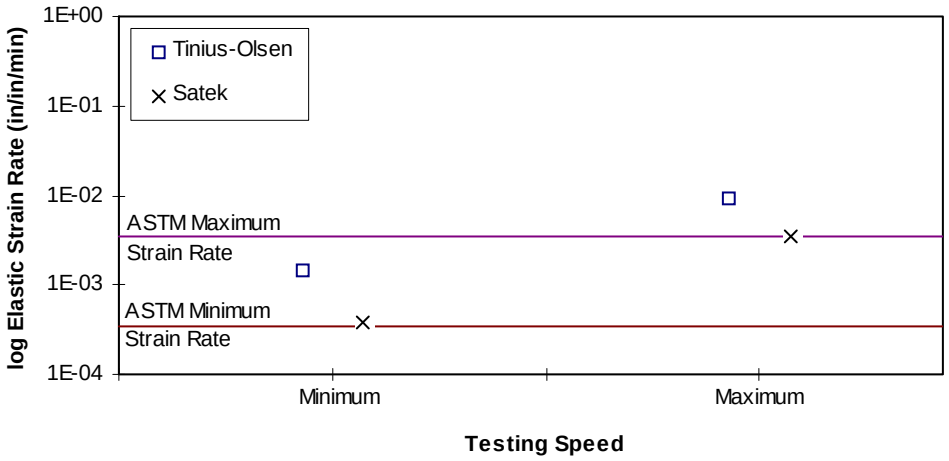

(a)

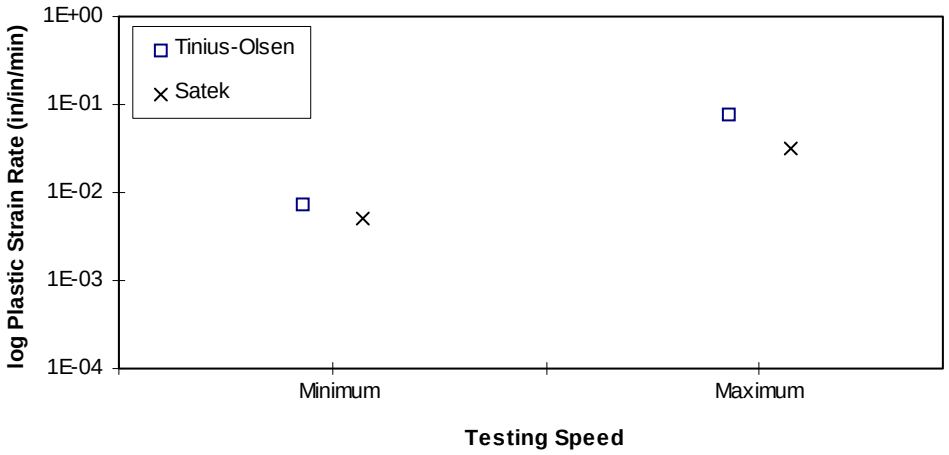

(b)

Figure 4-2: Strain rates at minimum, medium, and maximum test speeds for W36x150 web specimens: (a) elastic strain rate, and; (b) plastic strain rate

For a given crosshead speed, the hardness ratio increases as the specimen size increases. The larger specimen strains the machine more which results in a lower elastic strain rate in the specimen. Since the plastic strain rate is essentially equal to the crosshead speed, the hardness ratio will be greater for the larger specimen.

The machine stiffnesses calculated using the hardness ratios are listed in Table 4-1. The Tinius-Olsen machine has the highest stiffness while the hydraulic machines are much more flexible. While this trend is consistent with that reported in the literature, these values are generally higher. See Table 2-2. The machine stiffness varies between tests as described by Gray and Sharp (1989) and Hockett and Gillis (1971) though, in contrast to the findings of these authors, the trend is toward increased stiffness with the larger specimen.

4.1.3 Behavior of Machine at Yield

The behavior of the machines differ at the onset of yield. This is described in Section 2.3.2. Even though the Tinius-Olsen machine did not report a yield point, the hydraulic machines often reported one. This is apparent in Figure 4-3 in which the stress-strain curves of a Tinius-Olsen test specimen (D3) and a Southwark-Emery specimen (G3) normalized against the lower yield strength are superimposed.

The different paths of the yield drop reported by the mechanical and hydraulic machines which were described in Section 2.3.2 are shown in Figure 4-4.

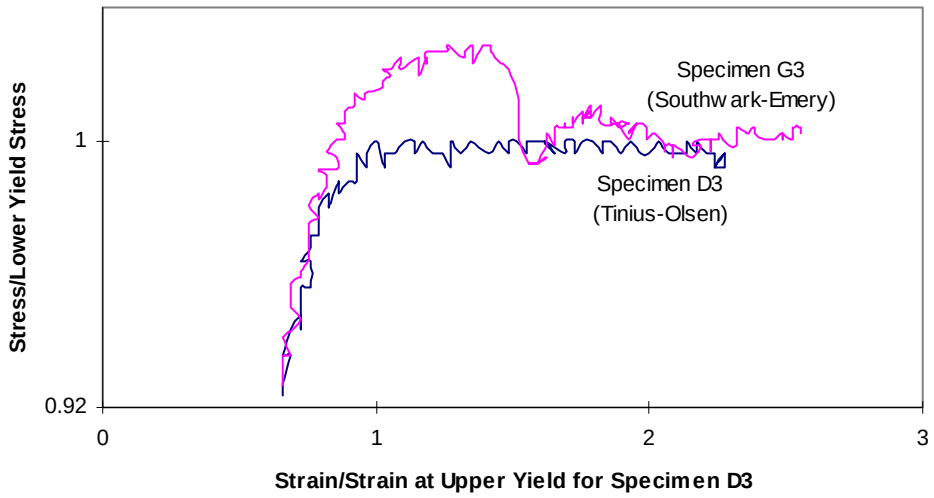

Figure 4-3: Yield points reported by Tinius-Olsen and Southwark-Emery machines.

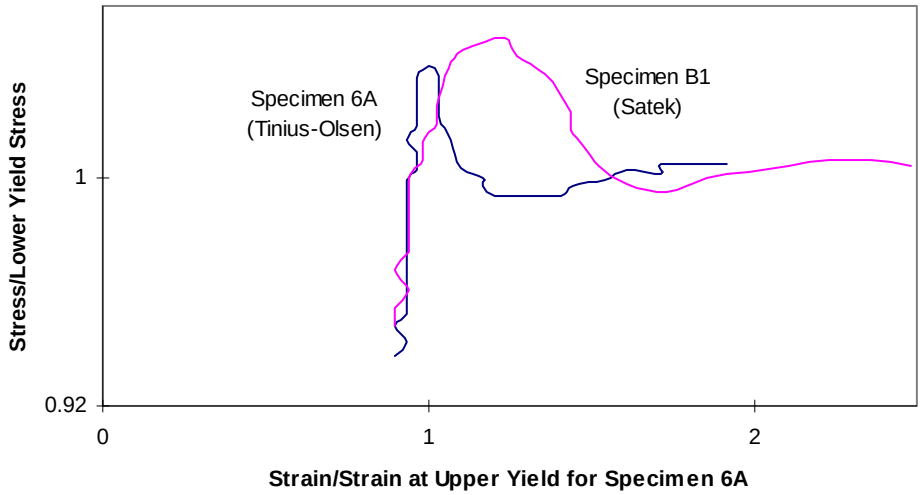

Figure 4-4: Yield drops reported by Tinius-Olsen and Satek machines.

4.2 PLATE SPECIMENS

4.2.1 General Summary of Results

The upper yield, the lower yield and the static yield strengths for all plate specimens including the base line specimens (shown shaded) are summarized in Figure 4-5 and Table 4-3. The upper yield is taken as the yield point, where one exists, or as the top of the knee on the stress-strain curve. The lower yield is taken as the stress corresponding to the 0.5% total extension under load. The stress-strain curves for each of the specimens are included in Appendix A2.

The lowest and highest values of yield strength are 38.76 ksi and 54.72 ksi. The former is a static yield measurement. Considering only ASTM designated yield strengths, the range becomes 44.14 ksi to 54.72 ksi. This is a difference of 10.58 ksi.

A major portion of this difference can be attributed to material variation rather than test variables. Specimens P1, P2 and P3 which are located along the original plate edge are significantly stronger than specimens located elsewhere in the plate. The difference in upper yield strength between specimens P3 and L1, both of which were tested at 0.2 in/min in the Tinius-Olsen machine, is 9.09 ksi. If specimens P1 to P3 are omitted, the lowest and highest values of ASTM-permitted yield strength are 44.14 ksi and 49.56 ksi. These are upper yield strengths for specimens J2 and N1 which were both tested in the same machine at the same rate. The difference of 5.42 ksi is an indication of the range in material

strength for all but specimens P1, P2 and P3. By comparison, Gray and Sharp's (1989) scatter

	T-O 0.20 in/min	Rhiele 0.5 in/min	T-O 0.5 in/min	Satek match D3	T-O 0.20 in/min	S-E 50 ksi/min	Satek 50 ksi/min	T-O 0.2 in/min	Satek 50 ksi/min	S-E 50 ksi/min	T-O 0.20 in/min	Satek match N3	T-O 0.5 in/min	Rhiele 0.5 in/min	T-O 0.20 in/min
	B3	**C3**	**D3**	**E3**	**F3**	**G3**	**H3**	**I3**	**J3**	**K3**	**L3**	**M3**	**N3**	**O3**	**P3**
UY	47.10	48.28	46.98	48.86	48.40	46.63	45.93	47.68	48.33	47.46	46.72	47.73	46.30	48.48	54.24
LY	46.72	48.28	46.98	47.76	48.21	45.32	44.57	47.88	47.14	46.33	46.72	46.82	45.54	48.48	54.24
Static	42.89	41.17	43.10	43.15	44.75	41.33	38.76		41.82	42.71	42.88	47.29	43.28	46.46	50.97

	Satek 100 ksi/min	S-E 100 ksi/min	T-O 0.20 in/min	S-E match D3	Rhiele 0.2 in/min	T-O 0.20 in/min	T-O match P2	T-O match C2	T-O match C1	T-O 0.20 in/min	Rhiele 0.2 in/min	S-E match N3	T-O 0.20 in/min	S-E 100 ksi/min	Satek 100 ksi/min
	B2	**C2**	**D2**	**E2**	**F2**	**G2**	**H2**	**I2**	**J2**	**K2**	**L2**	**M2**	**N2**	**O2**	**P2**
UY	48.38	48.43	48.00	48.17	47.37	47.28	46.22	47.96	49.56	46.41	46.25	47.91	46.95	49.22	54.72
LY	47.37	47.21	47.82	48.09	47.37	47.47	45.83	47.96	49.37	46.61	45.23	47.74	46.95	48.74	54.63
Static	41.99	42.72	44.99	41.99	44.32	43.00	42.33	45.83	47.23	43.17	41.17	42.04	43.52	44.62	49.17

	T-O 0.20 in/min	Rhiele 0.05 in/min	T-O 0.05 in/min	T-O 0.5 in/min	T-O 0.20 in/min	Satek 10 ksi/min	S-E 10 ksi/min	T-O 0.2 in/min	S-E 10 ksi/min	Satek 10 ksi/min	T-O 0.20 in/min	T-O 0.5 in/min	T-O 0.05 in/min	Rhiele 0.05 in/min	T-O 0.20 in/min
	B1	**C1**	**D1**	**E1**	**F1**	**G1**	**H1**	**I1**	**J1**	**K1**	**L1**	**M1**	**N1**	**O1**	**P1**
UY	45.22	46.66	47.88	48.58	45.99	46.30	45.27	46.59	47.30	47.40	45.15	46.93	44.14	47.76	51.39
LY	45.22	46.66	47.31	48.19	45.80	45.48	44.78	46.59	46.32	46.12	44.96	46.93	44.14	47.76	51.39
Static	41.99	42.10	44.73	44.09	42.14	40.27	41.18		43.54	40.28	41.56	42.65	43.29	46.24	48.83

Figure 4-5: Test results of plate specimens

Table 4-3: Test results of plate specimens: (a) base line specimens, and; (b) test specimens

(a)

Specimen	Area (in^2)	Load			Stress		
		Yield Point (kip)	0.5% Yld (kip)	Static Yield (kip)	Upper Yield (ksi)	Lower Yield (ksi)	Static Yield (ksi)
Tinius-Olsen							
B1	0.3646	16.49	16.49	15.31	45.22	45.22	41.99
F1	0.3601	16.56	16.49	15.17	45.98	45.79	42.13
L1	0.3667	16.56	16.49	15.24	45.15	44.96	41.56
P1	0.3626	18.64	18.64	17.53	51.39	51.39	48.34
D2	0.3680	17.67	17.60	16.56	48.00	47.82	44.99
G2	0.3560	16.83	16.90	15.31	47.28	47.48	43.00
K2	0.3627	16.83	16.90	15.66	46.41	46.61	43.17
N2	0.3630	17.04	17.04	15.80	46.95	46.95	43.52
B3	0.3618	17.04	16.90	15.52	47.10	46.72	42.89
F3	0.3607	17.46	17.39	16.14	48.40	48.21	44.75
L3	0.3604	16.83	16.83	15.45	46.71	46.71	42.87
P3	0.3603	19.54	19.54	18.36	54.22	54.22	50.95

band of yield strengths for specimens tested in machines similar to those used in this study was +/- 3 ksi.

It was mentioned in the previous section that the plate material did not have a yield point. This was true for the test specimens, but the practice specimens which were oriented perpendicular to these in the original plate did report a yield point. Gray (1997) offers an explanation for this observation. Rolling leads to orthotropic distribution of whatever is pinning the dislocations.

The pinning arrangement for specimens taken perpendicular to the rolling direction would not

(b)

Specimen	Area (in^2)	Load			Stress		
		Yield Point (kip)	0.5% Yld (kip)	Static Yield (kip)	Upper Yield (ksi)	Lower Yield (ksi)	Static Yield (ksi)
Tinius-Olsen							
N1	0.3641	16.07	16.07	15.76	44.14	44.14	43.29
D1	0.3632	17.39	17.18	16.25	47.88	47.30	44.73
I1	0.3614	16.83	16.83	N/A	46.58	46.58	N/A
I3	0.3589	17.11	17.11	N/A	47.68	47.68	N/A
D3	0.3657	17.18	17.18	15.76	46.98	46.98	43.10
N3	0.3681	17.04	16.77	15.93	46.30	45.55	43.29
H2	0.3567	16.49	16.35	15.10	46.22	45.83	42.33
I2	0.3583	17.18	17.18	16.42	47.96	47.96	45.83
J2	0.3564	17.67	17.60	16.83	49.56	49.37	47.23
E1	0.3551	17.25	17.11	15.66	48.58	48.19	44.09
M1	0.3557	16.70	16.70	15.17	46.93	46.93	42.65
Satek							
G1	0.3615	16.74	16.44	14.55	46.30	45.48	40.27
K1	0.3621	17.16	16.70	14.59	47.40	46.12	40.28
H3	0.3644	16.74	16.24	14.13	45.93	44.57	38.76
J3	0.3606	17.43	17.00	15.08	48.33	47.14	41.82
B2	0.3568	17.26	16.90	14.98	48.38	47.37	41.99
P2	0.3571	19.54	19.51	17.56	54.72	54.63	49.17
E3	0.3590	17.54	17.15	15.49	48.86	47.76	43.15
M3	0.3599	17.18	16.85	15.11	47.73	46.82	41.99
Southwark-Emery							
H1	0.3574	16.18	16.00	14.72	45.27	44.78	41.18
J1	0.3575	16.91	16.56	15.57	47.30	46.32	43.54
G3	0.3582	16.70	16.24	14.81	46.63	45.32	41.33
K3	0.3631	17.23	16.82	15.51	47.46	46.33	42.71
O2	0.3613	17.78	17.61	16.12	49.22	48.74	44.62
C2	0.3576	17.32	16.88	15.27	48.43	47.21	42.72
E2	0.3589	17.29	17.26	15.07	48.17	48.09	41.99
M2	0.3577	17.14	17.08	15.04	47.91	47.74	42.04
Riehle							
O1	0.3607	17.23	17.23	16.68	47.76	47.76	46.24
C1	0.3613	16.86	16.86	15.21	46.66	46.66	42.10
F2	0.3598	17.04	17.04	15.95	47.37	47.37	44.32
L2	0.3606	16.68	16.31	14.85	46.25	45.23	41.17
O3	0.3629	17.59	17.59	16.86	48.48	48.48	46.46
C3	0.3606	17.41	17.41	14.85	48.28	48.28	41.17

be as strong as specimens taken parallel to the rolling direction. In the former case, the stress to free the dislocations would be less than the upper yield and no yield point is observed.

4.2.2 Base Line Yield Strengths

The base line yield strengths, shown in Figure 4-6, are an attempt to eliminate the inherent variation in material strength when comparing the different test results. These values were found by interpolating between the results of the base line specimens which were tested at 0.2 in/min in the Tinius-Olsen machine. The yield strengths from all other test specimens were normalized against these base line values so that the influence of different testing procedures could be compared.

The general trend in strength appears to be a gradual increase from row 1 to row 3 and a gradual increase from columns B to N followed by a sharp jump at column P.

4.2.3 Influence of Testing Variables on the Yield Strength

Upper and Lower Yield Strengths Comparing the test results of individual specimens reveals very few consistent trends relating the influence of testing variables on the yield strengths. This is apparent both in the absolute values shown in Figure 4-5 and the normalized results shown in Figure 4-7. Consider, for example, specimens J2 and K2 which are adjacent to one another and which would presumably have very similar strengths. According to the results, the yield strength increases by approximately 3 ksi as the testing speed is decreased by a

	T-O 0.20 in/min	Rhiele 0.5 in/min	T-O 0.5 in/min	Satek match D3	T-O 0.20 in/min	S-E 50 ksi/min	Satek 50 ksi/min	T-O 0.2 in/min	Satek 50 ksi/min	S-E 50 ksi/min	T-O 0.20 in/min	Satek match N3	T-O 0.5 in/min	Rhiele 0.5 in/min	T-O 0.20 in/min
	B3	**C3**	**D3**	**E3**	**F3**	**G3**	**H3**	**I3**	**J3**	**K3**	**L3**	**M3**	**N3**	**O3**	**P3**
UY	47.10	47.46	47.83	48.16	48.40	48.28	48.06	47.68	47.43	47.16	46.72	48.31	50.00	52.28	54.24
LY	46.72	47.02	47.43	47.85	48.21	48.23	48.13	47.88	47.52	47.13	46.72	48.00	49.56	51.73	54.24
Static	42.89	43.77	44.33	44.63	44.75	44.35	43.90		43.10	42.88	42.88	44.30	46.08	48.27	50.97

	Satek 100 ksi/min	S-E 100 ksi/min	T-O 0.20 in/min	S-E match D3	Rhiele 0.2 in/min	T-O 0.20 in/min	T-O match P2	T-O match C2	T-O match C1	T-O 0.20 in/min	Rhiele 0.2 in/min	S-E match N3	T-O 0.20 in/min	S-E 100 ksi/min	Satek 100 ksi/min
	B2	**C2**	**D2**	**E2**	**F2**	**G2**	**H2**	**I2**	**J2**	**K2**	**L2**	**M2**	**N2**	**O2**	**P2**
UY	47.68	47.82	48.00	47.74	47.53	47.28	47.05	46.82	46.60	46.41	46.52	46.70	46.95	48.71	52.25
LY	47.27	47.53	47.82	47.69	47.60	47.47	47.25	47.03	46.80	46.61	46.64	46.75	46.95	48.84	52.23
Static	46.13	45.44	44.99	44.15	43.52	43.00	42.93	42.94	43.01	43.17	43.28	43.45	43.52	45.22	49.12

	T-O 0.20 in/min	Rhiele 0.05 in/min	T-O 0.05 in/min	T-O 0.5 in/min	T-O 0.20 in/min	Satek 10 ksi/min	S-E 10 ksi/min	T-O 0.2 in/min	S-E 10 ksi/min	Satek 10 ksi/min	T-O 0.20 in/min	T-O 0.5 in/min	T-O 0.05 in/min	Rhiele 0.05 in/min	T-O 0.20 in/min
	B1	**C1**	**D1**	**E1**	**F1**	**G1**	**H1**	**I1**	**J1**	**K1**	**L1**	**M1**	**N1**	**O1**	**P1**
UY	45.22	45.01	45.19	45.57	45.99	46.34	46.55	46.59	46.14	45.62	45.15	45.83	46.92	48.64	51.39
LY	45.22	44.86	44.99	45.36	45.80	46.21	46.47	46.59	46.00	45.36	44.96	45.32	46.31	47.94	51.39
Static	41.99	42.25	42.33	42.28	42.14	41.89	41.65		41.33	41.35	41.56	42.91	44.55	46.49	48.83

Figure 4-6: Base line yield strengths

factor of four. Contrary to this, two other specimens, G2 and H2, which are also side-by-side and which compare the same test variables as J2 and K2 (Tinius-Olsen at 0.2 and 0.05 in/min), agree with the well established fact that yield strength increases with testing speed, in this case by about 1 ksi.

A review of the normalized results also shows a number of contradictions. Each combination of machine and testing speed variable was tested with at least two specimens. Of the 15 pairs of specimens per test variable, only nine report a consistent increase or decrease in the lower yield compared to the base line value. Of the remaining six pairs, one test reports a value which is higher than the base line yield strength while the other test reports a lower value. For the case of the upper yield strength, six pairs agree and nine pairs conflict. Accounting for the possibility that the base line yield strengths were poorly interpolated by favorably increasing or decreasing them by an arbitrary 0.3 ksi does not improve the normalized results appreciably.

The difference between the absolute yield strengths and the base line yield strengths are shown in Figure 4-8. These number illustrate that even for the pairs which agree, one test may report a small change in yield strength for a given test procedure, while the other may report a large change. For example, the difference between absolute and base line is -3.56 ksi for specimen H3 and -0.36 ksi for specimen J3, a difference of 3.18 ksi. It seems that for a reliable conclusion to be drawn, the results should be in closer agreement. For the case of the lower yield,

	T-O 0.20 in/min	Rhiele 0.5 in/min	T-O 0.5 in/min	Satek match D3	T-O 0.20 in/min	S-E 50 ksi/min	Satek 50 ksi/min	T-O 0.2 in/min	Satek 50 ksi/min	S-E 50 ksi/min	T-O 0.20 in/min	Satek match N3	T-O 0.5 in/min	Rhiele 0.5 in/min	T-O 0.20 in/min
	B3	**C3**	**D3**	**E3**	**F3**	**G3**	**H3**	**I3**	**J3**	**K3**	**L3**	**M3**	**N3**	**O3**	**P3**
UY	1.00	1.02	0.98	1.01	1.00	0.97	0.96	1.00	1.02	1.01	1.00	0.99	0.93	0.93	1.00
LY	1.00	1.03	0.99	1.00	1.00	0.94	0.93	1.00	0.99	0.98	1.00	0.98	0.92	0.94	1.00
Static	1.00	0.94	0.97	0.97	1.00	0.93	0.88		0.97	1.00	1.00	1.07	0.94	0.96	1.00

	Satek 100 ksi/min	S-E 100 ksi/min	T-O 0.20 in/min	S-E match D3	Rhiele 0.2 in/min	T-O 0.20 in/min	T-O match P2	T-O match C2	T-O match C1	T-O 0.20 in/min	Rhiele 0.2 in/min	S-E match N3	T-O 0.20 in/min	S-E 100 ksi/min	Satek 100 ksi/min
	B2	**C2**	**D2**	**E2**	**F2**	**G2**	**H2**	**I2**	**J2**	**K2**	**L2**	**M2**	**N2**	**O2**	**P2**
UY	1.01	1.01	1.00	1.01	1.00	1.00	0.98	1.02	1.06	1.00	0.99	1.03	1.00	1.01	1.05
LY	1.00	0.99	1.00	1.01	1.00	1.00	0.97	1.02	1.05	1.00	0.97	1.02	1.00	1.00	1.05
Static	0.91	0.94	1.00	0.95	1.02	1.00	0.99	1.07	1.10	1.00	0.95	0.97	1.00	0.99	1.00

	T-O 0.20 in/min	Rhiele 0.05 in/min	T-O 0.05 in/min	T-O 0.5 in/min	T-O 0.20 in/min	Satek 10 ksi/min	S-E 10 ksi/min	T-O 0.2 in/min	S-E 10 ksi/min	Satek 10 ksi/min	T-O 0.20 in/min	T-O 0.5 in/min	T-O 0.05 in/min	Rhiele 0.05 in/min	T-O 0.20 in/min
	B1	**C1**	**D1**	**E1**	**F1**	**G1**	**H1**	**I1**	**J1**	**K1**	**L1**	**M1**	**N1**	**O1**	**P1**
UY	1.00	1.04	1.06	1.07	1.00	1.00	0.97	1.00	1.03	1.04	1.00	1.02	0.94	0.98	1.00
LY	1.00	1.04	1.05	1.06	1.00	0.98	0.96	1.00	1.01	1.02	1.00	1.04	0.95	1.00	1.00
Static	1.00	1.00	1.06	1.04	1.00	0.96	0.99		1.05	0.97	1.00	0.99	0.97	0.99	1.00

Figure 4-7: Normalized results

	T-O 0.20 in/min	Rhiele 0.5 in/min	T-O 0.5 in/min	Satek match D3	T-O 0.20 in/min	S-E 50 ksi/min	Satek 50 ksi/min	T-O 0.2 in/min	Satek 50 ksi/min	S-E 50 ksi/min	T-O 0.20 in/min	Satek match N3	T-O 0.5 in/min	Rhiele 0.5 in/min	T-O 0.20 in/min
	B3	**C3**	**D3**	**E3**	**F3**	**G3**	**H3**	**I3**	**J3**	**K3**	**L3**	**M3**	**N3**	**O3**	**P3**
UY	0.00	0.82	-0.85	0.70	0.00	-1.65	-2.13	47.68	0.90	0.30	0.00	-0.58	-3.70	-3.80	0.00
LY	0.00	1.26	-0.45	-0.09	0.00	-2.91	-3.56	47.88	-0.38	-0.80	0.00	-1.18	-4.02	-3.25	0.00
static	0.00	-2.60	-1.23	-1.48	0.00	-3.02	-5.14		-1.28	-0.17	0.00	2.99	-2.80	-1.81	0.00

	Satek 100 ksi/min	S-E 100 ksi/min	T-O 0.20 in/min	S-E match D3	Rhiele 0.2 in/min	T-O 0.20 in/min	T-O match P2	T-O match C2	T-O match C1	T-O 0.20 in/min	Rhiele 0.2 in/min	S-E match N3	T-O 0.20 in/min	S-E 100 ksi/min	Satek 100 ksi/min
	B2	**C2**	**D2**	**E2**	**F2**	**G2**	**H2**	**I2**	**J2**	**K2**	**L2**	**M2**	**N2**	**O2**	**P2**
UY	0.70	0.61	0.00	0.43	-0.16	0.00	-0.83	1.14	2.96	0.00	-0.27	1.20	0.00	0.51	2.47
LY	0.10	-0.32	0.00	0.40	-0.23	0.00	-1.42	0.93	2.57	0.00	-1.41	0.99	0.00	-0.10	2.40
static	-4.14	-2.72	0.00	-2.16	0.80	0.00	-0.60	2.89	4.22	0.00	-2.11	-1.41	0.00	-0.60	0.05

	T-O 0.20 in/min	Rhiele 0.05 in/min	T-O 0.05 in/min	T-O 0.5 in/min	T-O 0.20 in/min	Satek 10 ksi/min	S-E 10 ksi/min	T-O 0.2 in/min	S-E 10 ksi/min	Satek 10 ksi/min	T-O 0.20 in/min	T-O 0.500 in/min	T-O 0.05 in/min	Rhiele 0.05 in/min	T-O 0.20 in/min
	B1	**C1**	**D1**	**E1**	**F1**	**G1**	**H1**	**I1**	**J1**	**K1**	**L1**	**M1**	**N1**	**O1**	**P1**
UY	0.00	1.65	2.69	3.01	0.00	-0.04	-1.28	46.59	1.16	1.78	0.00	1.10	-2.78	-0.88	0.00
LY	0.00	1.80	2.32	2.83	0.00	-0.73	-1.69	46.59	0.32	0.76	0.00	1.61	-2.17	-0.18	0.00
static	0.00	-0.15	2.40	1.81	0.00	-1.62	-0.47		2.21	-1.07	0.00	-0.26	-1.26	-0.25	0.00

Figure 4-8: Difference between absolute yield strengths and base line yield strengths

the average difference between such values is 1.40 ksi. A similar result is obtained for the upper yield strengths.

Given these irregular results and the apparent large variation in material strength, the only reliable comparison of machines may be that obtained by averaging the results. Since the specimens are well distributed around the plate, the influence of material variation should be the same for each machine. Table 4-4 shows the average of all tests including the base line tests, columns 1; all tests minus P1, P2 and P3, column 2; the first six specimens listed under each machine in Table 4-3 which are equally distributed around the plate, column 3; and these six specimens minus P2, column 4.

Table 4-4: Average lower and upper yields reported by testing machines

Machine [1]	Avg	Machine [2]	Avg	Machine [3]	Avg	Machine [4]	Avg
Upper Yield							
Satek	48.46	Satek	47.56	Satek	48.51	Riehle	47.47
S-E	47.55	S-E	47.55	Riehle	47.47	S-E	47.39
Riehle	47.47	Riehle	47.47	S-E	47.39	Satek	47.27
T-O	47.46	T-O	46.95	T-O	46.59	T-O	46.59
Lower Yield							
Satek	47.49	Riehle	47.30	Satek	47.55	Riehle	47.30
T-O	47.33	S-E	46.82	Riehle	47.30	S-E	46.45
Riehle	47.30	T-O	46.81	S-E	46.45	T-O	46.37
S-E	46.82	Satek	46.46	T-O	46.37	Satek	46.13

For the upper yield, the Tinius-Olsen reports the lowest value for all combinations considered. For the lower yield, the order is consistent only for the cases where the “P” specimens are omitted. In these cases, the Satek reports the lowest lower yield and the Riehle machine reports the highest.

The magnitude difference between the average of each machine is more significant than the actual order. The largest difference between any two machines for a given combination is 1.92 ksi. This suggests that for normal production testing, the use of different machines may only account for a small variation in the results reported by different mills or by independent testing laboratories.

Strain rate sensitivity is found by plotting yield strength against strain rate and fitting a straight line to the data as shown in Figure 4-9 (a) and (b) for all plate specimens. Table 4-5 lists the results obtained from plotting the same combinations used in comparing machines. The average increase in lower yield for the different combinations is 0.82 ksi per decade increase in strain rate. This is lower than the 1.4 ksi value found by Gray and Sharp (1989) and Johnson and Murray (1967). The strain rate sensitivity of the upper yield for these tests is less than the lower yield. This disagrees with the findings of others (Gray and Sharp 1989, Johnson and Murray 1967, Chang and Lee 1987). This is most likely due to the absence of a yield point for most of the specimens.

Table 4-5: Strain rate sensitivity for various combinations of specimens

Increase in yield strength per decade increase in strain rate				
[1]	[2]	[3]	[4]	Avg
Upper Yield				
0.80	1.03	0.75	0.70	0.82
Upper Yield				
0.49	0.56	0.40	0.27	0.43

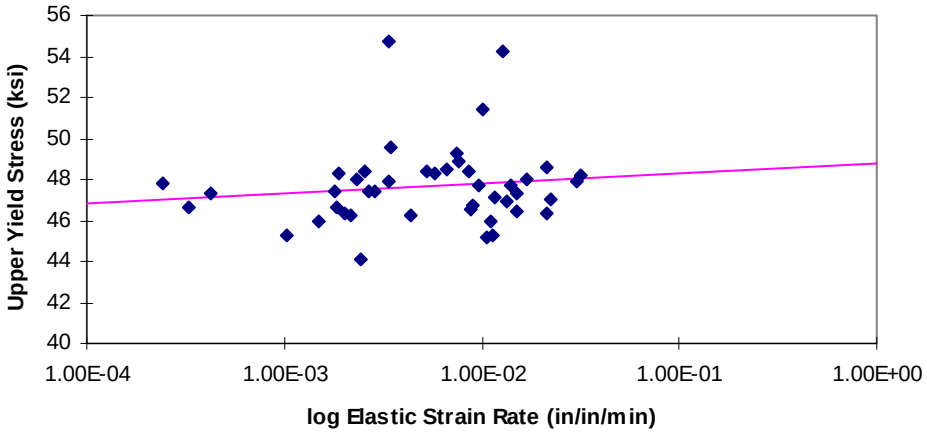

(a)

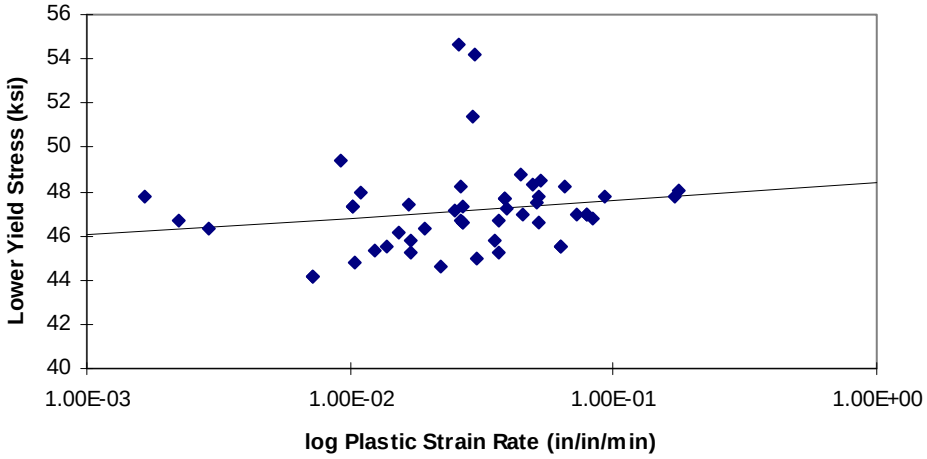

(b)

Figure 4-9: Strain rate sensitivity of plate specimens: (a) upper yield; and (b) lower yield.

Static Yield Table 4-6 shows the average static yield strengths using the same combinations of tests as above. The Satek machine reports the lowest static yield in all cases. If the static yield is independent of the machine, and, as above, assuming the material variation to be uniformly distributed among the specimens, then one would expect very close agreement in these values. However, the largest difference between the average of any two machines for a given case is 2.97 ksi which is greater than that found for either the upper or lower yield.

Table 4-6: Average static yields reported by testing machines

Machine [1]	Avg	Machine [2]	Avg	Machine [3]	Avg	Machine [4]	Avg
T-O	44.13	Riehle	43.57	T-O	43.60	T-O	43.60
Riehle	43.57	T-O	43.55	Riehle	43.57	Riehle	43.57
S-E	42.52	S-E	42.52	S-E	42.68	S-E	42.68
Satek	42.18	Satek	41.18	Satek	42.05	Satek	40.63

The strain rate sensitivity of the static yield for each machine is shown in Figure 4-11. The solid lines are an average of the data points and demonstrate that the static yield is dependent on the plastic strain rate. The data for the Tinius-Olsen contradicts the findings of Tall and Ketter (1958) who used the same machine and found that the static yield was relatively constant with respect to the speed of the test.

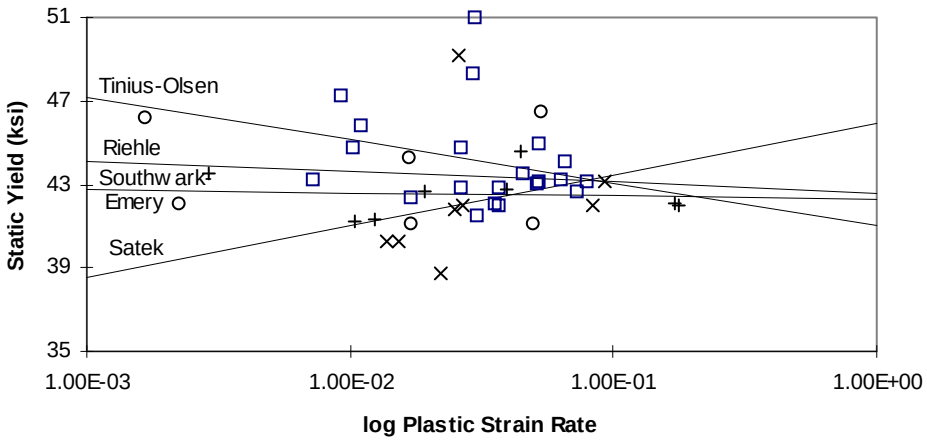

Figure 4-10: Strain rate sensitivity of the static yield

4.3 W36X150 WEB SPECIMENS

4.3.1 General Summary of Results

Specimens 4A to 6A and 4B to 6B were tested by Bo Jaquess at the University of Texas. These tests were conducted as part of a Round Robin sponsored by the American Institute of Steel Construction and will published along with the results from other labs in an upcoming report.

The upper yield, the average lower yield and the static yield strengths for all W36x150 web specimens are listed in Table 4-7. The stress-strain curves for each of the specimens are included in Appendix A2.

Table 4-7: Test Results of W36x150 specimens

Specimen	Machine	Test Speed	Area (in^2)	Load			Stress		
				Yld Pt (kip)	Plateau (kip)	Stat Yld (kip)	Up Yld (ksi)	Lwr Yld (ksi)	Stat Yld (ksi)
3A	T-O	0.4 in/min	0.9820	61.40	61.45	57.90	62.53	62.58	58.96
2A	Satek	115 ksi/min	1.0034	61.98	60.38	47.53	61.77	60.18	47.36
1A	Satek	11 ksi/min	0.9938	60.68	60.09	47.53	61.06	60.47	47.82
4A	T-O	0.05 in/min	0.9853	62.76	60.89	58.43	63.70	61.80	59.30
5A	T-O	2.0 in/min	0.9854	66.91	61.78	57.55	67.90	62.70	58.40
6A	T-O	0.4 in/min	1.4997	96.88	93.28	88.03	64.60	62.20	58.70
4B	T-O	0.4 in/min	1.0137	66.09	62.34	58.80	65.20	61.50	58.00
5B	T-O	0.05 in/min	1.0161	65.03	61.98	59.65	64.00	61.00	58.70
6B	T-O	1.5 in/min	1.0062	65.70	63.69	58.76	65.30	63.30	58.40
1B	Satek	58 ksi/min	1.0026	63.54	60.58	48.18	63.38	60.42	48.05
2B	Satek	8 ksi/min	0.9970	62.24	58.73	47.27	62.43	58.90	47.41
3B	T-O	0.4 in/min	0.9849	62.40	62.49	59.40	63.36	63.45	60.31

The lowest and highest values of yield strength are 47.36 ksi and 67.90 ksi. The former is a static yield measurement. Considering only ASTM designated yield strengths, the range becomes 58.90 ksi to 68.02 ksi. This is a difference of 9.12 ksi. Considering the average lower yield strength only, the range is 58.90 ksi to 64.79, a difference of 5.89 ksi.

The test results for the W36x150 web specimens shown in Table 4-7 rather graphically illustrate the potentially large variations possible in measured yield strength for a sample of steel. Depending on the coupon location, type of testing machine used, speed of testing, and definition of yield strength (upper, lower or static yield), the reported yield strength for the web of the W36x150 can vary from 47 to 68 ksi, i.e., a 21 ksi variation! Examination of the data in Table

4-7 suggests that the factor causing the largest variation is the definition of yield stress. For example, for specimen 2B, the difference between the upper yield point and the static yield is approximately 15 ksi. The influence of testing variables on the reported yield strength is discussed further in the following section.

4.3.2 INFLUENCE OF TESTING VARIABLES ON THE YIELD STRENGTH

Upper and Lower Yield Strengths The test results demonstrate the influence of testing procedures on the yield strength and suggest a pattern of material variation along the depth of the web. The upper and lower yield strengths of the six interior specimens tested in the Tinius-Olsen machine are controlled by the speed of the test. The yield strengths increase with testing speed with little apparent influence from material variation.

The yield strengths of the specimens tested by the Satek machine drop sharply from the adjacent Tinius-Olsen specimens. If a straight line interpolation between the specimens at the K-line and specimens 4A and 6B is assumed, then the results suggest that the Satek machine reports a lower yield than the Tinius-Olsen. However, with plastic deformation occurring in the first few inches of the web during the straightening process (see Section 2.2.2), it is likely that the specimens at the K-line will be stronger than adjacent specimens. It is possible, therefore, that the strength decreases slightly at the third points then increases sharply at the K-line. This is the general pattern shown in Massonet and Save (1965).

Further evidence of this includes the slight drop in lower yield strength from specimen 1A to 2A despite a ten-fold increase in testing speed while the strength drops substantially on the other side of the web for a drop in testing speed of similar magnitude. This suggests that the arrangement of testing speeds for the outer specimens on side B of the web compliment the material variation while on side A the testing speeds work against it.

Given this, the difference in yield strength reported by the two machines is difficult to ascertain. It does not seem likely that the Tinius-Olsen machine would report lower strengths than the Satek as the apparent material variation at these locations in the web would then be even greater. The relatively large differences in lower yield strength between the four Satek specimens and those adjacent to them, 2.88 ksi, 4.46 ksi, 1.33 ksi and 2.35 ksi, are greater than the difference between any other two adjacent specimens.

The most plausible conclusion is that the Satek machine reports a similar yield strength as the Tinius-Olsen, and may even report a lower strength, but that it seems unlikely that it reports a higher yield.

The strain rate sensitivity of the upper yield is greater than that of the lower yield. This is shown in Figure 4-11. According to these results, the upper yield strength increases 2.15 ksi per decade increase in elastic strain rate compared to 1.77 ksi for the lower yield. Consistent with the findings discussed in Section 4.1.2, the Satek specimens are seen to lie toward the lower end of the strain rates.

The yield drop from upper to lower yield does not seem to be greater for one machine over another. No yield drop was recorded for the specimens at the

K-line. One possibility for this may be the partial yielding of the web as described in Section 2.2.2 and shown in Illustration 2-1. The outside edge of these specimens was approximately 2 inches from the K-line. Yielding in this area does not appear to be uniform and, therefor, the mechanical properties will vary across the area of

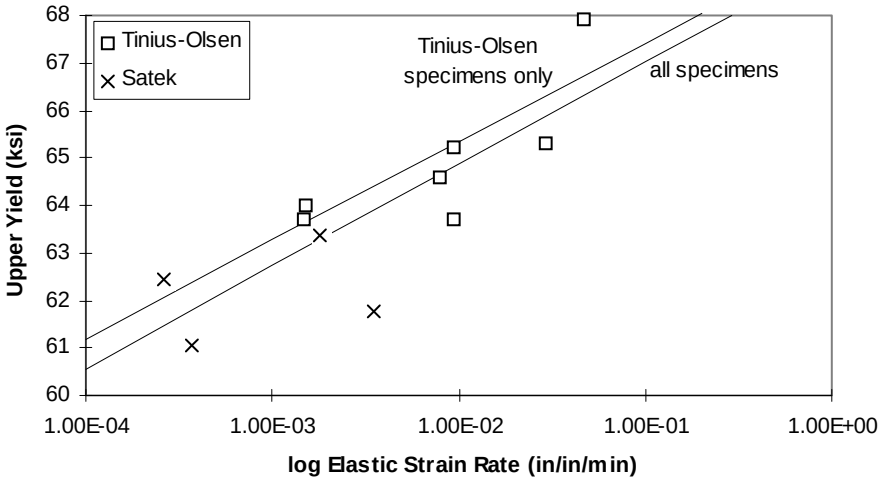

(a)

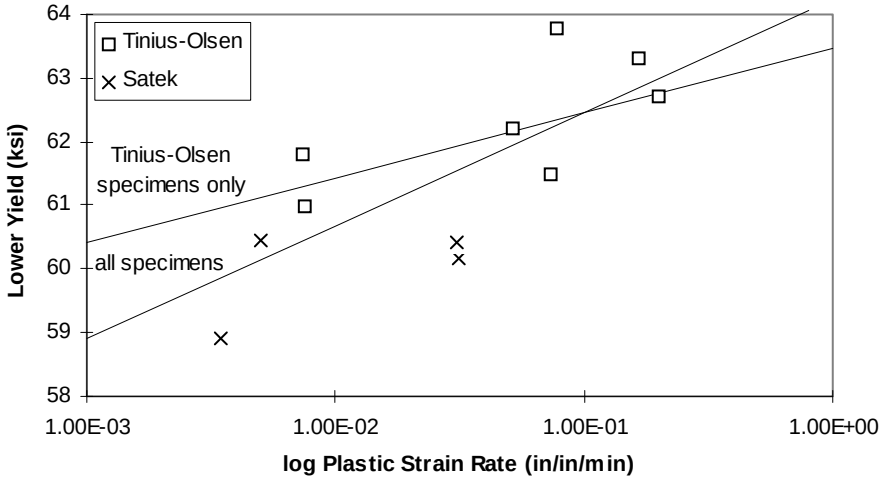

(b)

Figure 4-11: Strain rate sensitivity of W36x150 web specimens: (a) upper yield vs. elastic strain rate, and; (b) lower yield vs. elastic strain rate.

the specimen. During a test, portions of the specimen are yielding at different loads in a way similar to a specimen being poorly aligned in the grips. This has been shown to eliminate the yield point (Welter and Gockowski 1938). This hypothesis needs further study.

Static Yield The range in static yield strengths for each machine is less than the range of upper and lower yields. The average static yield drop reported by the Satek machine is 12.3 ksi compared to 3.5 ksi for the Tinius-Olsen machine.

4.4 DISCUSSION OF THE STATIC YIELD TEST

4.4.1 Interpretation of Test Results

In Sections 4.2.3 and 4.3.3 the static yield test results were presented. A number of problems were encountered in the testing and in the interpretation of the data which may have compromised the accuracy of the results. These include the behavior of the machines during the test and the performance of the data acquisition system.

Machines The change in load during the test is dependent on the performance of the machine. When the Tinius-Olsen machine is stopped, the load immediately drops about 200 pounds in an apparent response to the gears being

disengaged. For the plate specimens used in these tests, this load drop equates to about 0.5 ksi which is about 15% of the average static yield drop.

In the case of the hydraulic machines, the amount of load drop varied with the procedure. For the Satek machine, if the valve was shut off and the pump left on, the load would drop to a certain level after approximately 2 minutes, then begin to climb. If the pump was turned off, the load dropped to a lower value. Both procedures were employed for specimens E3 and M3. The latter is shown in Figure 4-12. The difference between the two static yields is 2.92 ksi.

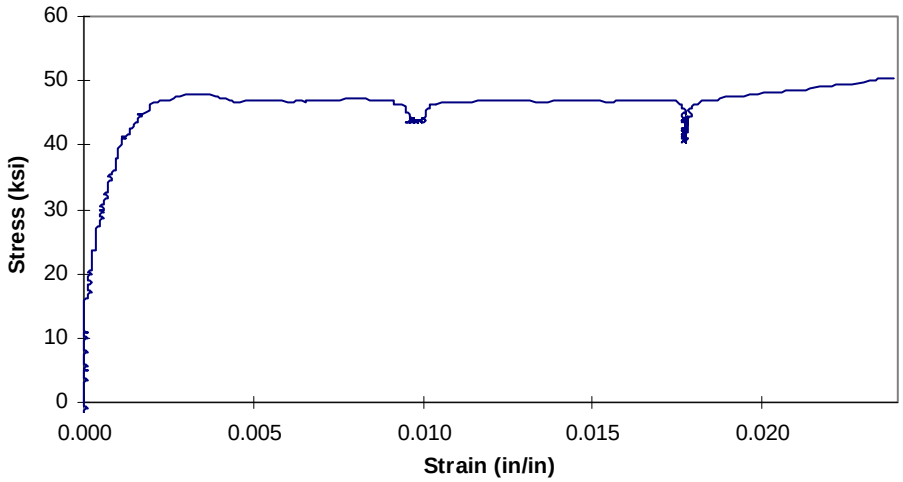

Figure 4-12: Stress-strain curve at yield plateau for specimen M3

For the Southwark-Emery, if both the valve and the pump were turned off, the load dropped sharply.

All static yields reported in the results were found with the pump off for the Satek machine and the pump on for the Southwark-Emery machine. In both cases, the load did not stabilize after 3 minutes. The stress-time curves in

Appendix 3 clearly show the stress decreasing throughout the static yield test. In only one test (W36 - 2B) was this unloading accompanied by a strain reversal.

Data Acquisition It is possible that strain reversal was occurring but that the extensometer did not record it. The extensometer was, at times, insensitive to small changes in the strain. Evidence of this includes stress-strain curves which report no change in strain up to about 0.5Fy or even higher followed by a sudden change in slope. Also, a specimen was loaded a number of times to approximately 0.8Fy then unloaded completely. In most cases, the extensometer reported a substantial residual strain even though the specimen was likely still elastic.

4.4.2 Validity of the Static Yield Test

Machines It is apparent that in most cases the static yield is partly a measure of machine relaxation. Evidence in the literature to support this was briefly presented in Section 2.4. The results of the machine relaxation tests described in Section 3.7 are summarized in Table 4-8 along with the average load drop recorded during static yield tests of all plate specimens. It is clear that a significant portion of the drop in load attributed to the static yield may actually be a function of the machine. It also appears that the greatest relaxation occurs for the hydraulic machines. This may be due, at least in part, to a small amount of leakage of the hydraulic fluid at the seals or valves.

Table 4-8: Machine relaxation tests

Load to	Drop to	Difference	
(kip)	(kip)	(kip)	(ksi)

Tinius-Olsen			
17.30	16.85	0.45	1.24
17.95	17.60	0.35	0.96
16.00	15.75	0.25	0.69
Satek			
17.07	14.60	2.47	6.80
16.96	14.79	2.17	5.98
16.77	14.30	2.47	6.80
Southwark-Emery			
16.20	15.40	0.80	2.20
17.25	16.45	0.80	2.20
17.08	16.33	0.75	2.07

A detailed look at the stress-strain curves during the static yield test indicate different behavior of the machines. In the case of the hydraulic machines, there is a rounding of the curve as the load drops and the deformation continues. This was typically followed by a vertical line as the load dropped without an increase in strain. For the Tinius-Olsen machine, the rounded portion was followed by a gradual negative slope as the deformation continued throughout the test.

Tall and Ketter (1958) argued this was a validation of the static yield test. However, it seems more plausible that this is instead an indication of the machine relaxing. Deformation of a specimen would stop completely in rigid machine. Furthermore, if the deformation does not stabilize, then the concept of a *static* yield falls apart.

Given the ample evidence that machine relaxation affects the results of the static yield tests, the only valid procedure may involve a closed loop machine operated in extensometer control mode to maintain a zero strain rate. This was the type of test conducted by Chang and Lee (1987).

Test Procedure The procedure for determining the static yield test involves stopping the machine and recording the load at the end of three minutes. However, the static yield is by definition the strength of the material corresponding to the point at which the specimen stops deforming ($\dot{\varepsilon} = 0$). This should occur within the three minutes of the standard test and may even occur in the first few seconds. Beyond that, the specimen may be experiencing stress relaxation as discussed in Section 2.4.2.

It was hoped that two values of static yield could be obtained from the test data: the load at the end of the three minutes and the load corresponding to the point of zero deformation; and that the latter would be a more reliable measure of the static yield. While the strain rate slowed to zero in the case of the hydraulic machines, the Tinius-Olsen tests never reached a point of zero strain rate. Also, determining the point at which the specimen stopped deforming was hampered by the precision of the data acquisition system.

Figure 4-13 illustrates this. The change in voltage output from the extensometer is read by the software in discrete steps equivalent to 0.000114 in/in of strain. This represents approximately 1/30 of the strain at yield. At the start of the static yield test, changes in the load are accompanied by relatively small changes in the strain. Unlike the continuous line reported by the data plotter, the software reports a series of steps until a point at which the strain appears to stabilize. As seen in the figure, this may not be the point at which the specimen stops deforming and, therefore, it is not clear which stress corresponds to zero strain rate. This is further complicated by the noise in the system which causes random jumps in the readings as seen in Figure 4-14.

Even if the data problem was resolved, interpretation of these results would need to include the effects of machine relaxation. Recall Guiu and Pratt's (1964) findings that the majority of relaxation occurred in the first 3 to 6 seconds after the machine was stopped.

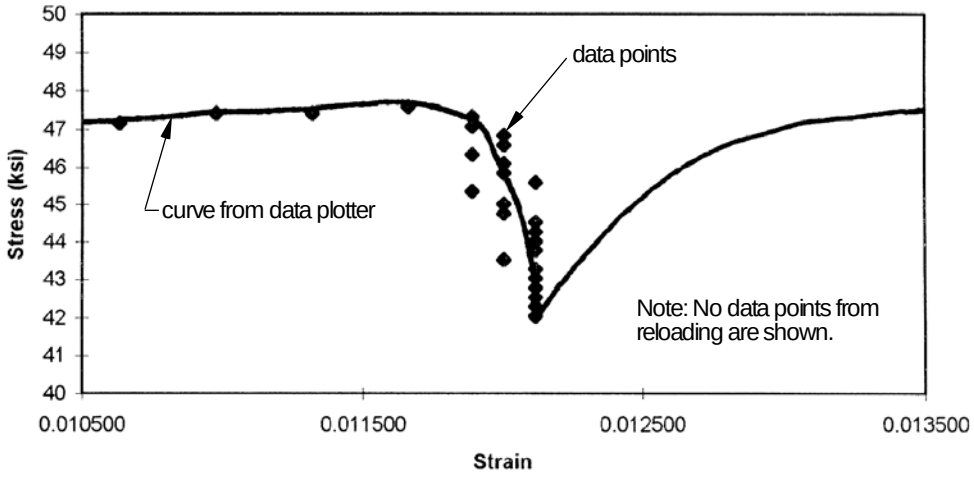

Figure 4-13: Data points and data plotter curve during static yield test

Chapter 5: Conclusion

An experimental study was conducted to evaluate the variations in the measured yield stress of structural steel caused by the use of different test machines and loading rates. This study was motivated by large discrepancies in yield stress measurements between mill certificates and independent laboratory tests recently reported in the literature.

The test results do not prove conclusively that one machine reports a higher or lower yield strength than another. However, it is clear that the difference between machines is not very significant in attempting to reconcile the discrepancy between mill certificates and independent laboratory tests. The largest difference between machines of 1.92 ksi from the plate tests (obtained by averaging the results) is much less than the 16 to 17 ksi reported by Shuey (1996), by Schriber (1996) and by Uang (1995).

Likewise, strain rate sensitivity was not found to be significant. An increase in strain rate from the minimum to the maximum testing speeds permitted by the *Standards*, equal to a factor of ten, should result in an increase in the lower yield strength of only about 1.5 ksi. The interpretation of the ASTM *Standards* in Section 2.5.2 represents a further increase in strain rate equal to the hardness ratio for a given machine. For a hardness ratio of 10, the minimum and maximum testing speeds would differ by a factor of 100 and the increase in lower yield strength from the former to the latter would likely be about 3 ksi.

Based on the results of this study, it appears that only a small portion of the discrepancy in the reported yield strength between mill certificates and independent laboratory tests can be attributed to variations in test procedures, i.e., to the use of different test machines and different strain rates within the current ASTM limits. Variations due to these causes are likely in the range of 3 to 5 ksi. It appears that the bulk of the discrepancy in reported yield strengths may be due to variations in the definition of yield strength (upper vs. lower vs. static yield strength), and variation of material properties throughout a section including variation between flange and web, variation within flange and web, and variation along the length of the member.

Test procedures, therefor, may account for some portion of the discrepancy between mill certificates and independent labs, but the bulk of the difference is likely due to other factors such as the use of the yield point to represent the strength of the material, the sampling of the web rather than the flange and variation in the mechanical properties of the material.

Test results also suggest that the measured static yield strength is machine and strain rate dependent. Beyond these findings, no firm conclusion is drawn regarding the reliability or even the validity of the static yield test. The study points out some possible shortcomings in the technique which should be investigated further before the static yield is proposed for material standardization. These include the effects of machine relaxation, variation in the machine response to the static yield test, the duration of the test, and the influence of stress relaxation on the test results.

Appendix A1

A1 CALIBRATION

A1.1 Extensometer

The output calibration of the extensometer was 2.135 mV/V, i.e., 2.135 mV of output signal per volt of excitation when the extensometer is fully extended. This was verified by an Epsilon shunt calibration module. With an excitation of 10 volts and the output signal amplified 500 times, the resulting voltage-deformation curve had a slope of 5.3385 volts/inch. This was verified by imposing a series of known displacements and recording the output signals. This was accomplished using a milling machine with digital displacement readout accurate to 0.0005 inch.

A1.2 Load Indicating Systems

Accuracy of Load Indicators The load indicator of each machine was checked using a Strainsense Load Cell System with a 100 kip load cell which had been calibrated by National Standards Testing Laboratory in May 1997. All machines agreed closely with the Strainsense load cell.

Load-Voltage Curve The slope of the load-voltage curve was required to convert the voltage read by Lab View to engineering units. For each machine, Table 4-1 lists the excitation voltage, the load scale, the load-voltage curve based on full scale and the curve based on data from loading a specimen a number of times from zero to 30 kips in roughly 2 kip increments and recording the voltage. The slope of the curve was found by fitting a straight line through the data using a

regression analysis. In the case of the Satek machine, the Strainsense load cell was used in place of the specimen.

Table A1-1: Load-voltage calibration

Machine	Excitation Voltage	Load Scale	Slope of Load-Voltage Curve (V/kip)	
			Full Scale	From Data
Tinius-Olsen	10 Volts	0 to 120 kip	0.0833	0.0704
Satek	10 Volts	0 to 300 kn (67.45 kip)	0.1483	0.1483
	10 Volts	0 to 1200 kn (269.78 kip)	0.0371	0.0374
Southwark-Emery	10 Volts	0 to 60 kip	0.1667	0.1667
Riehle	10 Volts	0 to 600 kip	0.0167	0.0266

In all cases the slope found from the data was used in the analysis of test data.

Appendix A2

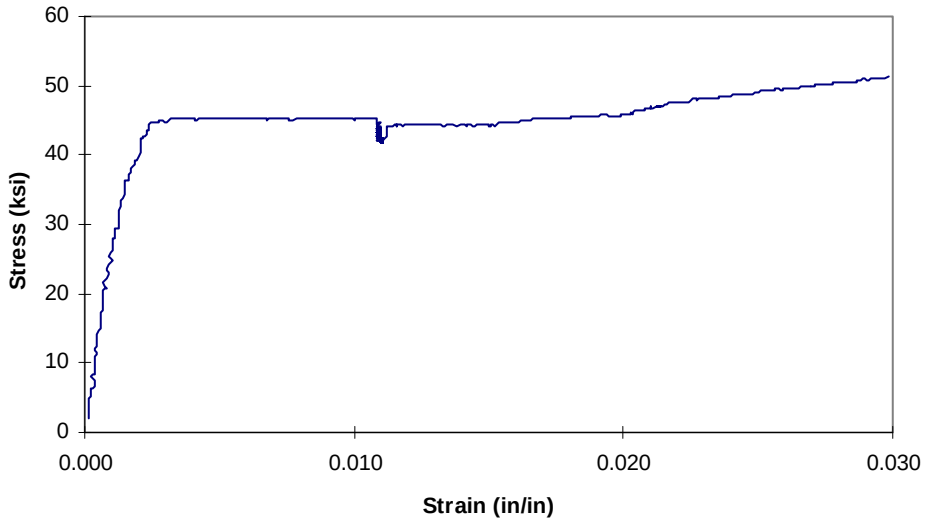

Figure A2-1: Specimen B1. Stress-strain curve: zero through start of strain hardening.

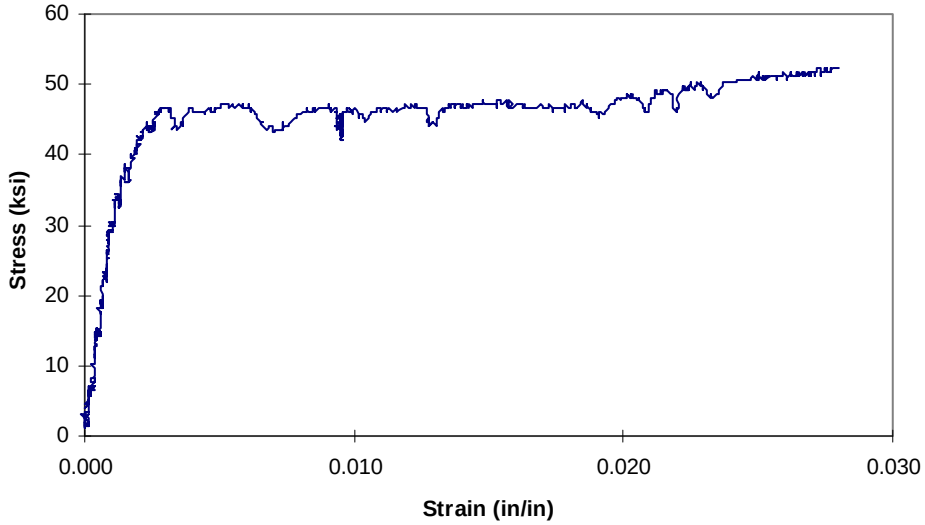

Figure A2-2: Specimen C1. Stress-strain curve: zero through start of strain hardening.

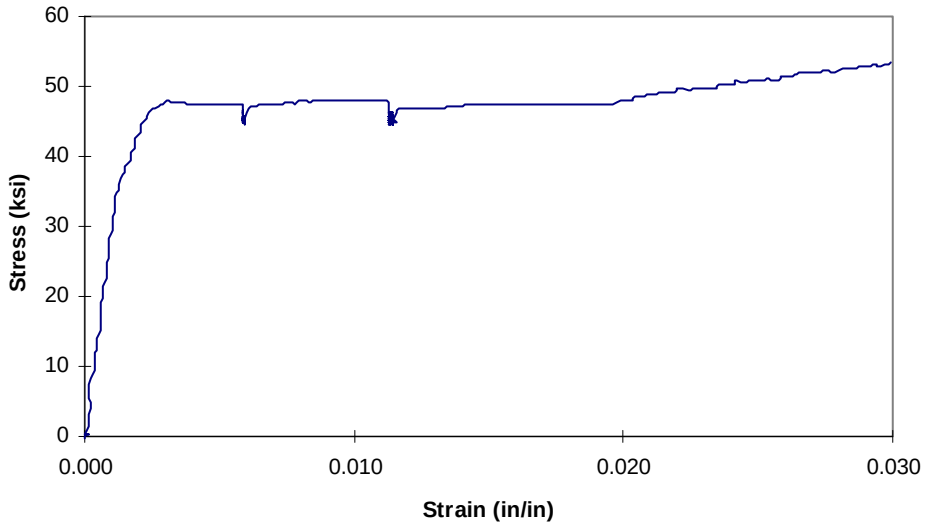

Figure A2-3: Specimen D1. Stress-strain curve: zero through start of strain hardening.

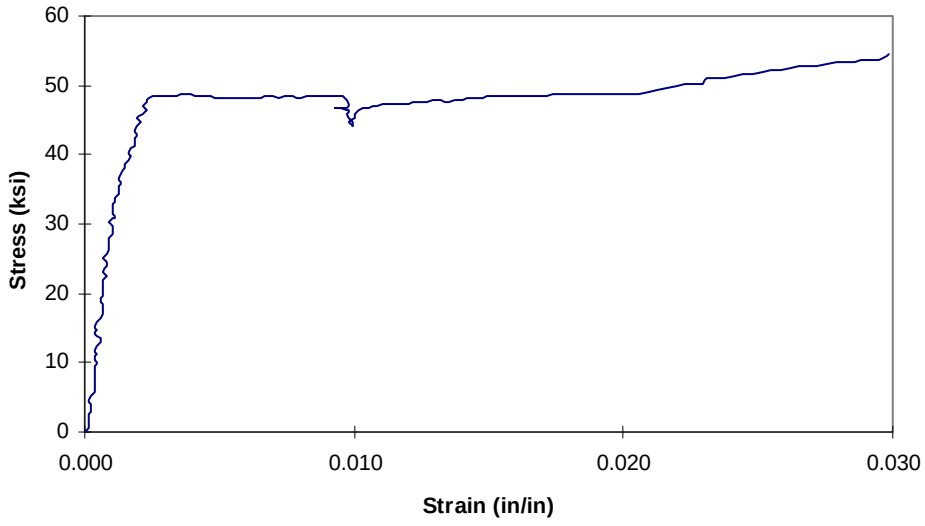

Figure A2-4: Specimen E1. Stress-strain curve: zero through start of strain hardening.

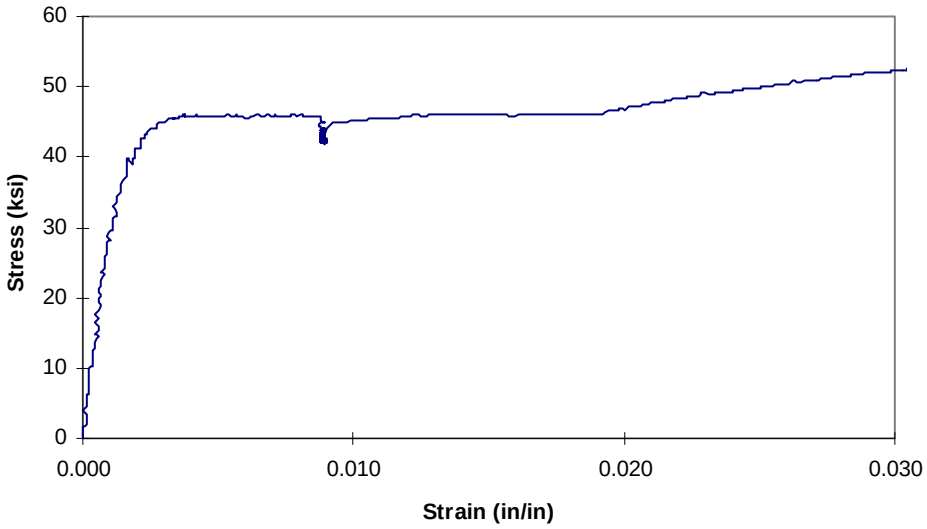

Figure A2-5: Specimen F1. Stress-strain curve: zero through start of strain hardening.

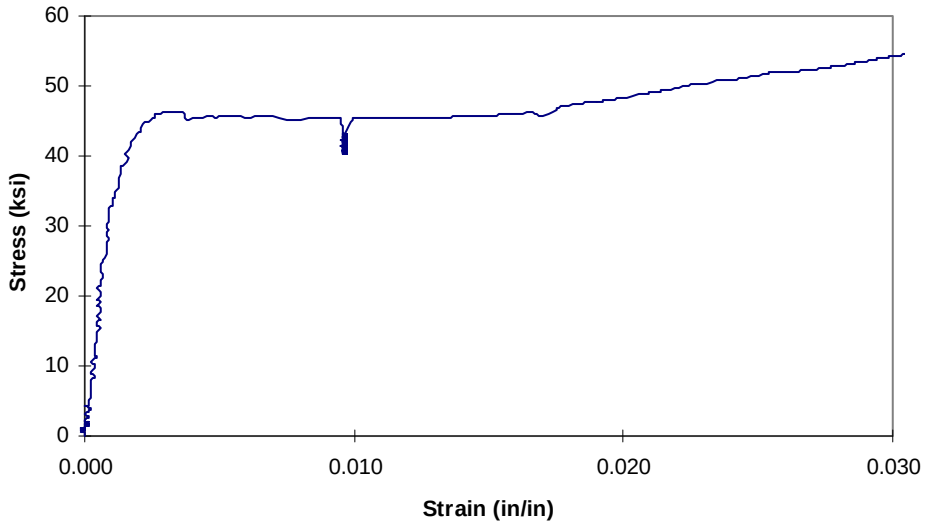

Figure A2-6: Specimen G1. Stress-strain curve: zero through start of strain hardening.

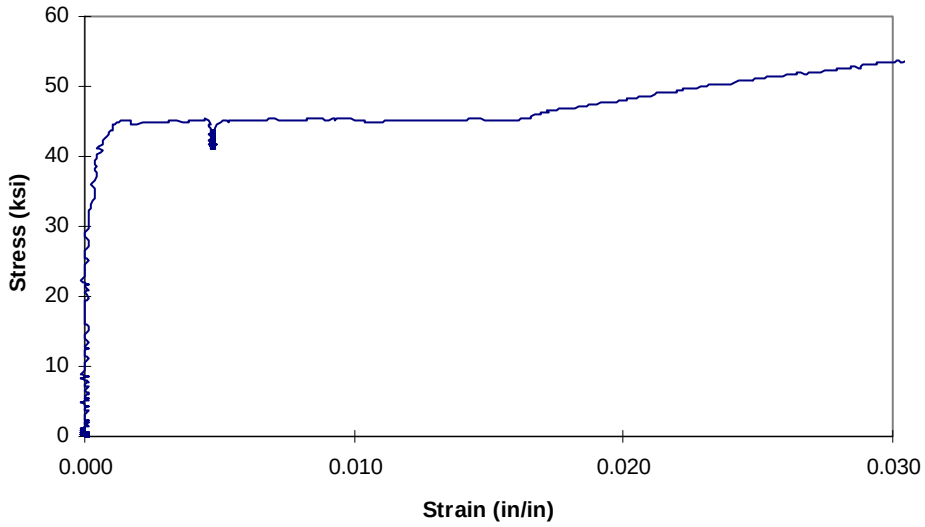

Figure A2-7: Specimen H1. Stress-strain curve: zero through start of strain hardening.

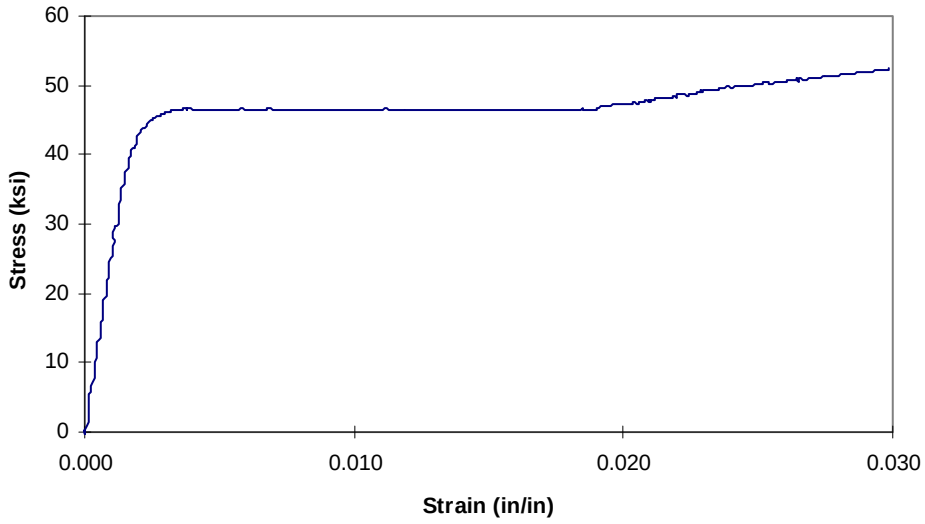

Figure A2-8: Specimen I1. Stress-strain curve: zero through start of strain hardening.

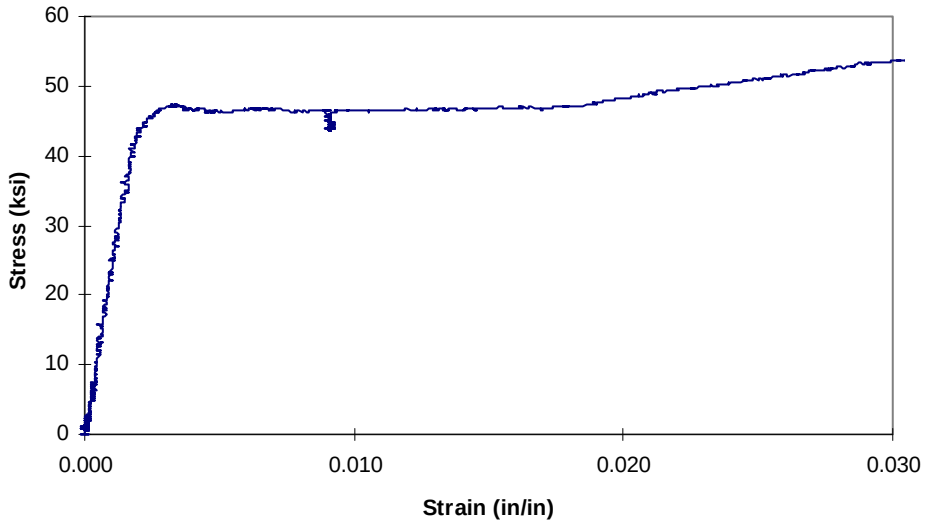

Figure A2-9: Specimen J1. Stress-strain curve: zero through start of strain hardening.

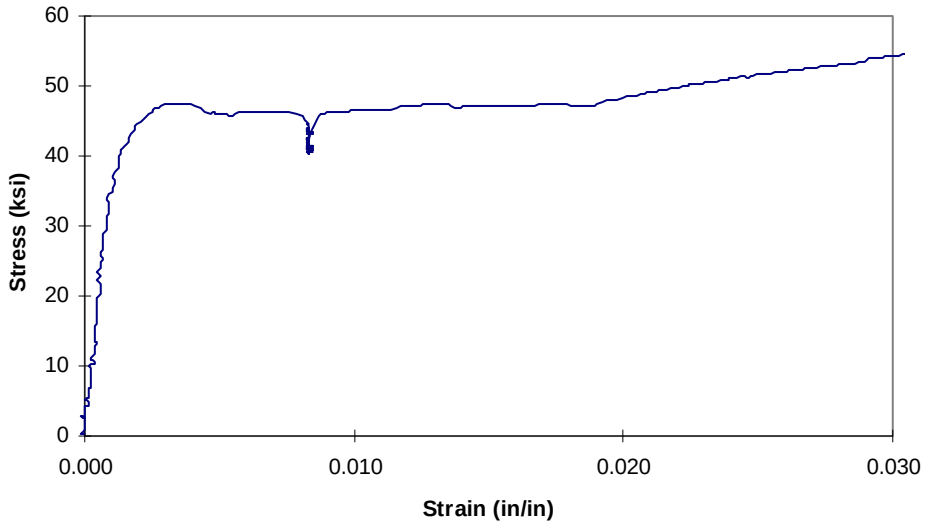

Figure A2-10: Specimen K1. Stress-strain curve: zero through start of strain hardening.

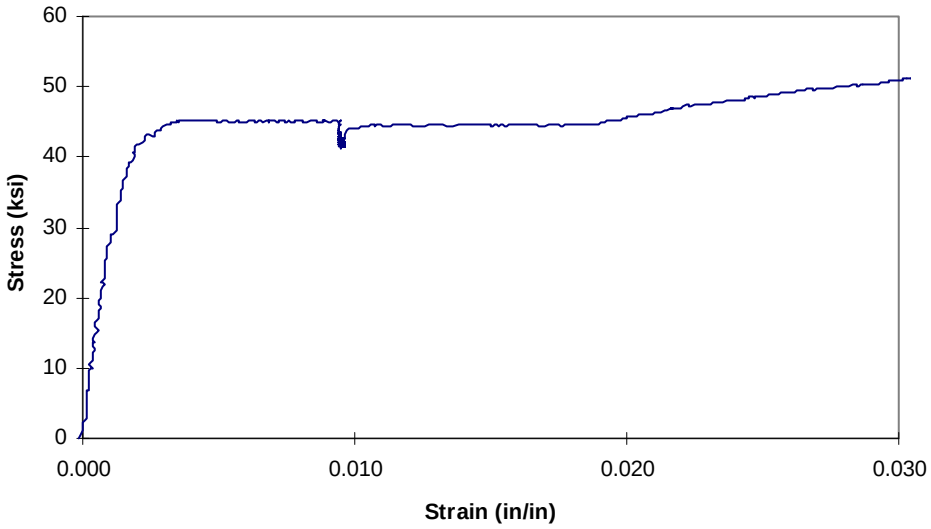

Figure A2-11: Specimen L1. Stress-strain curve: zero through start of strain hardening.

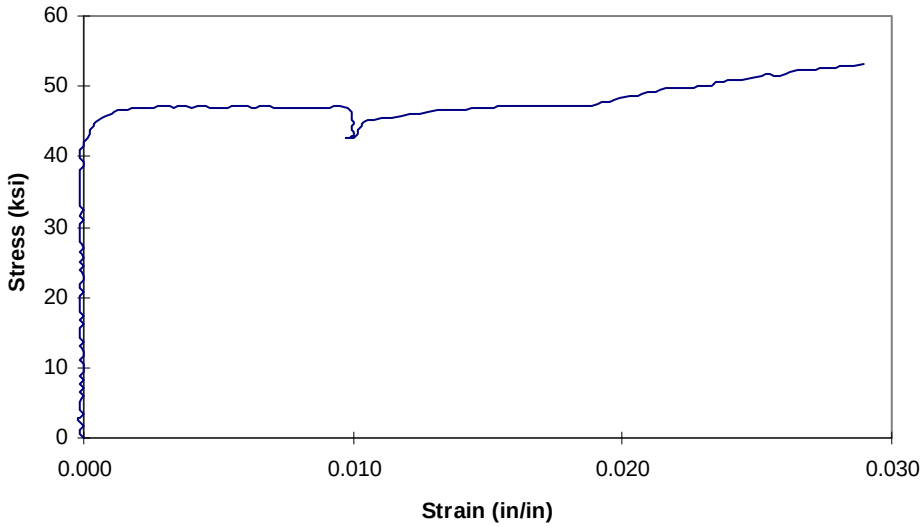

Figure A2-12: Specimen M1. Stress-strain curve: zero through start of strain hardening.

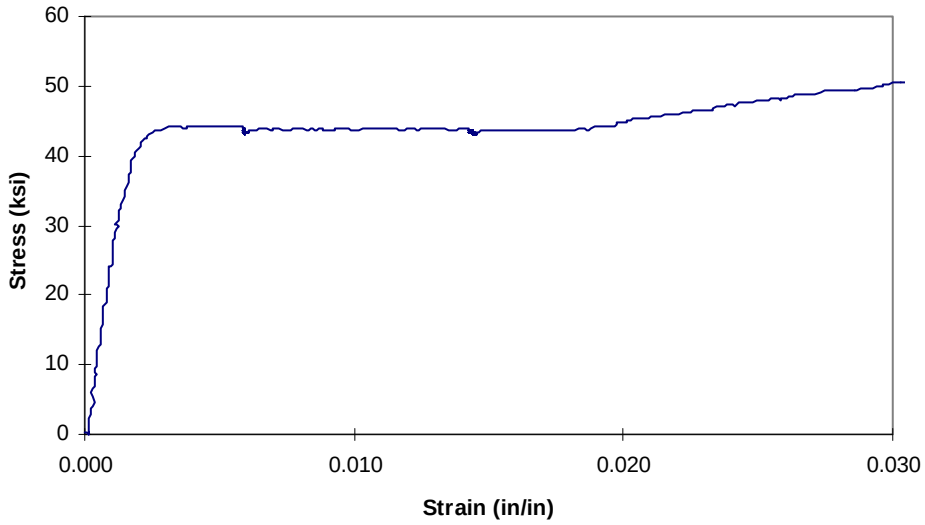

Figure A2-13: Specimen N1. Stress-strain curve: zero through start of strain hardening.

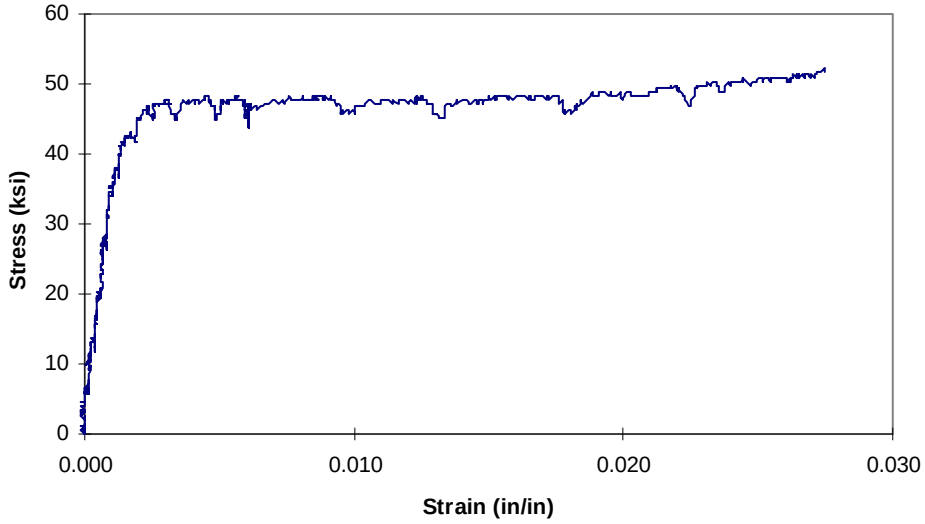

Figure A2-14: Specimen O1. Stress-strain curve: zero through start of strain hardening.

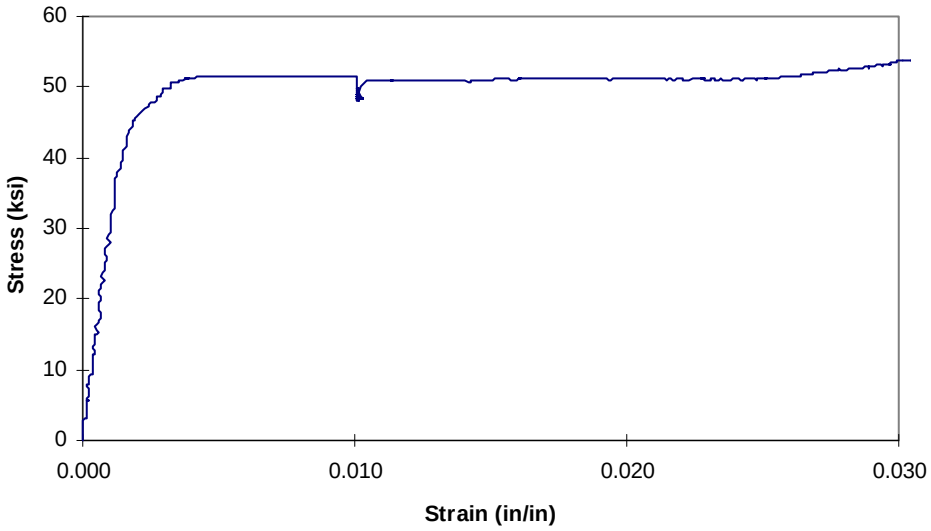

Figure A2-15: Specimen P1. Stress-strain curve: zero through start of strain hardening.

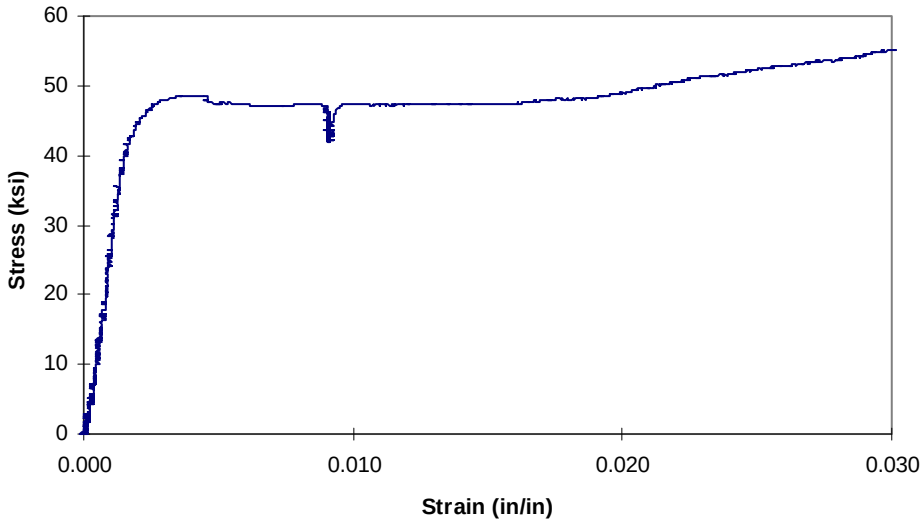

Figure A2-16: Specimen B2. Stress-strain curve: zero through start of strain hardening.

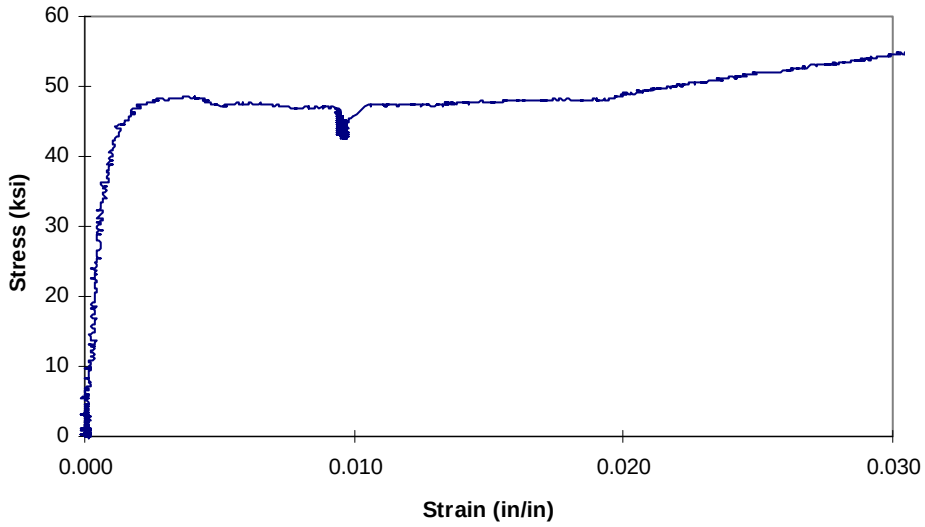

Figure A2-17: Specimen C2. Stress-strain curve: zero through start of strain hardening.

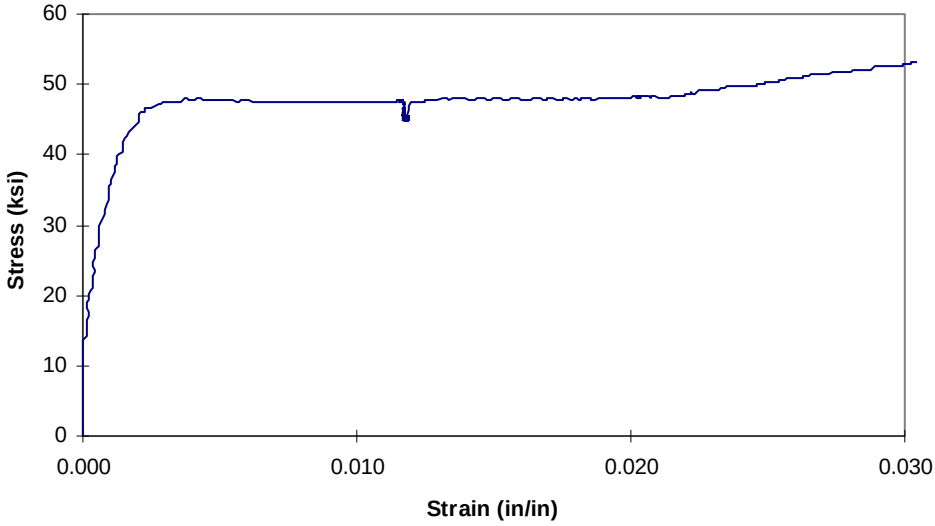

Figure A2-18: Specimen D2. Stress-strain curve: zero through start of strain hardening.

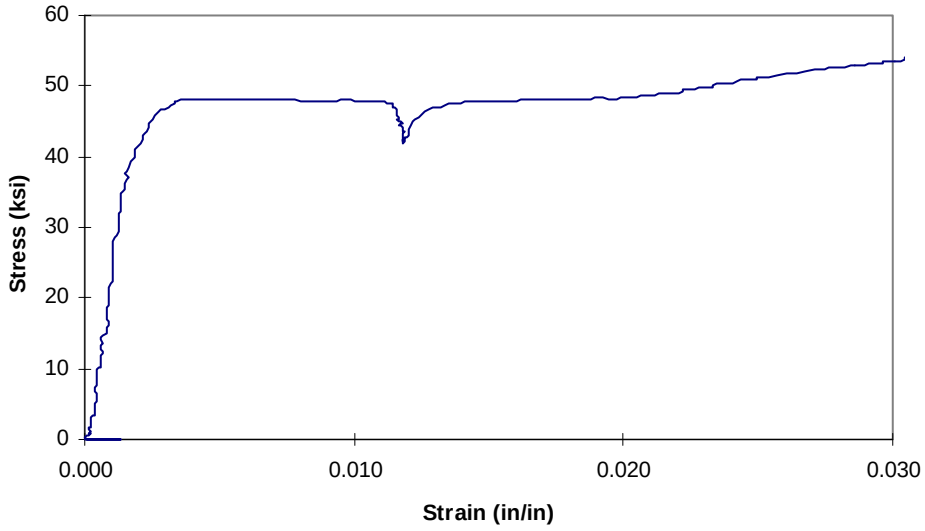

Figure A2-19: Specimen E2. Stress-strain curve: zero through start of strain hardening.

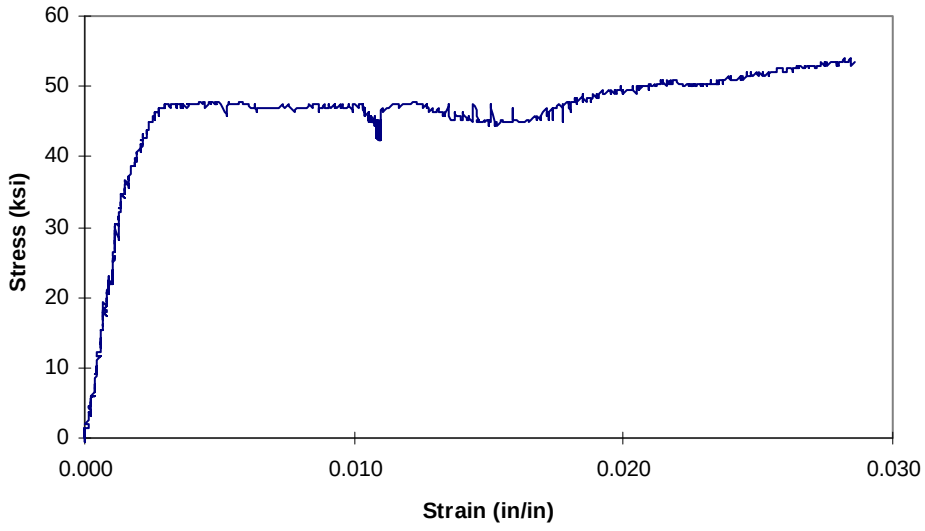

Figure A2-20: Specimen F2. Stress-strain curve: zero through start of strain hardening.

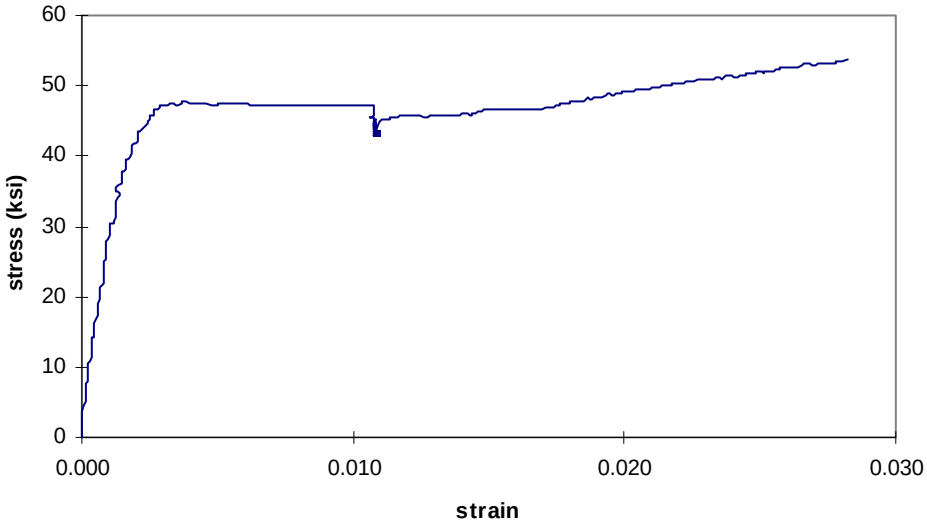

Figure A2-21: Specimen G2. Stress-strain curve: zero through start of strain hardening.

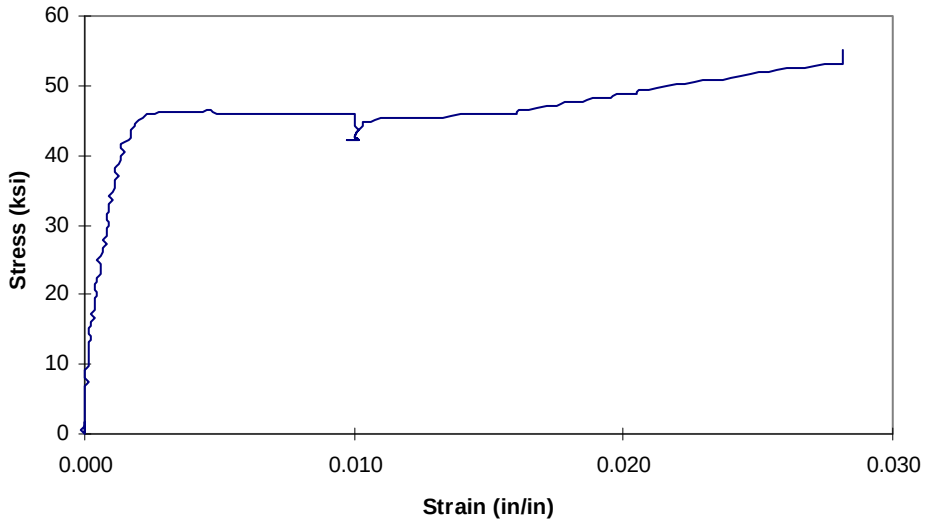

Figure A2-22: Specimen H2. Stress-strain curve: zero through start of strain hardening.

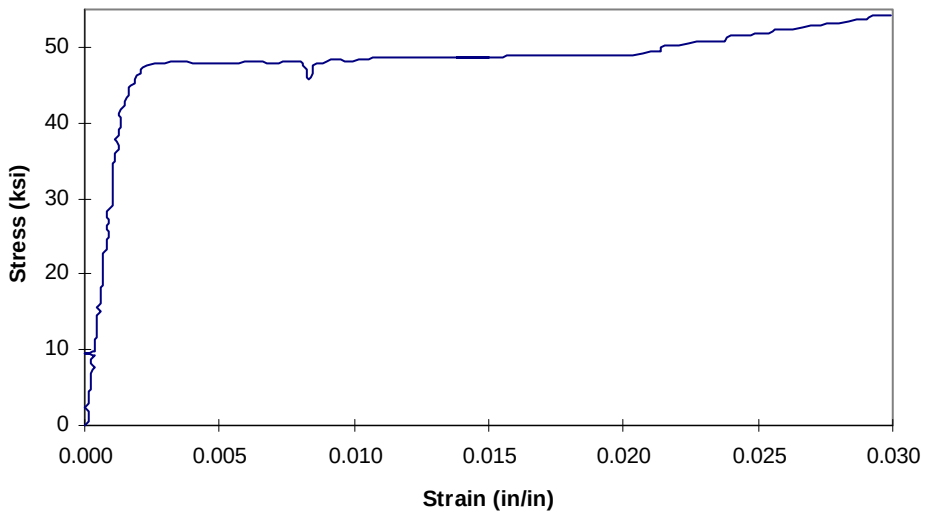

Figure A2-23: Specimen I2. Stress-strain curve: zero through start of strain hardening.

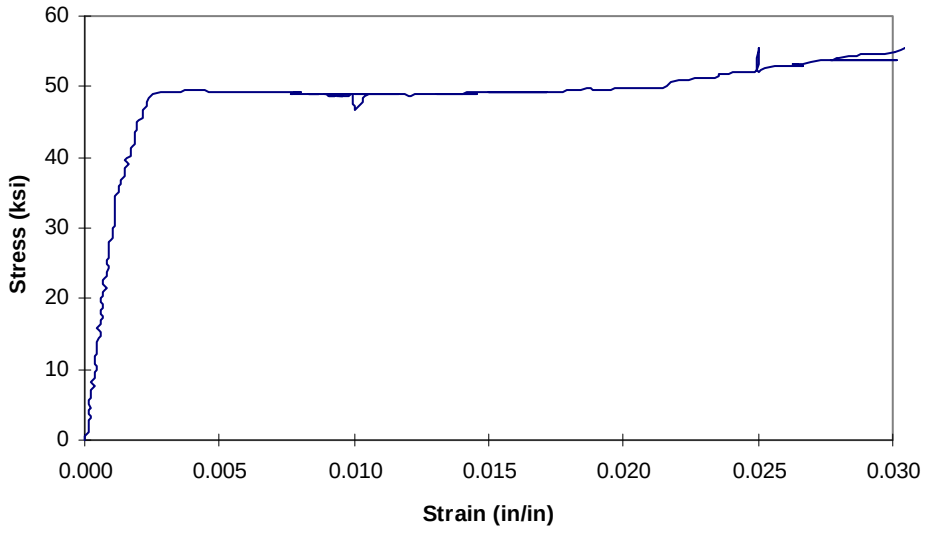

Figure A2-24: Specimen J2. Stress-strain curve: zero through start of strain hardening.

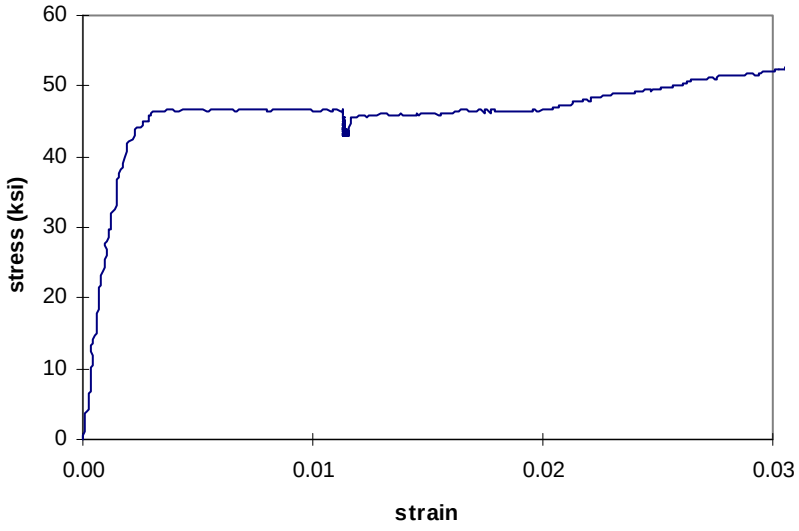

Figure A2-25: Specimen K2. Stress-strain curve: zero through start of strain hardening.

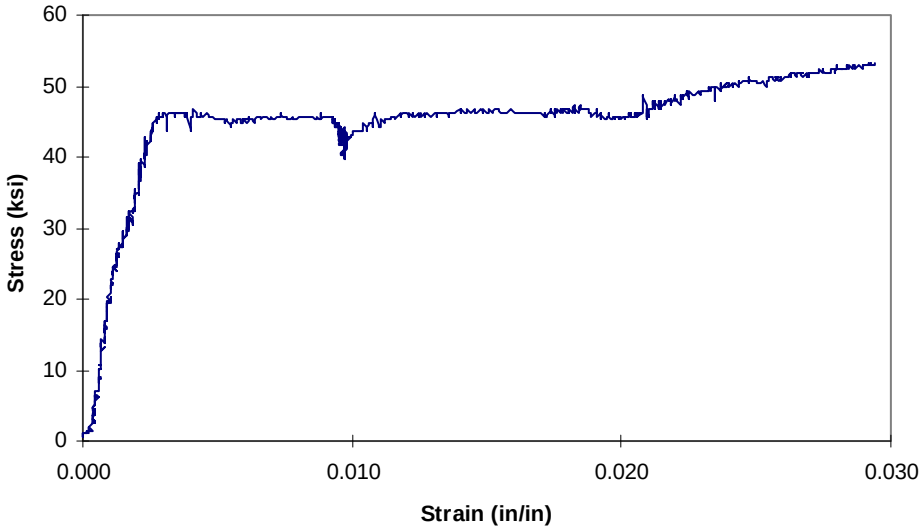

Figure A2-26: Specimen L2. Stress-strain curve: zero through start of strain hardening.

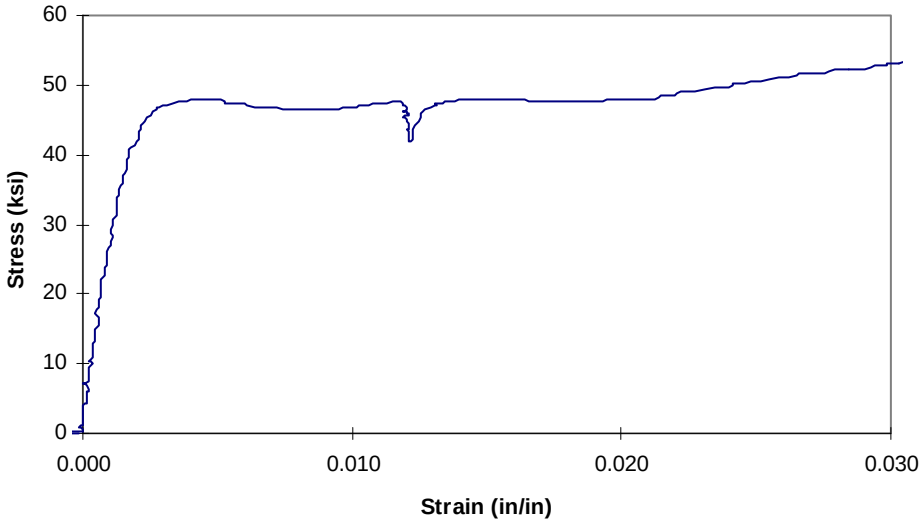

Figure A2-27: Specimen M2. Stress-strain curve: zero through start of strain hardening.

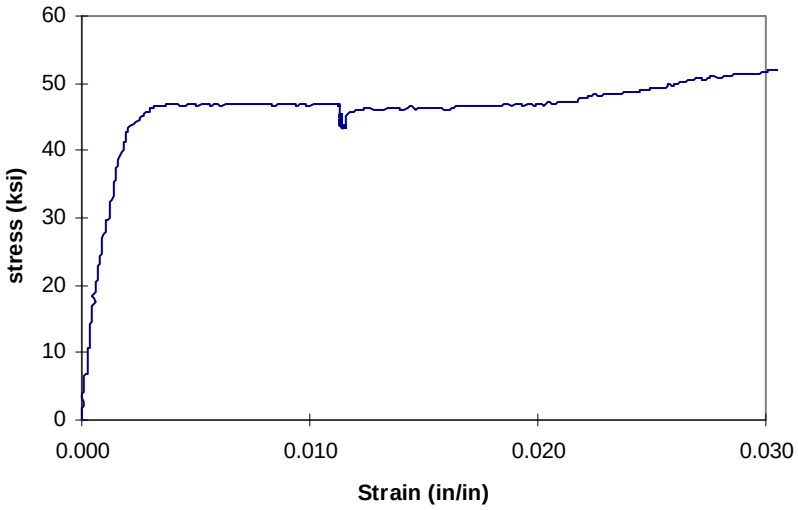

Figure A2-28: Specimen N2. Stress-strain curve: zero through start of strain hardening.

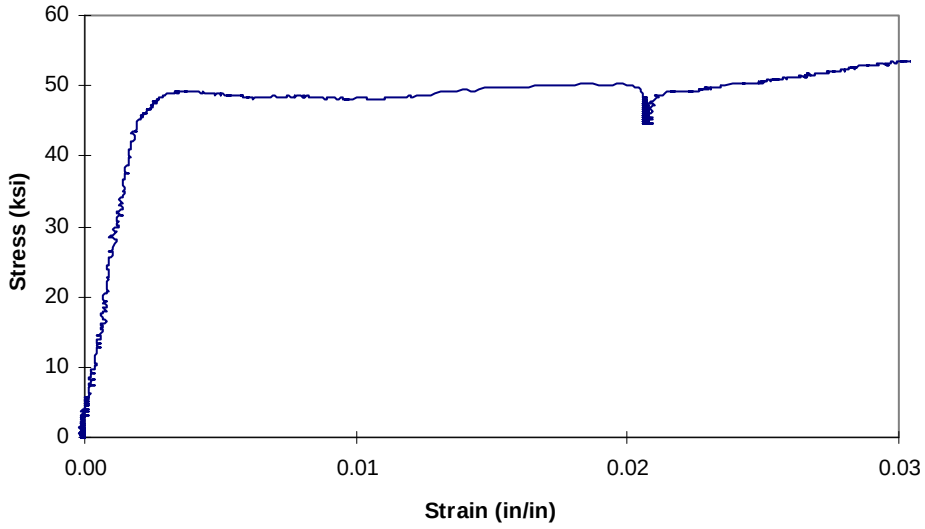

Figure A2-29: Specimen O2. Stress-strain curve: zero through start of strain hardening.

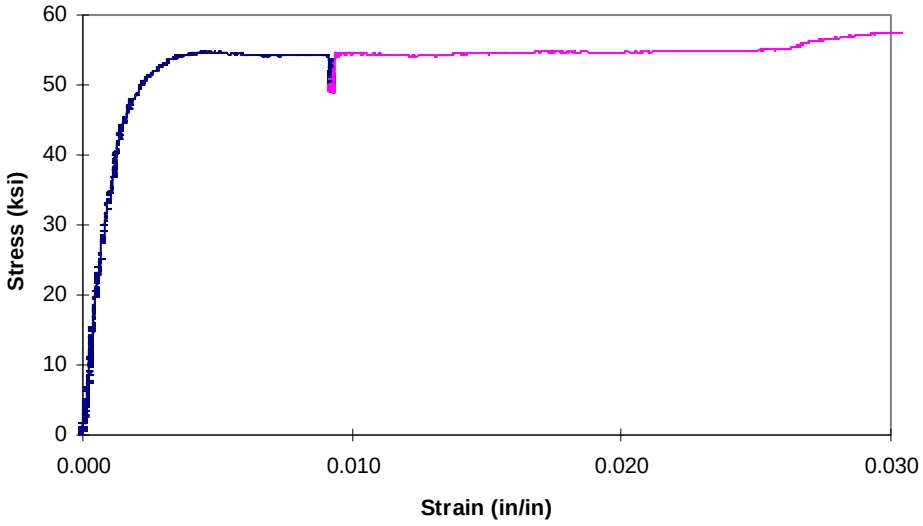

Figure A2-30: Specimen P2. Stress-strain curve: zero through start of strain hardening.

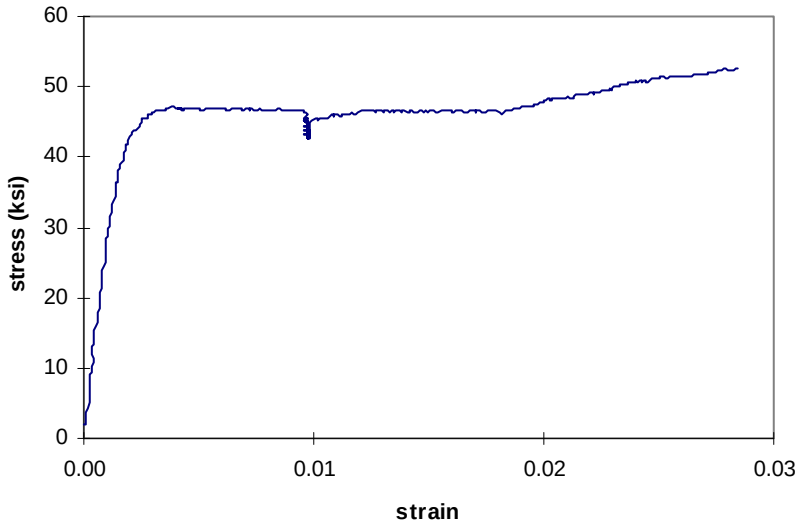

Figure A2-31: Specimen B3. Stress-strain curve: zero through start of strain hardening.

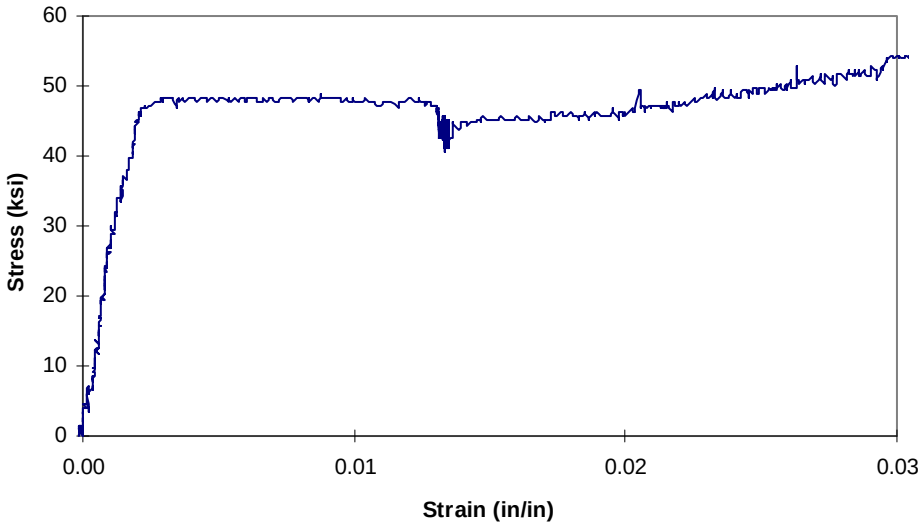

Figure A2-32: Specimen C3. Stress-strain curve: zero through start of strain hardening.

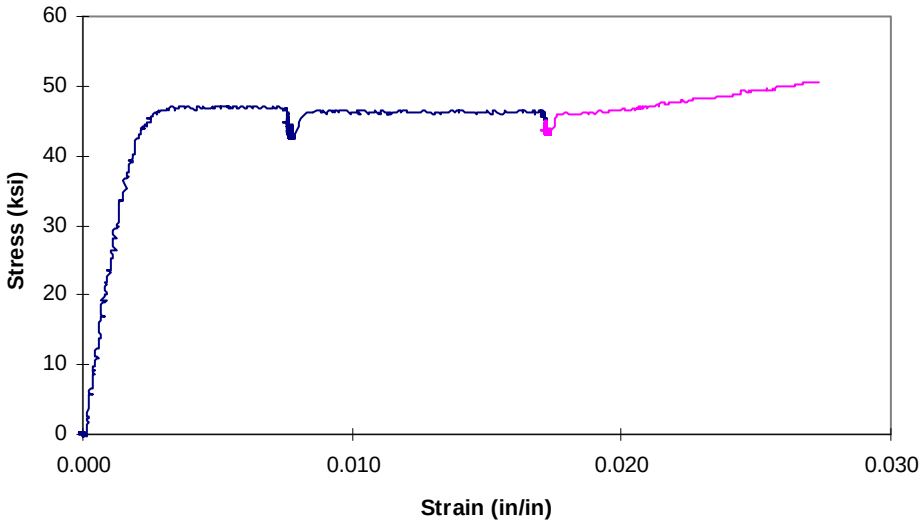

Figure A2-33: Specimen D3. Stress-strain curve: zero through start of strain hardening.

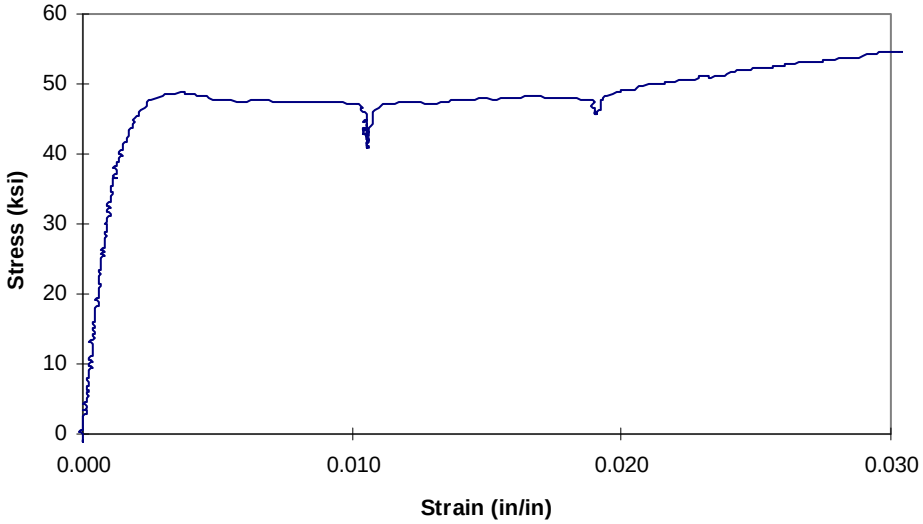

Figure A2-34: Specimen E3. Stress-strain curve: zero through start of strain hardening.

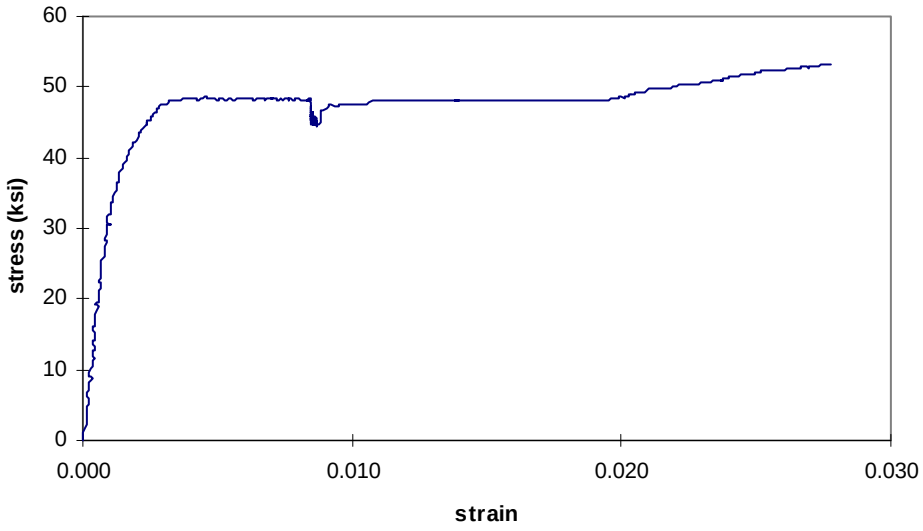

Figure A2-35: Specimen F3. Stress-strain curve: zero through start of strain hardening.

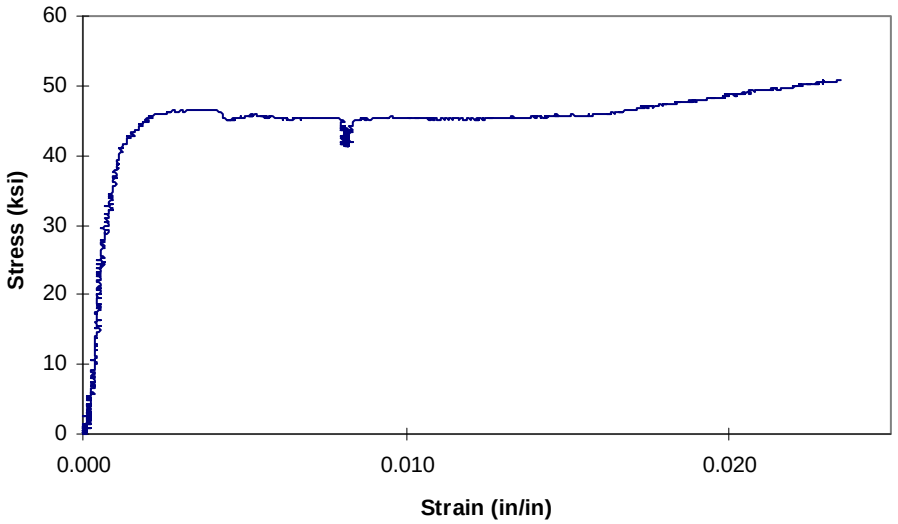

Figure A2-36: Specimen G3. Stress-strain curve: zero through start of strain hardening.

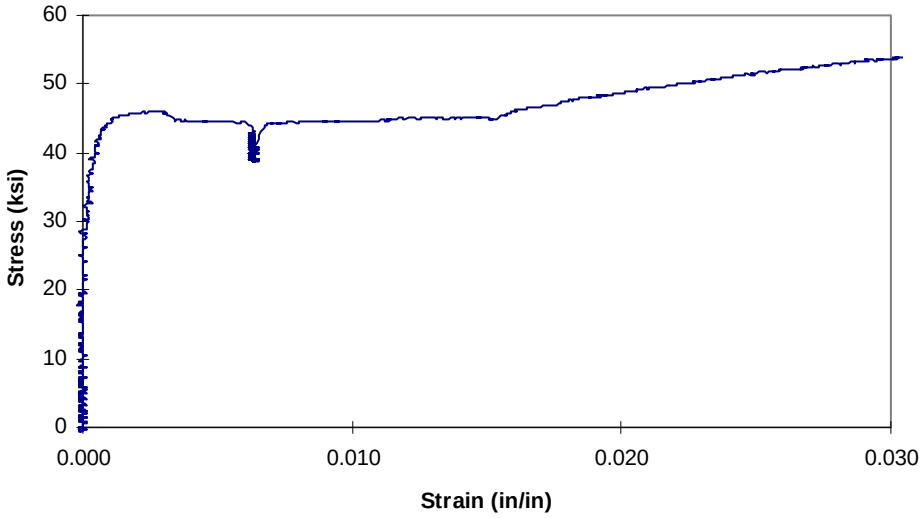

Figure A2-37: Specimen H3. Stress-strain curve: zero through start of strain hardening.

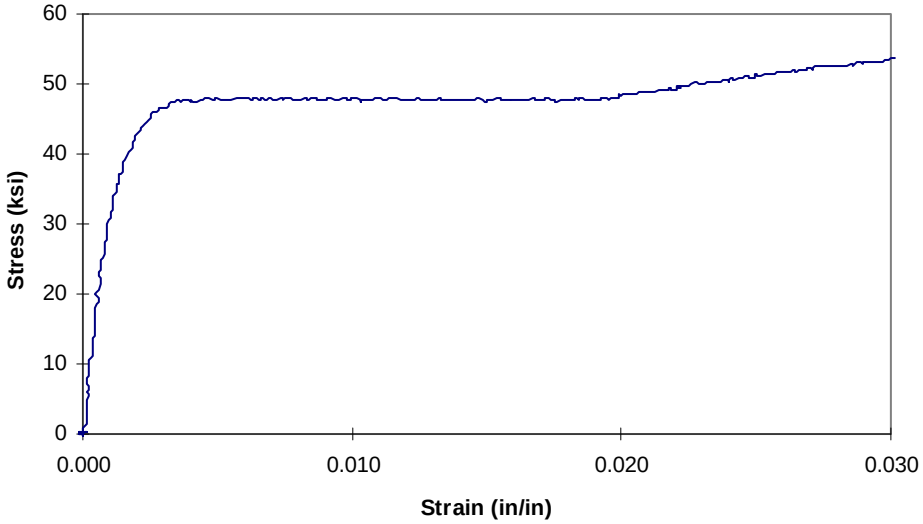

Figure A2-38: Specimen I3. Stress-strain curve: zero through start of strain hardening.

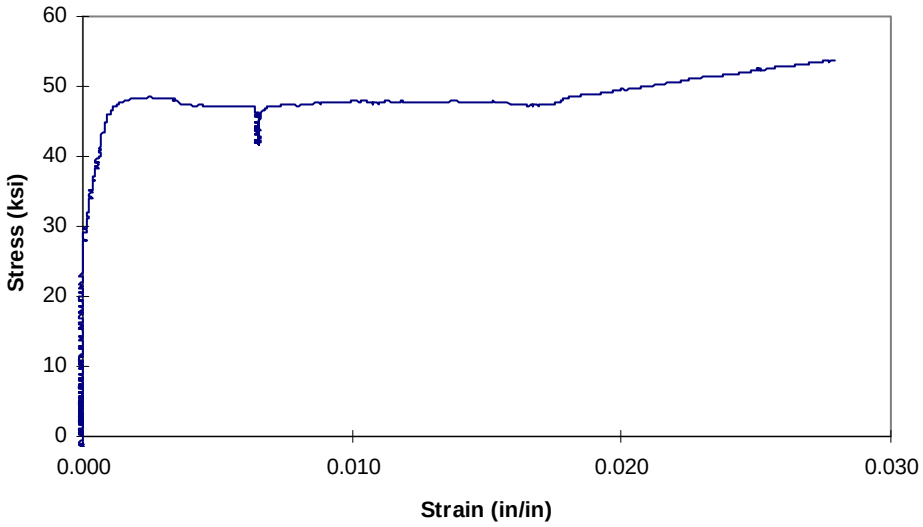

Figure A2-39: Specimen J3. Stress-strain curve: zero through start of strain hardening.

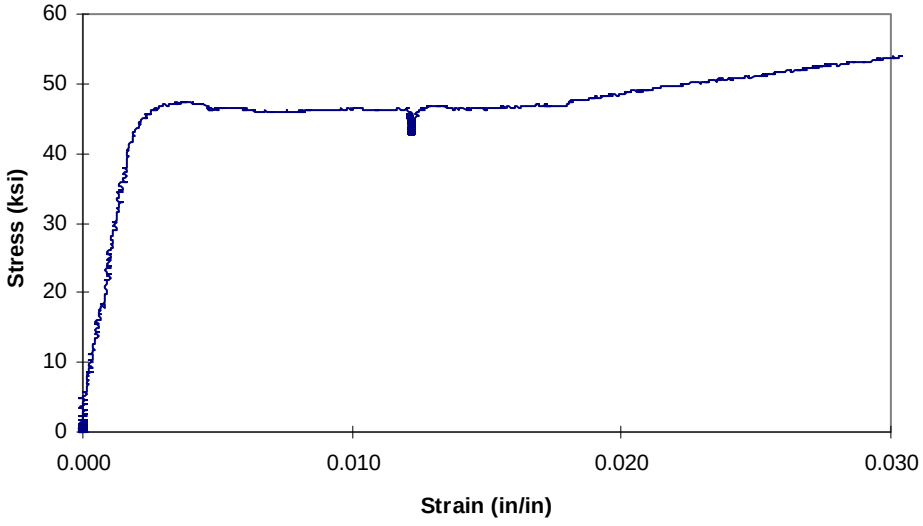

Figure A2-40: Specimen K3. Stress-strain curve: zero through start of strain hardening.

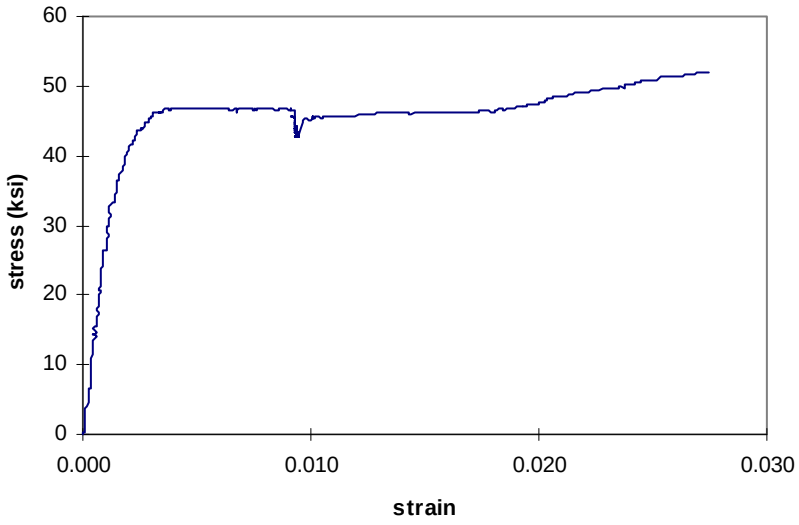

Figure A2-41: Specimen L3. Stress-strain curve: zero through start of strain hardening.

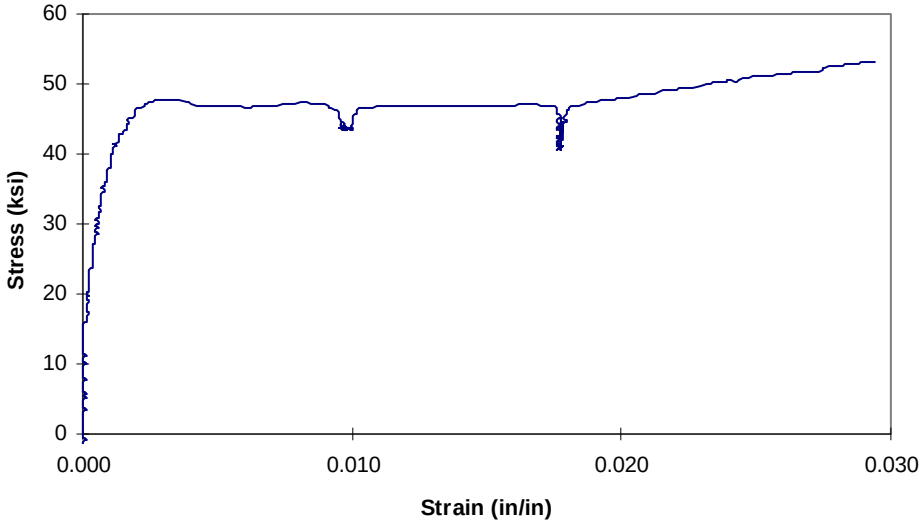

Figure A2-42: Specimen M3. Stress-strain curve: zero through start of strain hardening.

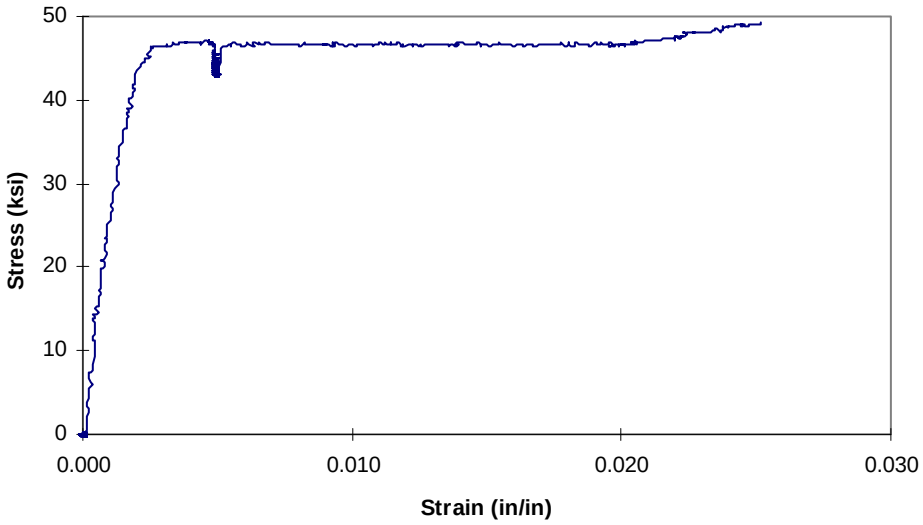

Figure A2-43: Specimen N3. Stress-strain curve: zero through start of strain hardening.

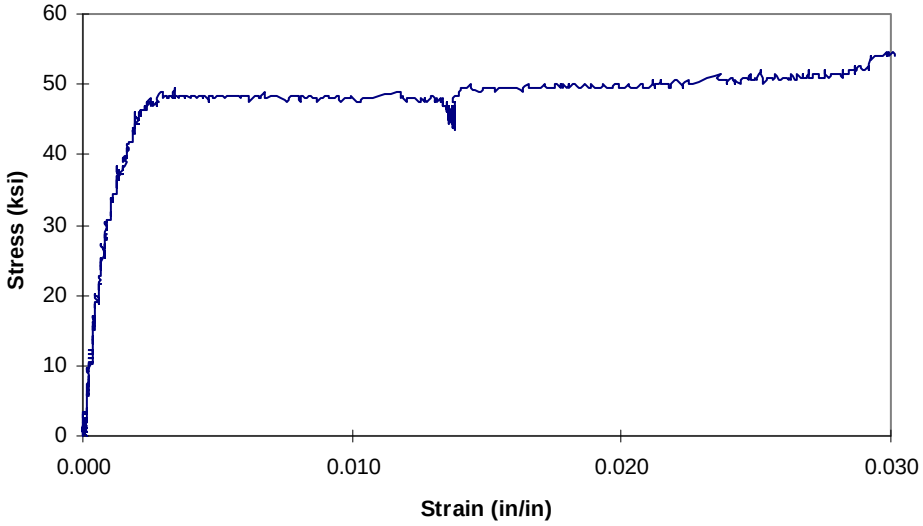

Figure A2-44: Specimen O3. Stress-strain curve: zero through start of strain hardening.

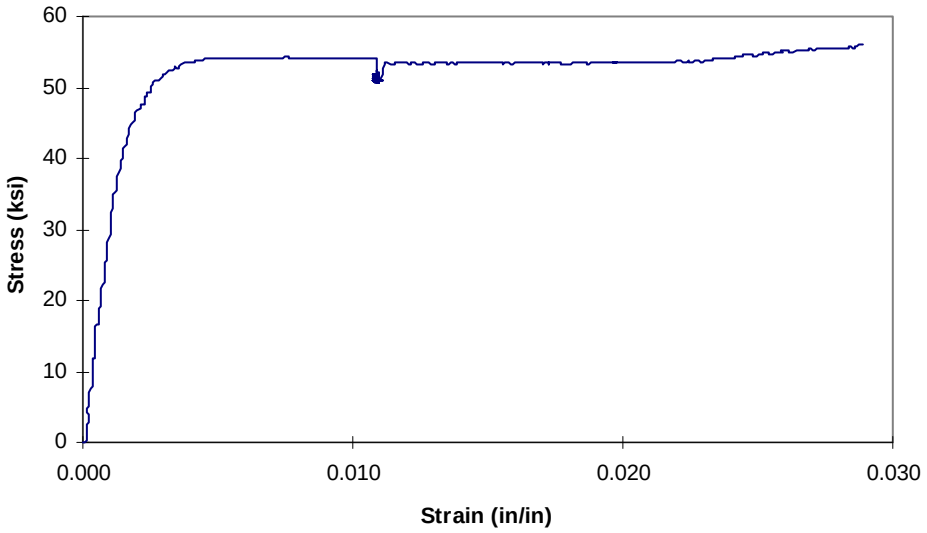

Figure A2-45: Specimen P3. Stress-strain curve: zero through start of strain hardening.

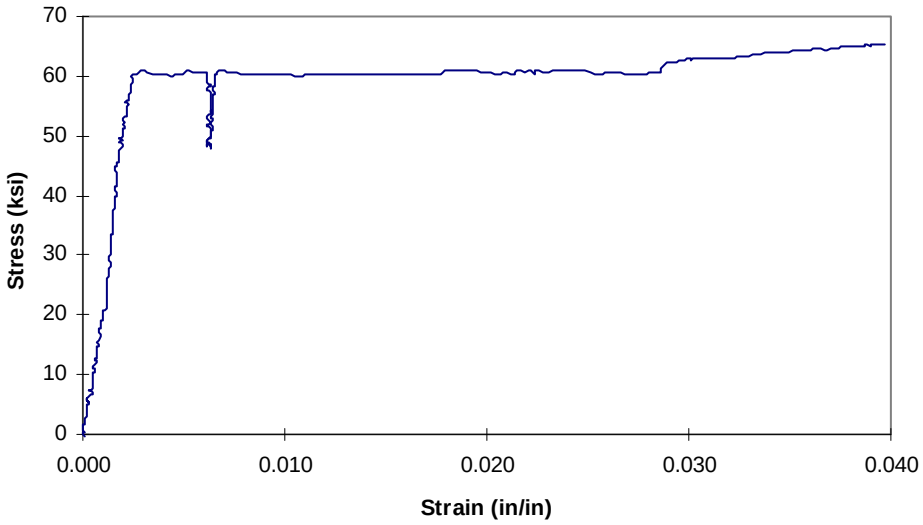

Figure A2-46: Specimen 1A. Stress-strain curve: zero through start of strain hardening.

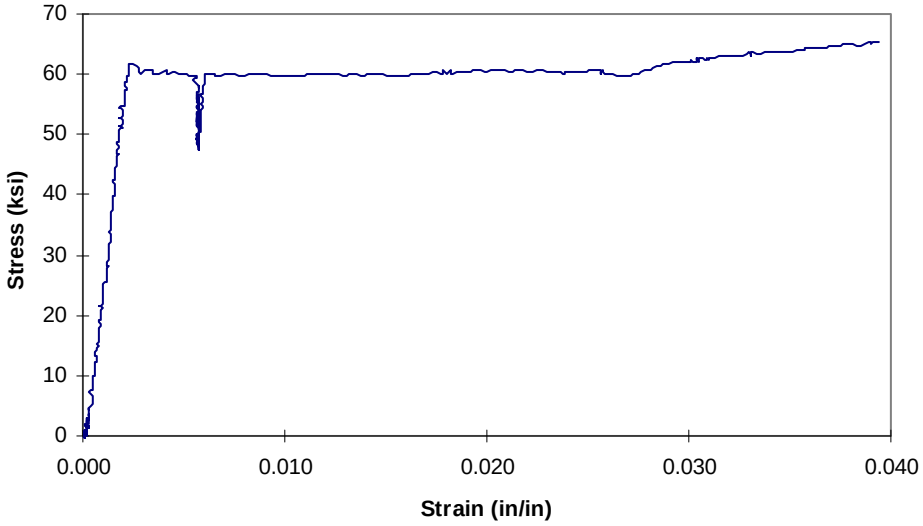

Figure A2-47: Specimen 2A. Stress-strain curve: zero through start of strain hardening.

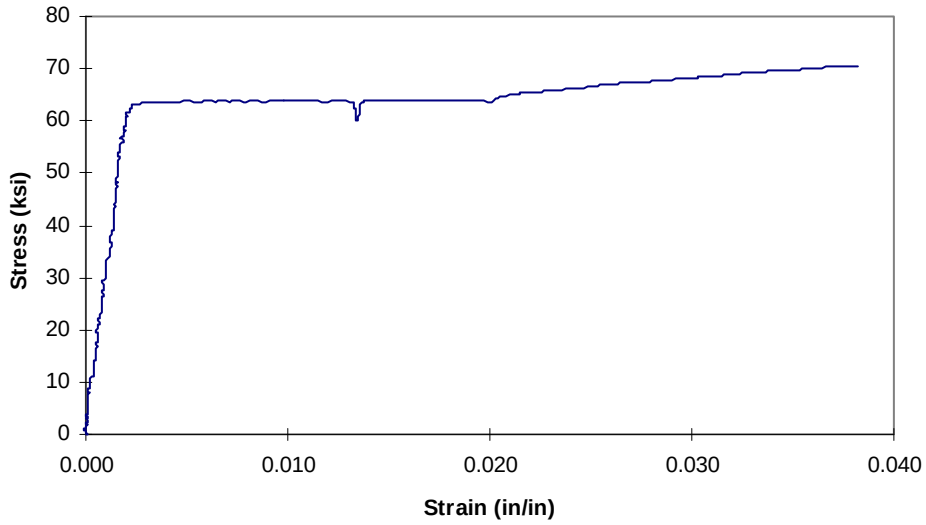

Figure A2-48: Specimen 3A. Stress-strain curve: zero through start of strain hardening.

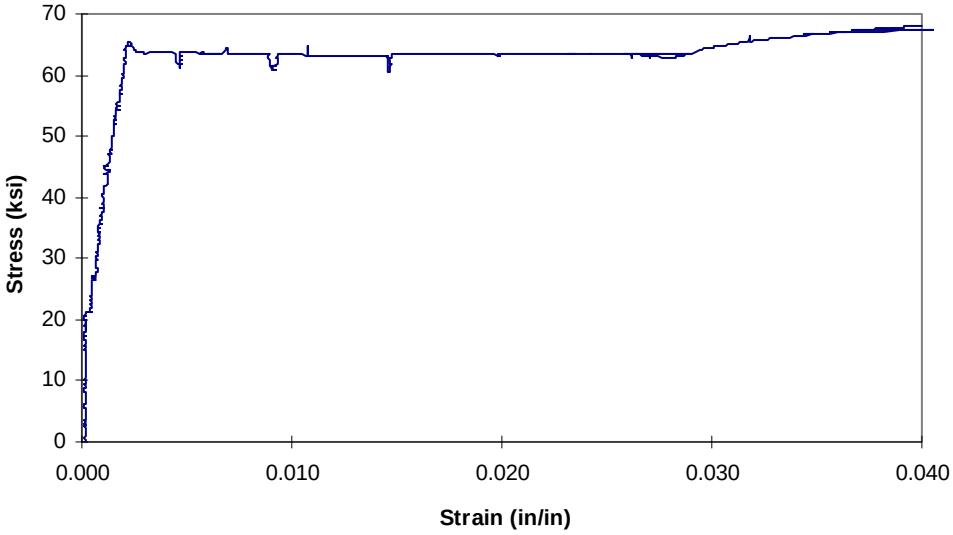

Figure A2-49: Specimen 4A. Stress-strain curve: zero through start of strain hardening.

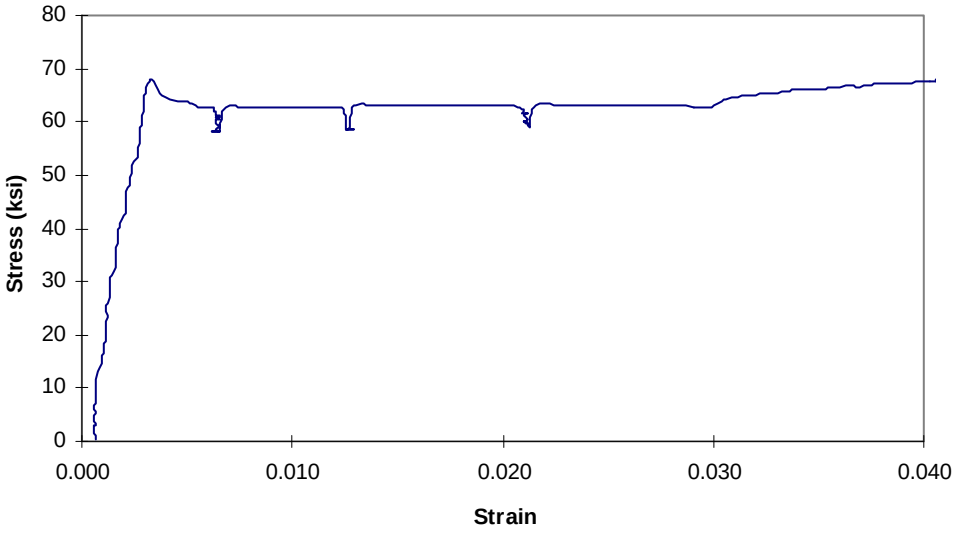

Figure A2-50: Specimen 5A. Stress-strain curve: zero through start of strain hardening.

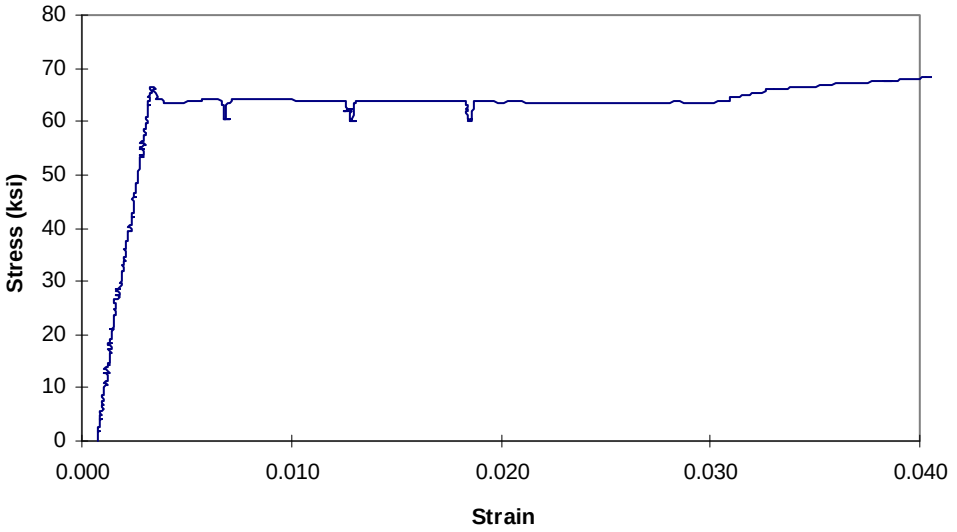

Figure A2-51: Specimen 6A. Stress-strain curve: zero through start of strain hardening.

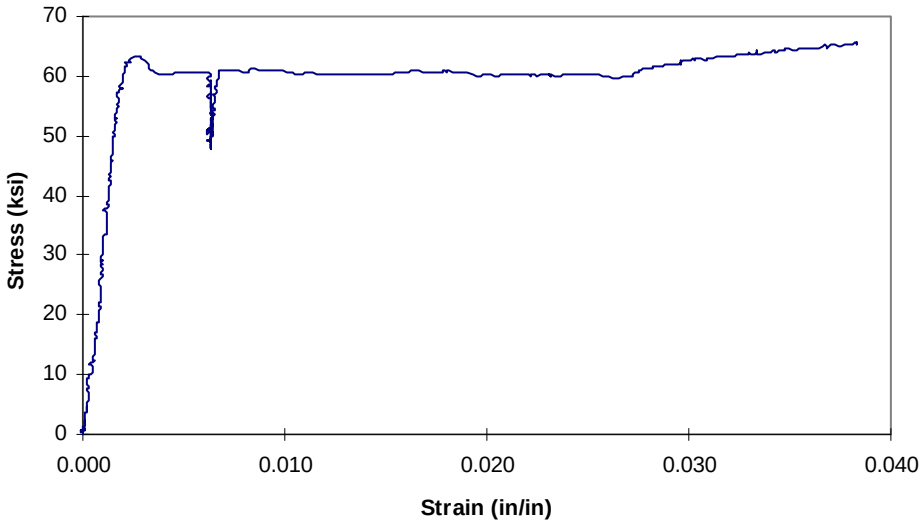

Figure A2-52: Specimen 1B. Stress-strain curve: zero through start of strain hardening.

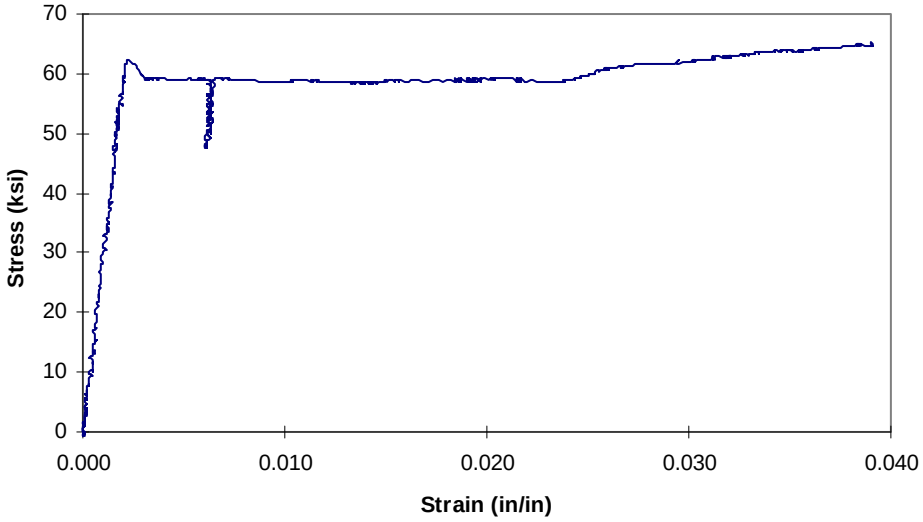

Figure A2-53: Specimen 2B. Stress-strain curve: zero through start of strain hardening.

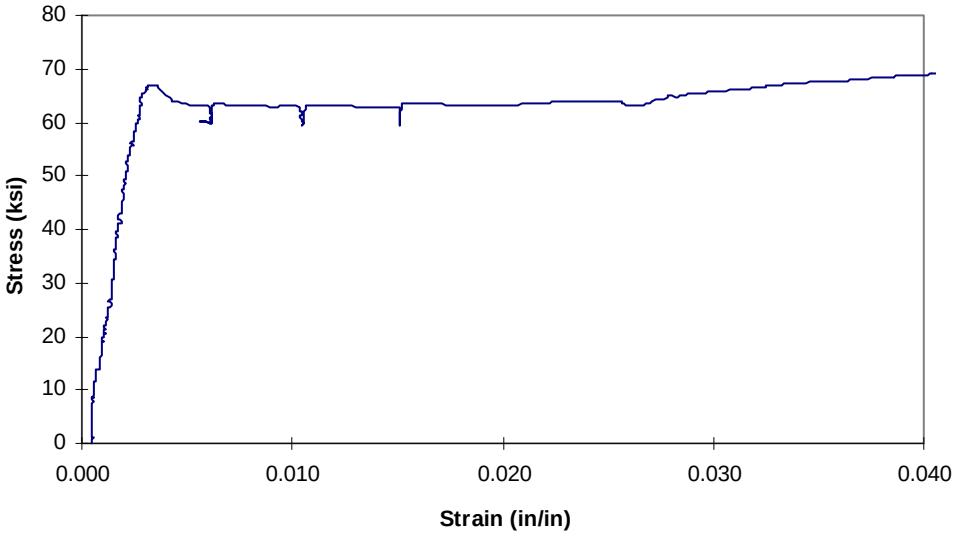

Figure A2-54: Specimen 4B. Stress-strain curve: zero through start of strain hardening.

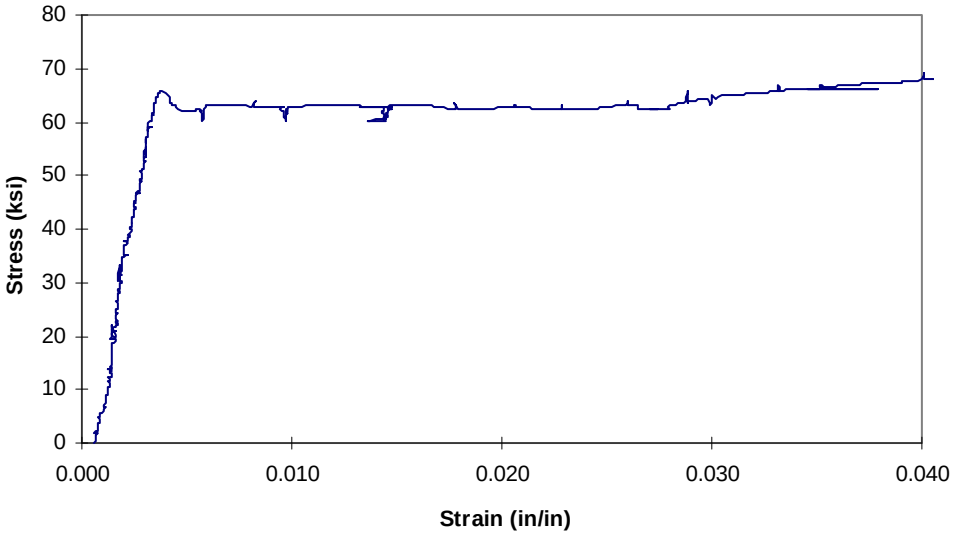

Figure A2-55: Specimen 5B. Stress-strain curve: zero through start of strain hardening.

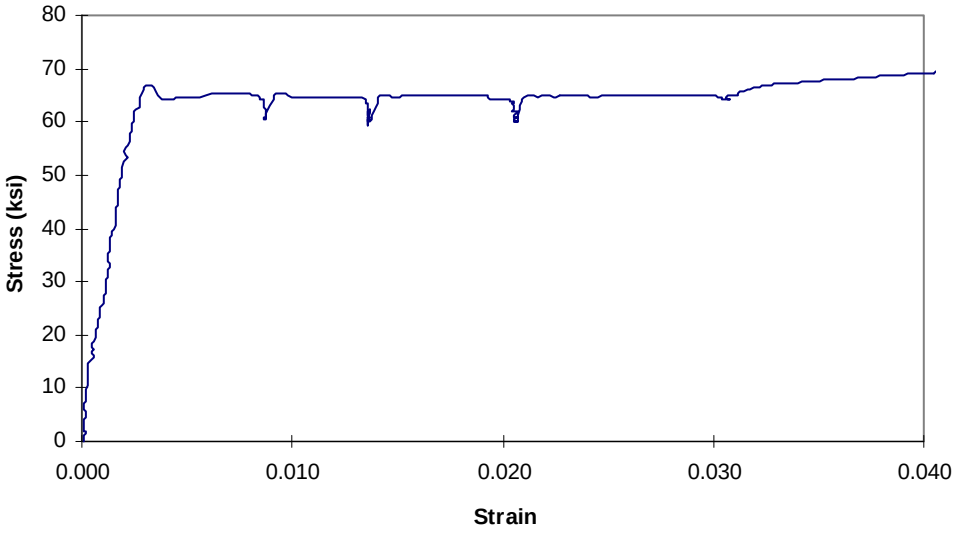

Figure A2-56: Specimen 6B. Stress-strain curve: zero through start of strain hardening.

Appendix A3

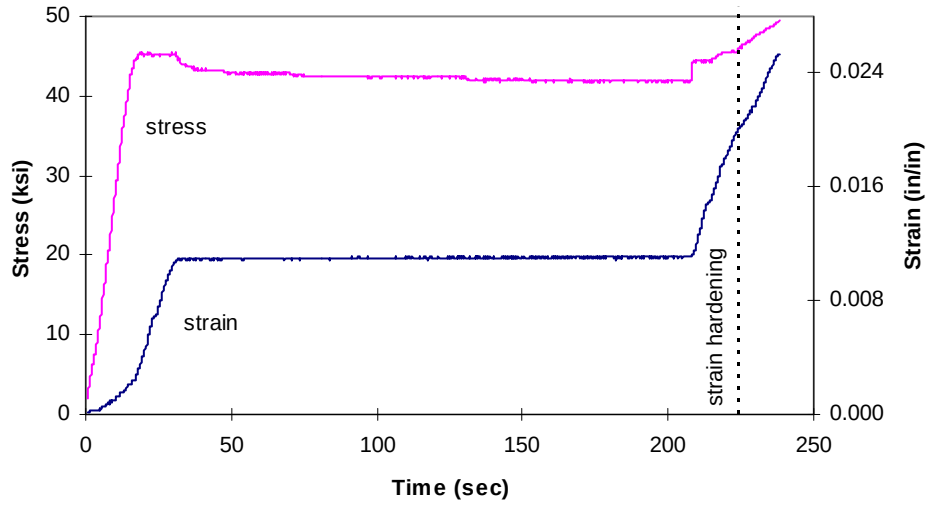

(a)

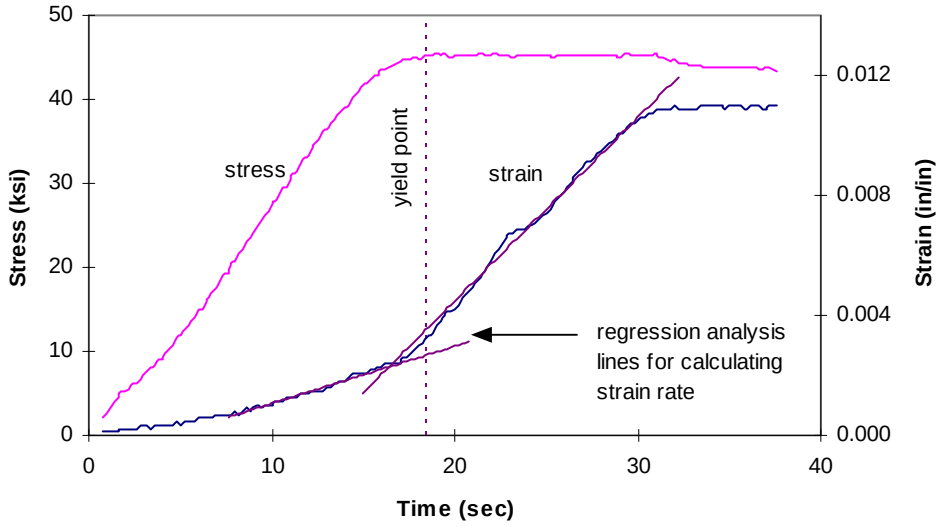

(b)

Figure A3-1:Specimen B1. Stress-time and strain-time curves: (a) zero through start of strain hardening; (b) zero through start of static yield.

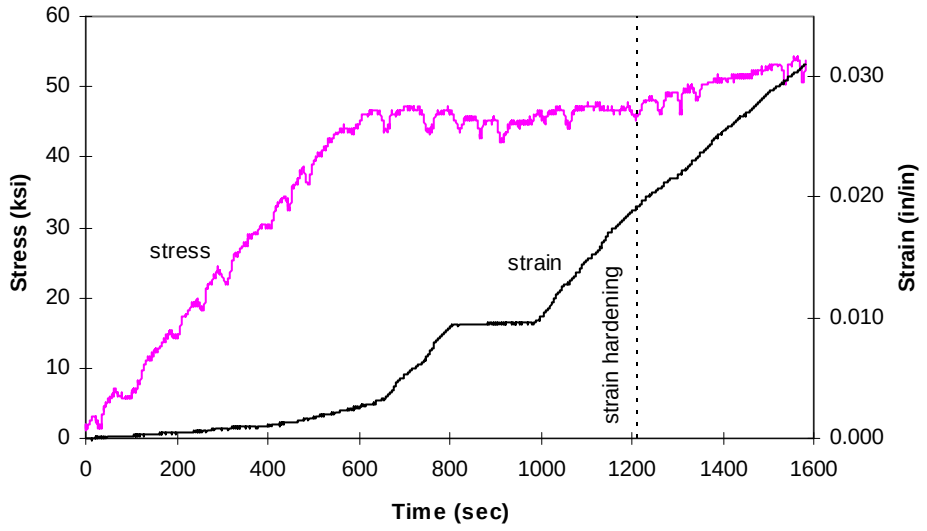

(a)

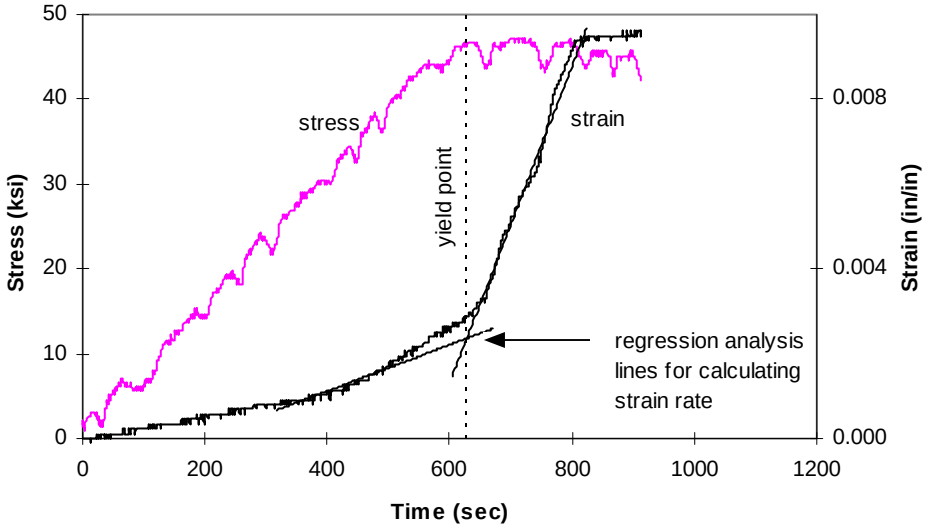

(b)

Figure A3-2: Specimen C1. Stress-time and strain-time curves: (a) zero through start of strain hardening; (b) zero through start of static yield.

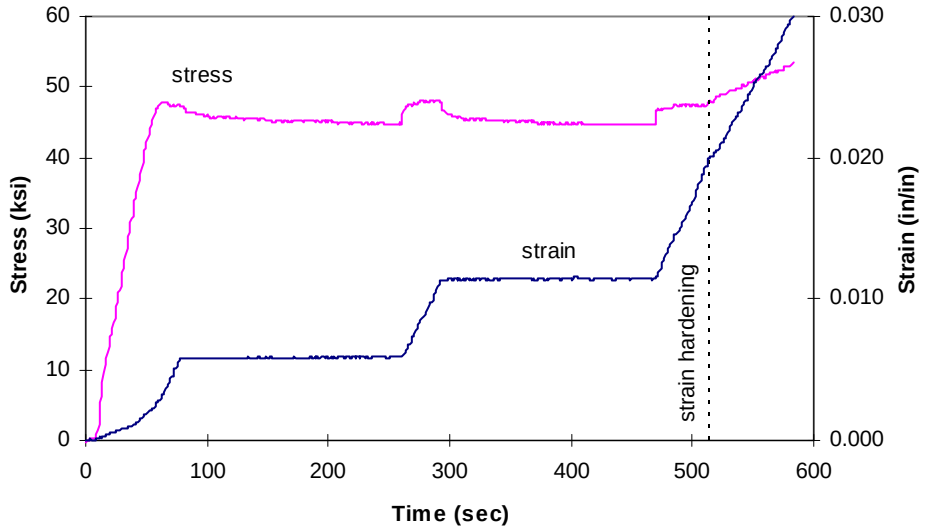

(a)

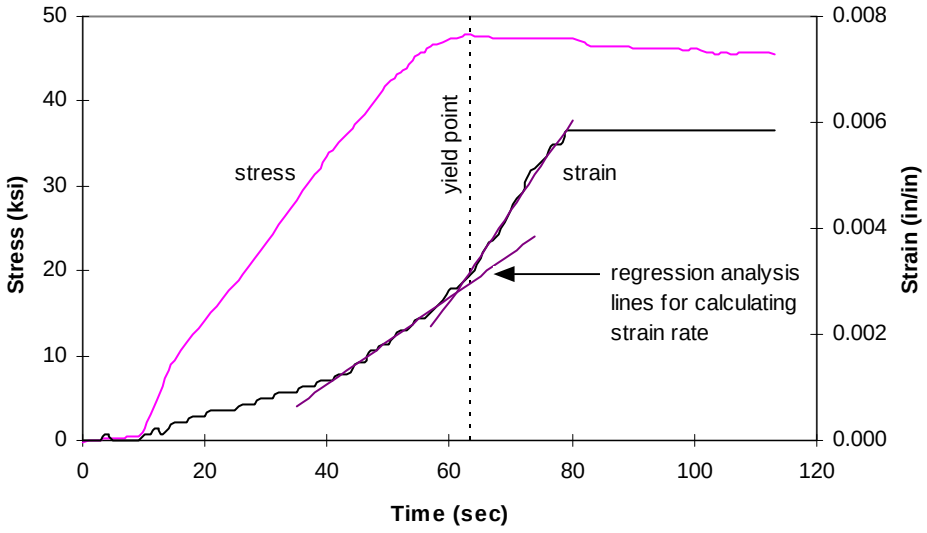

(b)

Figure A3-3: Specimen D1. Stress-time and strain-time curves: (a) zero through start of strain hardening; (b) zero through start of static yield.

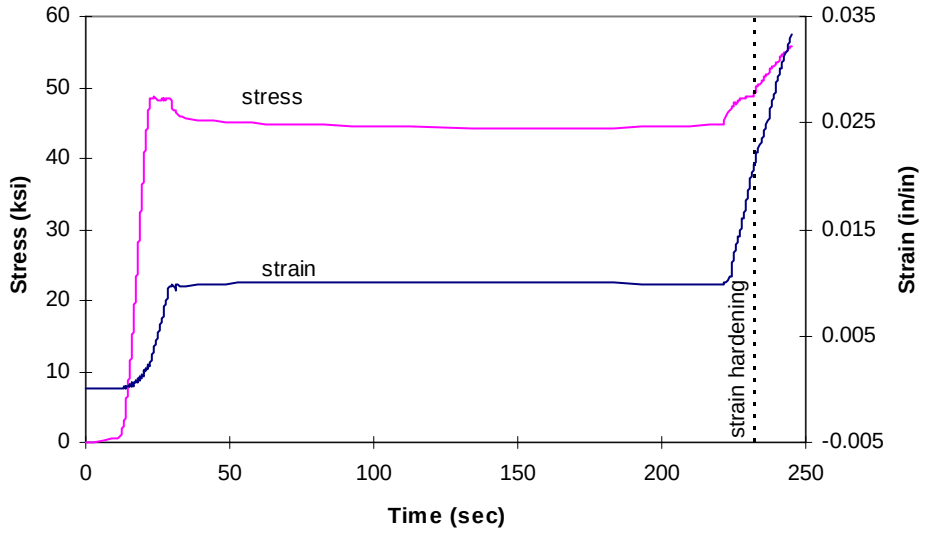

(a)

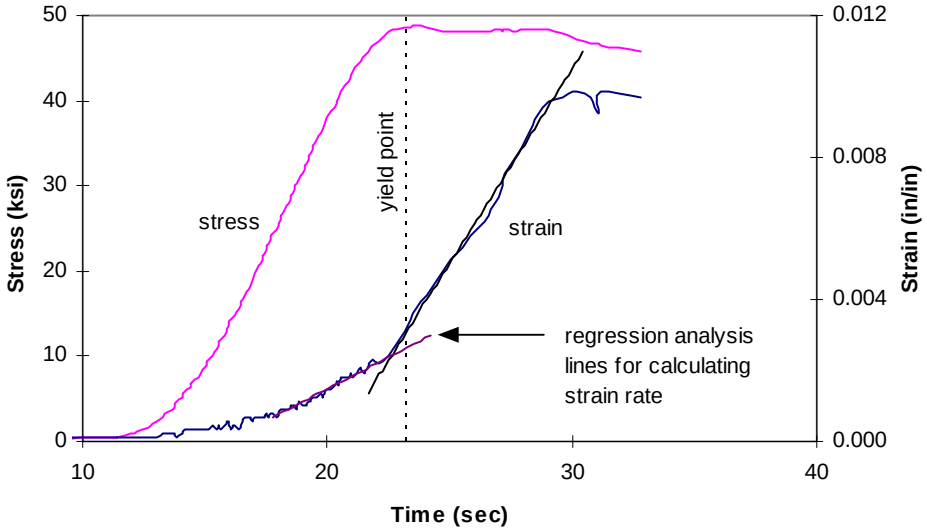

(b)

Figure A3-4: Specimen E1. Stress-time and strain-time curves: (a) zero through start of strain hardening; (b) zero through start of static yield.

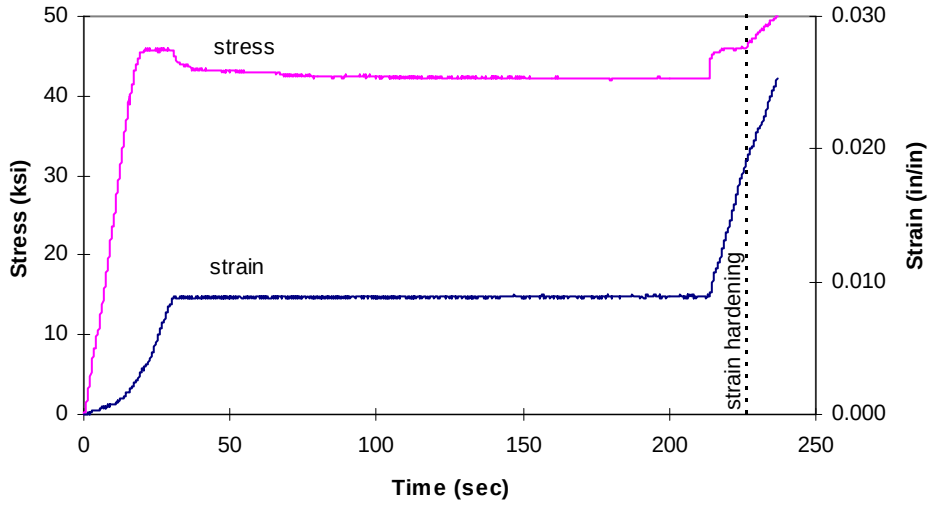

(a)

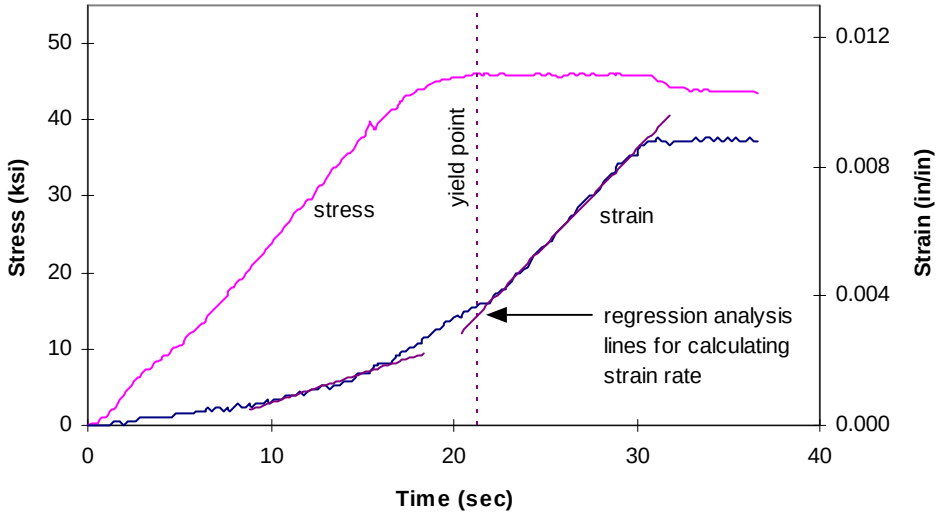

(b)

Figure A3-5: Specimen F1. Stress-time and strain-time curves: (a) zero through start of strain hardening; (b) zero through start of static yield.

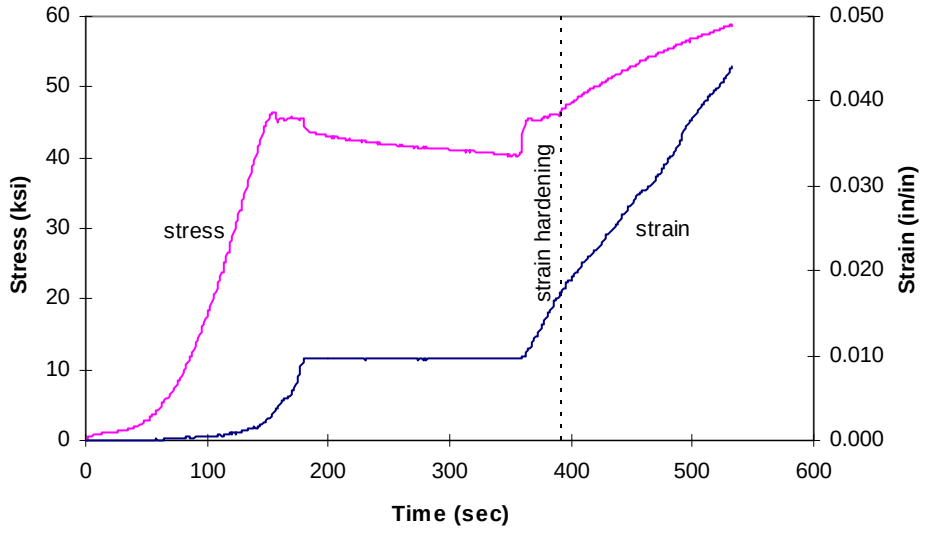

(a)

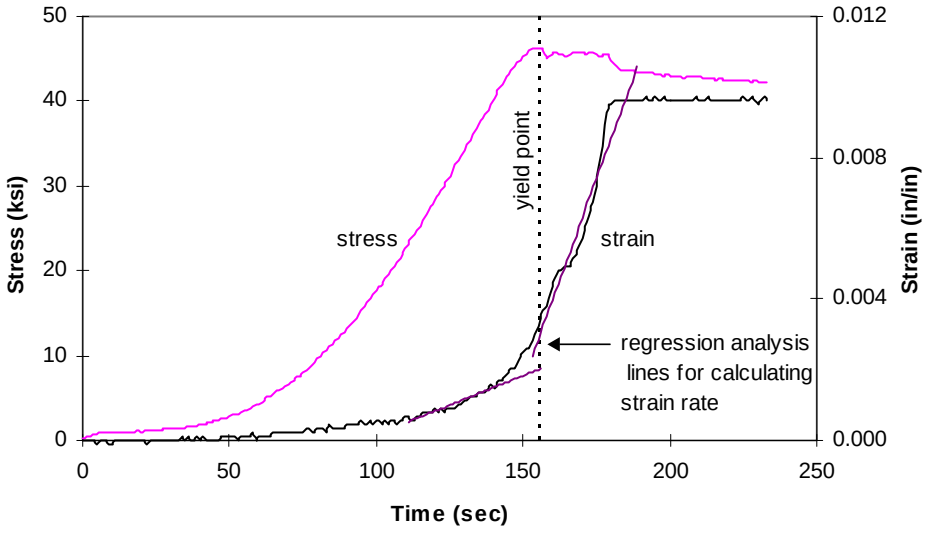

(b)

Figure A3-6: Specimen G1. Stress-time and strain-time curves: (a) zero through start of strain hardening; (b) zero through start of static yield.

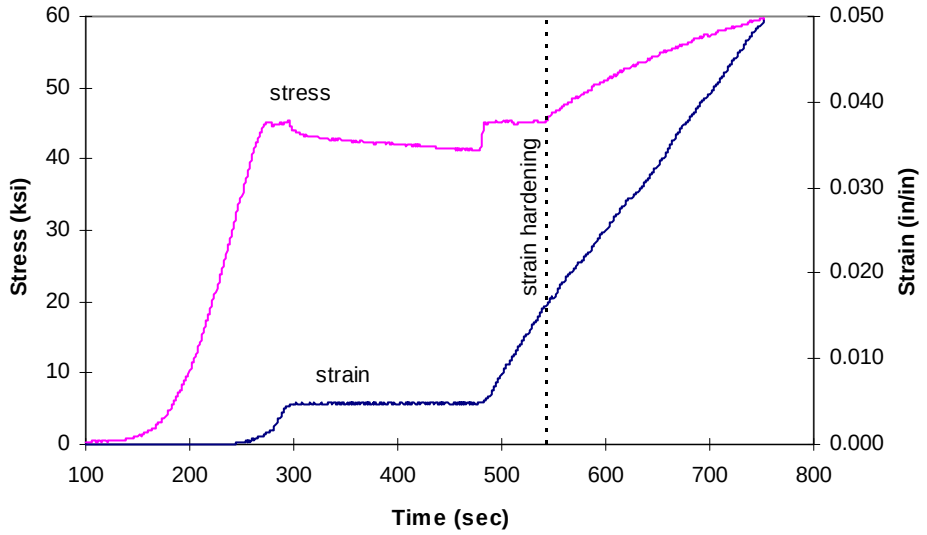

(a)

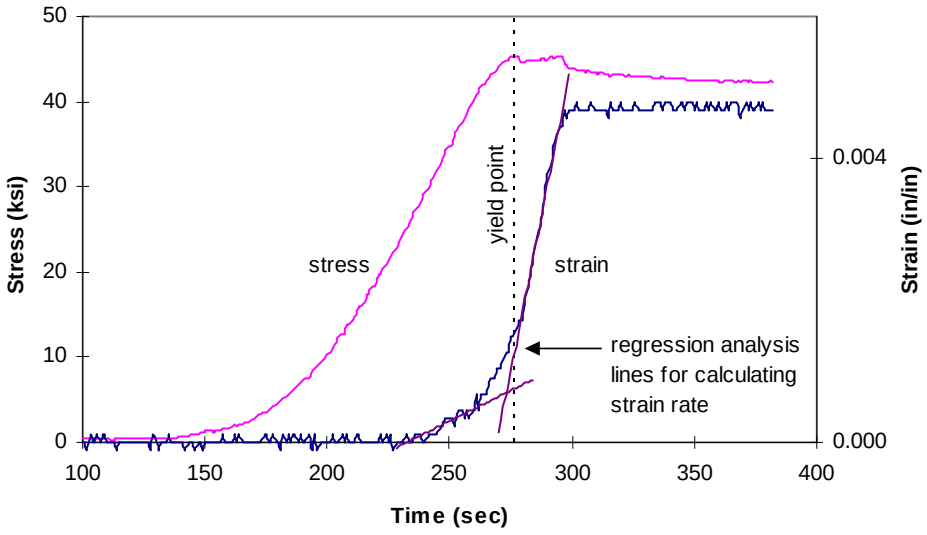

(b)

Figure A3-7:Specimen H1. Stress-time and strain-time curves: (a) zero through start of strain hardening; (b) zero through start of static yield.

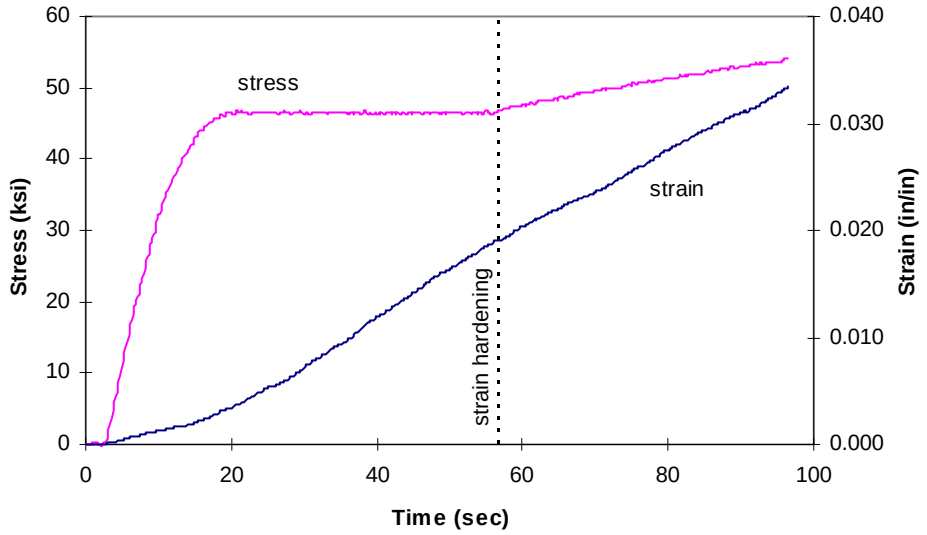

(a)

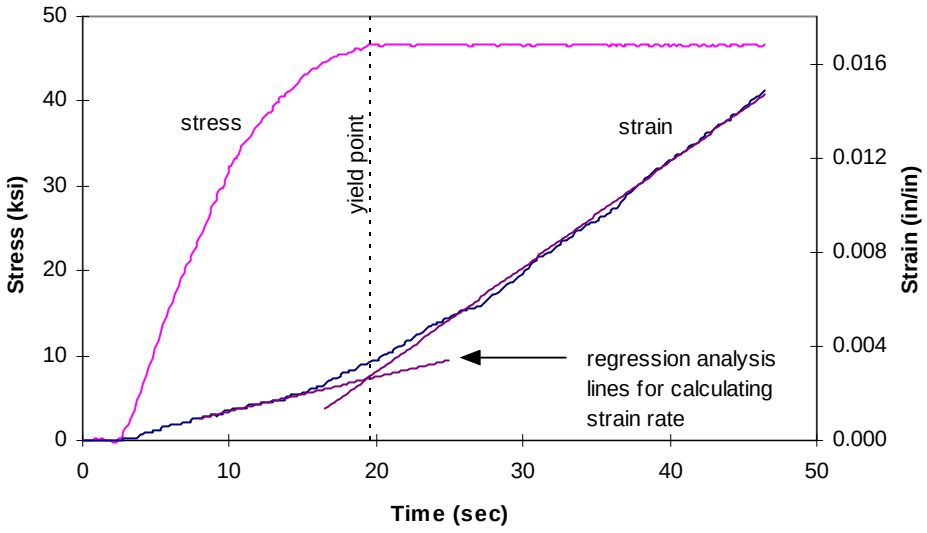

(b)

Figure A3-8: Specimen I1. Stress-time and strain-time curves: (a) zero through start of strain hardening; (b) zero through start of yield.

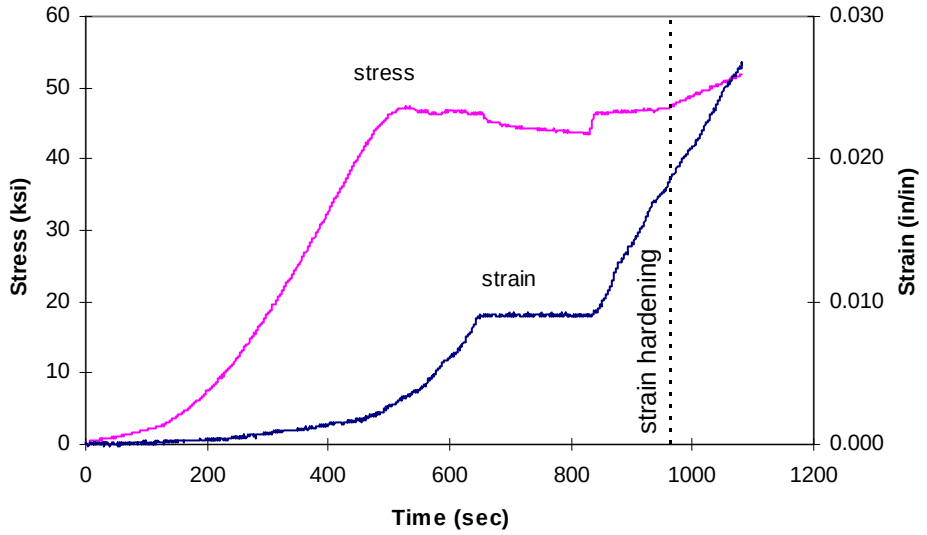

(a)

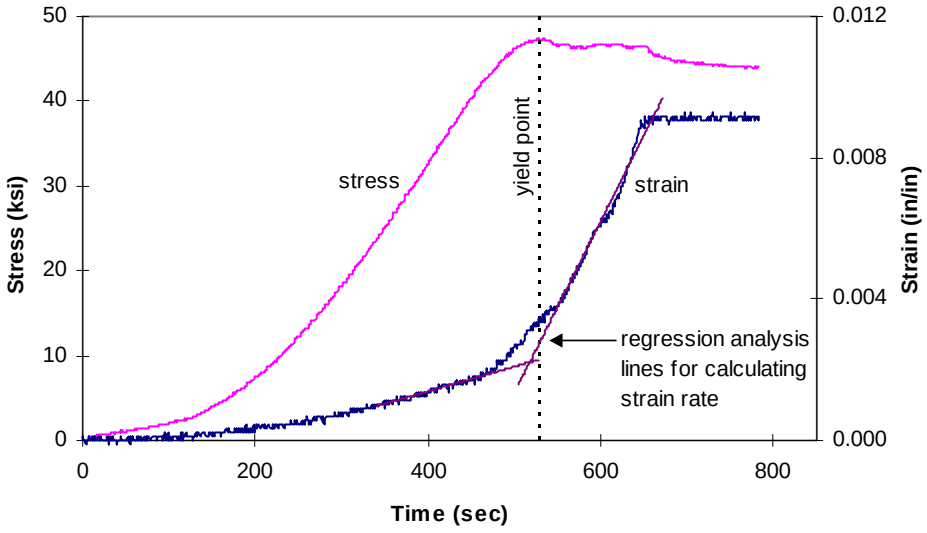

(b)

Figure A3-9: Specimen J1. Stress-time and strain-time curves: (a) zero through start of strain hardening; (b) zero through start of yield.

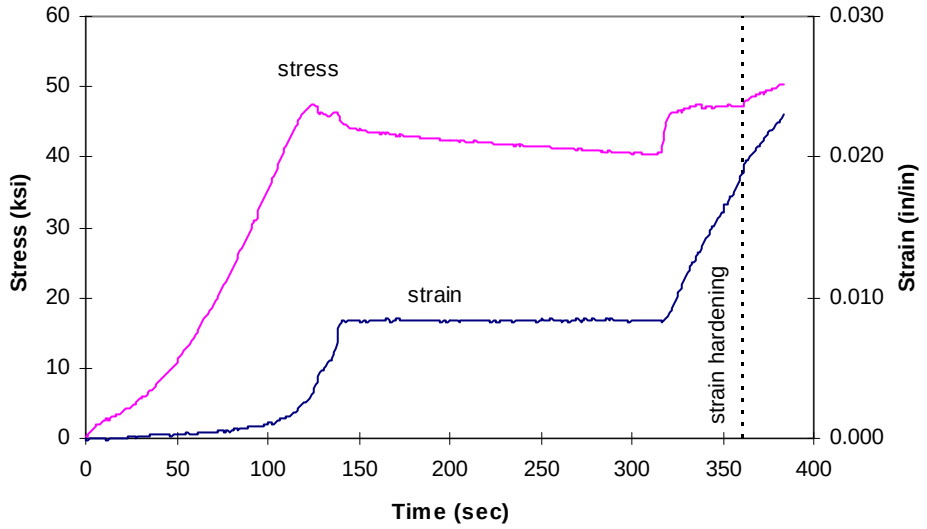

(a)

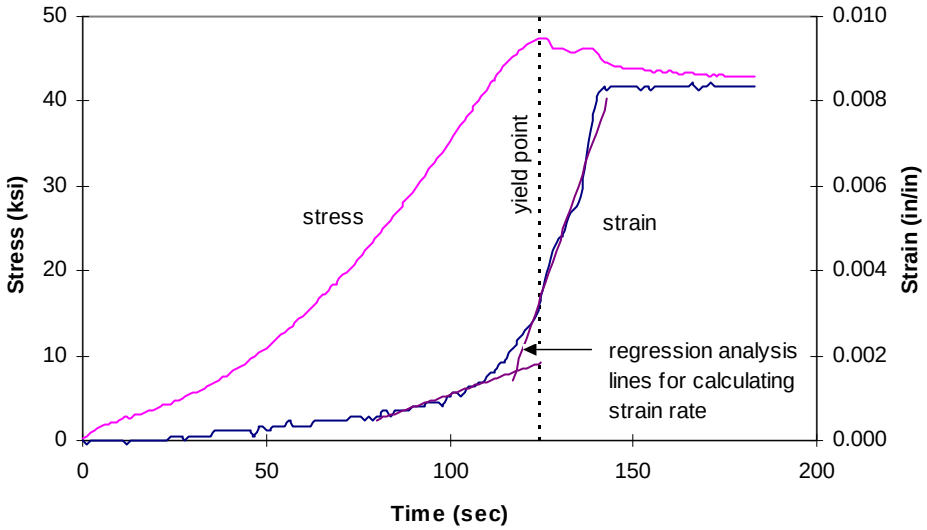

(b)

Figure A3-10: Specimen K1. Stress-time and strain-time curves: (a) zero through start of strain hardening; (b) zero through start of yield.

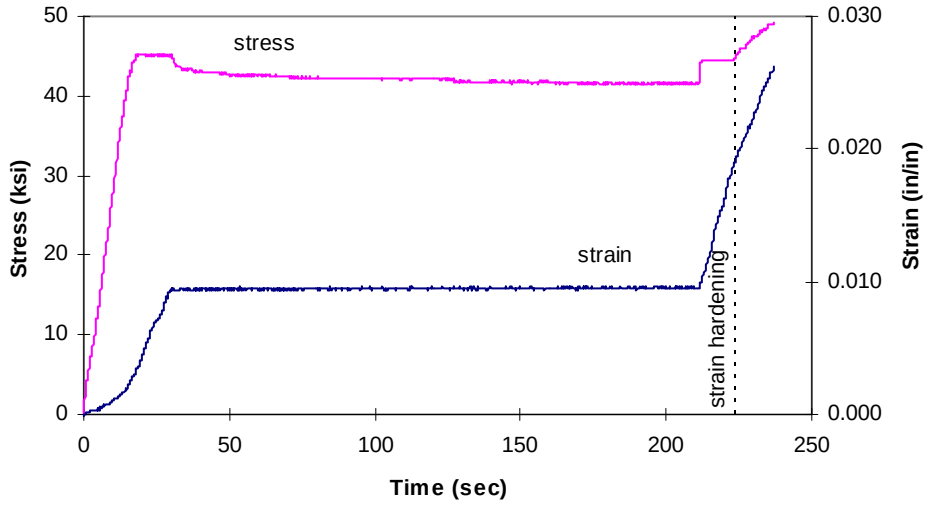

(a)

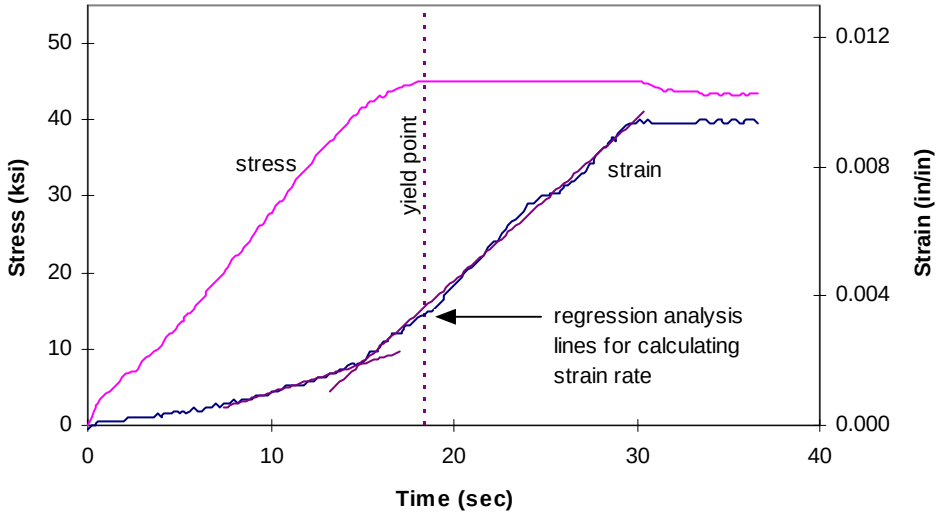

(b)

Figure A3-11: Specimen L1. Stress-time and strain-time curves: (a) zero through start of strain hardening; (b) zero through start of yield.

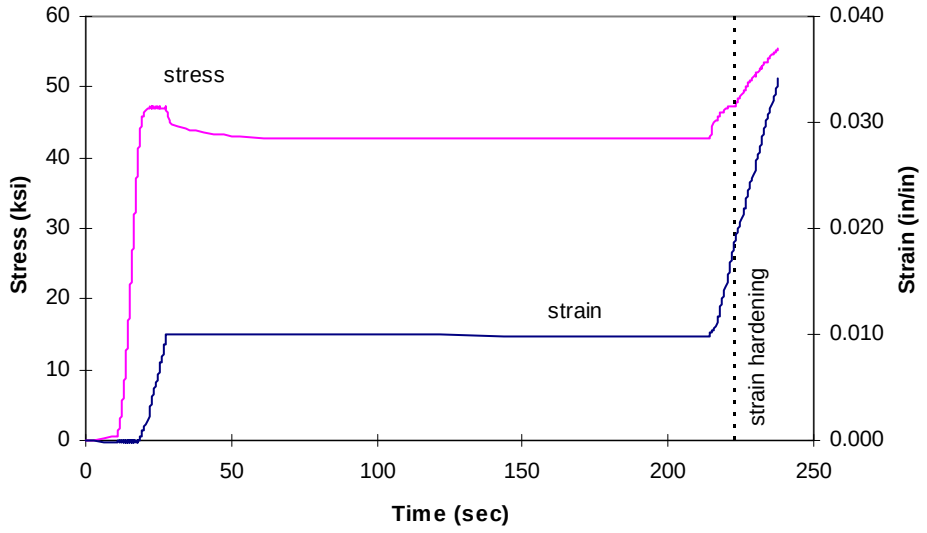

(a)

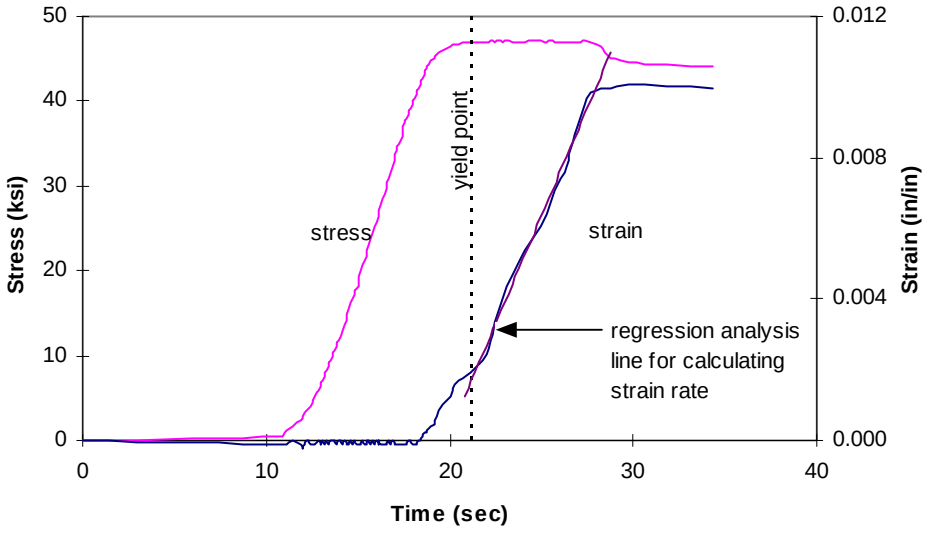

(b)

Figure A3-12: Specimen M1. Stress-time and strain-time curves: (a) zero through start of strain hardening; (b) zero through start of yield.

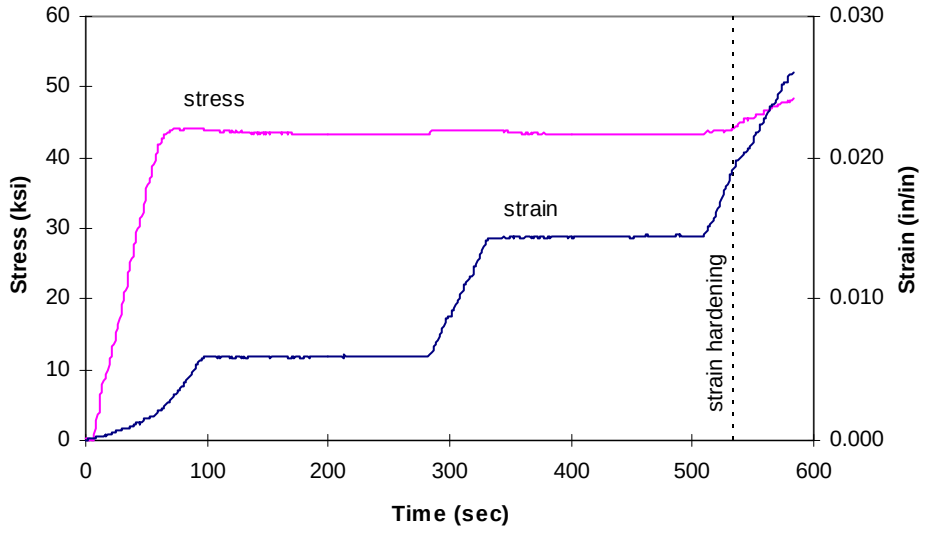

(a)

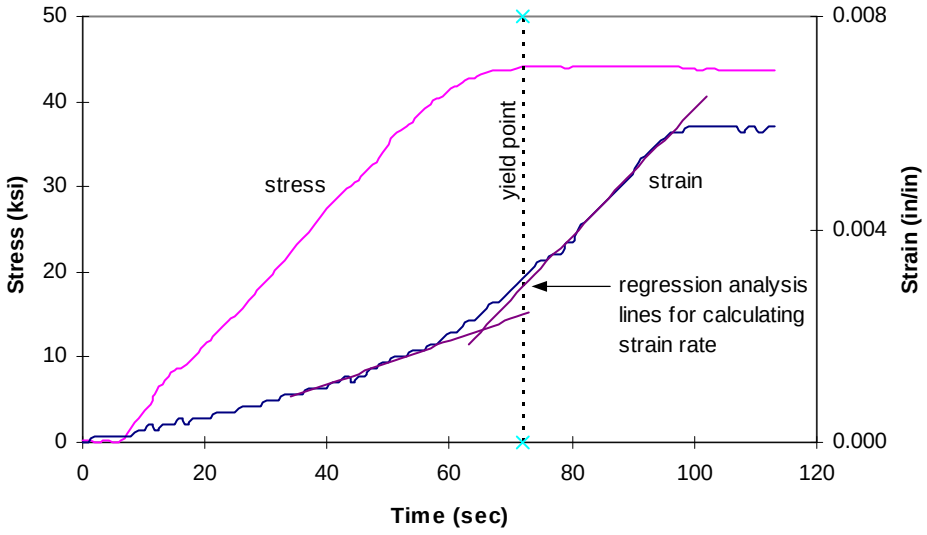

(b)

Figure A3-13: Specimen N1. Stress-time and strain-time curves: (a) zero through start of strain hardening; (b) zero through start of yield.

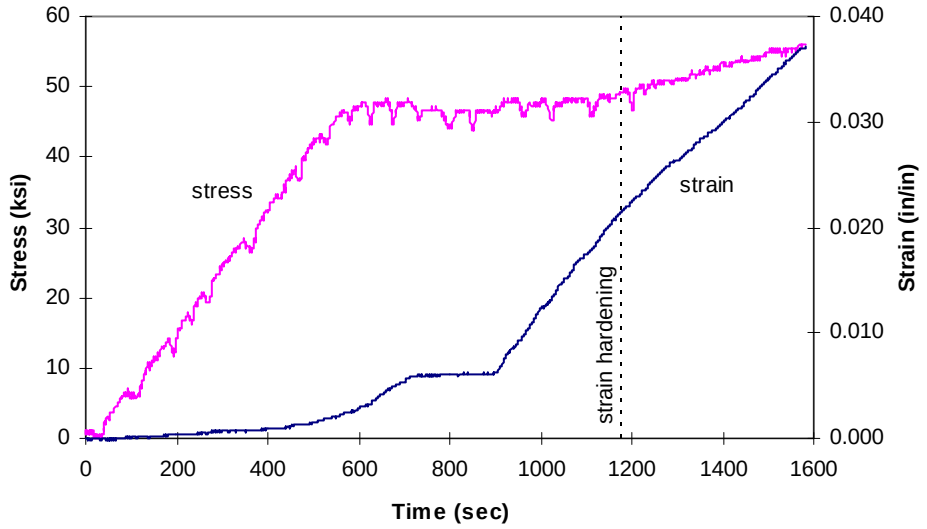

(a)

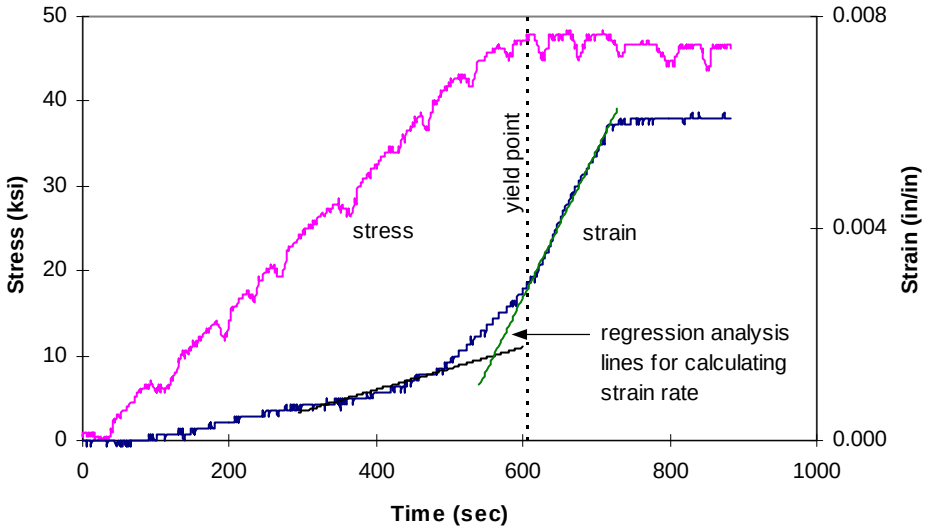

(b)

Figure A3-14: Specimen O1. Stress-time and strain-time curves: (a) zero through start of strain hardening; (b) zero through start of yield.

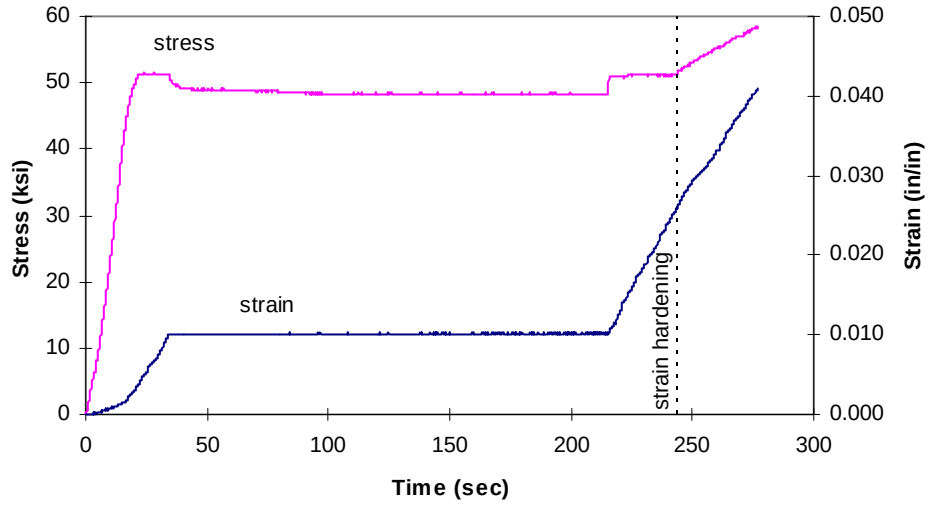

(a)

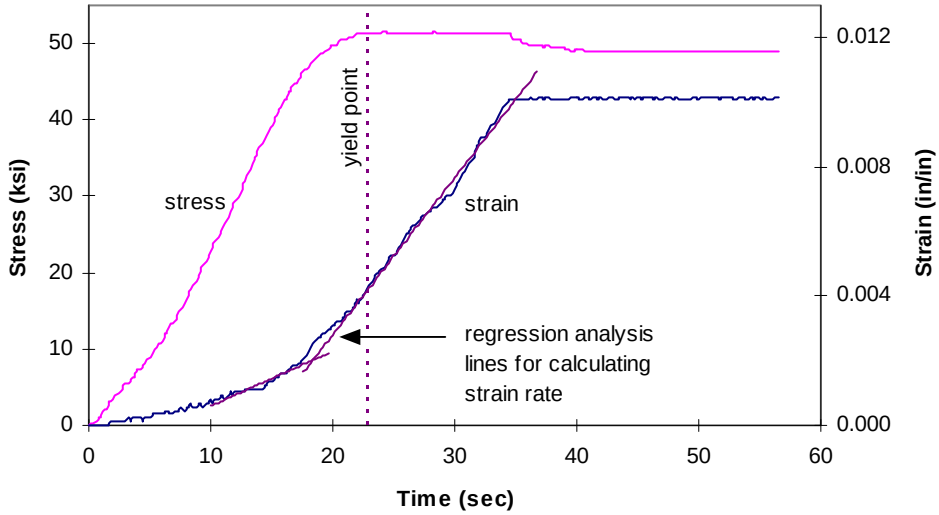

(b)

Figure A3-15: Specimen P1. Stress-time and strain-time curves: (a) zero through start of strain hardening; (b) zero through start of yield.

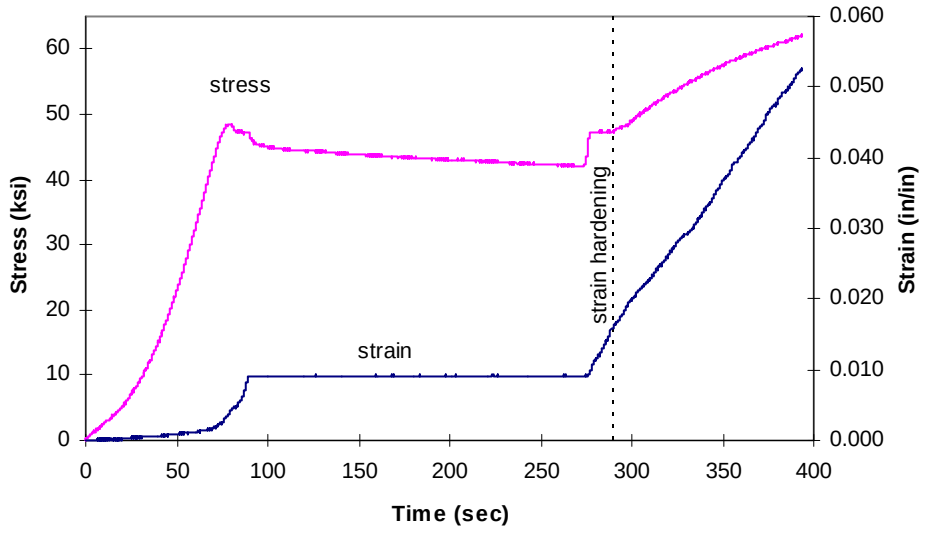

(a)

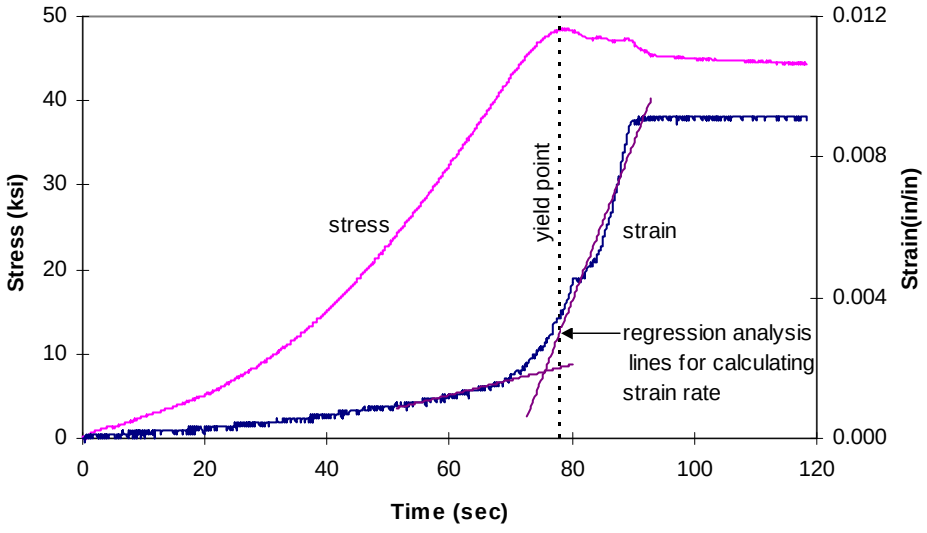

(b)

Figure A3-16: Specimen B2. Stress-time and strain-time curves: (a) zero through start of strain hardening; (b) zero through start of yield.

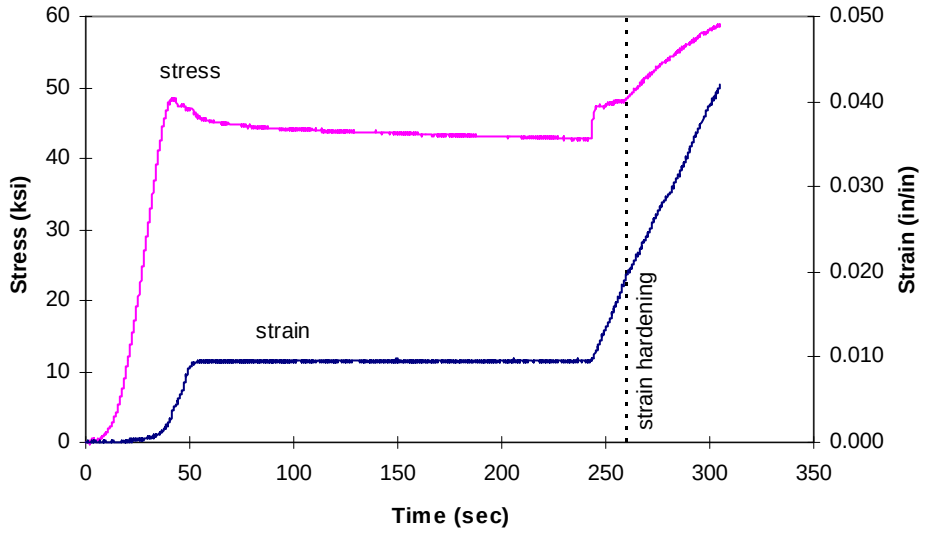

(a)

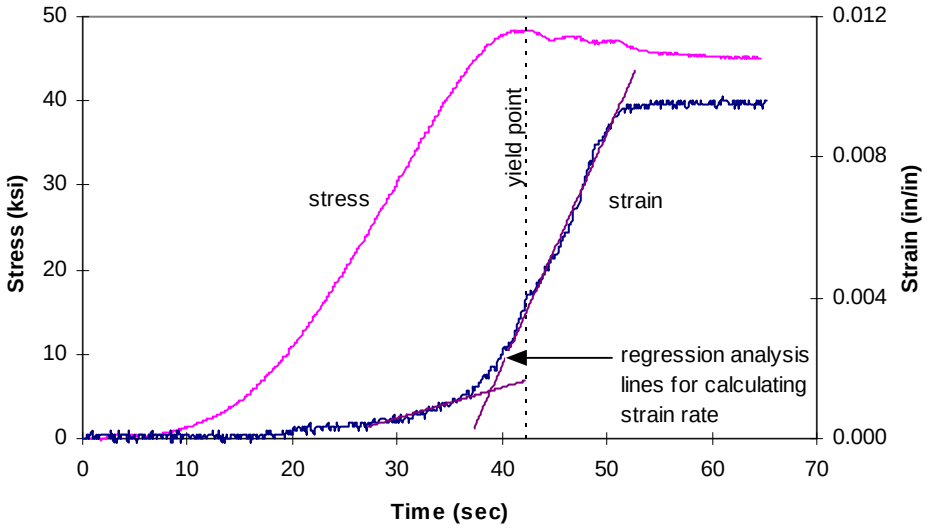

(b)

Figure A3-17: Specimen C2. Stress-time and strain-time curves: (a) zero through start of strain hardening; (b) zero through start of yield.

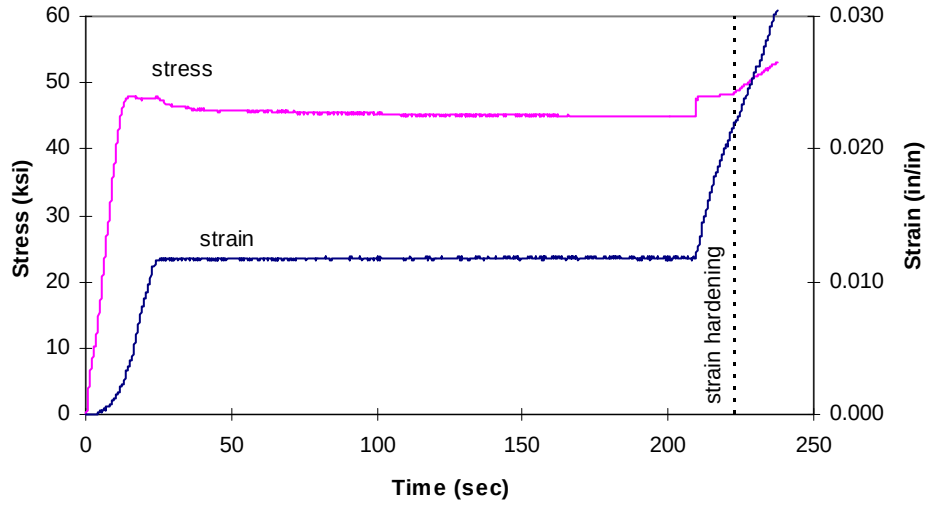

(a)

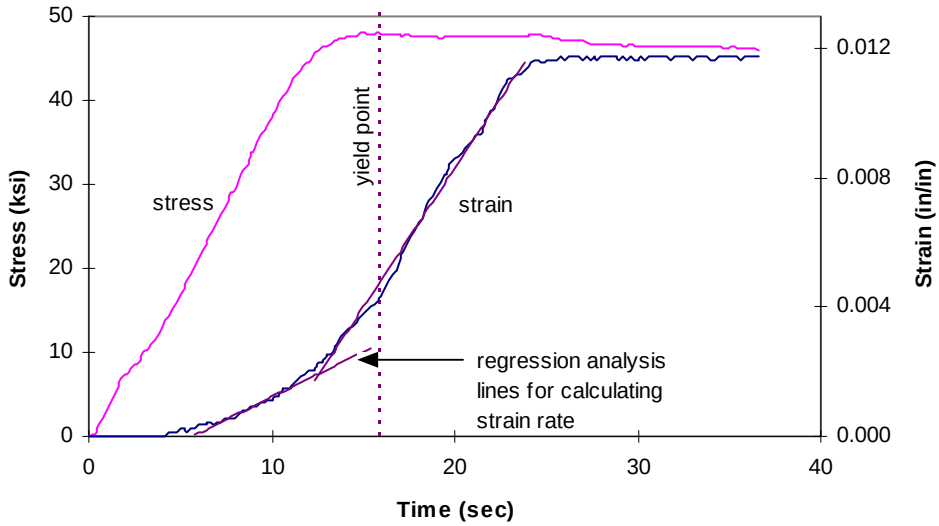

(b)

Figure A3-18: Specimen D2. Stress-time and strain-time curves: (a) zero through start of strain hardening; (b) zero through start of static yield.

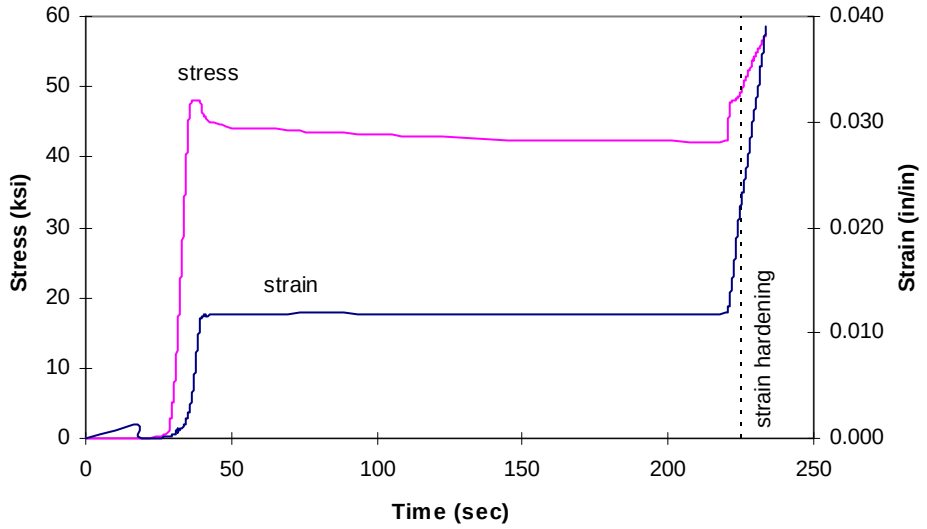

(a)

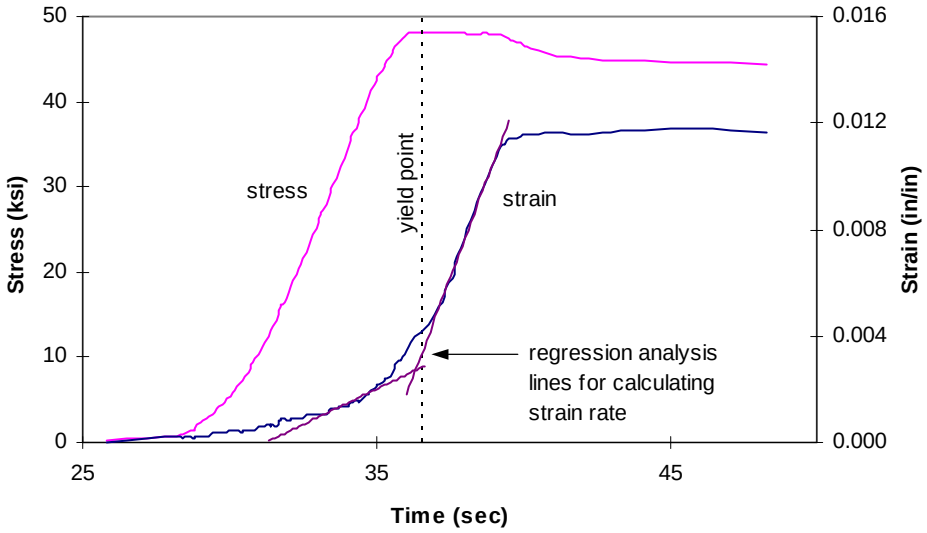

(b)

Figure A3-19: Specimen E2. Stress-time and strain-time curves: (a) zero through start of strain hardening; (b) zero through start of static yield.

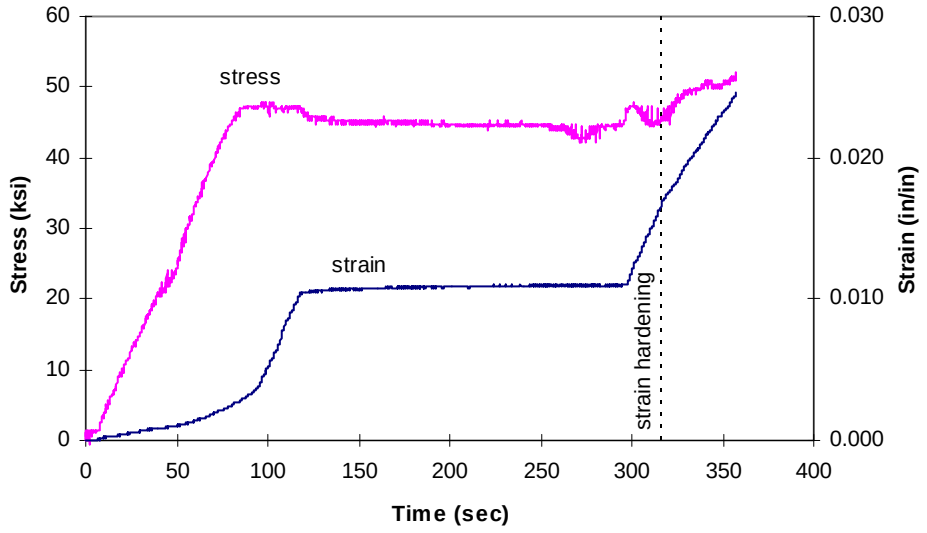

(a)

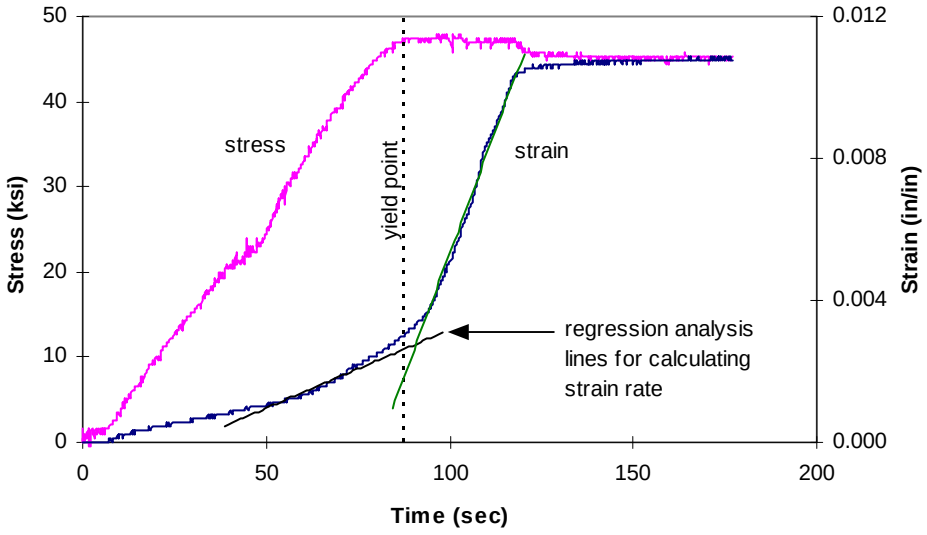

(b)

Figure A3-20: Specimen F2. Stress-time and strain-time curves: (a) zero through start of strain hardening; (b) zero through start of static yield.

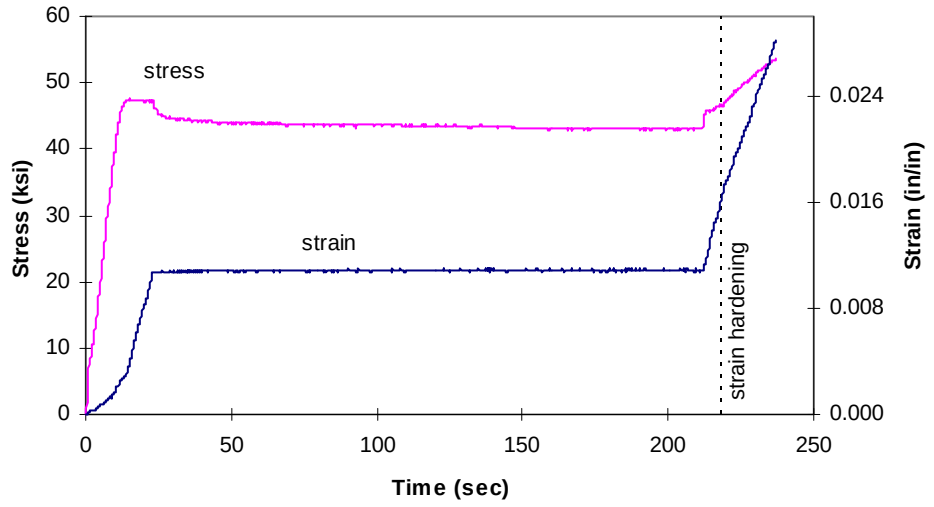

(a)

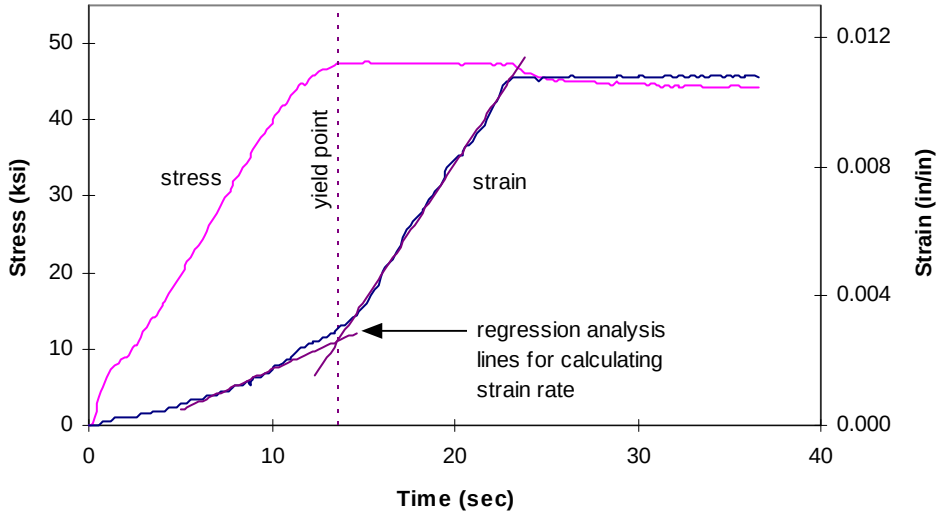

(b)

Figure A3-21: Specimen G2. Stress-time and strain-time curves: (a) zero through start of strain hardening; (b) zero through start of static yield.

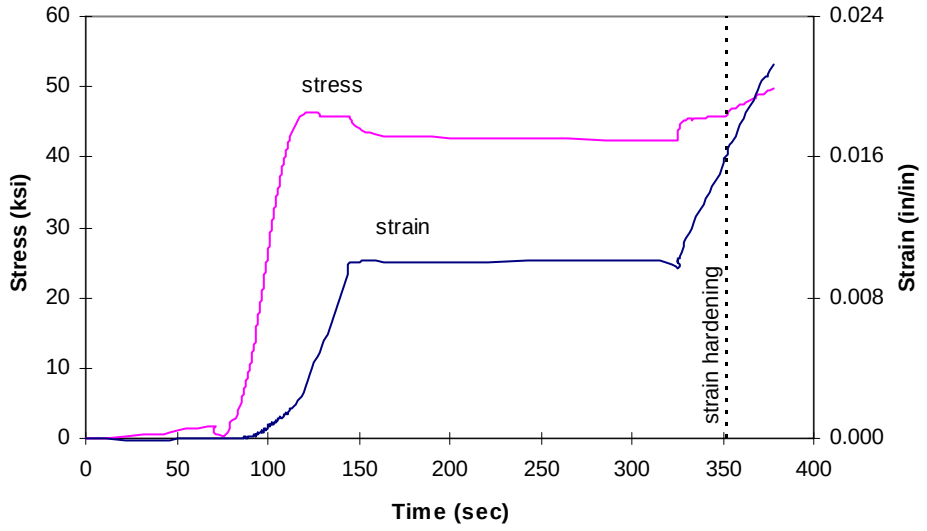

(a)

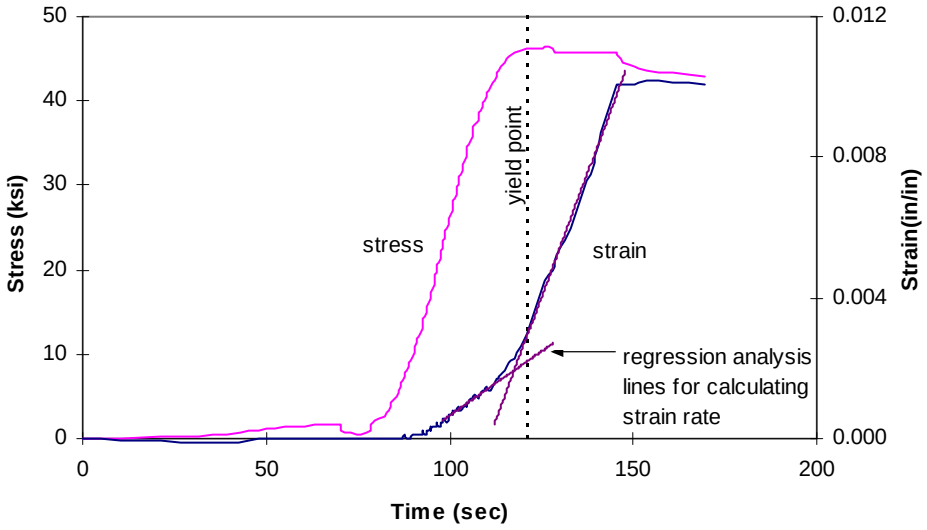

(b)

Figure A3-22: Specimen H2. Stress-time and strain-time curves: (a) zero through start of strain hardening; (b) zero through start of static yield.

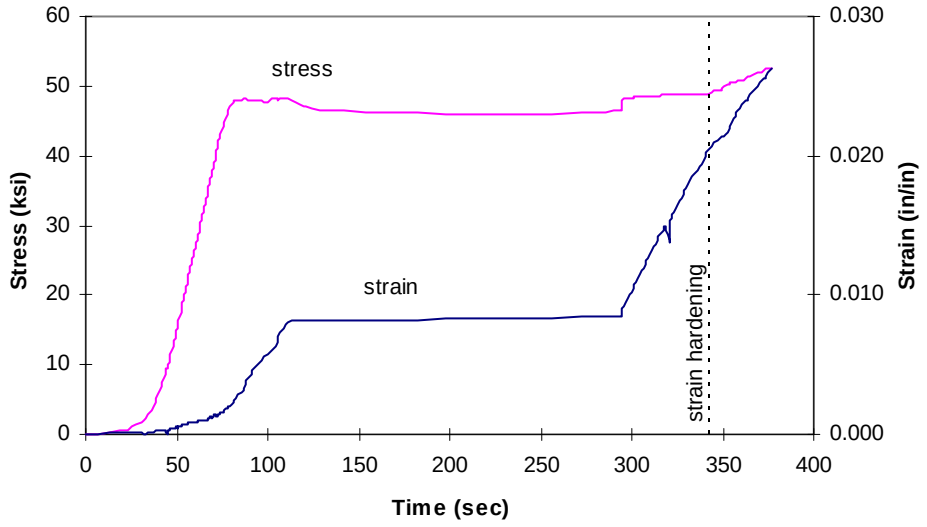

(a)

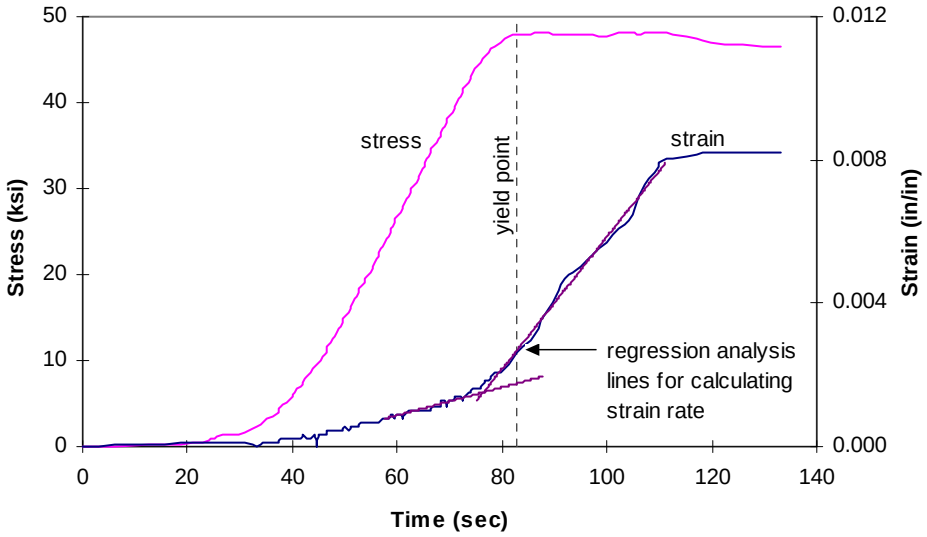

(b)

Figure A3-23: Specimen I2. Stress-time and strain-time curves: (a) zero through start of strain hardening; (b) zero through start of static yield.

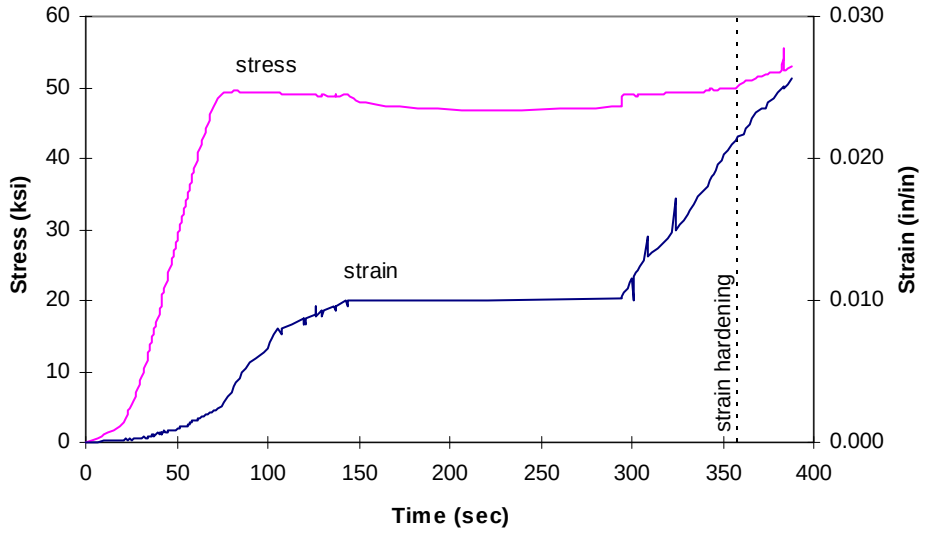

(a)

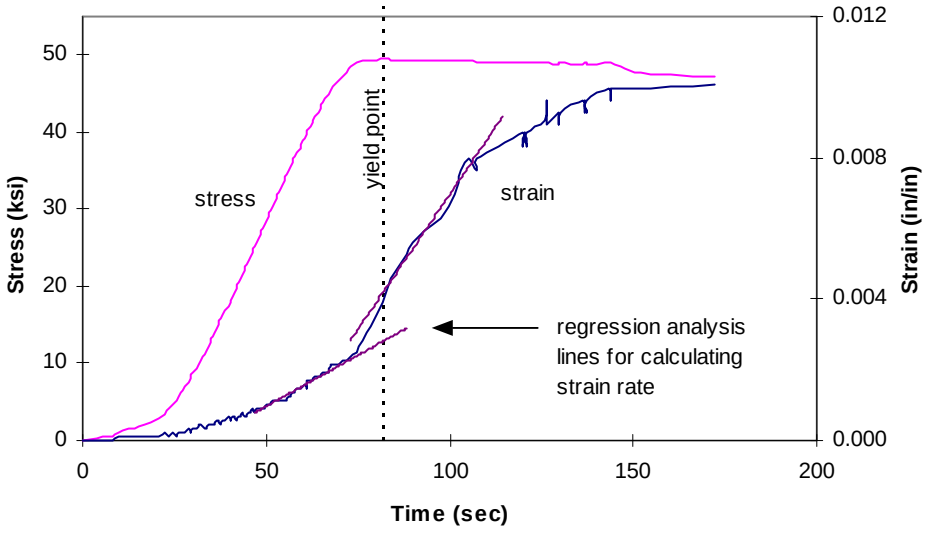

(b)

Figure A3-24: Specimen J2. Stress-time and strain-time curves: (a) zero through start of strain hardening; (b) zero through start of static yield.

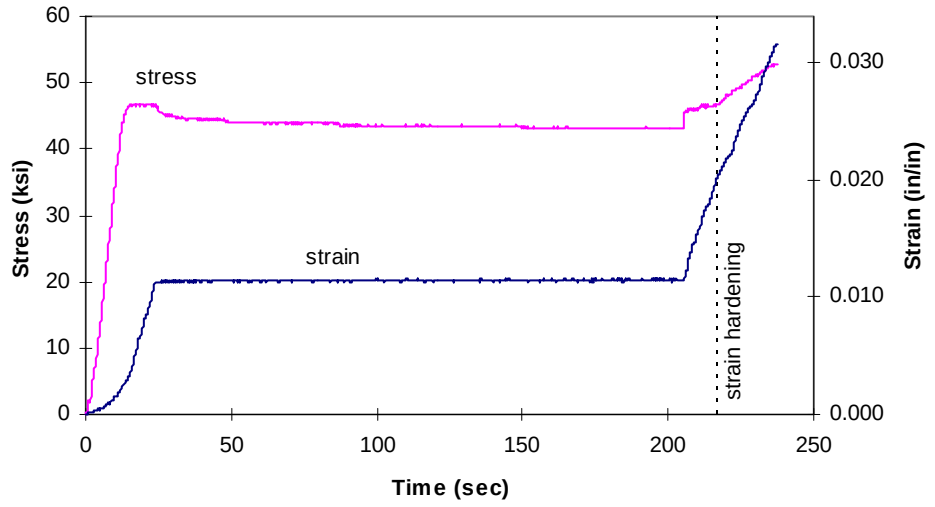

(a)

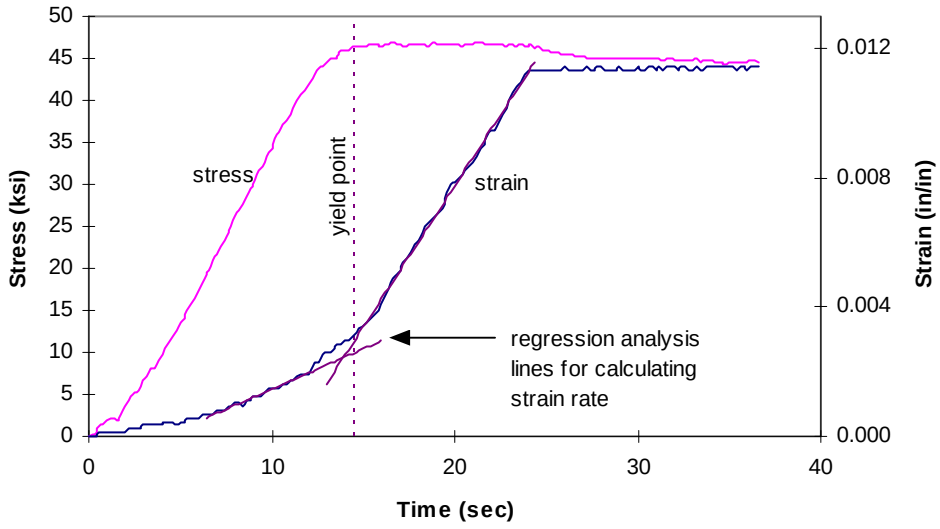

(b)

Figure A3-25: Specimen K2. Stress-time and strain-time curves: (a) zero through start of strain hardening; (b) zero through start of static yield.

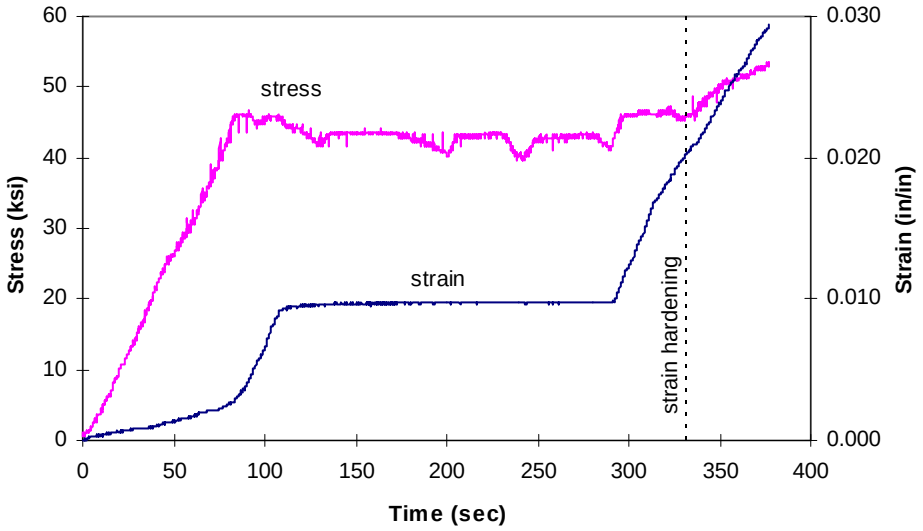

(a)

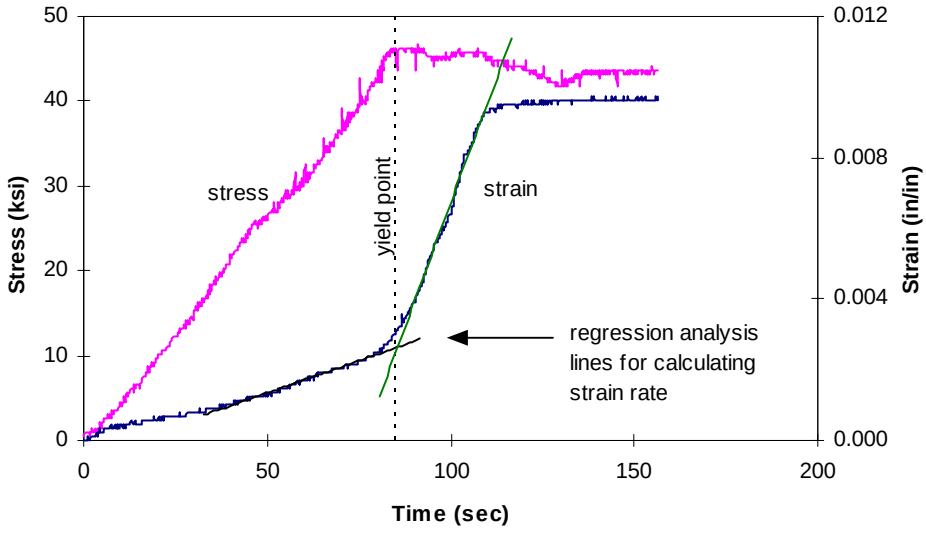

(b)

Figure A3-26: Specimen L2. Stress-time and strain-time curves: (a) zero through start of strain hardening; (b) zero through start of static yield.

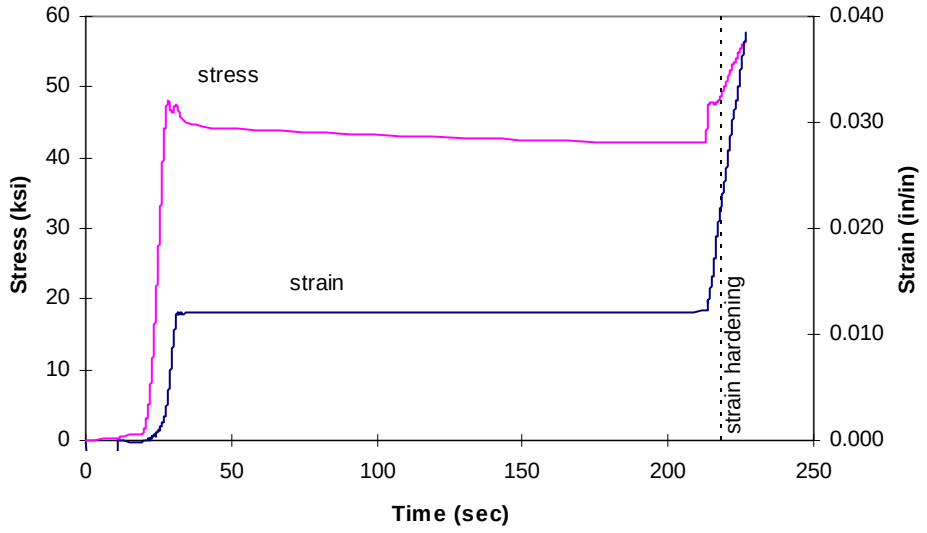

(a)

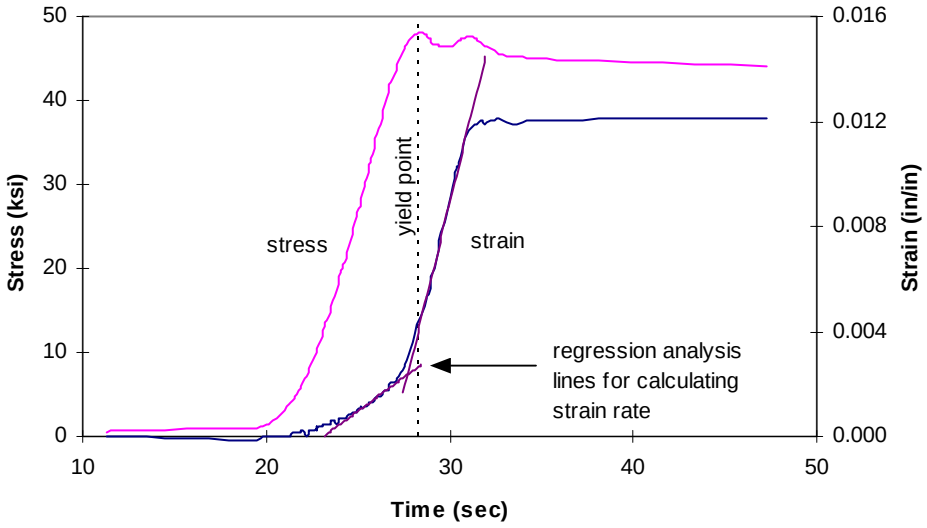

(b)

Figure A3-27: Specimen M2. Stress-time and strain-time curves: (a) zero through start of strain hardening; (b) zero through start of static yield.

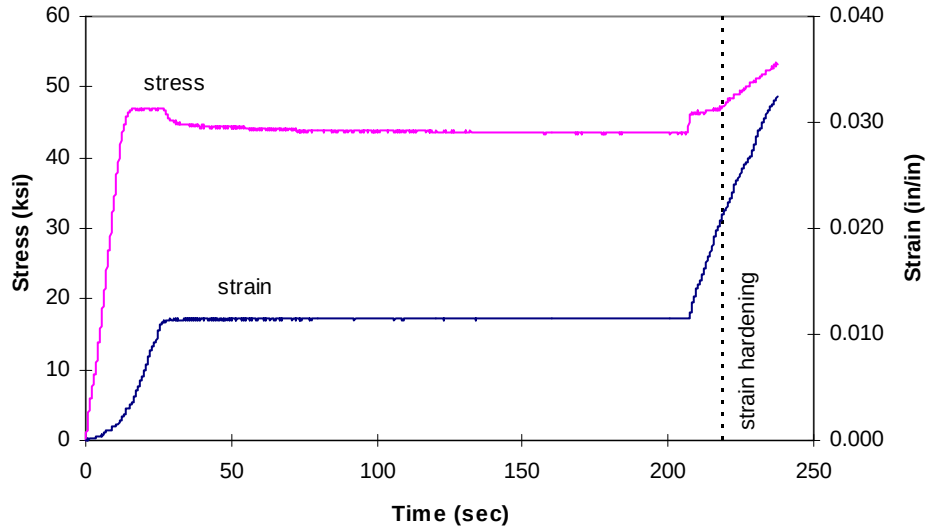

(a)

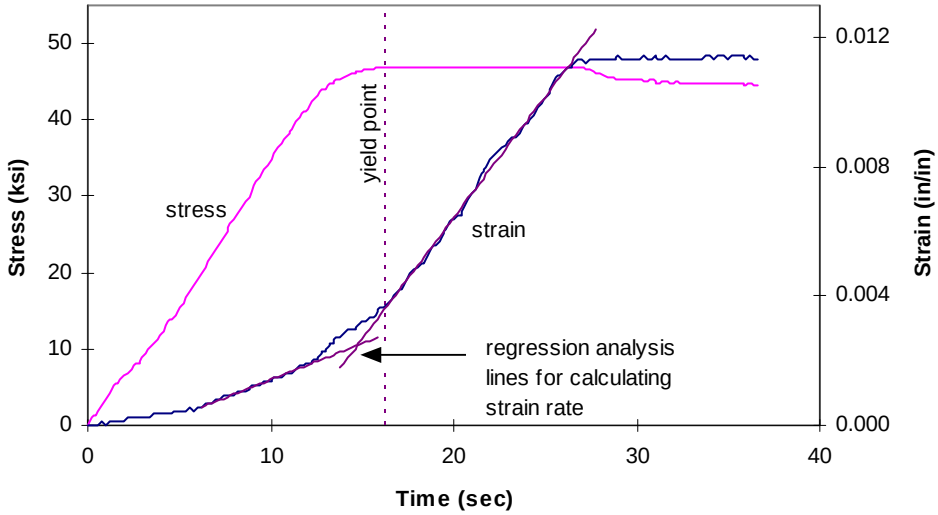

(b)

Figure A3-28: Specimen N2. Stress-time and strain-time curves: (a) zero through start of strain hardening; (b) zero through start of static yield.

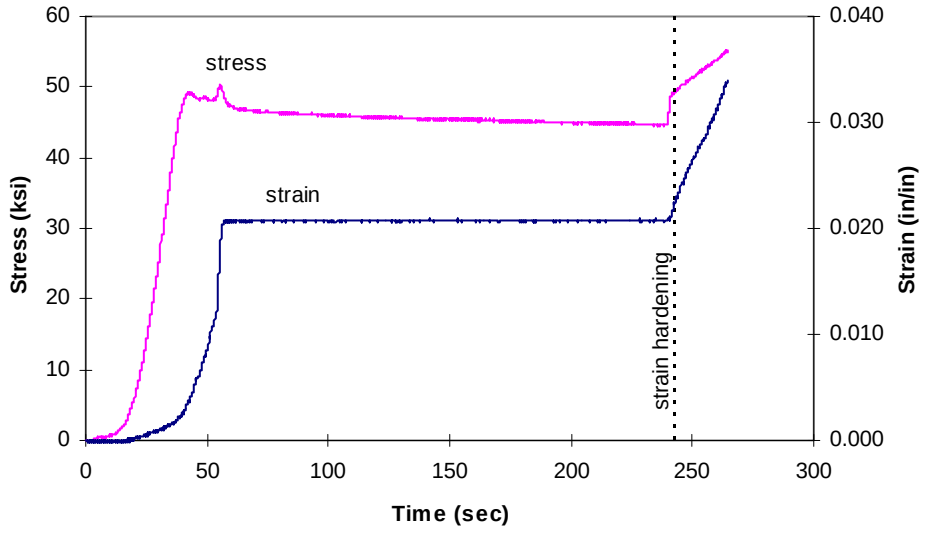

(a)

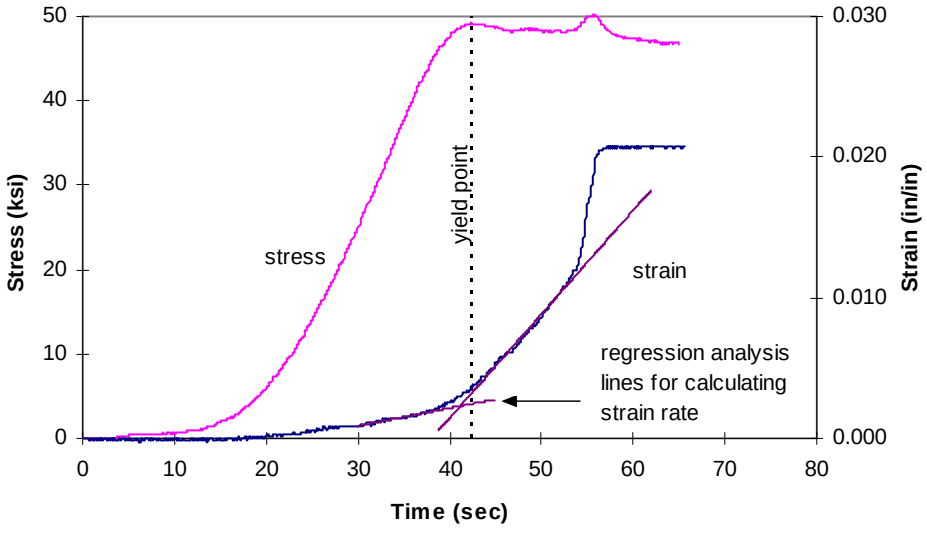

(b)

Figure A3-29: Specimen O2. Stress-time and strain-time curves: (a) zero through start of strain hardening; (b) zero through start of static yield.

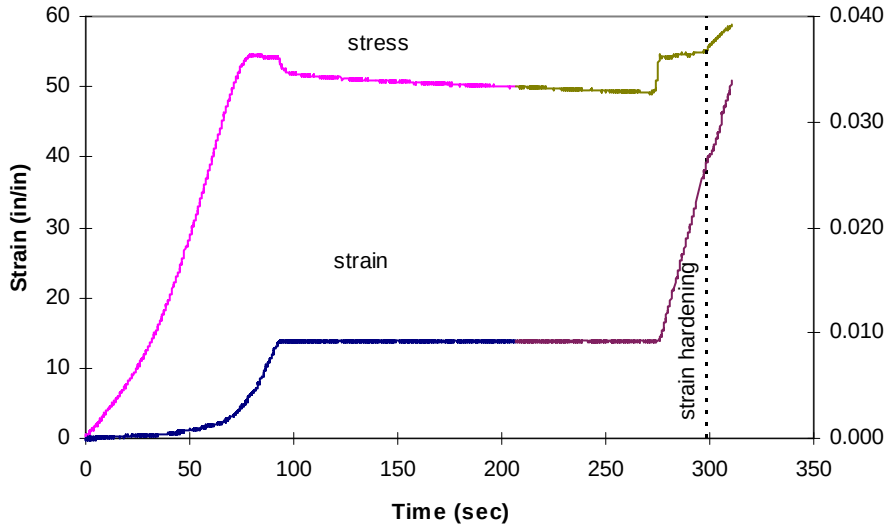

(a)

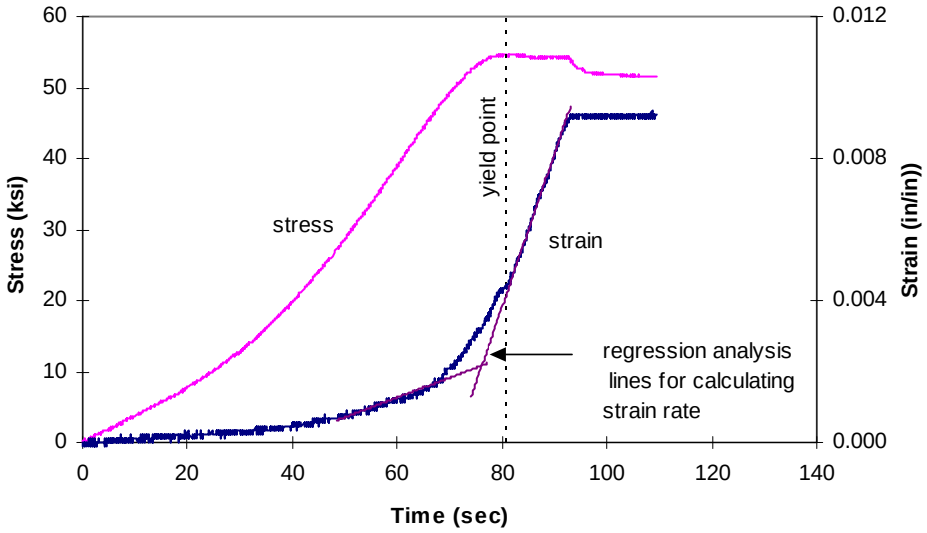

(b)

Figure A3-30: Specimen P2. Stress-time and strain-time curves: (a) zero through start of strain hardening; (b) zero through start of static yield.

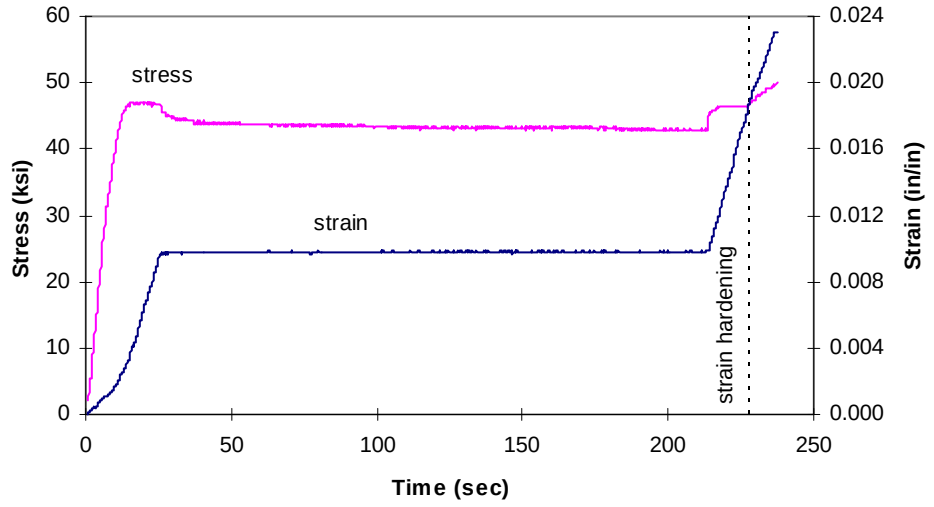

(a)

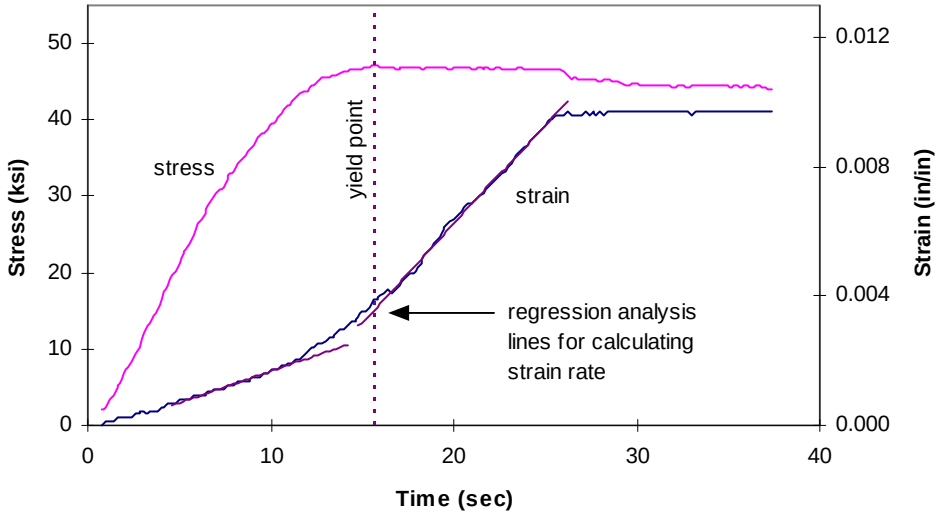

(b)

Figure A3-31: Specimen B3. Stress-time and strain-time curves: (a) zero through start of strain hardening; (b) zero through start of static yield.

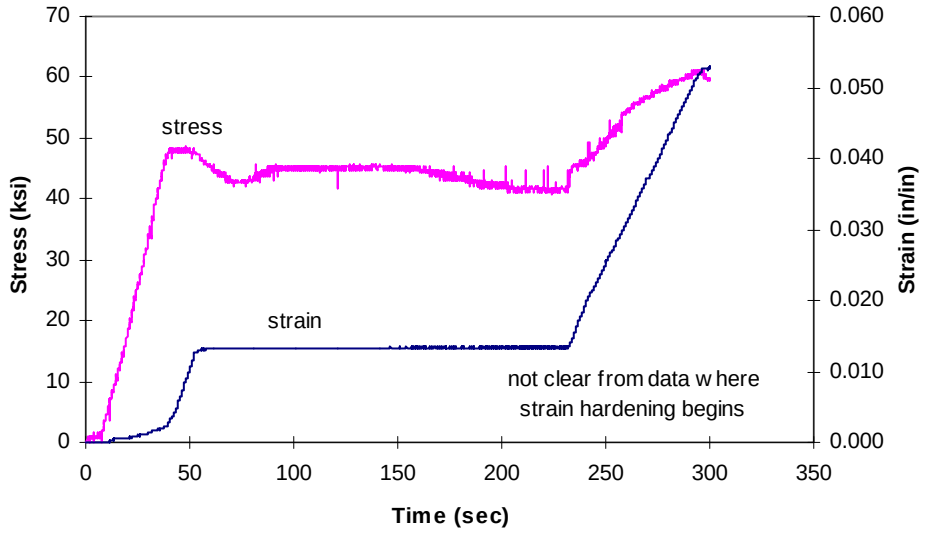

(a)

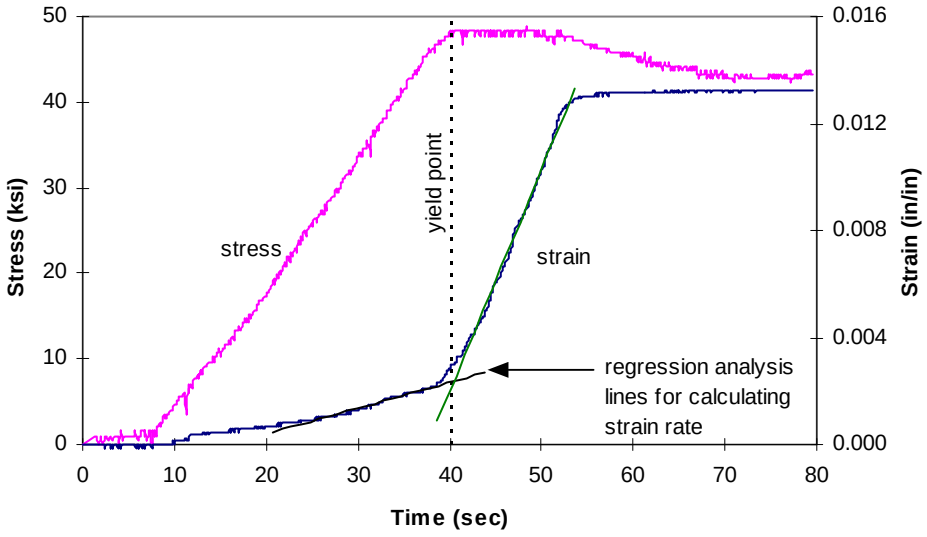

(b)

Figure A3-32: Specimen C3. Stress-time and strain-time curves: (a) zero through start of strain hardening; (b) zero through start of static yield.

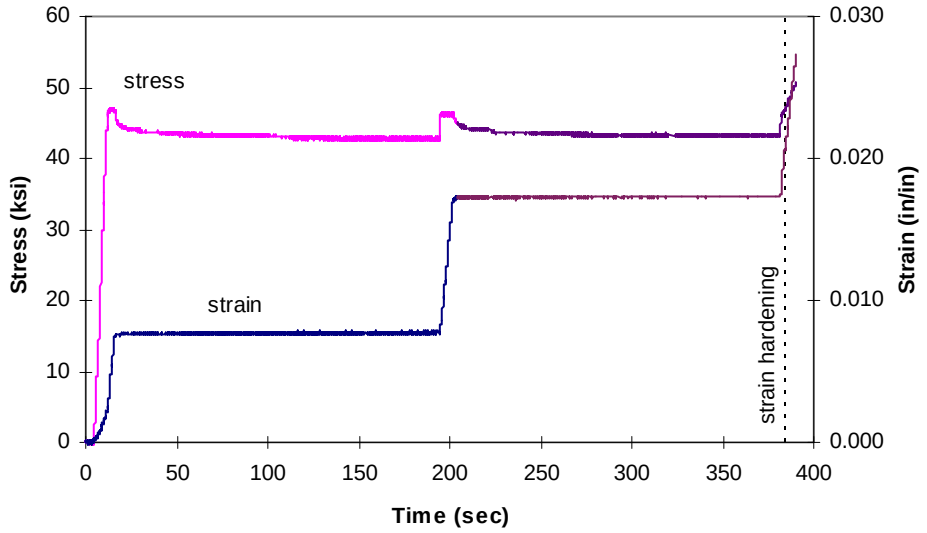

(a)

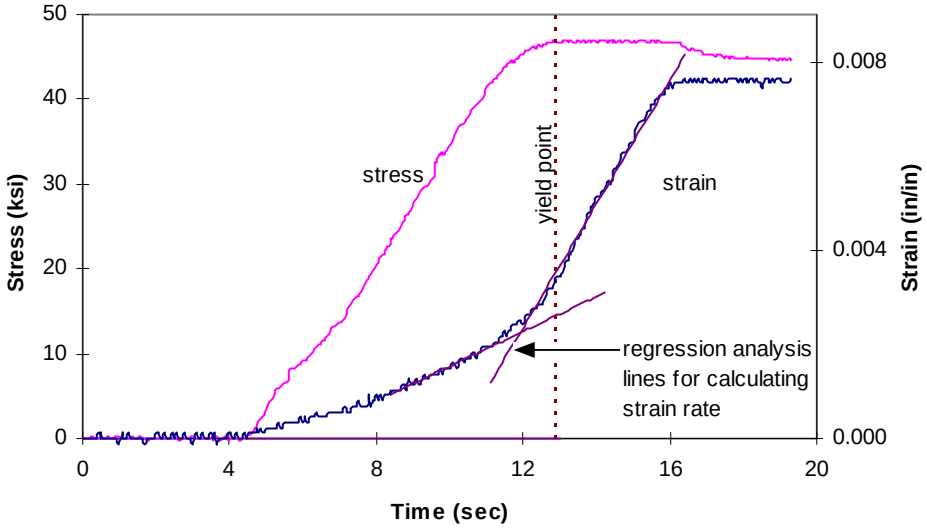

(b)

Figure A3-33: Specimen D3. Stress-time and strain-time curves: (a) zero through start of strain hardening; (b) zero through start of static yield.

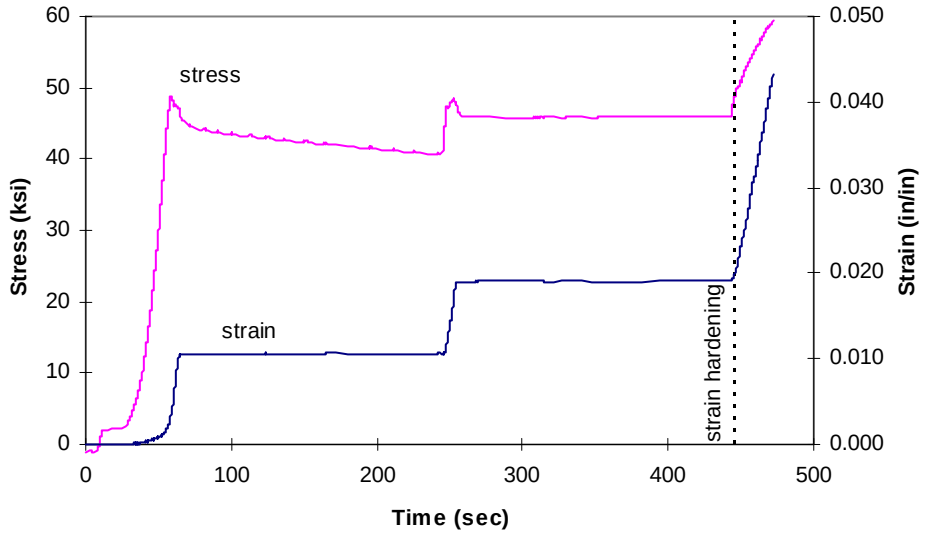

(a)

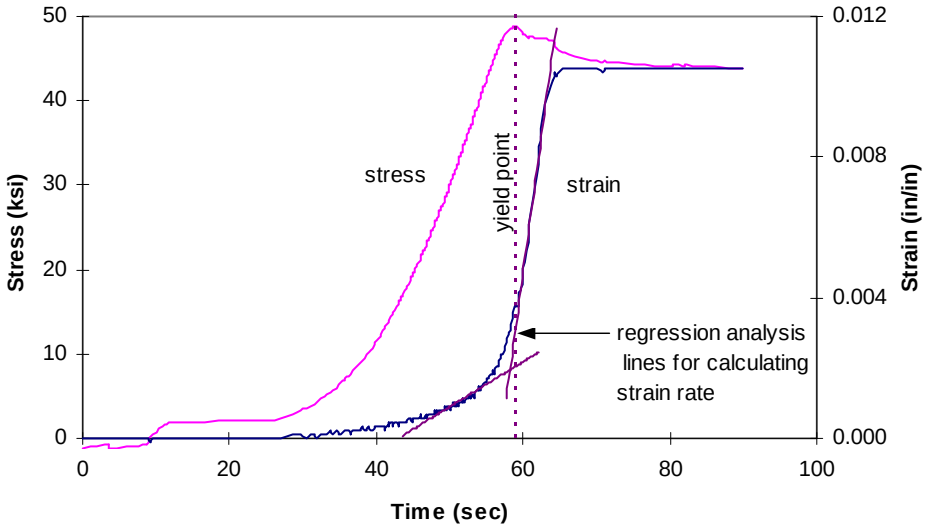

(b)

Figure A3-34: Specimen E3. Stress-time and strain-time curves: (a) zero through start of strain hardening; (b) zero through start of static yield.

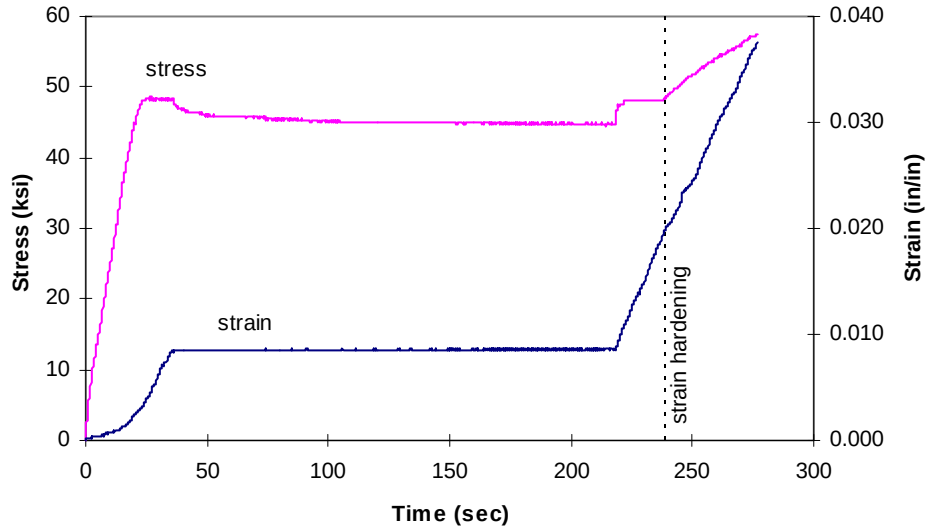

(a)

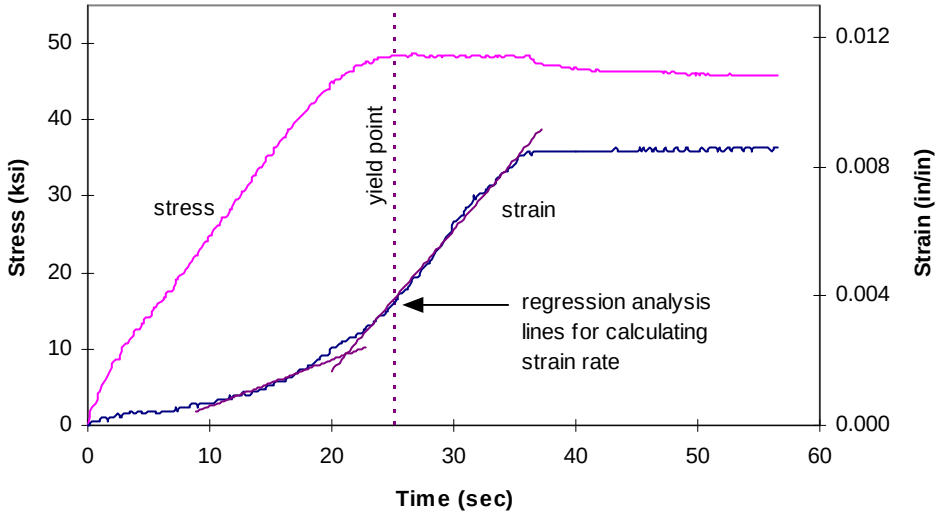

(b)

Figure A3-35: Specimen F3. Stress-time and strain-time curves: (a) zero through start of strain hardening; (b) zero through start of static yield.

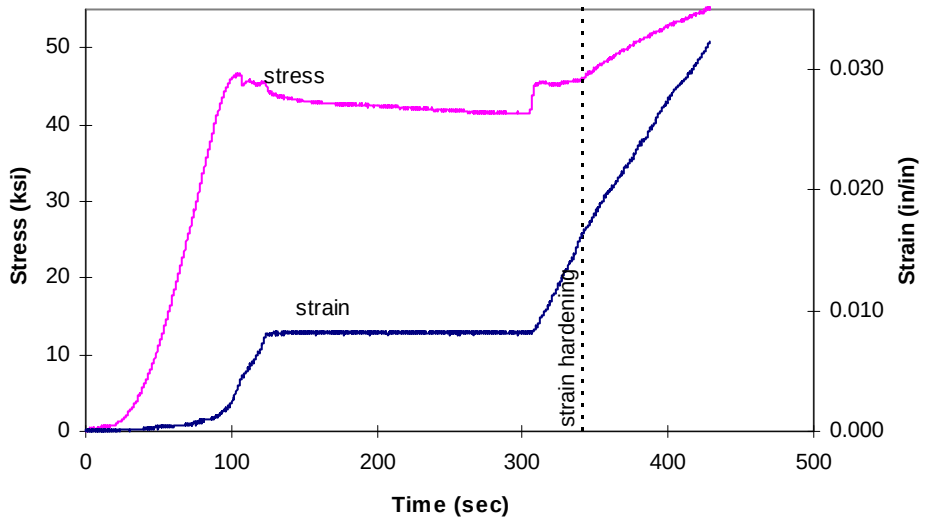

(a)

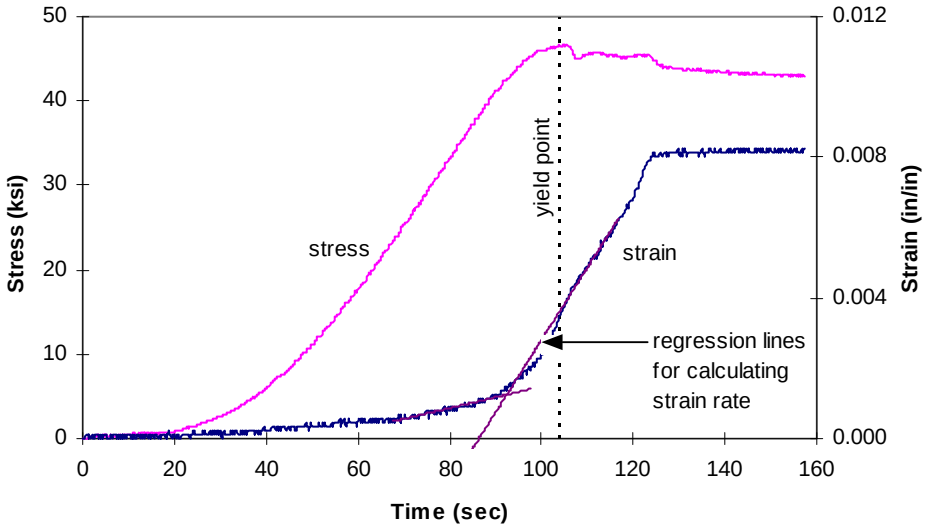

(b)

Figure A3-36: Specimen G3. Stress-time and strain-time curves: (a) zero through start of strain hardening; (b) zero through start of static yield.

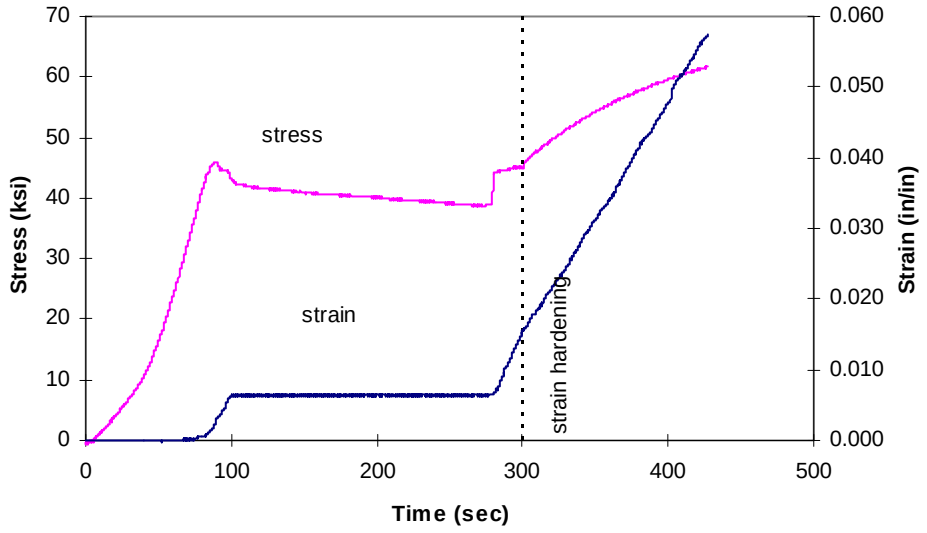

(a)

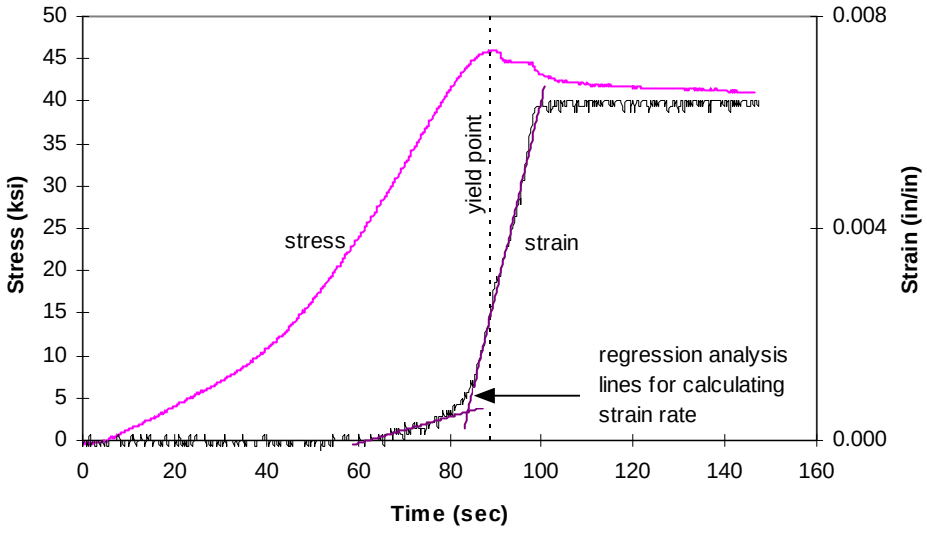

(b)

Figure A3-37: Specimen H3. Stress-time and strain-time curves: (a) zero through start of strain hardening; (b) zero through start of static yield.

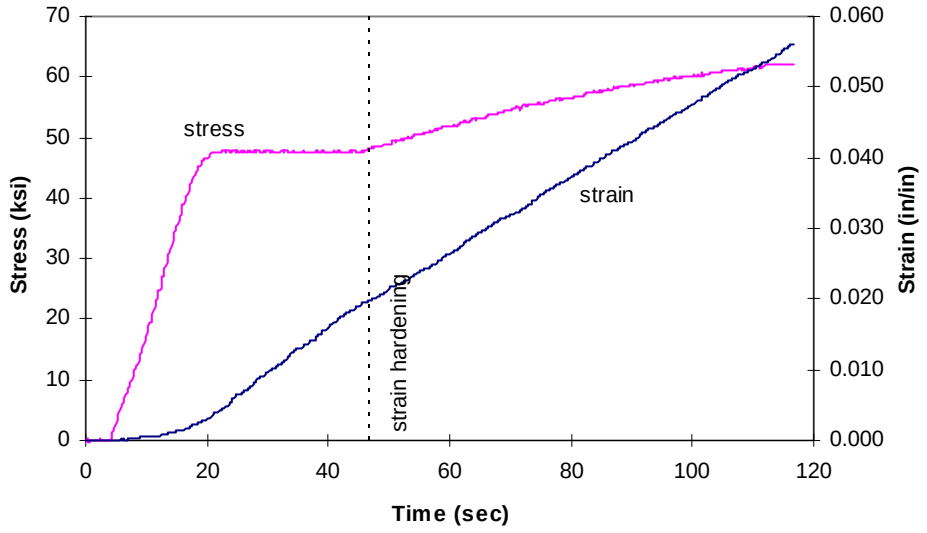

(a)

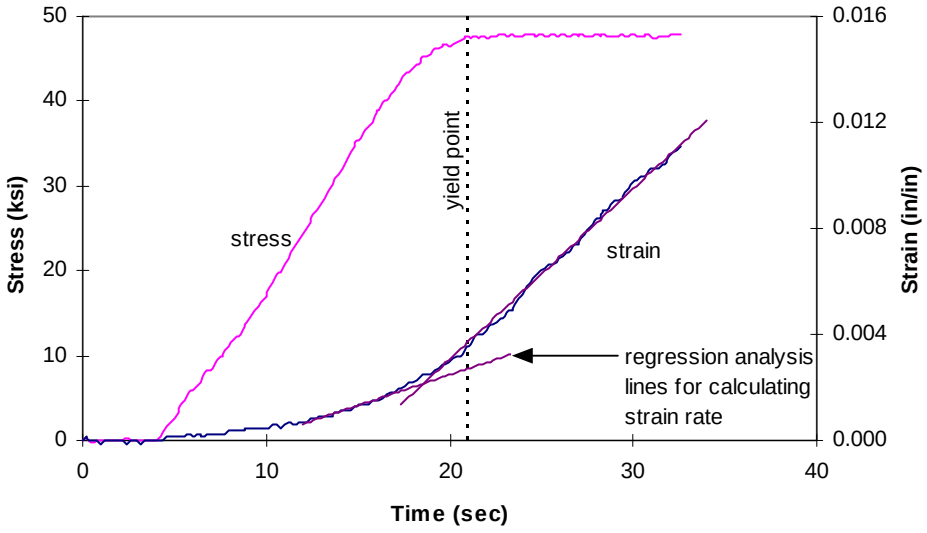

(b)

Figure A3-38: Specimen I3. Stress-time and strain-time curves: (a) zero through start of strain hardening; (b) zero through start of yielding.

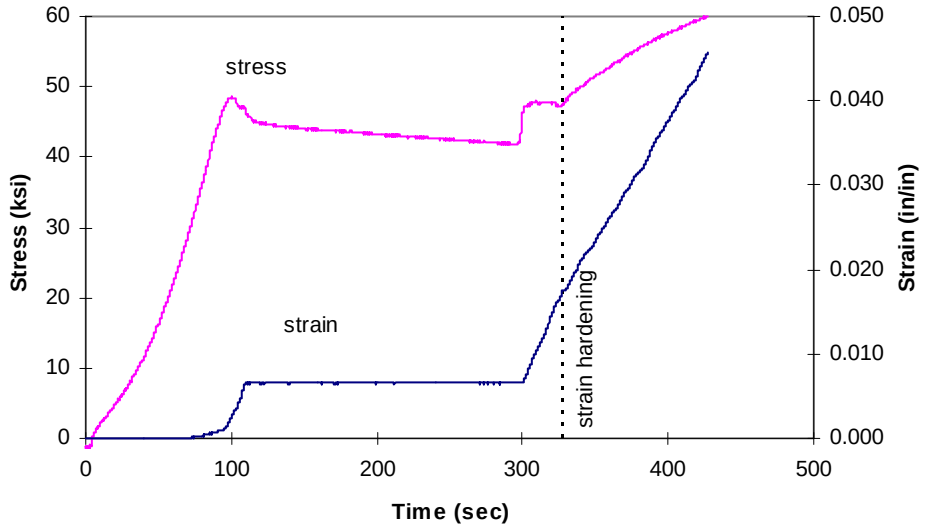

(a)

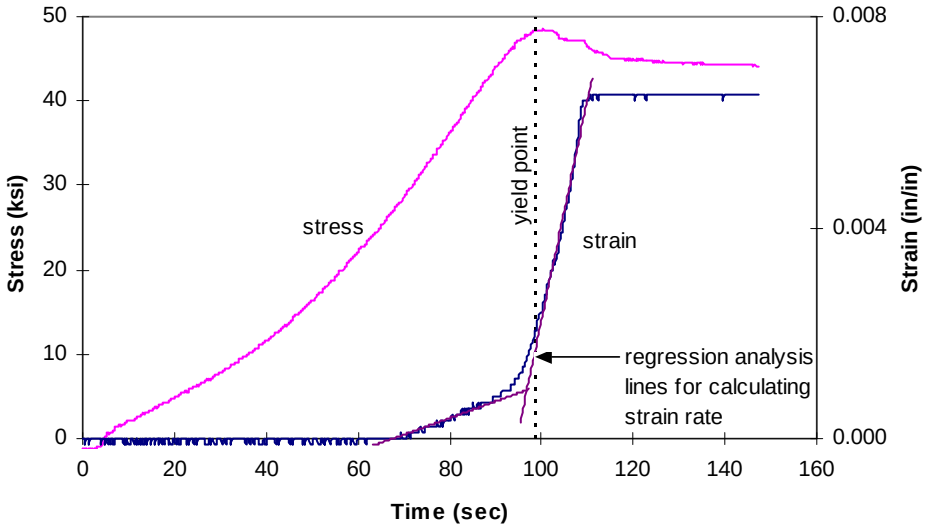

(b)

Figure A3-39: Specimen J3. Stress-time and strain-time curves: (a) zero through start of strain hardening; (b) zero through start of static yield.

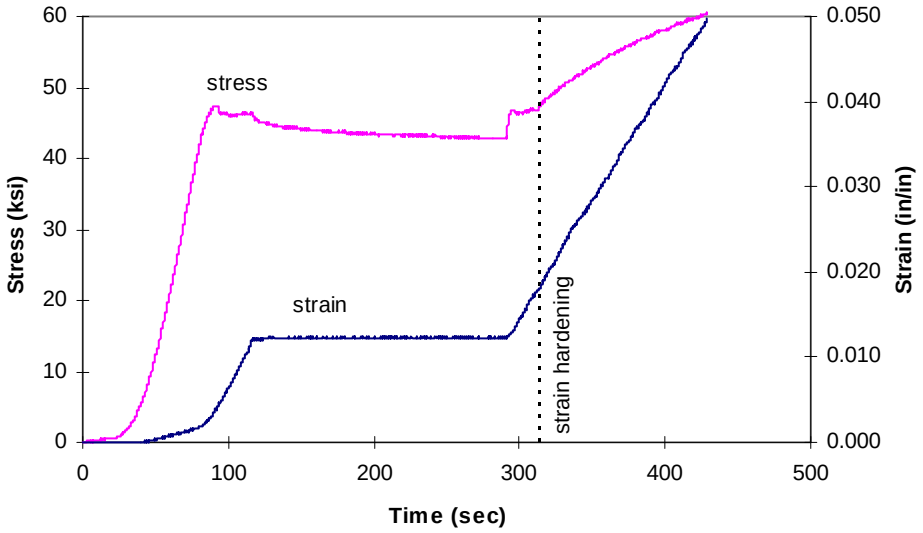

(a)

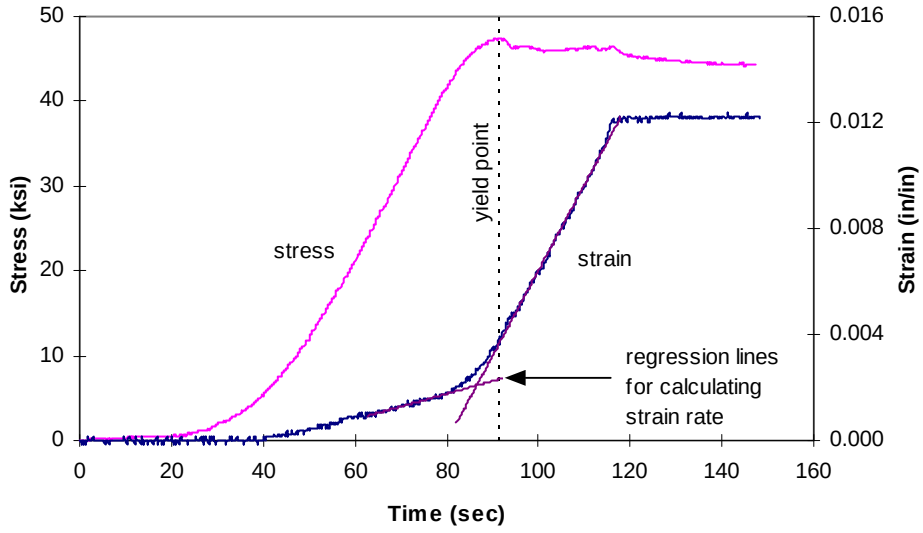

(b)

Figure A3-40: Specimen K3. Stress-time and strain-time curves: (a) zero through start of strain hardening; (b) zero through start of static yield.

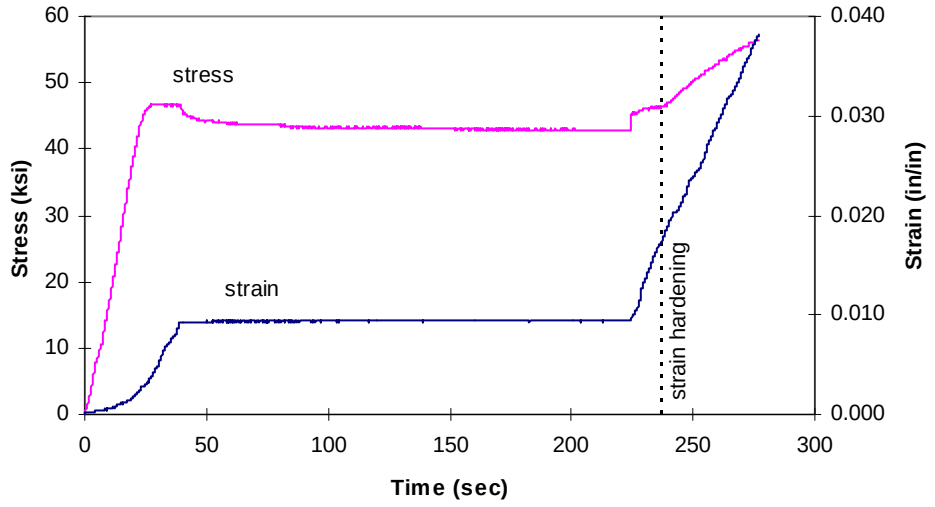

(a)

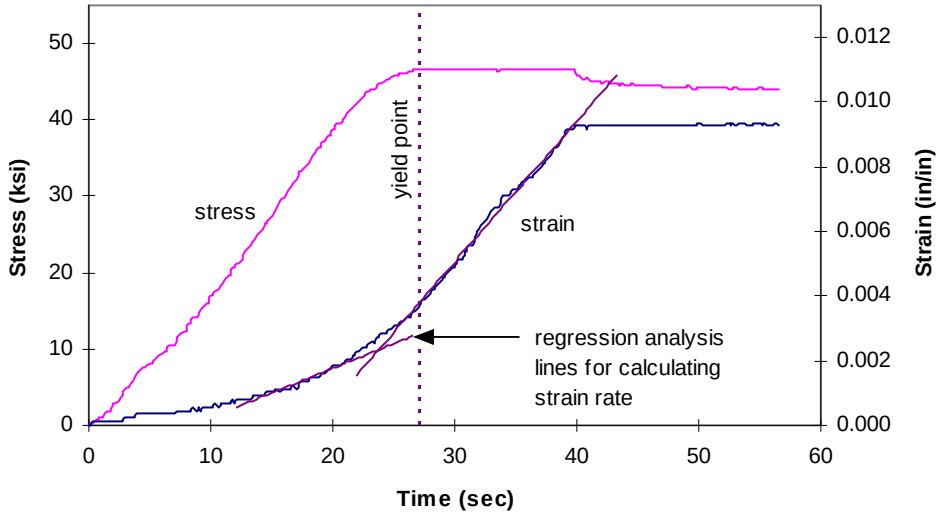

(b)

Figure A3-41: Specimen L3. Stress-time and strain-time curves: (a) zero through start of strain hardening; (b) zero through start of static yield.

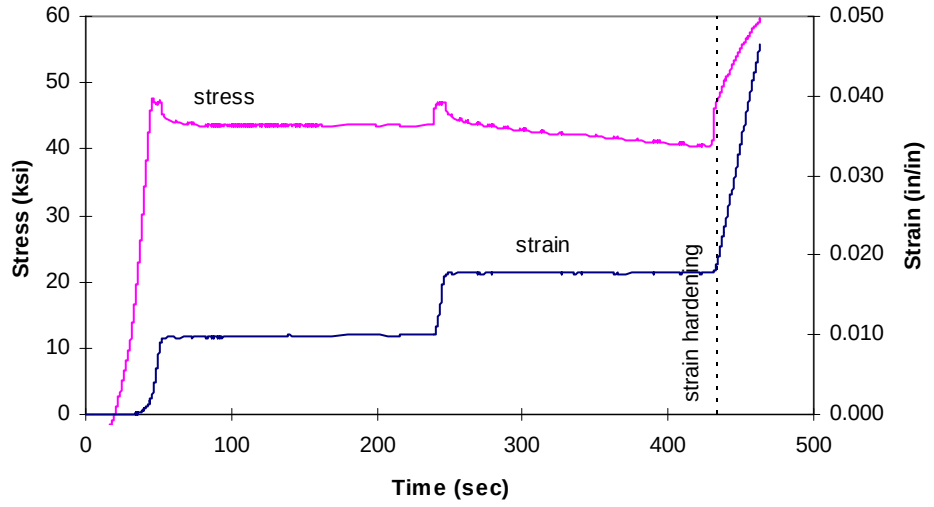

(a)

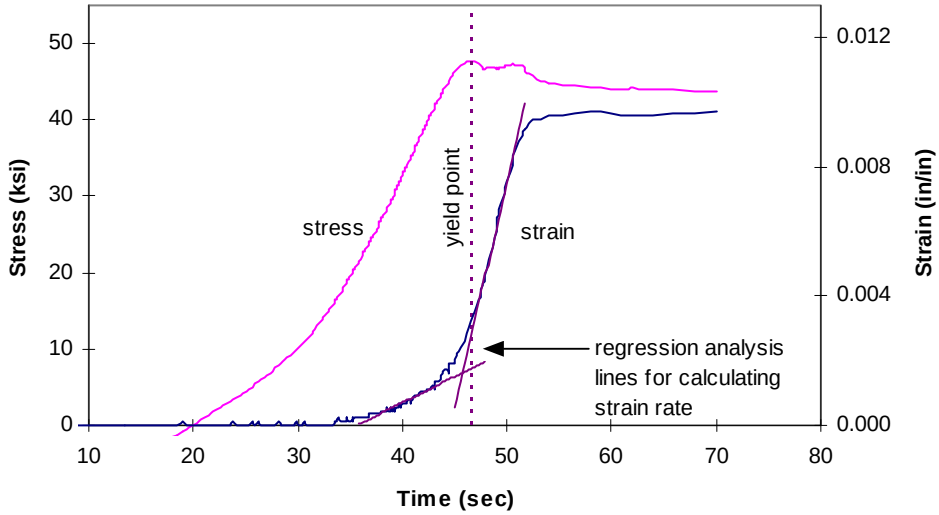

(b)

Figure A3-42: Specimen M3. Stress-time and strain-time curves: (a) zero through start of strain hardening; (b) zero through start of static yield.

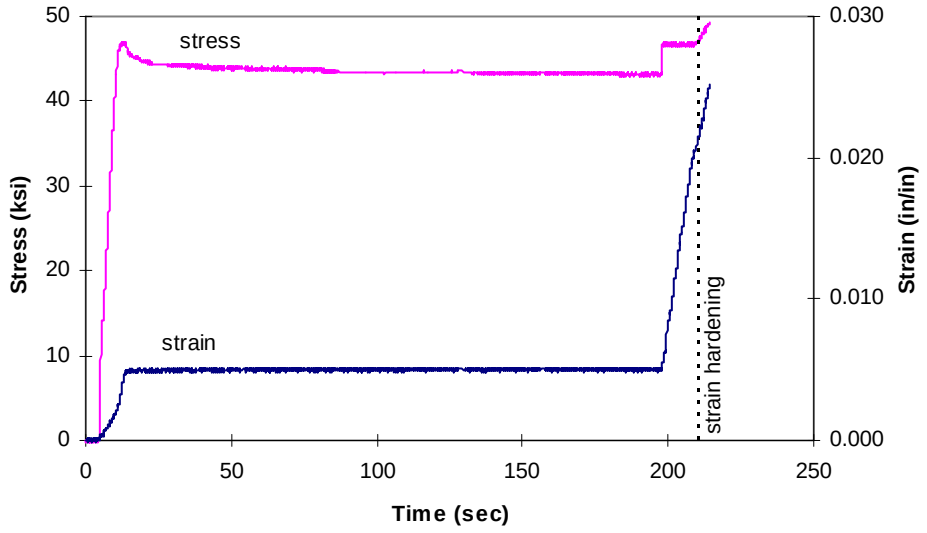

(a)

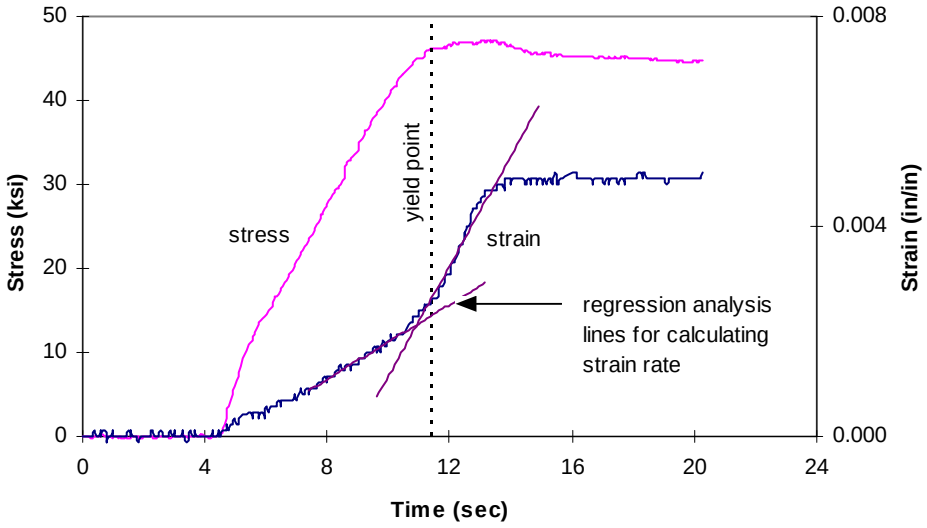

(b)

Figure A3-43: Specimen N3. Stress-time and strain-time curves: (a) zero through start of strain hardening; (b) zero through start of static yield.

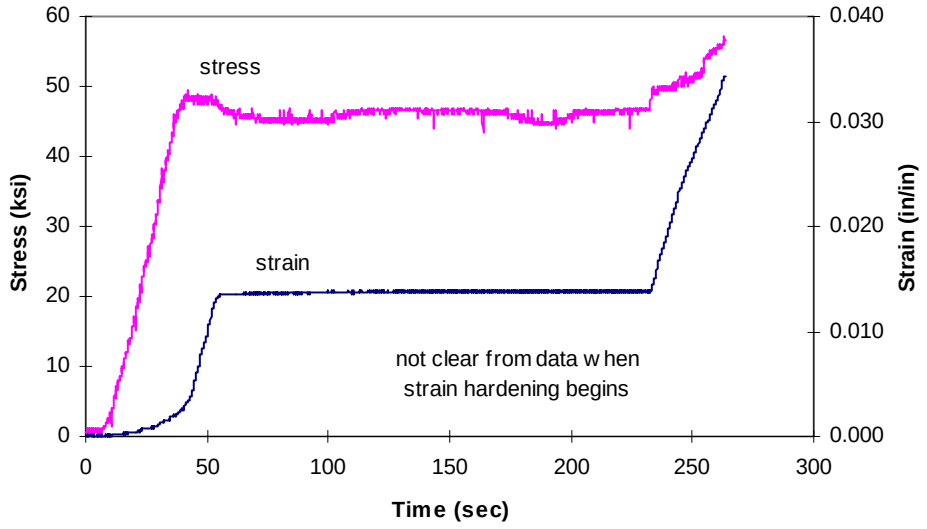

(a)

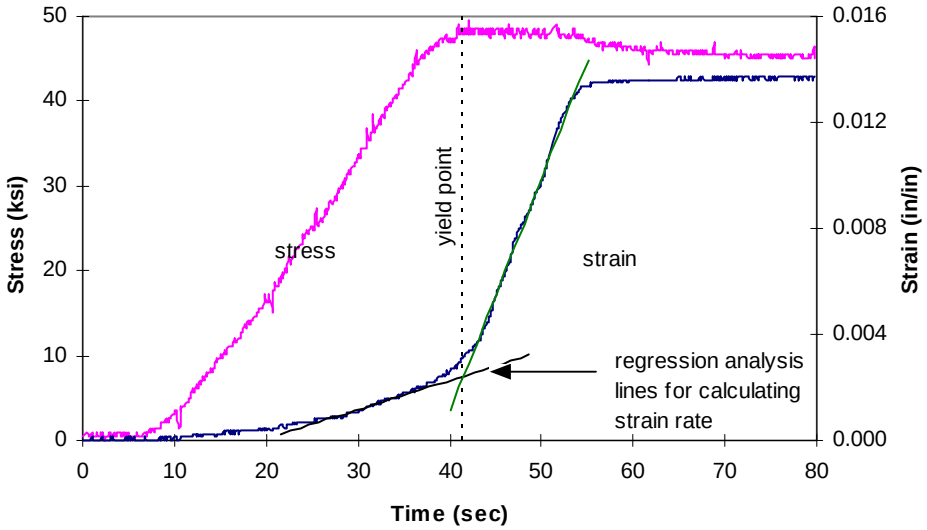

(b)

Figure A3-44: Specimen O3. Stress-time and strain-time curves: (a) zero through start of strain hardening; (b) zero through start of static yield.

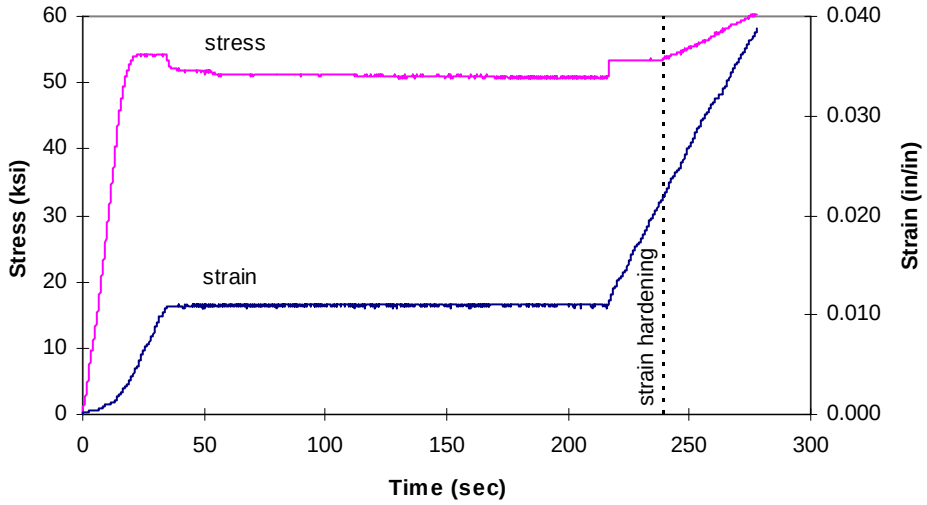

(a)

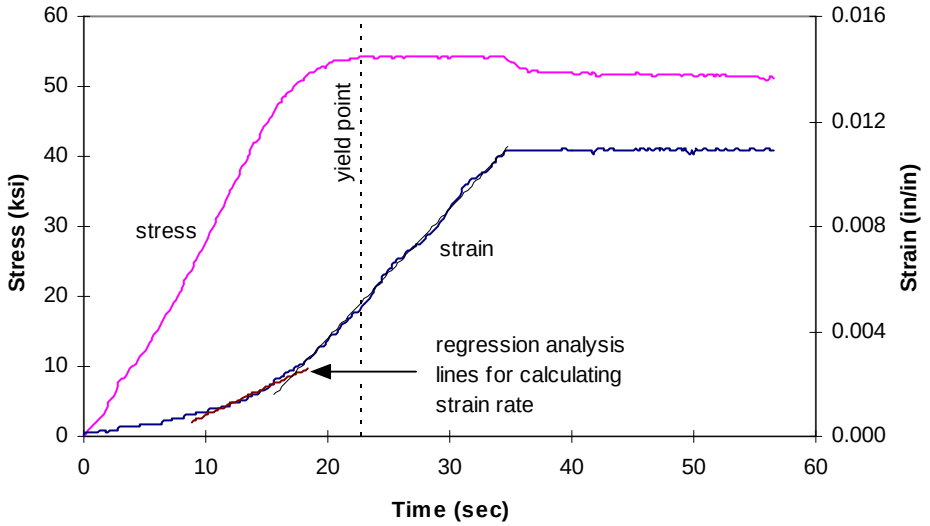

(b)

Figure A3-45: Specimen P3. Stress-time and strain-time curves: (a) zero through start of strain hardening; (b) zero through start of static yield.

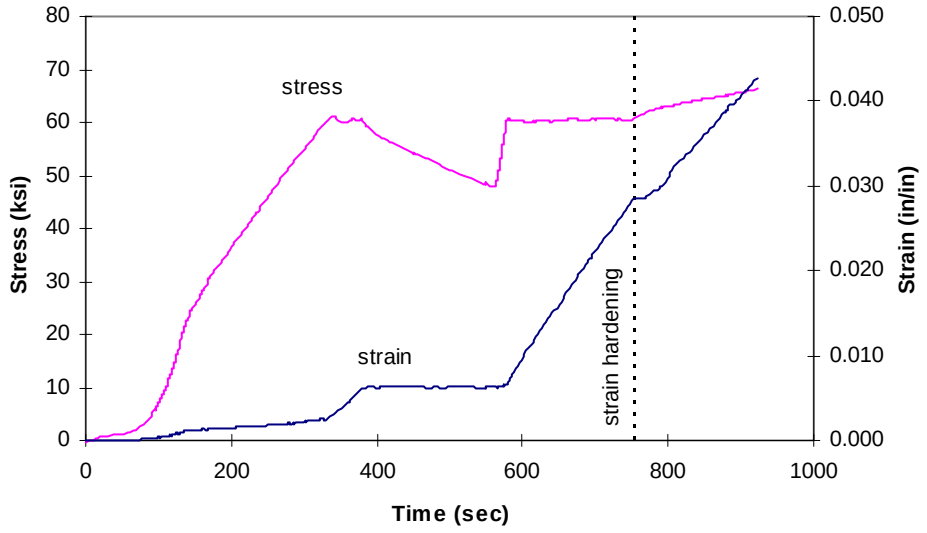

(a)

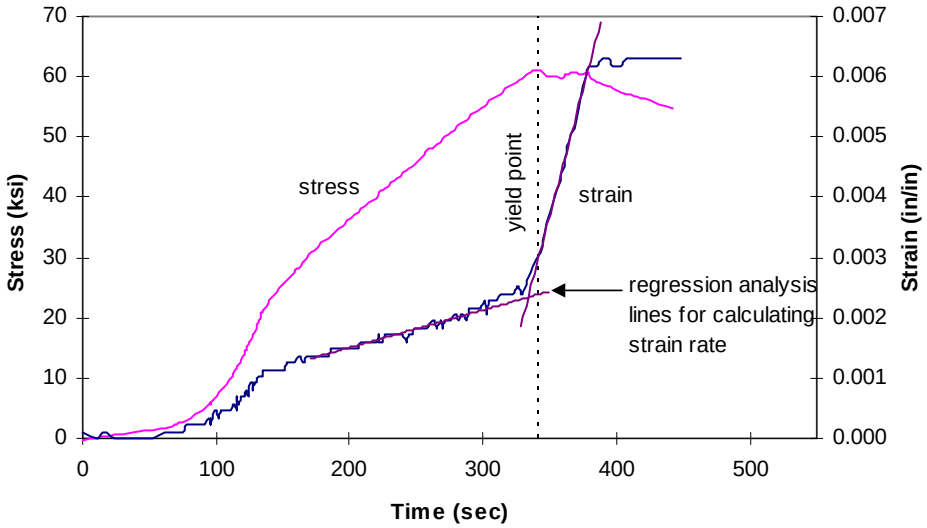

(b)

Figure A3-46: Specimen 1A. Stress-time and strain-time curves: (a) zero through start of strain hardening; (b) zero through start of static yield.

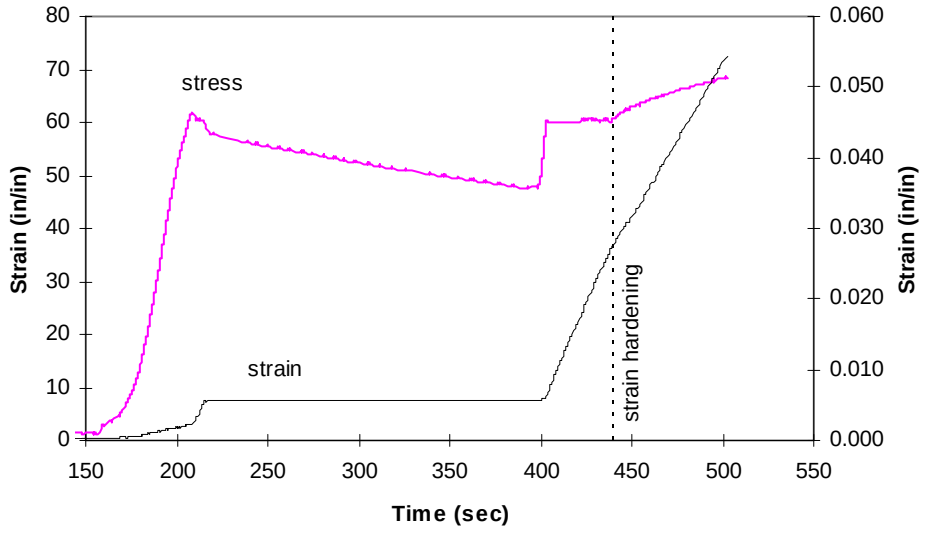

(a)

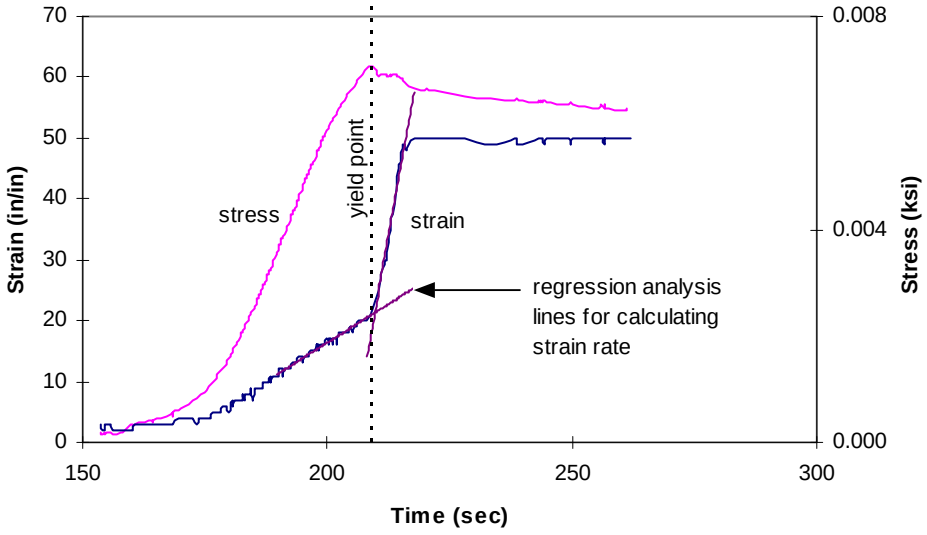

(b)

Figure A3-47: Specimen 2A. Stress-time and strain-time curves: (a) zero through start of strain hardening; (b) zero through start of static yield.

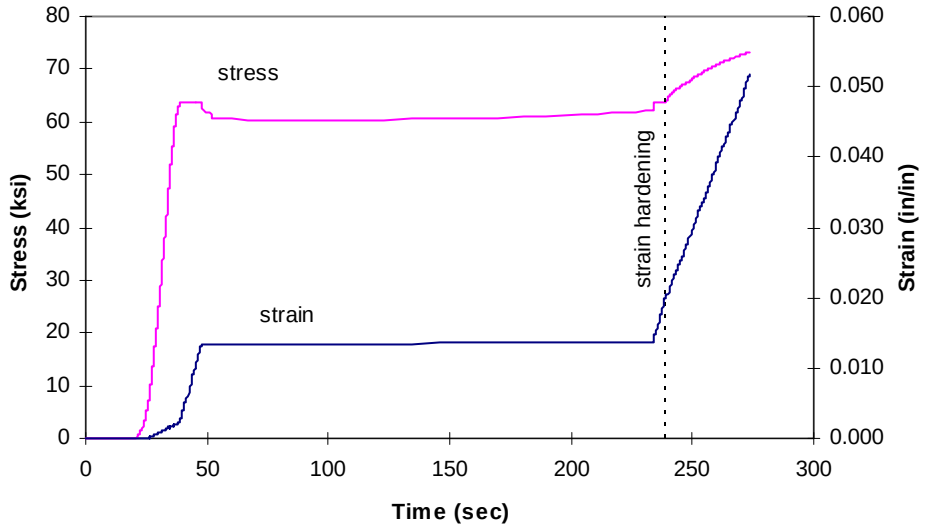

(a)

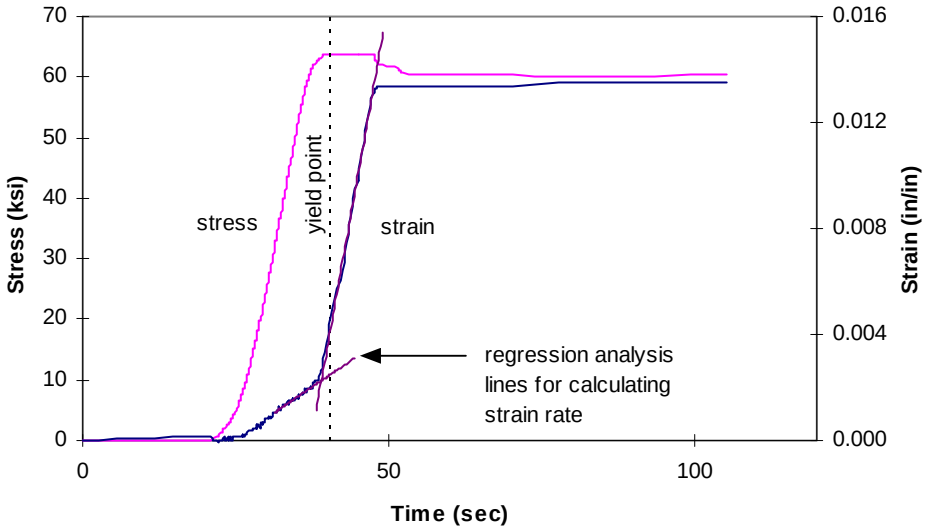

(b)

Figure A3-48: Specimen 3A. Stress-time and strain-time curves: (a) zero through start of strain hardening; (b) zero through start of static yield.

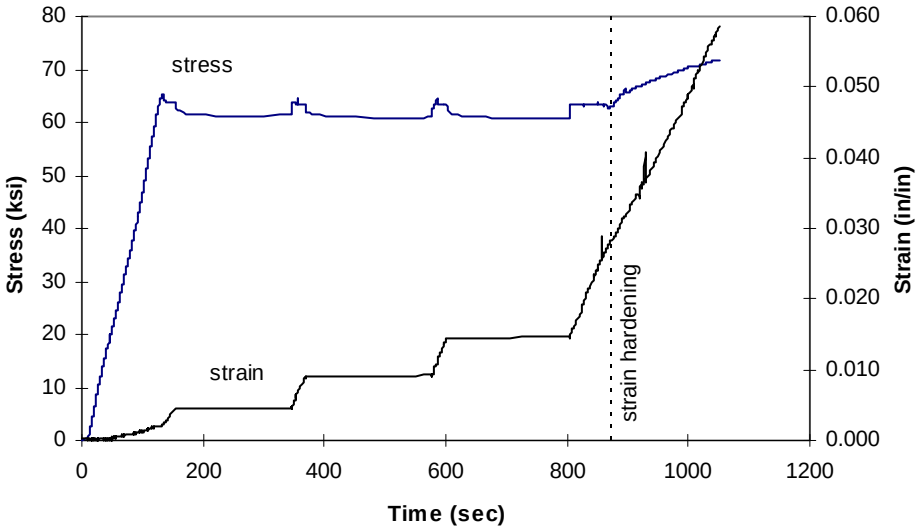

(a)

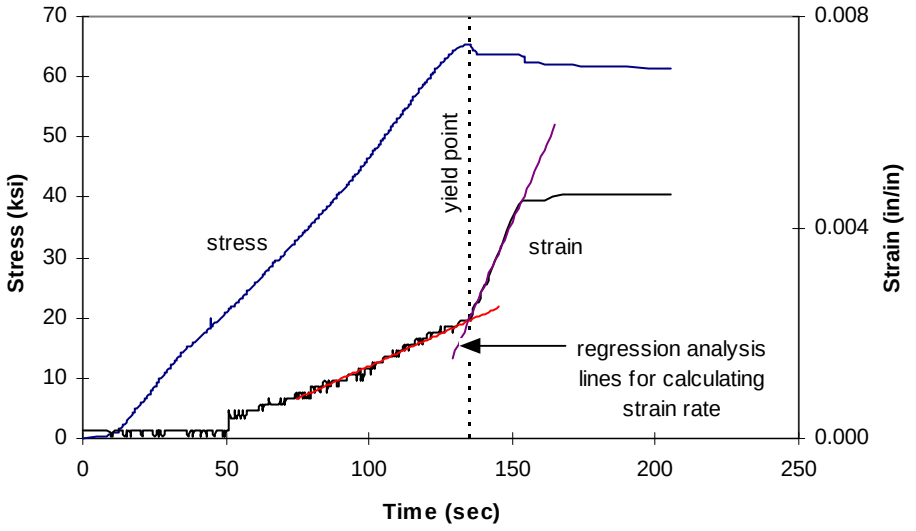

(b)

Figure A3-49: Specimen 4A. Stress-time and strain-time curves: (a) zero through start of strain hardening; (b) zero through start of static yield.

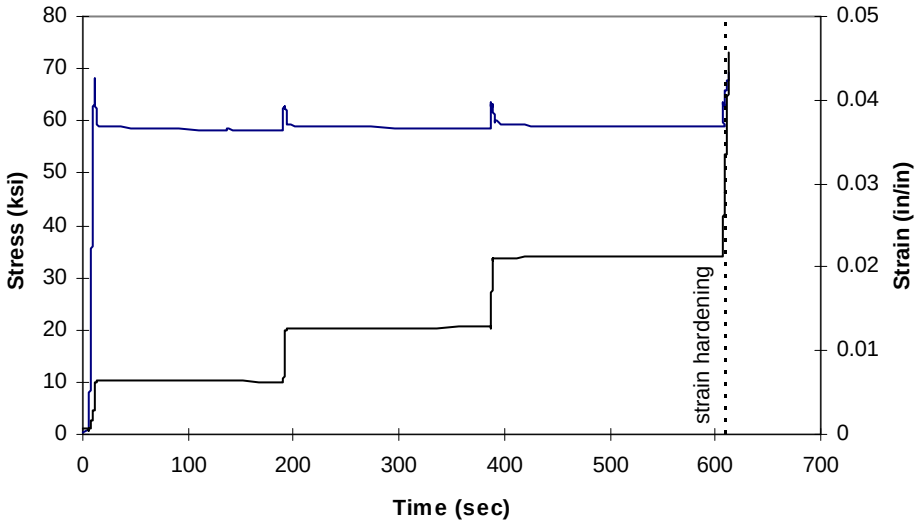

(a)

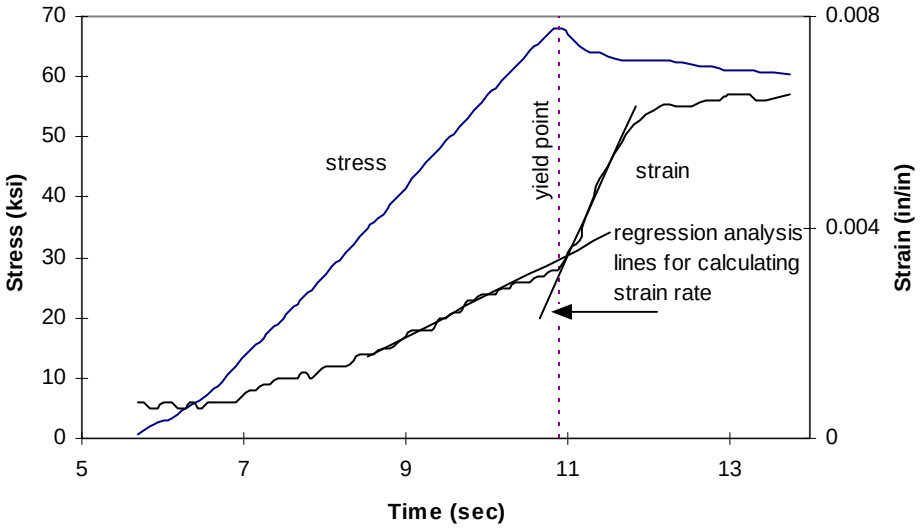

(b)

Figure A3-50: Specimen 5A. Stress-time and strain-time curves: (a) zero through start of strain hardening; (b) zero through start of static yield.

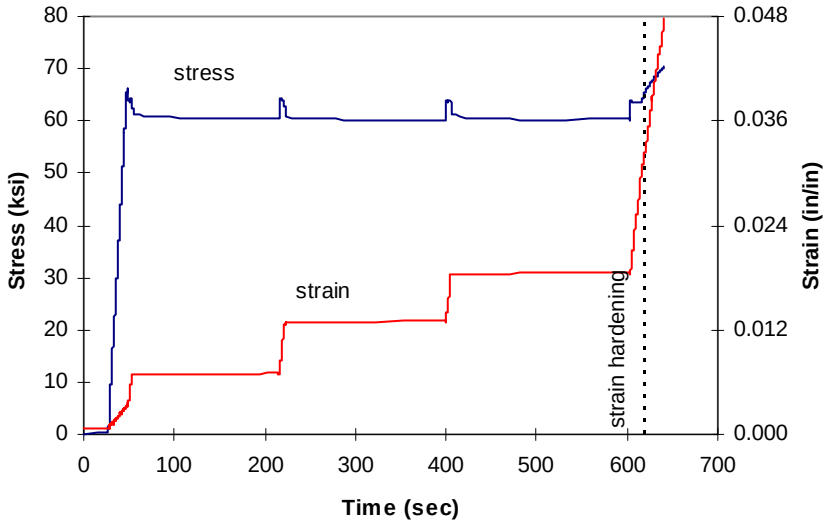

(a)

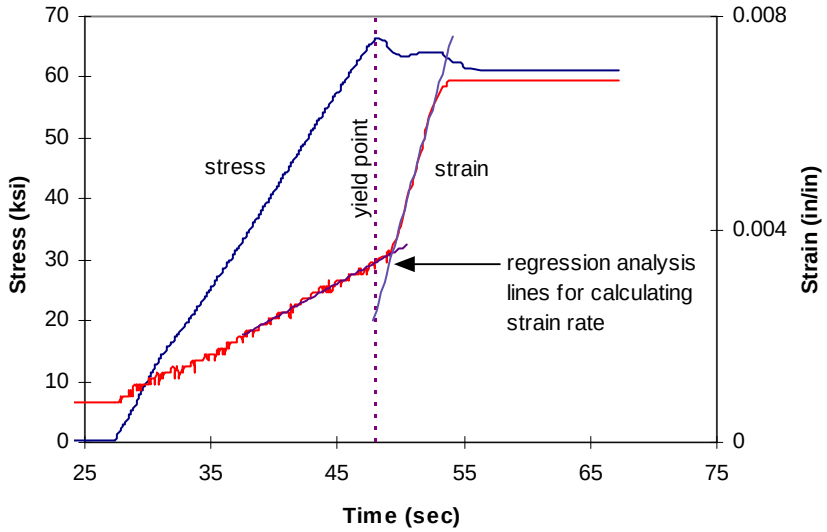

(b)

Figure A3-51: Specimen 6A. Stress-time and strain-time curves: (a) zero through start of strain hardening; (b) zero through start of static yield.

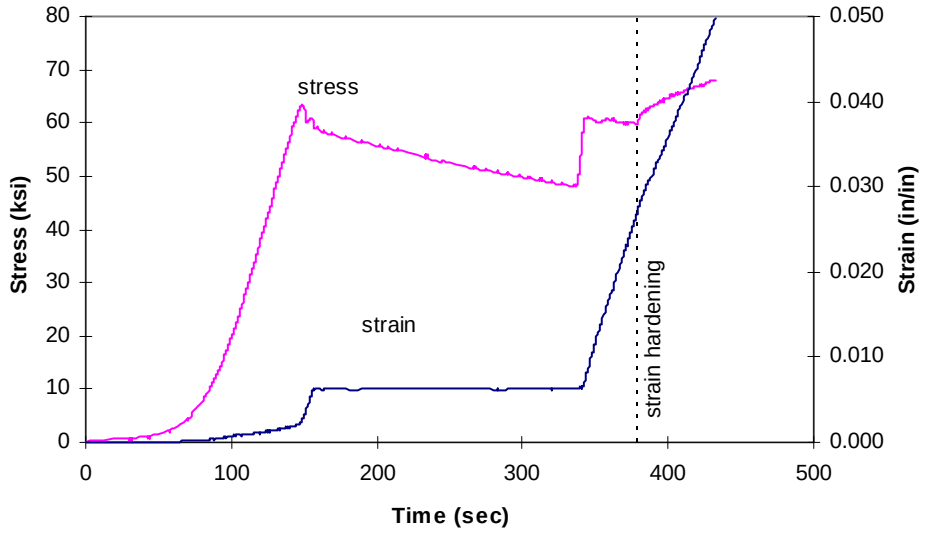

(a)

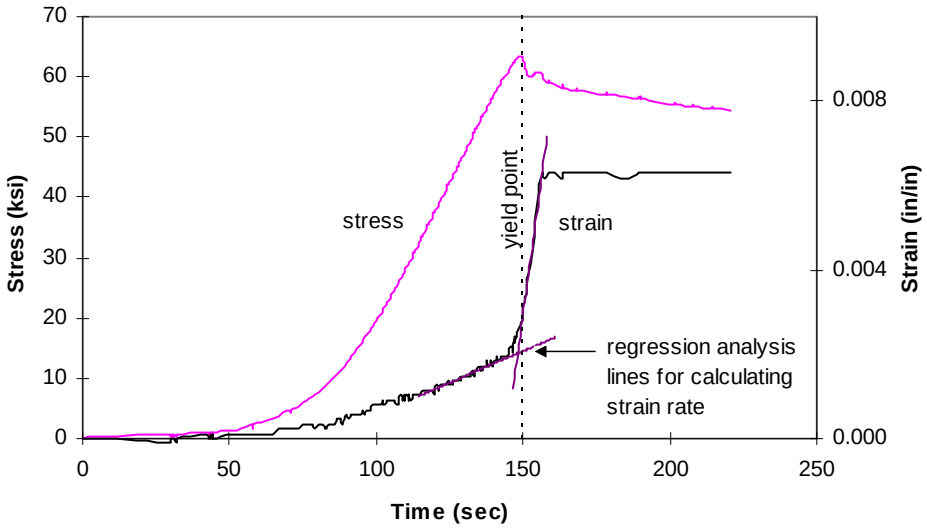

(b)

Figure A3-52: Specimen 1B. Stress-time and strain-time curves: (a) zero through start of strain hardening; (b) zero through start of static yield.

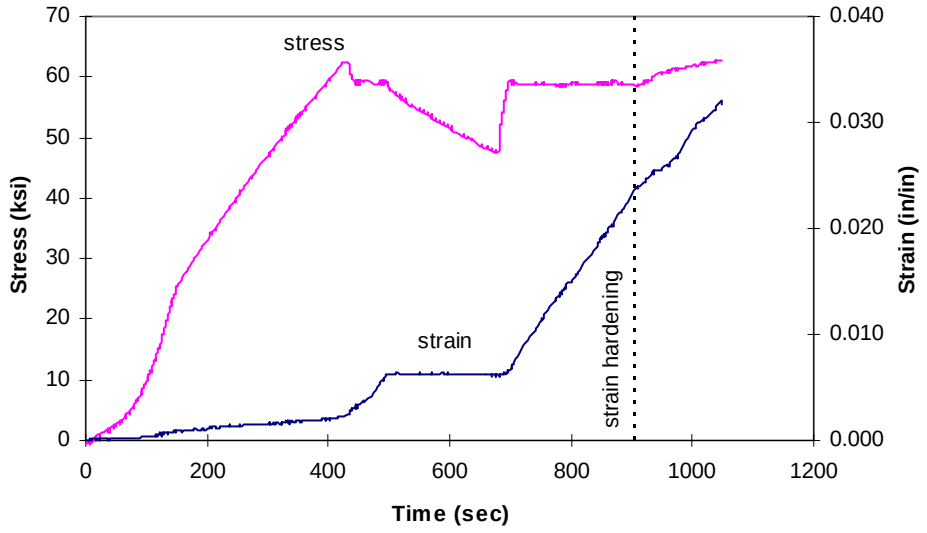

(a)

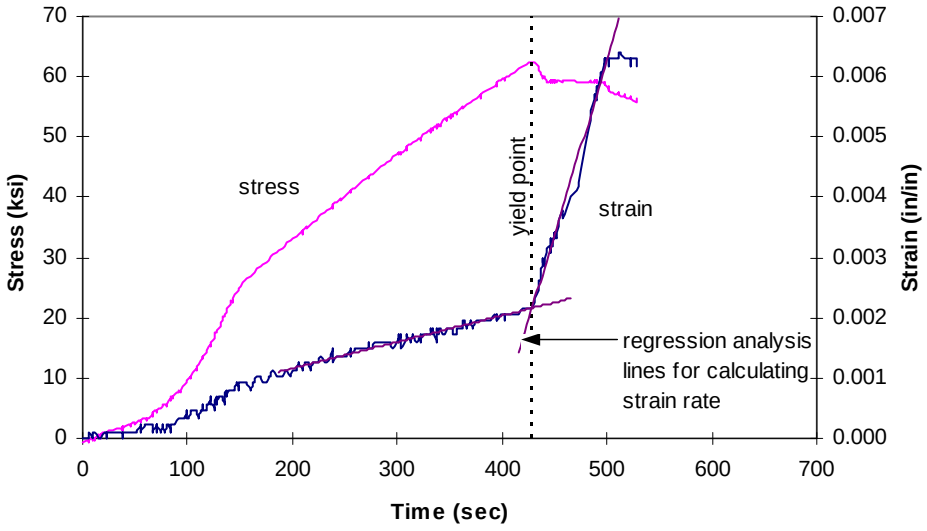

(b)

Figure A3-53: Specimen 2B. Stress-time and strain-time curves: (a) zero through start of strain hardening; (b) zero through start of static yield.

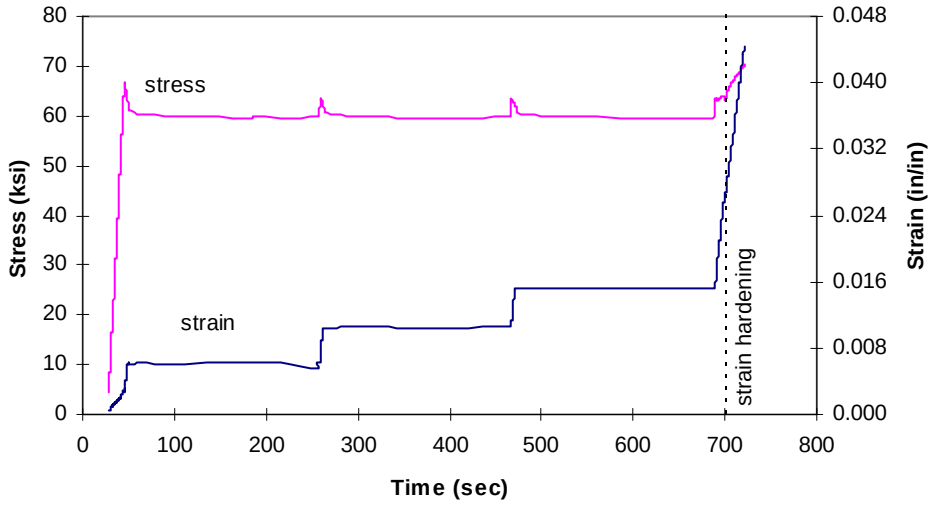

(a)

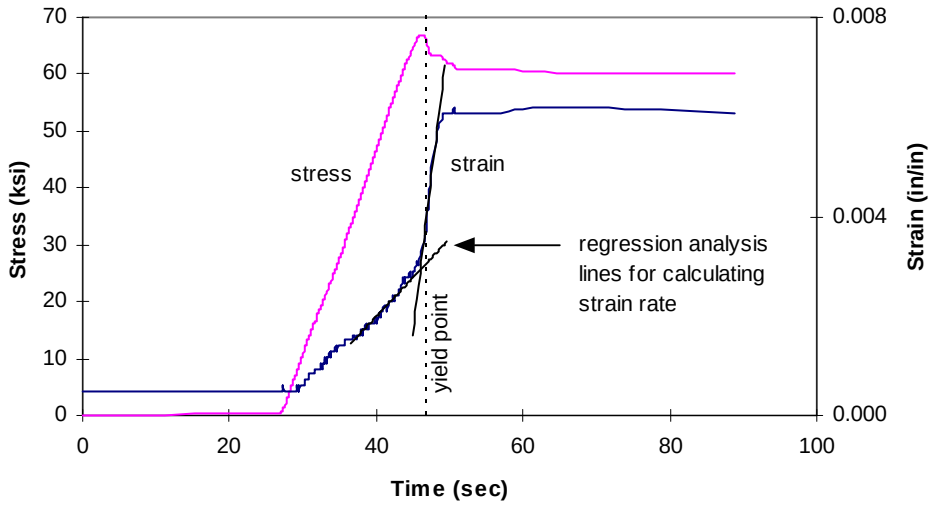

(b)

Figure A3-54: Specimen 4B. Stress-time and strain-time curves: (a) zero through start of strain hardening; (b) zero through start of static yield.

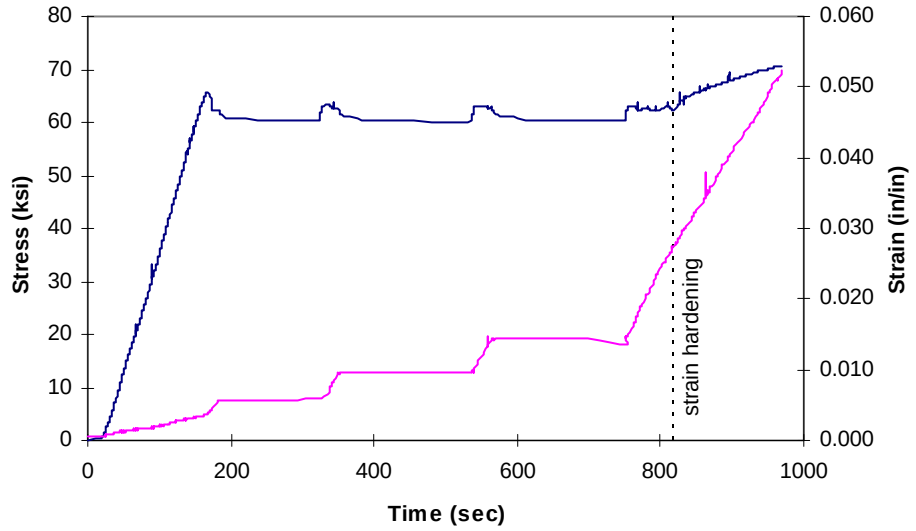

(a)

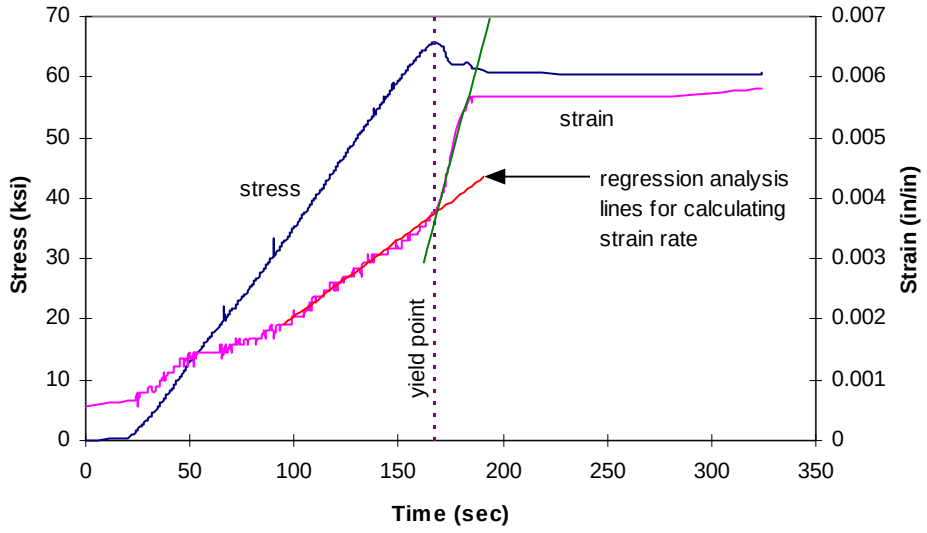

(b)

Figure A3-55: Specimen 5B. Stress-time and strain-time curves: (a) zero through start of strain hardening; (b) zero through start of static yield.

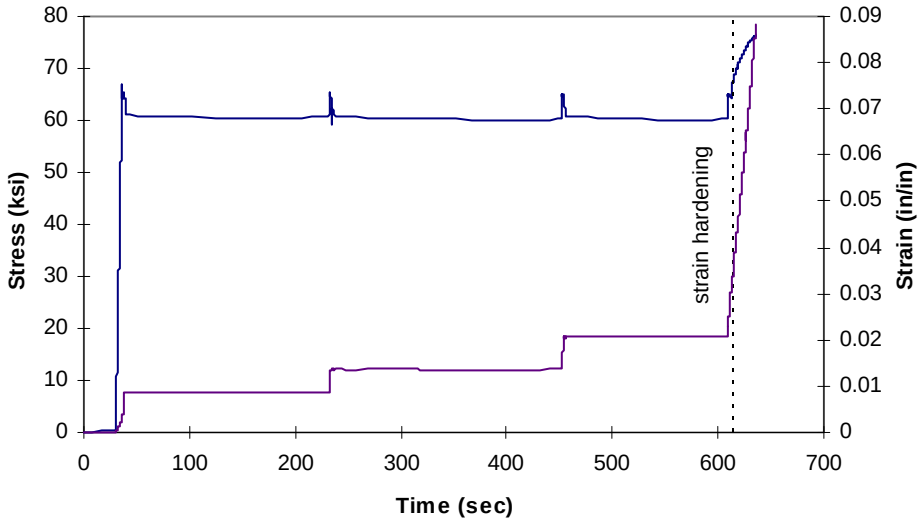

(a)

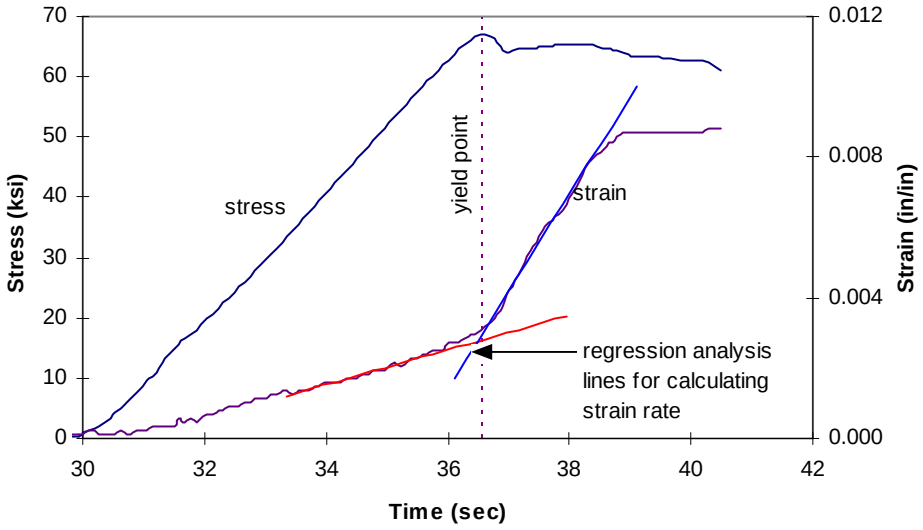

(b)

Figure A3-56: Specimen 6B. Stress-time and strain-time curves: (a) zero through start of strain hardening; (b) zero through start of static yield.

References

Alpsten, G. (1970). "Discussion on Significance of Upper and Lower Yield Point of Structural Steels." *Jernkontorets Annaler*, Vol. 154, 479-484.

Avery, D. H., and Findley, W. N. (1974). "Quasistatic Mechanical Testing." in *Techniques of Metal Research*, Vol. 5, Pt. 1, R.F. Bunshah (ed.), Wiley-Intersciences, New York.

Baker, M. J. (1969). "Variations in the Mechanical Properties of Structural Steels." *Symposium on Concepts of Structures and Methods of Design*, IABSE, London.

Barsom, J. M. (1987). "Material Considerations in Structural Steel Design." *Engineering Journal*, 24(3), 127-139.

Butler, J. F. (1962). "Effect of Luders Front Number on the Yield Point of Iron." *Acta Metallurgica*, 10(3), 258-259.

Callister, W. D. (1994). *Material Science and Engineering*, 3rd edition, John Wiley & Sons, Inc., New York.

Chang, K. C., and Lee, G. C. (1987). "Strain Rate Effect on Structural Steel Under Cyclic Loading." *Journal of Engineering Mechanics*, ASCE, 113(9), 1292-1301.

Christian, J. W. (1964). “The Stress Dependence of Dislocation Velocity and Its Relation to the Strain Rate Sensitivity,” *Acta Metallurgica*, 12(1), 99-102.

Cottrell, A. H. (1967). *Introduction to Metallurgy*, St. Martins’s Press, New York.

Davis, H. E., Troxell, G. E., and Wiskoal, C. T. (1941). *Testing and Inspection of Engineering Materials*, McGraw-Hill, New York.

Davis, E. A. (1938). “The Effect of the Speed of Stretching and the Rate of Loading on the Yielding of Mild Steel.” *Journal of Applied Mechanics*, ASME, 5(4), A138-A140.

Dieter, G. E., *Mechanical Metallurgy*, McGraw-Hill, New York, N.Y., 1986.

Fisher, J. C., and Rogers, H. C. (1956). “Propagation of Luders Bands in Steel Wires.” *Acta Metallurgica*, 4(2), 180-185.

Frank, K. H. (1997). “The Physical and Metallurgical Properties of Structural Steels.” in *Metallurgy, Fracture Mechanics, Welding, Moment Connections and Frame System Behavior*, Background Reports SAC 95-09, 1-1 to 1-22.

Fry, L. H. (1940). “Speed in Tension Testing and its Influence on Yield Point Values.” *Proceedings*, ASTM, 625-636.

Galambos, T. V. and Ravindra, M. K. (1978). "Properties of Steel for Use in LRFD." *Journal of Structural Engineering*, ASCE, 104(9), 1459-1467.

"General Requirements for Rolled or Welded Structural Quality Steel," CAN/CSA-G40.20-M92, Canadian Standards Association, Ontario, 1992.

Gillis, P. P. (1997). Telephone conversation, July 2, 1997.

Gray, T. G. F. (1997). Electronic mail correspondence, July 10, 1997.

Gray, T. G. F., and Sharp, J. (1989). "Influence of Machine Type and Strain Rate Interaction in Tension Testing." in *Factors that Affect the Precision of Mechanical Tests, ASTM STP 1025*, R. Papirno and H. C. Weiss, Eds., American Society for Testing and Materials, Philadelphia, 187-205.

Gray, T. G. F., and McCombe, A. (1992). "Influence of Specimen Dimension and Grip in Tensile Testing Steel to EN 10 002." *Ironmaking and Steelmaking*, Vol. 19, 402-408.

Guiu, F. and Pratt, P. L. (1964). "Stress Relaxation and the Plastic Deformation of Solids." Physical Stata Solidi, 6(11) 111-120.

Haasen, P. (1996). *Physical Metallurgy*, 3rd ed., Cambridge University Press, Cambridge.

Hahn, G. T. (1962). “A Model for Yielding with Special Reference to the Yield-Point Phenomena of Iron and Related BCC Metals.” *Acta Metallurgica*, 10(8), 727-738.

Hahner, P. (1993). “Modelling of Propagating Plastic Instabilities.” *Scripta Metallurgica et Materialia*, 29, 1171-1176.

Hall, E. O. (1970). *Yield Point Phenomena in Metals and Alloys*, Plenum Press, New York.

Hamstad, M. A., and Gillis, P. P. (1966). “Effective Strain Rates in Low Speed Uniaxial Tension Tests.” *Materials Research and Standards*, 6(11), 569-573.

Hockett, J. E., and Gillis, P. P. (1971). “Mechanical Testing Machine Stiffness.” *International Journal of Mechanical Sciences*, 13(3), 251-264.

Hutchison, M. M. (1957). “High Upper Yield Points in Steel.” *Journal of the Iron and Steel Institute*, August, 186, 431-432.

Hutchison, M. M. (1973). “Considerations Relevant to Lower Yield Stresses.” *Metal Science Journal*, Vol. 7, 26-31.

Ingwall, C. T. (1970). “Influence of Test Conditions on the Level of the Upper and Lower Yield Stress of Steels for Welded Structures.” *Jernkontorets Annaler*, Vol. 154, 71-91.

"Interim Guidelines: Evaluation, Repair, Modification and Design of Steel Moment Frames." (1995). FEMA Rep. No. 267, Federal Emergency Management Agency (FEMA), Washington, D.C.

Johnson, R. F. and Murray, J. D. (1967). "The Effect of Rate of Straining on the 0.2% Proof Stress and Lower Yield Stress of Steel," *High Temperature Properties of Steel*, Publication 97, Iron and Steel Institute, London, 79-85.

Kraft, J. M. (1962). "An Interpretation of Lower Yield Point Plastic Flow in the Dynamic Testing of Mild Steel." *Acta Metallurgica*, 10(2), 85-93.

Leblois, C. and Massonnet, C. (1972). "Influence of the Upper Yield Stress on the Behavior of Mild Steel in Bending and Torsion." *International Journal of Mechanical Sciences*, 14(2), 95-115.

Lessells, J. and Barr, R. R. (1965). "A Test Machine for High Temperature Lower Yield or Proof Stress Testing." *Iron & Steel*, 38(1), 2-9.

Load and Resistance Factor Design Specification for Structural Steel Buildings (LRFD). (1993). American Institute of Steel Construction, Chicago, Il.

"Making, Shaping and Treating of Steel." Association of Iron and Steel Engineers, 10th ed., 1985.

Manjoine, M. J. (1944). "Influence of Rate of Strain and Temperature on Yield Stresses of Mild Steel." *Journal of Applied Mechanics*, ASME, 11(4), A211-A218.

Massonet, C. E. and Save, M. A. (1965). *Plastic Analysis and Design*, Blaisdell Publishing Company, New York.

Meguid, S. A. and Malvern, L. E. (1982). "An Experimental Investigation into Load Relaxation in Aluminum (HE30TB) and Mild Steel (EN1A)." *International Journal of Mechanical Sciences*, 24(5), 299-312.

Meyers, M. A. and Chawla, K. K. (1984). *Mechanical Metallurgy*, Prentice-Hall, Englewood Cliffs, NJ.

Moon, D. W., and Vreeland, T. (1968). "Stress Dependence of Mobile Dislocation Density and Dislocation Velocity From Luders Band Front Propagation Velocity." *Scripta Metallurgica*, 2(1), 35-40.

Moon, D. W., and Vreeland, T.(1969). "The Initiation of Yielding in Silicon-Iron." *Acta Metallurgica*, 17(8), 989-996.

"NEHRP Recommended Provsions for Seismic Regulations for New Buildings." (1994). FEMA Rep. No. 222, Federal Emergency Management Agency (FEMA), Washington, D.C.

Petch, N. J. (1964). "The Upper Yield Stress of Polycrystalline Iron." *Acta Metallurgica*, 12(1), 59-65.

Petch, N.J. (1990). “Theory of Yield Point and of Strain-Aging in Steel.” in *Advances in Physical Metallurgy*, J. A. Charles and G. C. Smith, Eds, The Institute of Metals, London, 11-25.

Rao, N. R. N., Lohrmann, M., and Tall, L. (1964). *Effect of Strain Rate on the Yield Stress of Structural Steels*, Lehigh University Fritz Engineering Laboratory, Report No. 249.23.

Schriber, H. W. (1996) Letter to Nester Iwankiw of American Institute of Steel Construction, April 22, 1996

Shuey, B. (1996). M.S. Thesis, The University of Texas at Austin.

“Statistical Analysis of Tensile Data for Wide Flange Structural Shapes.” (1994). American Iron and Steel Institute, Washington, D.C.

Tall, L. and Ketter, R. L. (1958). *Residual Stress and the Compressive Properties of Steel*, Lehigh University Fritz Engineering Laboratory, Report No. 220A.33.

Tall, L. and Alpsten, G. (1969). “On the Scatter and Yield Strength and Residual Stresses in Steel Members.” in *Symposium on Concepts of Structures and Methods of Design*, IABSE, London.

Tanaka, K. and Ishikawa, H. (1976). “Effect of Rigidity of Testing Machine on the Behavior of Tensile Deformation in Mild Steel.” in *Proceedings of the 19th Japan Congress of Materials Research*, Iron and Steel Institute, London.

Taraldsen, A. (1976). "Yield Point Standardization." *Journal of Testing and Evaluation,* JTEVA, 4(2), 126-132.

"Standard Practice for Verification and Classification of Extensometers," (1996). E83, *Annual Book of ASTM Standards*, Vol. 03.01, American Society for Testing and Materials, Philadelphia.

"Standard Specifications for Carbon Structural Steel," (1994). A36, *Annual Book of ASTM Standards*, Vol. 01.04, American Society for Testing and Materials, Philadelphia.

"Standard Specifications for General Requirements for Rolled Structural Steel Bars, Plates, Shapes and Sheet Piling." (1994). A6, *Annual Book of ASTM Standards*, Vol. 01.04, American Society for Testing and Materials, Philadelphia.

"Standard Terminology Relating to Methods of Mechanical Testing," (1989). E6, *Annual Book of ASTM Standards*, Vol. 03.01, American Society for Testing and Materials, Philadelphia.

"Standard Test Methods and Definitions for Mechanical Testing of Steel Products," (1995). A370, *Annual Book of ASTM Standards*, Vol. 01.04, American Society for Testing and Materials, Philadelphia.

"Standard Test Methods for Tension Testing of Metallic Materials." (1996). E8, *Annual Book of ASTM Standards*, Vol. 03.01, American Society for Testing and Materials, Philadelphia.

"Tensile Testing of Metallic Materials." (1990). BS EN 10 002-1, British Standards Institution, London.

Uang, C.M. and Latham, C.T. (1995). "Cyclic Testing of Full-Scale MNH-SMRF Moment Connections." Report No. TR-95/01, Structural Systems Research, University of California at San Diego.

Uniform Building Code. (1994). International Conference of Building Officials, Whittier, CA.

"The Variation of Product Analysis - Carbon Steel Plates and Wide Flange Shapes," American Iron and Steel Institute, Washington, D. C., Sep., 1974.

Welter, G. and Gockowski, S. (1938). "Some Fundamental Factors Regarding the Stress-Strain Diagram for Mild Steel." *Metallurgia*, July, 99-101.

Welter, G. and Gockowski, S. (1939). "Influence of the Resiliency of the Test Machine and of the Loading Speed upon the Determination of the Yield Point for Mild Steel." *Metallurgia*, Aug, 143-148.